STUDIA UNIVERSITATIS
BABEŞ-BOLYAI

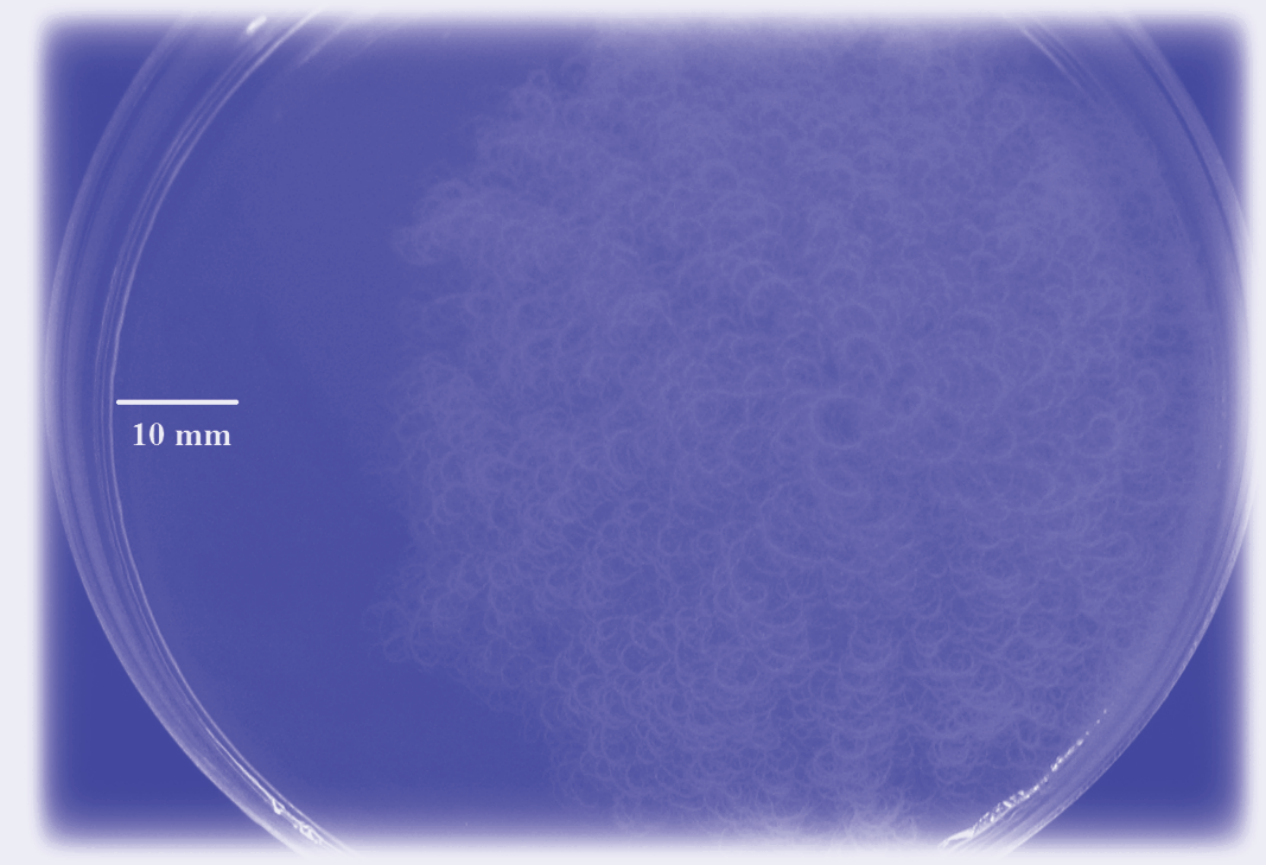

BIOLOGIA

1/2014

STUDIA
UNIVERSITATIS BABEŞ-BOLYAI

BIOLOGIA

1 / 2014
January – June

YEAR **Volume 59 (LIX) 2014**
MONTH **JUNE**
ISSUE **1**

STUDIA
UNIVERSITATIS BABEŞ-BOLYAI

BIOLOGIA

1

STUDIA UBB EDITORIAL OFFICE: B.P. Hasdeu no. 51, 400371 Cluj-Napoca, Romania,
Phone + 40 264 405352, www.studia.ubbcluj.ro

SUMAR – CONTENTS – SOMMAIRE – INHALT

REGULAR ARTICLES

SHORT COMMUNICATION

REVIEW

All authors are responsible for submitting manuscripts in comprehensible US or UK English and ensuring scientific accuracy.

Original pictures on front cover: A biofilm-associated phenotype: 48-hours colony of *Bacillus mycoides* isolated from drinking water © Anca Farkas

STUDIA UNIVERSITATIS BABEŞ-BOLYAI BIOLOGIA, LIX, 1, 2014 (p. 5-20)

EFFECT OF DIFFERENT DISINFECTANTS AGAINST BIOFILM BACTERIA

ANCA FARKAS[1]✉, BRÎNDUȘA BOCOȘ[2], MIHAIL DRĂGAN BULARDA[1] and CORNELIA CRĂCIUNAȘ[1]

SUMMARY. Drinking water biofilms represent a potential reservoir for water contamination. The biofilm mode of life provides multiple advantages for its inhabitants, including specific mechanisms of resistance against antimicrobials. The aim of the present study is to assess the effect of several disinfectants on biofilm consortia. The experiment was set in order to address the most stringent issues in drinking water systems: biofilms resilience, microbial diversity and bacterial resistance. Four chlorine-based agents commonly used in drinking water treatment (sodium dichloroisocyanurate, sodium hypochlorite, chloramine-T and chlorine dioxide) and one mixed cleaning agent (containing sulphamic acid, hydrochloric acid, hydrogen peroxide and acetic acid) were tested for their antibacterial properties. The assessment of disinfectants' efficacy on a wide variety of bacteria brings novel outcomes. The average log reduction values (LRV) indicated the mixed cleaning agent as the most efficient product in bacterial inactivation (LRV = 3.673), followed by sodium dichloroisocyanurate (LRV = 1.122), sodium hypochlorite (LRV = 0.979), chloramine-T (LRV = 0.885) and chlorine dioxide (LRV = 0.657).

Keywords: biofilm bacteria, chlorine-based disinfectants, drinking water, mixed cleaning agents.

Introduction

Drinking water safety is the priority of both the professionals in drinking water industry as well as of the public health authorities. Although waterborne diseases occur rarely in developed countries, outbreaks with public health risks were reported in the near past due to malfunctioning of drinking water treatment plants and distribution networks, which failed to maintain an adequate level of disinfectant to

[1] *Babeş-Bolyai University, Faculty of Biology and Geology, M. Kogălniceanu 1, 400084 Cluj-Napoca, Romania.*

[2] *National Public Health Institute – Regional Public Health Center of Cluj, 6-8 Pasteur Street, Cluj-Napoca, Romania.*

✉ ***Corresponding author: Anca Farkas**, Babeş-Bolyai University, Faculty of Biology and Geology, M. Kogălniceanu 1, 400084 Cluj-Napoca, Romania. E-mail: farkasanca@yahoo.com.*

prevent the growth of pathogens and/or harboured the pathogens (Simões and Simões, 2013). The assessment of treatment efficiency in drinking water treatment plants is accomplished by routine monitoring of inlet and outlet bulk fluids. Microbiological monitoring is based on the values of planktonic bacteria: heterotrophic plate counts (HPC) and faecal indicators (coliform bacteria, Escherichia coli, intestinal enterococci and Clostridium perfringens). HPC offers general and unspecific information on the water microbiota. The presence of faecal indicators warns of microbial contamination with pathogenic bacteria, viruses or protozoa. However, multispecies biofilms proved to be the main mode of bacterial organisation in aquatic environments (Costerton *et al*., 1987). A dynamic exchange of individuals occurs between the attached and planktonic state. The biofilm mode of life provides multiple advantages for its inhabitants, including specific mechanisms of resistance against antimicrobials: slow penetration of disinfectant, stress response defence, metabolic gradients and the presence of persister cells (Chambless *et al*., 2006). Drinking water-associated biofilms may harbour pathogenic species, thus representing a potential reservoir for water contamination (Szewzyk *et al.,* 2000; Wingender and Flemming, 2011; Farkas *et al*., 2012).

In order to overcome the microbiological hazards in drinking water, a number of successive treatment procedures are generally used. Current practices involve multiple barriers to remove raw water pollution and to control bacterial regrowth in distribution systems (Butiuc-Keul, 2014). Chemical disinfection is considered the essential and most direct treatment to inactivate or destroy pathogenic and other microbes in drinking water (Sobsey, 2002). In Europe, it often consists in pretreatment oxidation, primary disinfection and secondary inactivation. While the first two procedures target the optimal removal of raw water contaminants, the last one aims to restrict microbial growth in drinking water distribution systems by maintaining disinfectant residuals at certain levels. Technical barriers (coagulation-flocculation, precipitation, adsorption and filtration) are also designed to modify chemical and physical properties. Such treatments result in assimilable organic carbon reducing, rather than pathogen elimination (Stanfield *et al*., 2003). However, nutrient limitation in bulk water restricts microbial multiplication.

Chemical disinfection procedures are designed based on the type (surface or groundwater) and the quality of the source (LeChevallier and Au, 2004), using gaseous chlorine, monochloramine, chlorine dioxide, ozone, as well as UV irradiation. Chlorination is traditionally applied in drinking water treatment, especially as primary disinfection. Gaseous chlorine is either used for shock chlorination, or dosed as a residual disinfectant. A disadvantage of chemical treatment is the release of trihalometanes (THM) and of other halogenated disinfection by-products (DBP). However, the risks to human health from DBP are extremely small in comparison with the risks associated with inadequate disinfection. By-product formation may be controlled by treatment process optimization (WHO,

2008). The poor efficacy of residual chlorine disinfectant in drinking water to inactivate waterborne pathogens in distribution systems has been observed previously (Payment, 1999). Alternative agents available to water systems exceeding drinking water standards in DBP precursors removal include chlorine dioxide and monochloramines. While chlorine dioxide is increasingly used as either primary or secondary disinfectant, monochloramine is recommended and used as secondary disinfectant only, due to its longer persistence and biofilm penetration (WHO, 2000; LeChevallier and Au, 2004).

The present study investigates the bactericide and bacteriostatic effect of five solutions against biofilm consortia. The experiment was set in order to adress the most stringent issues in drinking water systems: biofilms resilience, microbial diversity and bacterial resistance. Antimicrobial substances commonly used in water industry as well as commercially available products recommended for water disinfection were chosen to be tested. The aim of the paper is to compare the bacterial inactivation performance of conventional chlorine-based disinfectants with the antimicrobial efficiency of a mixed cleaning agent. The hypothesis to be tested is that an innovative solution to be used for drinking water systems cleaning and disinfection should have bactericidal effects and also be capable to disintegrate the biofilm matrix.

Materials and methods

Sampling

In order to obtain mature and structured biofilms, polypropylene coupons with a surface area of 60 cm^2 were immersed for 90 days (Boe Hansen *et al.,* 2002; Martiny *et al.,* 2003) in the settling step of a drinking water facility in Cluj (Fig. 1).

The raw water is abstracted from Tarniţa Lake, falling within A1 quality category (Farkas *et al*., 2011). During the biofilm growth, the average values for few physico-chemical parameters were recorded, as following: temperature 10.8 °C, turbidity 1.52 NTU, pH 7.35, organic substances 2.32 mg/L, dissolved oxygen 10.16 mg/L, total organic compounds 2.64 mg/L, ammonium 0.04 mg/L, nitrites 0.015 mg/L and nitrates 2.78 mg/L.

Disinfection procedure

The polypropylene coupons containing the 90-day-old biofilms were collected and transported to laboratory. All laboratory procedures were performed in sterile conditions. Five biofilm coupons were exposed to disinfectant solutions, while a control coupon was kept in sterile raw water, for two hours. Three chlorine compounds-generating reagents (sodium dichloroisocyanurate, sodium hypochlorite and chloramine-T), one chlorine dioxide-generating product and one mixed cleaning agent (containing hydrochloric acid, sulphamic acid and hydrogen peroxide) were tested for their antibacterial properties (Table 1). Disinfectant solutions were

prepared in sterile raw water, based on laboratory or commercially available products, as shown in Table 1. Solid compounds (Clorom, Chloramine-T tablets) were dissolved in sterile raw water. Liquid reagents (sodium hypochlorite) were diluted in sterile raw water. Aliquots of stock solutions were diluted in sterile raw water up to a concentration of 1.1mg/L free chlorine/chloramine (SR EN ISO 7393-1/2002) and of 1.1mg/L chlorine dioxide. Chlorine dioxide was generated by mixing the precursors delivered in kits, as per manufacturers' instructions. The mixed cleaning agent Floran was prepared using three solutions delivered by the producer: Topix, Filtrasan and Oxis.

Chlorine and chloramine consumptions were measured after disinfection. Disinfectant residuals were inactivated by the addition of 0.5% sodium thiosulphate solution (SR EN ISO 19458/2007).

Table 1.

Disinfectants tested for their antibacterial effect on drinking water biofilms

Active components	**Commercial name**	**Producer**
Sodium dichloroisocyanurate	Clorom	G&M, Romania
Sodium hypochlorite	Sodium hypochlorite solution	Penta, Czech Republic
N-chloro-*p*-toluene sulphonamide	Chloramine-T	Sintofarm, Romania
Chlorine dioxide	TwinOxide	TwinOxide, Netherlands
Topix 40% vol: sulphamic acid, phosphatidic acid; Filtrasan 40% vol: hydrochloric acid, sodium triphosphate, lactic acid, ascorbic acid; Oxis 20% vol: hydrogen peroxide, acetic acid, peracetic acid.	Floran	Mosslein, Germany

Biofilm analyses

Biomass was harvested from each coupon and 7 g biofilm were homogenized. Two subsamples of 1 g weight each were further used for preparing the stock suspensions. Two series of dilutions up to 10^{-9} (control biofilm) and 10^{-6} (disinfected biofilm) were prepared from each subsample (SR EN ISO 6887-1/ 2002).

Different culture media, specific for the fourteen types of bacteria targeted were inoculated with three to five successive dilutions. Viable and cultivable heterotrophic bacteria, faecal indicators, opportunistic pathogens, bacteria involved in nitrogen and sulphur cycling together with iron and manganese bacteria were estimated per gram of biofilm.

HPCs were enumerated in R2A Agar, after 7 days incubation at 22°C (SR EN ISO 6222/2004). The presence of opportunistic pathogens (*Aeromonas hydrophila* and *Pseudomonas aeruginosa*) and of faecal indicators (*Escherichia coli*, intestinal enterococci, *Clostridium perfringens*) was assessed by membrane filtration, as described by available standard methods.

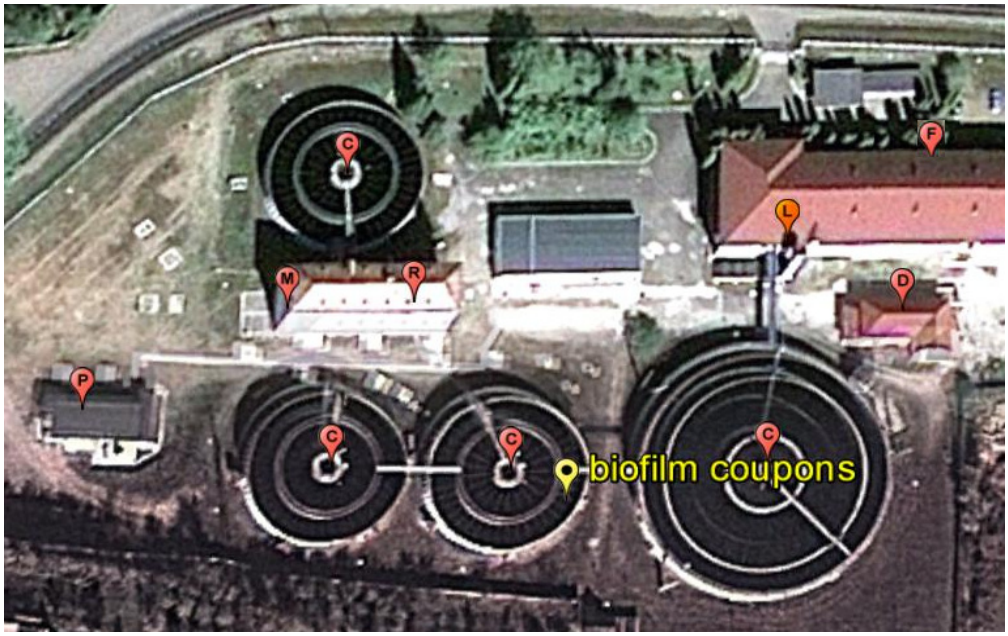

Figure 1. The drinking water treatment plant of Cluj with the position of the immersed polypropylene coupons. M – microstraining; P – prechlorination; R – reagents addition for coagulation and flocculation; C – clarification; F – rapid sand filtration; D – final disinfection by chlorination; L – laboratory.

The incidence of *A. hydrophila* in biofilm samples was measured by inoculation in Ryan's agar. Further confirmatory testing was applied to the colonies that were positive for oxidase, able to ferment trehalose, indole producing and resistant to vibriostatic agent O129 (2,4-diamino-6,7-diisopropyl pteridine) (HPA W9, US EPA 1605). *P. aeruginosa* was cultured on cetrimide agar, counting the fluorescent, oxidase-positive colonies (HPA W6, SR EN ISO 16266/2008). Typical yellow colonies with yellow discoloration developed on Chapman Agar were considered *E. coli* if oxidase-negative and indole positive (SR EN ISO 9308-2/1990). Red to brown colonies on Slanetz and Bartley Agar were enumerated as enterococci if able to produce bile aesculin hydrolysis (SR EN ISO 7899-2/2002). Presumptive colonies of *C. perfringens* were detected on mCP agar, if turned pink to purple after exposure to ammonium hydroxide (Council Directive 98/83/EEC).

Specific growth media were prepared for diverse physiological groups of bacteria, estimated by the most probable number method (Farkas *et al*., 2013). Ammonifying bacteria grown in Peptone Broth supplemented with mineral salts and red phenol were detected by the addition of Nessler reagent. Denitrifying bacteria cultured in Allen Broth were able to produce gaseous nitrogen and nitrogen oxides. Peptone medium, as well as Oppenheimer and Gunkel Broth, Starkey Broth and Postgate Broth were used for the recovery of bacteria involved in sulphur cycling, based on their ability to produce hydrogen sulphide (sulphur reducing bacteria), to precipitate sulphide and iron salts (sulphate reducing bacteria) or to generate sulphur deposits (sulphur oxidizers). Iron reducing bacteria were detected in Ottow's culture medium, recognized by the pink staining of the bivalent iron ions resulted from Fe^{3+} reduction with α-α-dipiridil. Manganese bacteria were grown in modified Manganese Agar and stained with leucoberbelin blue.

Statistics

The experimental procedure was performed in duplicate. Descriptive analyses including average, mean and standard deviation were calculated. Statistical significance testing was performed to assess the differences between data obtained in the two series of biofilm suspensions. Student test was carried out to verify whether the differences in the two series of biofilm suspensions were significant. Because of the limited replications, Wilcoxon rank-sum test was run for each parameter separately. Microsoft Office Excel and Wessa Statistics Software (Holliday, 2012) were used.

The efficiency of each disinfectant was assessed based on the log reduction value (LRV) for each type of bacteria (Hamilton, 2010), based on Eq. (1):

$$LRV = \log10 \text{ (viable bacteria in control / viable bacteria in disinfected biofilm)} \quad (1)$$

Results and discussion

Viable and cultivable HPC, opportunistic pathogens, faecal indicators, bacteria involved in nitrogen cycling, iron and manganese bacteria and bacteria involved in sulphur cycling were measured in control and in disinfected biofilms (Fig. 2). This is the first extensive research on such a wide variety of bacteria. Previously, the antimicrobial effect of different types of disinfectants was assessed mostly on HPC and faecal indicators, especially *E. coli* (LeChevallier *et al*., 1988; Gagnon *et al*., 2005; Volk *et al*., 2010; Kephart and Stoeckel, 2011).

A similar eficacy in reducing bacterial growth was observed in biofilms treated with sodium dichloroisocyanurate and sodium hypochlorite. Differences were observed in their action against opportunistic pathogens and sulphur bacteria.

Sodium dichloroisocyanurate proved to better inactivate aeromonads, pseudomonads and *Clostridium*. It also reduced the viability of sulphur reducers to a greater extent, compared to sodium hypochlorite, while the last registered a higher antibacterial effect against sulphur oxidizers.

When added to water, sodium dichloroisocyanurate rapidly hydrolyses to release free available chlorine and establishes a complex series of equilibria involving six chlorinated and four non-chlorinated isocyanurates (Kuznesov, 2004). The overall hydrolysis reaction can be considered as (Eq. 2):

$$C_3N_3O_3Cl_2Na + 2H_2O \leftrightarrow C_3N_3O_3H_2Na + 2HOCl \quad (2)$$

The antimicrobial effect of chlorine in water is based on its products of dissociation, hypoclorous acid (HOCl) and hypoclorite ions (OCl-), where act as oxidants. They can remove or assist in the removal of some chemicals: pesticides, manganese (II), iron (II), arsenite, hydrogen sulphide, sulphite, bromide, iodide, and nitrite (WHO, 2000; 2003; 2007).

$$Cl_2 + H_2O \rightarrow HOCl + H^+ + Cl^- \quad (3)$$

$$HOCl \leftrightarrow H^+ + OCl^- \quad (4)$$

Sodium hypochlorite disinfection is also based on the action of hypochlorite ions resulted from hypochlorous acid dissociation:

$$NaOCl + H_2O \rightarrow HOCl + Na^+ + OH^- \quad (5)$$

When using sodium dichloroisocyanurate in water disinfection, hypochlorous acid is consumed into an oxidation reaction with organic material, while chloroisocyanurates function as reservoir chlorine, rapidly dissociating to release more HOCl (WHO, 2007). This may explain the higher efficiency of sodium dichloroisocyanurate in biofilm bacteria inactivation, when compared with sodium hypochlorite.

Chloramine-T and chlorine dioxide had similar effects against biofilm bacteria, with one major exception. Intestinal enterococci displayed an increased resistance to chlorine dioxide, while no enterococcal growth was observed in any other disinfected sample. Chlorine dioxide was the second most efficient solution against *E. coli* bacteria, after Floran mixed cleaning agent.

Chloramine-T used in this experiment is an organic chloramine, different than generic chloramine resulted from the combination of chlorine with ammonia. In water, chloramine-T, as a sodium salt of chlorinated arylsulphonamide, dissociates to yield hypochlorite and the sulphonamide moiety. It is therefore used as a mild disinfectant and a biocide.

$$CH_3\text{-}C_6H_4\text{-}SO_2NClNa + H_2O \leftrightarrow CH_3\text{-}C_6H_4\text{-}SO_2NH_2 + OCl^- + Na^+ \quad (6)$$

Chlorine dioxide is a powerful oxidizing agent that dissolves in water, decomposing with the slow formation of chlorite and chlorate:

$$2ClO_2 + H_2O \rightarrow ClO_2^- + ClO_3^- + 2H^+ \quad (7)$$

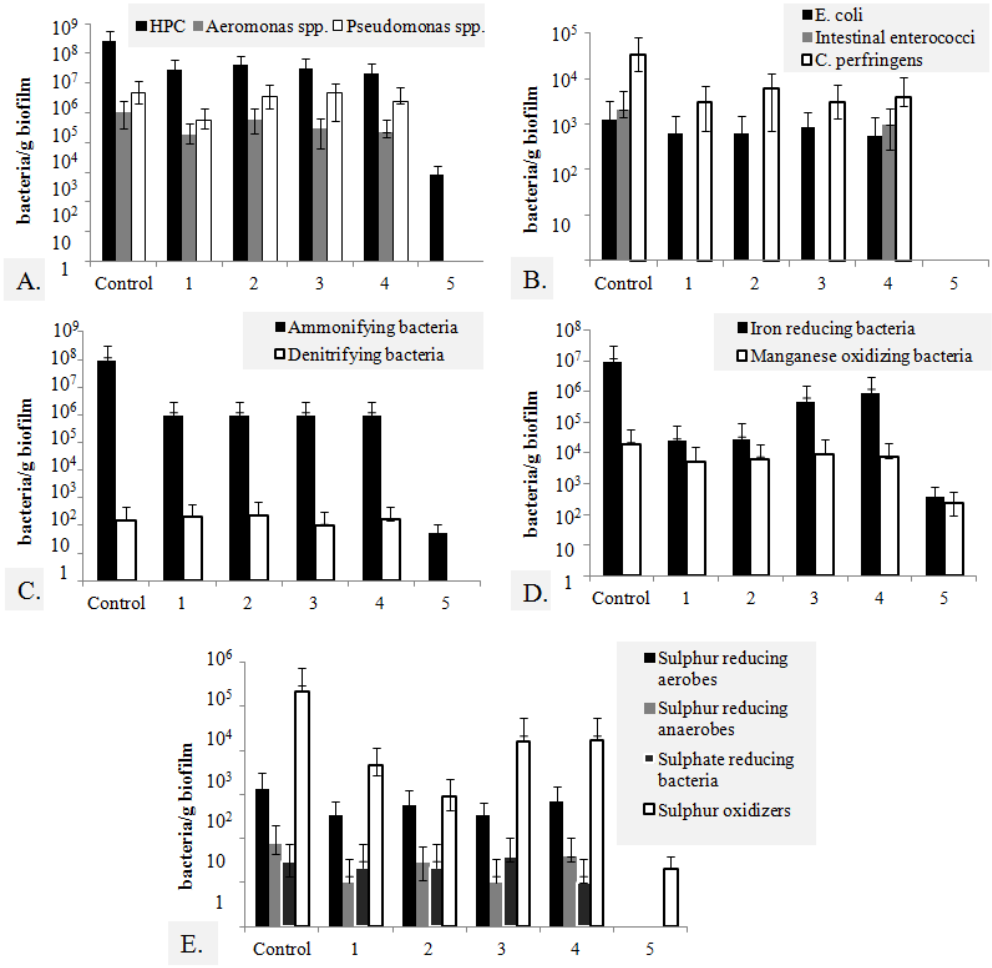

Figure 2. Comparative colony counts in control biofilm and in disinfected biofilms after applying: 1 – sodium dichloroisocyanurate; 2 – sodium hypochlorite; 3 – chloramine-T; 4 – chlorine dioxide; 5 – Floran. A – HPC and opportunistic pathogens; B – faecal indicators; C – bacteria involved in nitrogen cycling; D – iron and manganese bacteria; E – bacteria involved in sulphur cycling

In drinking water, 50-70% of chlorine dioxide is converted to chlorite and 30% to chlorate and chloride (Werdehoff and Singer, 1987). It can be involved in a variety of redox reactions, such as the oxidation of iodide, sulphide, iron (II) and manganese (II) ions (WHO, 2000).

Chloramine-T solution was observed to be the only disinfectant with antimicrobial effect against denitrifying bacteria. It had no inhibitory action against sulphate reducing bacteria (SRB). Rather the contrary, an increment in sulphate reduction occurred within the biofilms exposed for two hours in 1.1 mg / L chloramine-T solution. Such results may explain the enhanced corrosion rates in pipe surfaces when applying chloramine-T disinfection, SRB being recognised as one important physiological group of bacteria involved in biocorrosion (Beech and Flemming, 2000; Coetser and Cloete, 2005). Sungur *et al*. (2010) also found chloramine (1.5 ppm, for 3 hours) to be efficient in HPC reduction in water and biofilms, as well as in planktonic SRB inactivation, but significantly ineffective against SRB in biofilms.

A p-value < 0.05 was considered to indicate that data obtained from two series of biofilm suspensions were significantly different. Student's test showed that no significant differences registered between the means of bacterial populations in the two subsamples of control, as well as in disinfected biofilms. Wilcoxon test revealed the absence of any significant difference for 13 of the 14 parameters investigated. Significant differences in the two series of biofilm suspensions (p-value < 0.05) occurred in the case of manganese bacteria (Table 2).

Residual chlorine concentrations after two hours disinfection are presented in Table 3. Sodium hypochlorite was the most rapidly consumed (residual 0.15 mg / L), while chloramite-T dissociated slowly (residual 0.8 mg / L). Chlorine dioxide proved to be able to persist longer, when compared with sodium dichloroisocyanurate and sodium hypochlorite.

No cells of aeromonads, pseudomonads, faecal indicators, denitrifiers, sulphur and sulphate reducing bacteria were recovered from biofilms treated with the mixed cleaning agent Floran. Recommended by the manufacturer for biofilms control in drinking water systems, Floran proved a high efficiency in bacterial inactivation. The performance of Mosslein cleaning solutions was tested previously in the drinking water treatment plant of Voila. Effects such as biofilm removal and sand filters conditioning were observed (Niculaie *et al.,* 2010).

Based on the average log reduction values of all bacterial types, the most effective disinfection in present investigation was achieved by the use of the mixed cleaning agent Floran (LRV = 3.673), followed by sodium dichloroisocyanurate (LRV = 1.122), sodium hypochlorite (LRV = 0.979), chloramine-T (LRV = 0.885) and chlorine dioxide (LRV = 0.657). As it can be seen in Table 4, of the five disinfectants tested, Floran was the most powerful agent in inactivating biofilm bacteria. It was able to reduce microbial viability in a percentage range from 96.66% (LRV = 1.477) to 99.99994% (LRV = 6.227).

Other studies on the comparative efficiency of disinfectants, targeting an inactivation of 99% (2 log) for planktonic HPC and *E. coli*, indicated the following ranking: hypochlorous acid followed by chlorine dioxide, hypochlorite ion and monochloramine (LeChevallier *et al.,* 1988; LeChevallier and Au, 2004).

Table 2.

Bacterial counts and standard deviations in control and disinfected biofilms. 1 – sodium dichloroisocyanurate; 2 – sodium hypochlorite; 3 – chloramine-T; 4 – chlorine dioxide; 5 – Floran. I, II – replicates. In rows – p-values for Wilcoxon test, assessing significant differences for each parameter, in replicates. In columns – p-values for Student's test, assessing significant differences for the 14 parameters in the two series of biofilm suspensions.

Type of bacteria	Sample	Control	1	2	3	4	5	Wilcoxon test, p-value
HPC	I	28272727	3214348	4307878	3398919	2420760	856	0.5887
	II	26818181	2704894	3908485	3091989	1879543	798	
	SD	1028519	360238	282413	217032	382698	41	-
A. hydrophila	I	127272	24000	75000	33235	33300	0	0.5211
	II	83692	11240	45120	24600	12100	0	
	SD	30815	9022	21128	6105	14990	0	-
P. aeruginosa	I	633333	75000	454000	496000	400000	0	0.2615
	II	340000	33000	250000	420000	102000	0	
	SD	207417	29698	144249	53740	210717	0	-
E. coli	I	1700	490	460	950	330	0	0.7393
	II	800	800	800	800	800	0	
	SD	636	219	240	106	332	0	-
Intestinal enterococci	I	3000	0	0	0	1200	0	0.7750
	II	1040	0	0	0	800	0	
	SD	1385	0	0	0	282	0	-
C. perfringens	I	43540	2500	5500	3950	5820	0	0.6303
	II	23166	3520	6520	2050	2200	0	
	SD	14406	721	721	1343	2559	0	-
Amonifying bacteria	I	5400000	1800000	1800000	1800000	1800000	55	0.2442
	II	80000000	36000	36000	36000	36000	55	
	SD	23460844	1247336	1247336	1247336	1247336	0	-
Denitrifying bacteria	I	36	54	54	18	60	0	0.0533
	II	280	340	420	180	280	0	
	SD	172	202	258	114	155	0	-
Iron reducing bacteria	I	470000	3600	3600	3600	3600	330	0.0869
	II	18000000	45000	54000	920000	1800000	430	
	SD	12395581	29274	35638	647992	1270246	71	-
Manganese oxidizing bacteria	I	35455	9090	11364	15455	12273	290	0.0411
	II	3000	1100	700	1900	2400	164	
	SD	22949	5649	7540	9584	6981	89	-

Table 2. continued

Sulphur reducing aerobes	I	1700	340	640	330	790	0	0.6279
	II	970	330	520	330	620	0	
	SD	516	7	84	0	120	0	-
Sulphur reducing anaerobes	I	110	20	20	20	60	0	0.2504
	II	45	0	36	0	18	0	
	SD	45	14	11	14	29	0	-
Sulphate reducing bacteria	I	20	45	45	60	20	0	0.0552
	II	40	0	0	18	0	0	
	SD	14	31	31	29	14	0	-
Sulphur oxidizing bacteria	I	430000	6400	1240	32000	32000	20	0.1481
	II	4700	2600	600	680	1400	20	
	SD	300732	2687	452	22146	21637	0	-
Student's test	p-value	0.2959	0.2234	0.2067	0.5429	0.7500	0.6409	-

No evidence of a direct correlation between chlorine consumption and the average LRV was found in the present experiment.

Previous studies assessing the effectiveness of chlorine dioxide as a disinfectant on planktonic bacteria in sewage systems indicated LRV ranging from 4.06 to 6.57 CFU/100ml (Kephart and Stoeckel, 2011). Ozone plus chlorine dioxide disinfection revealed LRV greater than 5 in removal of planktonic *C. perfringens* (Payment and Franco, 1993). In the present study, the action of chlorine-based agents resulted in *C. perfringens* log inactivation from 1.046 to 0.744 (91% to 81.98%), while Floran solution was able to reduce the active *Clostridium* cells with 99.997% (LRV = 4.523).

Even if chlorine dioxide was the most efficient chlorine-based disinfectant against heterotrophic bacteria (LRV = 1.108), as well as against *E. coli* (LRV = 0.345), its overall inhibitory effect against the fourteen types of bacteria was weaker than expected. Previous research studies reported a log-inactivation of 1.6-1.8 for suspended cells and just less than 1 log inactivation of biofilm heterotrophs (at a low concentration of 0.25mg/l, for 12 weeks) (Gagnon *et al.,* 2005). It is possible that longer contact time to be needed in order to achieve a more effective disinfection.

Table 3.

Chlorine residuals after two hours disinfection

Disinfectant	**mg / L**
Sodium dichloroisocyanurate	0.3
Sodium hypochlorite	0.15
Chloramine-T	0.8
Chlorine dioxide	0.6

Table 4.

Log reduction values in biofilm bacteria disinfected with:
1 – sodium dichloroisocyanurate; 2 – sodium hypochlorite; 3 – chloramine-T;
4 – chlorine dioxide; 5 – Floran solutions

Type of bacteria	***Log reduction value*** *(bacteria/g of biofilm)*				
	1	**2**	**3**	**4**	**5**
HPC	0.969	0.826	0.929	1.108	4.523
A. hydrophila	0.777	0.245	0.562	0.667	5.023
P. aeruginosa	0.955	0.141	0.026	0.288	5.687
E. coli	0.287	0.298	0.155	0.345	3.097
Intestinal enterococci	3.305	3.305	3.305	0.305	3.305
C. perfringens	1.045	0.744	1.046	0.920	4.523
Ammonifying bacteria	2.004	2.004	2.004	2.004	6.227
Denitrifying bacteria	-0.096	-0.176	0.203	-0.032	2.199
Iron reducing bacteria	2.580	2.506	1.301	1.010	4.386
Manganese oxidizing bacteria	0.577	0.503	0.346	0.418	1.928
Sulphur reducing aerobes	0.600	0.362	0.607	0.277	3.125
Sulphur reducing anaerobes	0.889	0.442	0.889	0.298	1.889
Sulphate reducing bacteria	0.125	0.125	-0.114	0.477	1.477
Sulphur oxidizing bacteria	1.684	2.373	1.124	1.114	4.036
Average LRV	**1.122**	**0.979**	**0.885**	**0.657**	**3.673**

When comparing results of similar investigations, realized on planktonic cells, to disinfectants efficacy on attached bacteria, as revealed by the present study, biofilm organization proves its protective features. The reduced antimicrobial impacts may be explained by slow penetration of disinfectants into the biofilm matrix. A direct measurement by the use of microelectrodes showed that chlorine concentrations in biofilms were typically only 20% or less of the concentration in the bulk liquid (de Beer *et al.,* 1994). Another explanation resides in the possibility of sublethal antimicrobial dosage, which may result in adaptative stress responses within the bacterial cells. Injured bacteria may react through a series of cellular repair and response mechanisms. The effects in terms of public health risks include the emergence of resistant variants, pathogens exhibiting enhanced virulence and bacteria entering the viable but nonculturable state (Wesche *et al*., 2009).

With respect to the increments in the recovery of denitrifying bacteria from biofilms exposed to chlorine-based agents and the enhanced sulphate reduction activity registered in biofilms treated with chloramine-T, we consider they may represent hormetic effects. Hormesis, a familiar term in toxicology, is a biphasic dose-response phenomenon characterized by a low-dose stimulation and a high-dose inhibition (Calabrese, 2008; Kaplan, 2011).

Therefore, drinking water treatment strategies should consider both the lower susceptibility of biofilm bacteria to disinfectants and the increased resistance of detached cells (Steed and Falkinham, 2006), which can survive and adhere to other surfaces to initiate biofilm formation downstream. Removal of deposits from the distribution systems also contributes to drinking water quality improvement (Lehtola *et al.,* 2004).

The mixed cleaning agent Floran demonstrated not just a bactericidal/bacteriostatic effect, but it was able to disintegrate the whole biofilm structure. As known, the efficient cleaning and disinfection implies not only killing the cells within the biofilm, but also disintegration of the biofilm matrix, so that the biofilm can be completely removed from the surface. Any leftover organic material provides nutrients that facilitate the rapid formation of a new biofilm (Wirtanen *et al.,* 2002; Luppens *et al.,* 2003).

Selection of the appropriate procedures in order to achieve drinking water safety is essential, since biofilm recovery after inefficient treatment could lead to populations of resistant bacteria, which may be recalcitrant to subsequent disinfection process (Simões *et al.,* 2004). To achieve efficient disinfection by the use of chlorine-based disinfectants, mechanical removal of biofilms prior to water disinfection is recommended. Also, investigations about the composition of microbial consortia and the physiological activities in the associated biofilms should be considered, due to the specificity of metabolic interactions between bacteria with different physiological requirements (Farkas *et al*., 2013).

Conclusions

After two hours exposure to disinfectant solutions based on the commonly used and commercially available chlorine-based products, in the recommended concentrations, significant numbers of bacteria were able to survive in drinking water biofilms.

None of the chlorine-based antimicrobials tested were able to completely inactivate the opportunistic pathogens or faecal bacteria embedded in biofilms. Moreover, increments in rates of sulphate reduction or in denitrification occurred in biofilms after applying chlorine-based disinfectants. Such aspects are important, considering the role of biofilms in biocorrosion.

The use of mixed cleaning agents proved to be the most efficient procedure for the inactivation of bacterial populations in drinking water associated biofilms. The maximum antimicrobial effect was achieved in biofilms treated with Floran (LRV = 3.673). Neither opportunistic pathogens nor faecal bacteria were viable in biofilms after treatment and the biofilm matrix was disintegrated.

REFERENCES

Beech, I.B., Flemming, H.C. (2000) Microbiological fundamentals, In: *Simple methods for the investigation of the role of biofilms in corrosion*, Beech, I., Bergel, A., Mollica, A., Flemming, H.C., Scotto, V., Sand, W. (eds.), Biocorrosion, 00-02, pp. 3-15

Boe-Hansen, R., Albrechtsen, H.J., Arvin, E., Jørgensen, C. (2002) Dynamics of biofilm formation in a model drinking water distribution system, *J. Water Supply Res. T.*, **51**, 399-406

Butiuc-Keul, A. (2014) *General Biotechnology* (in Romanian), Universitary Press of Cluj, pp. 210

Calabrese, E.J. (2008) Hormesis: why it is important to toxicology and toxicologists, *Environ. Toxicol. Chem.*, **27**, 1451-1474

Chambless, J.D., Hunt, S.M., Stewart, P.S. (2006) A three-dimensional computer model of four hypothetical mechanisms protecting biofilms from antimicrobials, *Appl. Environ. Microbiol.*, **72**, 2005-2013

Coetser, S.E., Cloete, T.E. (2005) Biofouling and biocorrosion in industrial water systems, *Crit. Rev. Microbiol.*, **31**, 213-232

Costerton, J.W., Cheng, K.J., Gessey, G.G., Ladd, T.I., Nickel, J.C., Dasgupta, M., Marrie, T.J. (1987) Bacterial biofilms in nature and disease*, Ann. Rev. Microbiol.*, **41**, 435-464

de Beer, D., Srinivasan, R., Stewart, P.S. (1994) Direct measurement of chlorine penetration into biofilms during disinfection, *Appl. Environ. Microbiol.*, **60**, 4339-4344

Farkas, A., Bogătean, M., Ciatarâș, D., Bocoș, B., Țigan, Ș. (2011) *The new drinking water source of Cluj brings improvements in raw water quality*, Danube – Black Sea Regional Young Water Professionals Conf. Proc., Bucharest, 3-9

Farkas, A., Drăgan-Bularda, M., Ciatarâș, D., Bocoș, B., Țigan, Ș. (2012) Opportunistic pathogens and faecal indicators assessment in drinking water associated biofilms in Cluj, Romania. *J. Water Health*, **10**, 471-483

Farkas, A., Drăgan-Bularda, M., Muntean, V., Ciatarâș, D., Țigan, Ș. (2013) Microbial activity in drinking water associated biofilms. *Cent. Eur. J. Biol.*, **8**, 201-214

Gagnon, G.A., Rand, J.L., O'Leary, K.O., Rygel, A.C., Chauret, C., Andrews, R.C. (2005) Disinfectant efficacy of chlorite and chlorine dioxide in drinking water biofilms, *Water Res.*, **39**, 1809-1817

Hamilton, M.A. (2010) *The log reduction measure of disinfectant efficacy*, Center for Biofilm Engineering, http://www.biofilm.montana.edu/files/CBE/documents/KSA-SM-07.pdf

Holliday, I.E. (2012) Wilcoxon-Mann-Whitney Test (v1.0.5) in Free Statistics Software (v1.1.23-r7), Office for Research Development and Education, http://www.wessa.net/ rwasp_ReddyMoores%20Wilcoxon%20MannWitney%20Test.wasp/

Kaplan, J.B. (2011) Antibiotic-induced biofilm formation*, Int. J. Artif. Organs***, 34**, 737-751

Kephart, C.M., Stoeckel, D.M. (2011) *Results of an evaluation of the effectiveness of chlorine dioxide as a disinfectant for onsite household sewage treatment systems*, US Geological Survey Open-File Report, http://pubs.usgs.gov/of/2011/1096/pdf/ofr2011-1096.pdf

Kuznesof, P.M. (2004) *Sodium dichloroisocyanurate. Chemical and technical assessment*, 61st Joint FAO/WHO Expert Committee on Food Additives, http://www.fao.org/ fileadmin/ templates/agns/pdf/jecfa/cta/61/NaDCC.pdf

LeChevallier, M.W., Cawthon, C.D., Lee, R.G. (1988) Factors promoting survival of bacteria in chlorinated water supplies, *Appl. Environ. Microbiol.*, **54**, 649-654

LeChevallier, M.W., Au, K.K. (2004) *Water Treatment and Pathogen Control*, IWA Publishing

Lehtola, M.J., Nissinen, T.K., Miettinen, I.T., Martikainen, P.J., Vartiainen, T. (2004) Removal of soft deposits from the distribution system improves the drinking water quality, *Water Res.*, **34**, 601-610

Luppens, S.B.I., Reij, M.W., Rombouts, F.M, Abee, T. (2003) Factors that affect disinfection of pathogenic biofilms, In: *Biofilms in medicine, industry and environmental biotechnology,* Lens, P., O'Flaherty, V., Moran, A.P., Stoodley, P., Mahony, T. (eds.), IWA Publishing, pp. 473-502

Martiny, A.C., Jørgensen, T.M., Albrechtsen, H.J., Arvin, E., Molin, S. (2003) Long-term succession of structure and diversity of a biofilm formed in a model drinking water distribution system, *Appl. Environ. Microbiol.,* **69,** 6899-6907

Niculaie, S., Mares, C., Poienaru, G., Gologan, D., Sinca, A. (2010) *The use of ecological solutions Mosslein for biofilm limitation in drinking water production and distribution systems* (in Romanian), Ecomediu Conf. Fascicle, Romanian Water Association, pp. 26-27

Payment, P., Franco, E. (1993) *Clostridium perfringens* and somatic coliphages as indicators of the efficiency of drinking water treatment for viruses and protozoan cysts, *Appl. Environ. Microbiol.*, **59**, 2418-2424

Payment, P. (1999) Poor efficacy of residual chlorine disinfectant in drinking water to inactivate waterborne pathogens in distribution systems, *Can. J. Microbiol*., **45**, 709-715

Simões, M., Pereira, M.O., Vieira, M.J. (2004) *Biofilm recovery after treatment with an anionic and cationic surfactant at sublethal concentrations,* Int. Conf. Biofilms 2004: Structure and Activity of Biofilms, pp. 200-204

Simões, L.C., Simões, M. (2013) Biofilms in drinking water: problems and solutions, *RSC Adv*., **3**, 2520–2533

Sobsey, M.D. (2002) *Managing Water in the Home: Accelerated Health Gains from Improved Water Supply*, World Health Organization, Geneva, http://www.who.int/ water_sanitation_ health/dwq/WSH02.07.pdf

Stanfield, G., LeChevallier, M.W., Snoozi, M. (2003) *Treatment efficiency in assessing microbial safety of drinking water*, IWA Publishing, 159-178

Steed, K.A., Falkinham III, J.O., (2006) Effect of growth in biofilms on chlorine susceptibility of *Mycobacterium avium* and *Mycobacterium intracellulare, Appl. Environ. Microbiol.*, **72**, 4007-4011

Sungur, E. I., Türetgen, I., Javaherdashti, R., Çotuk, A. (2010) Monitoring and disinfection of biofilm-associated sulfate reducing bacteria on different substrata in a simulated recirculating cooling tower system, *Turk. J. Biol.*, **3**, 389-397

Szewzyk, U., Szewzyk, R., Manz, W., Schleifer, K.H. (2000) Microbiological safety of drinking water, *Ann. Rev. Microbiol.*, **54**, 81-127

Volk, C.J., Hofmann, R., Chauret, C., Gagnon, G.A., Rangers, G., Andrews, R.C. (2010) Implementation of chlorine dioxide disinfection: Effects of the treatment change on drinking water quality in a full-scale distribution system, *J. Environ. Sci. Eng.,* **1,** 323-330

Werdehoff, K.S., Singer, P.C. (1987) Chlorine dioxide effects on THMPF, TOXFP, and the formation of inorganic by-products, *J. Am. Water Works Ass.*, **79**, 107-113

Wesche, A.M., Gurthler, J.B., Marks, B.P., Ryser, E.T. (2009) Stress, sublethal injury, resuscitation, and virulence of bacterial foodborne pathogens, *J. Food Protect.*, **5**, 1121-1138

Wingender, J., Flemming, H.C. (2011) Biofilms in drinking water and their role as reservoir for pathogens, *Int. J. Hyg. Envir. Heal.*, **213**, 190-197

Wirtanen, G., Langsrud, S., Salo, S., Olofson, U., Alnas, H., Neuman, M., Homleid, J.P., Mattila-Sandholm, T. (2002) *Evaluation of sanitation procedures for use in dairies*, VTT Technical Research Centre of Finland, http://www.vtt.fi/inf/pdf/publications/2002/P481.pdf

WHO (2000) *Disinfectants and Disinfectant By-Products*, World Health Organization, Geneva, http://whqlibdoc.who.int/ehc/WHO_EHC_216.pdf

WHO (2003) *Chlorine in Drinking Water*, World Health Organization, Geneva, http://www.who.int/water_sanitation_health/dwq/chlorine.pdf

WHO (2007) *Sodium Dichloroisocyanurate in Drinking Water*, World Health Organization, Geneva,http://www.who.int/water_sanitation_health/dwq/chemicals/second_addendum_sodium_dichloroisocyanurate.pdf

WHO (2008) *Guidelines for Drinking Water Quality*, 3rd edition, World Health Organization, Geneva, http://www.who.int/water_sanitation_health/dwq/fulltext.pdf

STUDIA UNIVERSITATIS BABEŞ-BOLYAI BIOLOGIA, LIX, 1, 2014 (p. 21-39)

EFFECTS OF MICROAEROBIOSIS ON PHOTOSYNTHESIS IN THE CYANOBACTERIUM *SYNECHOCOCCUS* SP. PCC 7002

EDINA SZEKERES[1], VICTOR BERCEA[2], NICOLAE DRAGOŞ[1] and BOGDAN DRUGĂ[2]✉

SUMMARY. In this study the effect of microaerobiosis on photochemical activity in the cyanobacterium *Synechococcus* sp. PCC 7002 is presented, by measuring chlorophyll fluorescence. Microaerobiosis was achieved by argon bubbling for 120 minutes, with samples being taken in four specific time periods.

In vitro measurements of absorption showed dominancy in chlorophyll a and the presence of carotenoids. Maximum fluorescence Fm decreased after 15 minutes of exposure to argon bubbling. Decline of Fm attests the large number of closed reaction centers, as well as plastoquinone reduction and growth of fluorescence emission. Variable fluorescence, expressing the difference between Fm and F0, showed positive values compared to the control, except after 60 minutes of argon treatment. Maximal quantum yield (Fv/Fm) of PS II photosynthesis was weakly stimulated by the argon treatment, except at 60 minutes of argon effect when negative values were observed. The coefficients of photochemical quenching, qP and qL, were maintained at higher values, except when 30 minute exposure to argon treatment.

By exposure to argon, the Pm signal was high in the first 30 minutes, followed by a significant decrease towards the end of the stress treatment suggesting a decrease in the reduction state of P700 reaction center compared to oxidized state. Moreover, effective PS I photochemical quantum yield Y(I) dropped significantly in the first 30 minute compared to the control. The decrease in quantum yield Y(I) reveals decreased reduction state due to the lack of limitation by the acceptor, respectively, decrease in photochemical energy conversion in PS I. The interchange of oxidative/reduced state of the plastoquinone nuclei was revealed in the kinetics of the chlorophyll fluorescence induction by pulse saturation in control. Fluorescence kinetics showed on the logarithmic scale revealed important modifications in I – P spectrum due to reduction of the plastoquinone nuclei.

Keywords: Cyanobacteria, fluorescence, microaerobiosis, photosynthesis, *Synechococcus*.

[1] *Faculty of Biology and Geology, Babeş-Bolyai University, Cluj-Napoca, Romania.*
[2] *Institute of Biological Research, Cluj-Napoca, Romania.*
✉ ***Corresponding author: Bogdan Drugă**, Institute of Biological Research, Cluj-Napoca, Romania. Email: bogdan.druga@icbcluj.ro.*

Introduction

Cyanobacteria are among the very few groups of bacteria that can perform oxygenic photosynthesis and their photochemical reactions are similar to those of superior plants (Bryant, 1987). They have three types of antenna systems: chlorophyll antenna system associated with photosystems PS I and PS II of the thylakoid membrane and an external antenna complex comprised of phycobilisomes that are attached to PS II and PS I (Gant, 1975; 1981; Glazer, 1982; 1985; Mondori and Melis, 1986). The components of the phycobilisome are the phycobiliproteins that are responsible for the blue-green pigmentation, that have an absorption spectra of 470-650 nm, while the chlorophyll complex can absorb the light at 430-440 and 670-680 nm. This separation of the absorption bands allows analysis of the relative contribution of phycobiliproteins and chlorophyll a to the action spectrum of PS I and PS II (Wang *et al.,* 1977; Butler, 1978; Diner, 1979).

The main environmental factors affecting the photosynthesis in cyanobacteria are: temperature, light intensity, UV light, drought and salinity, temperature being the major factor that controls this process. By decreasing the temperature the photosynthetic electron transport and carbon fixation is limited and this can induce a reduction in the ability to convert light. The accumulation of light energy leads to the damage of the photosystem PS II and photoinhibition, making it the most thermolabile aspect of the photosynthetic complex (Davison, 1991; Zak and Pakrasi, 2000). Stoichiometry of the photosynthetic apparatus and phycobilisomes is regulated by both light and temperature (enzyme phosphorylation, electron transport and plastoquinone diffusion), although the initial photochemical reactions are independent of temperature (Davison, 1991; Miskiewicz *et al.,* 2002; Murakami, 1997). Photosynthetic acclimatization to low temperatures mimics the mechanism of acclimatization to high light (Campbell *et al.,* 1995).

Cyanobacteria rely on their ability to sense the action of these external factors and to use their ability to adjust morphologically, physiologically and molecularly which give rise to acclimatization to environmental changes (Huner *et al.,* 1996; 1998). Photosynthetic acclimatization is not due to temperature rise or irradiation, but rather is due to the interaction of these factors (Köhler *et al.,* 2005; Miskiewicz *et al.,* 2000; Nicklisch *et al.,* 2008; Wieland and Kühl, 2000). The direct effects of temperature act synergistically with other environmental factors (Robarts and Zohary, 1987; Bhogavalli *et al.,* 2012).

Several studies show that cyanobacteria have a large spectrum of adaptive strategies (Tang and Vincent, 1999): 1. – tend to have a low photosynthetic capacity at decreased temperatures due to depressed Rubisco activity. 2 – decreased number of chlorophylls and pigments in the light-harvesting complex. Low temperatures can lead to a decrease in the chlorophyll levels (Young, 1993), although carotenoid levels can remain intact because of the photoinhibition (Falk *et al.,* 1990; Davison, 1991; Krause, 1993). Carotenoids can act as a protective screen which blocks the harmful effect of high light at these lowered temperatures (Krause, 1993).

The process of light absorption in cyanobacteria takes place in phycobilisomes and photosystems PS I and PS II (Glazer, 1989; Bryant, 1995; van Thor *et al.,* 1998). The light-harvesting antenna of cyanobacteria does not contain chlorophyll. Phycobilisomes have a central core, mainly composed of the phycobiliproteins: phycoerythrin, phycocyanin and allophycocyanin (Fig. 1). These are polypeptides which contain phycocyanobilin in the form of trimer or hexamer complex. The complex can be bound to the membrane surface of thylakoids (Arteni *et al.,* 2009).

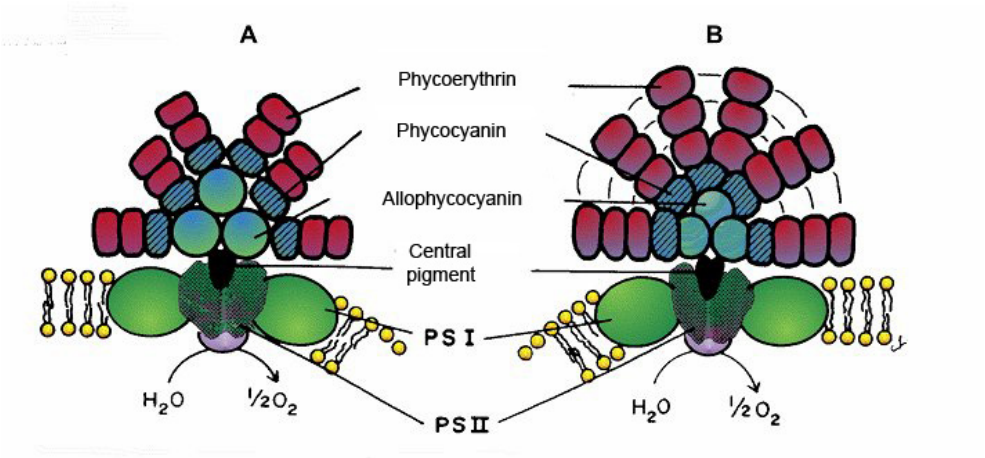

Figure 1. Structural model of a hemidiscoidal phycobilisome (A) and a hemispherical phycobilisome (B) (Gantt, 1986)

Resonance energy transfer from phycocyanin to allophycocyanin is a Förster type energy transfer that has a rate of 45-120 ps. Other investigations targeted the phycobilisome of PS II or PS I (Harnischfeger and Codd, 1978; Mimuro and Fujita, 1978; Kawamura *et al.,* 1979; Redlinger and Gantt, 1982; Ley, 1984), and by measurements of static electricity they concluded values of μs (Holzwarth *et al.,* 1990; van Thor *et al.,* 1998). The central core pigments have a very efficient resonance energy transfer chain with a yield of over 95% (Glazer, 1989). Phycobilins that form the phycobilisomes have a high fluorescence.

The basic aspects of photosynthetic light-harvesting and electron transport can be measured in a fast and non-invasive way by analyzing the chlorophyll fluorescence. The photosynthetic system of cyanobacteria is a link between metabolic processes (iron, nitrogen and carbon fixation), therefore chlorophyll fluorescence signals can provide fast and real-time information about photosynthesis and all phases of acclimatization.

Fluorescence analyses depend on the moment when a pigment absorbs a photon of energy and enters a state of electronic excitation, this is followed by: - photochemical reactions that take place in specific chlorophyll molecules of the photosynthetic reaction centers, the excited electron of the pigment molecule enters the electron transport chain; - heat dissipation that brings bag excited electrons to their initial state by giving off heat; - excited energy transfer to surrounding pigment molecules occurs in the light-harvesting antenna system; - fluorescent emission at a wavelength similar to the photon absorbs initially. These are competing processes, and changes in the fluorescence emission reflect in a corresponding way changes in the competing deexcitation pathways. For every kind of pigment, fluorescence emission levels rely upon concentration of the pigment, intensity of excitation light and production of fluorescence or fluorescence emission efficiency (Campbell *et al.,* 1998). Chlorophyll associated with PS II has a different fluorescence emission from that associated with PS I (Pfündel, 1998). The amount of chlorophyll combined with photosystems depends on the species, and its variability is induced by stress (Riethman and Sherman, 1988; Straus, 1994; Falkowski and Raven, 1997; Boekema *et al.,* 2001).

After illumination, chlorophyll molecules in PS II get in an excited singlet state (Chl a*). The energy resulted from the excited state is transferred to the reaction center for its further utilization in photochemical charge separation and conversion to chemical energy necessary in photosynthesis (photochemical) or can be dissipated as heat (non-photochemical diminution) either it can be reemitted as fluorescence. The sum of these energies is equivalent with the absorbed light energy. These three processes compete with each other, thus fluorescence will be higher when less energy is used in photochemical reactions or this energy is emitted in the form of heat. By measuring the amount of chlorophyll fluorescence, the efficiency of photochemical processes and of non-photochemical quenching can be determined (Krause and Weis, 1991). The wavelength of emitted fluorescence is higher than the wavelength of the absorbed light.

In the dark, all of the reaction centers are open, and the photochemical processes are maximized, while fluorescence emission is very low (F0, fluorescence in the absence of photosynthetic light) (Fig. 2). Illumination with strong light leads to charge separation in the reaction centers, while electrons move toward the first electron acceptor, QA. When QA is reduced, reaction centers are in a closed state, and photochemical processes are in a transitional blocked state. Reaction centers are closed because they are incapable of further electron accepting. Closing of the reaction centers result in a reduced efficiency of photochemical processes and increased fluorescence (van Kooten and Snel, 1990).

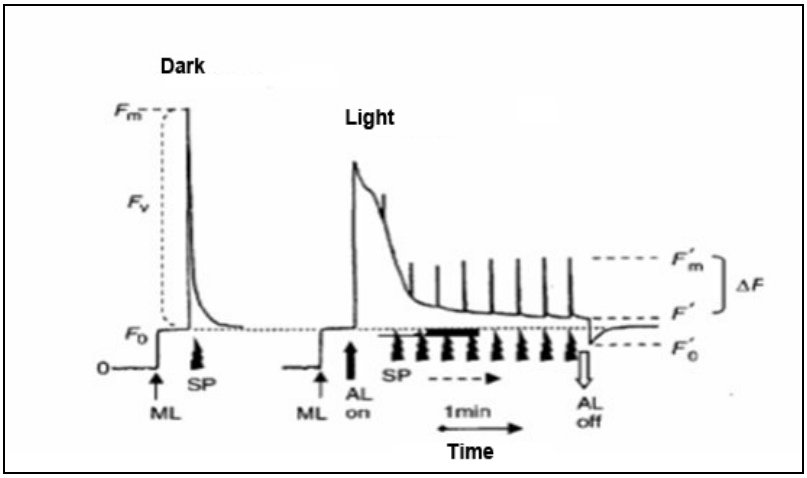

Figure 2. Model of pulse saturation method (adapted from Schreiber, 1986). Minimal and maximal fluorescence, F0 and Fm, measured on samples adapted to dark using modulated measuring light ML and saturation pulse of light SP. If actinic light AC and a series of saturation pluses is used for illumination F´ and F´m can be reached. When illumination is stopped F´0 can be obtained

Because photochemical production is minimal, fluorescence dissipation and production are proportional, and fluorescence production of the closed centers is noted Fm. As fluorescence production becomes proportional with the closed level of PS II, opening of the reaction centers act as fluorescence reducers (quencher), process noted with qP (photochemical reduction) (Genty *et al.,* 1989). qP values between 0-1 indicate the level of QA oxidation.

The difference between Fm (all QA reduced) and F0 (all QA oxidized) is called variable fluorescence Fv. Ratio between Fv/Fm is 0,65-0,80 for the samples adapted to dark and shows the photochemical production in PS II. Productions can vary with irradiation and physiological treatment. When the photosynthetic system is exposed to light the decrease of maximal fluorescence occurs and F´m is obtained. This phenomenon is called non-photochemical quenching NPQ, resulting in energy dissipation as heat. This non-photochemical diminution is the opposite of photochemical reactions and it is considered to be a protection valve against damages caused by excess irradiation.

In cyanobacteria, PS I and phycobilisomes significantly contributes to the fluorescence affecting the Fv/Fm parameter. Phycobiliproteins contribute to fluorescence to by overlapping the emission of chlorophylls influencing F0 (Campbell *et al*., 1998; Cruz *et al.,* 2005).

There is an inverse correlation between photochemistry and fluorescence emission. Photochemistry and fluorescent photochemical quenching (qP) are maximized when the reaction centers and PS II are open, while fluorescence is weak.

When all reaction centers are closed, qP decreases, and also fluorescence reaches a maximum level. Fluorescence is regulated by the oxidized state of the primary acceptor QA. When QA is oxidized, minimum level of fluorescence is achieved, while fluorescence reaches maximum level when QA is fully reduced (Bissati *et al.,* 2000).

In this study we present the effects of microaerobiosis achieved with argon bubbling, on photochemical activity of photosynthesis in the cyanobacterium *Synechococcus* sp. PCC 7002.

Materials and methods

The wild type *Synechococcus* sp. strain PCC 7002 is maintained in the Collection of Cyanobacteria and Algae of the Institute of Biological Research in Cluj-Napoca, Romania. For this experiment, the cells were photoautotrophically grown in flasks with A^+ medium (Stevens *et al.,* 1973). Light was provided by cool-white fluorescent lamps (250 μmol m^{-2} s^{-1}), while the standard growth temperature was 38°C, this value being maintained with a water bath within ±1°C. The density of the photon flux was measured using a QSPAR Quantum Sensor (Hansatech Instruments Ltd, Norfolk, United Kingdom) light meter while cell growth was monitored by the optical density at 550 nm (OD_{550}) with a model Shimadzu UV-1700 spectrophotometer (Shimadzu Corporation, Kyoto, Japan).

Cells were grown for 5 days, until they reached exponential growth phase, and then they were bubbled with argon in otherwise standard conditions for 120 minutes.

For monitoring PS I and PS II activity, chlorophyll fluorescence was measured with a Waltz Dual–100 analyzer. Identification of assimilation pigments was based on the maximum absorption peaks measured with a Jasco V-630 spectrophotometer, and their concentration was determined according to Arnon (1949), Lichtenthaler and Wellburn (1983).

Results and discussion

The *Synechococcus* sp. PCC 7002 culture had an optical density of OD_{680} = 1.166, given the density of biomass whose pigment components absorb light at 680 nm. *In vivo* absorption of cellular suspension revealed spectral regions of absorption of photosynthetic apparatus components and main absorption peaks (Fig. 3). Carotenoids absorb light in the blue range of spectrum (490 nm), chlorophyll a at 439 nm and in the red range of spectrum at 680 nm. The absorption spectrum of phycobilins is at 631 nm. Summation of phycobiliproteins and chlorophyll a gives rise to the ability of cyanobacteria to efficiently capture light (Mur *et al.,* 1999). *In vitro* measurements of absorption showed a dominancy in chlorophyll a (432, 664 nm) and the presence of carotenoids (481 nm) (Fig. 3 B).

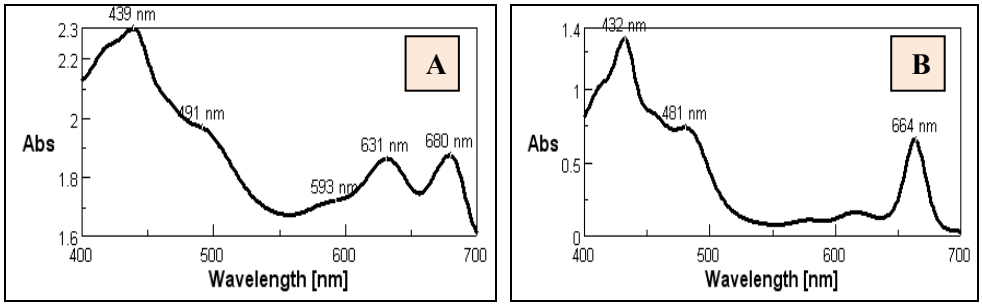

Figure 3. The *in vivo* absorption spectrum (A), and pigment extract spectrum (B) in *Synechococcus* sp. PCC 7002 grown under standard conditions

Assimilatory pigment contents were identified in *Synechococcus* sp. PCC 7002 and they are presented in Table 1. The photosynthetic apparatus in cyanobacteria include chlorophyll *a* (665 nm), which together with different types of carotenoids and phycobiliproteins form the light-harvesting unit. Pigment concentration was determined at the initial control state, before the application of stress treatment.

Composition specificity in assimilation pigments and their concentration is affected by the physiological development of cyanobacteria. Carotenoids can influence the photosynthetic membrane stability having a role in regulation of photosynthetic membrane dynamics (Szalontai *et al.,* 2012).

Table 1.

Assimilating pigments measured in the control sample (mg/l)

	Amount [mg/l]	λ_{nm}
Chlorophyll a	5,714	665
Carotene	0,606	451
Zeaxanthin (+ Cryptoxanthin)	0,451	452
Total carotenoids	1,057	
a/c	5,40	

Evolution of chlorophyll fluorescence parameters in *Synechococcus* sp. PCC 7002 under the effects of argon treatment are presented in Fig. 4. Minimal fluorescence yield F_0, decreased up to 94% after 120 minutes of exposure to argon. Basal fluorescence yield show that the primary acceptor Q_A is in oxidized form, and RC II reaction center are opened, this is a state when photochemical process and use of the excitation energy are maximized, also all redox components of PS II are oxidized. F_0 is the fluorescence emitted by chlorophyll molecules from the antenna before excitation is transferred to the reaction center.

By applying a saturation pulse, fluorescence rises from baseline to maximum value Fm, the primary electron acceptor of PS II becomes fully reduced, also photochemistry is blocked and reaction centers are closed. Maximum fluorescence Fm decreased after 15 minutes of exposure to argon bubbling. Decline of F_m attests the increasing number of closed reaction centers, as well as plastoquinone reduction and growth of fluorescence emission. Variable fluorescence, expressing the difference between Fm and F_0, showed positive values compared to the control, except after 60 minutes of argon treatment. F_0 and Fm are emitted by the chlorophyll molecules from the antenna (Krause and Weis, 1991). All reductions noted for opening and closing of the reaction centers of PS II exhibits a functional imbalance. Decreased Fm yielded low values for variable fluorescence Fv against the control.

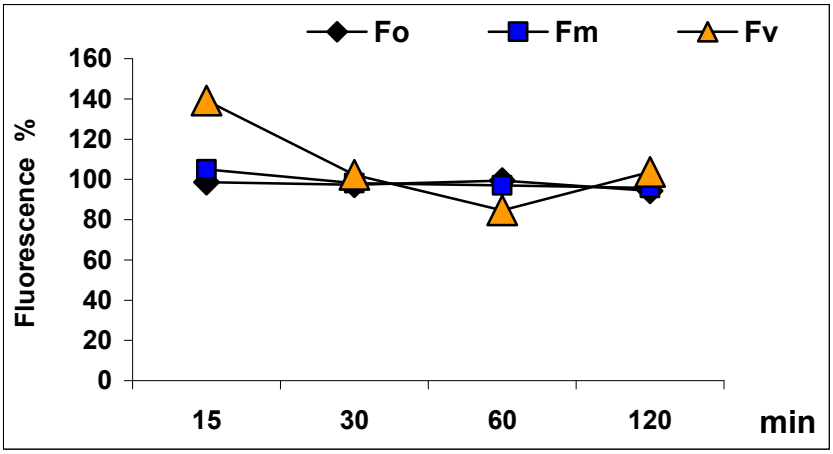

Figure 4. Evolution of chlorophyll fluorescence parameters in *Synechococcus* sp. PCC 7002 under microoxic conditions

Maximal quantum yield (Fv/Fm) of PS II photosynthesis weakly stimulated by the argon treatment, except at 60 minutes of argon effect when negative values were observed compared with the control. Fv/Fm allows the determination of maximum quantum yield (efficiency) of PS II photochemistry, or of the photosynthetic electron transport. Final value recorded was 0.167 that represent 20% of the theoretical value, respectively the proportion of photoinhibited reaction centers. Fv/Fm has a theoretical value of 0.82 and indicates the maximum fraction of photons absorbed and used in photochemical reactions. Values below 0.82 indicate the amount of photoinhibited PS II reaction centers. Maximum production of fluorescence when all the centers are closed represents only 3% of the light absorbed. When the centers are open, fluorescence represents 0,6% (Krause and Weis, 1991).

Effective quantum yield (YII) decreased after 15 minutes of argon treatment (Fig. 5). Y (II) corresponds to the fraction of photochemical converted energy.

Quantum yield of non-regulated energy dissipation Y (NO) dropped, reaching 94% after 15 minutes of stress condition, compared to the control. Theoretically, the quantum yield of non-regulated energy dissipation summarizes the energy dissipation processes that occur in antennas of the photosystems. Because of the decrease in fluorescence emission due to photoinhibition, non-regulated energy dissipation is slightly lower.

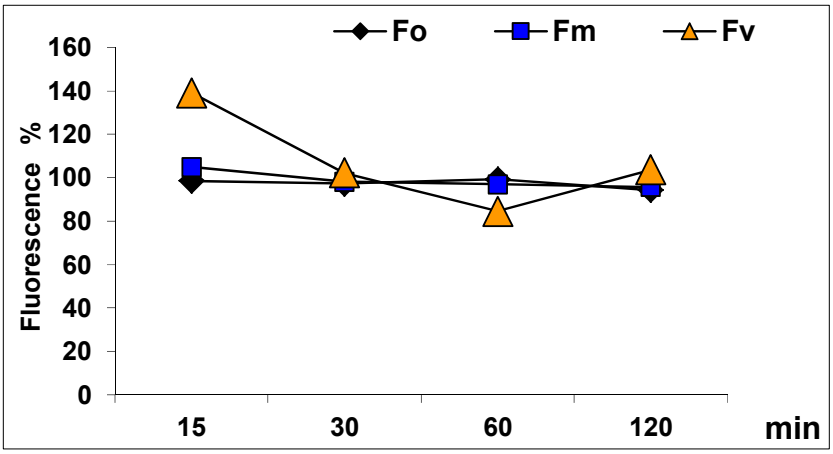

Figure 5. Evolution of quantum yields in PS II in *Synechococcus* sp. PCC 7002 under microoxic conditions

Coefficient of photochemical quenching, qP and qL, were maintained at higher values, except when 30 minute exposure to argon treatment (Fig. 6). qP is a measure of the overall „openness", and the high values observed proves the high open state of the RC II reaction centers, respectively the heavily oxidized state of the primary acceptor Q_A. He coefficient of photochemical quenching qL, is a measure of the fraction of open PS II reaction centers, high values observed in our cyanobacterial suspensions indicate the high amount of opened PS II reaction centers. qP allows the estimation of the oxidized quinone acceptor fraction of opened PS II or PS I reaction centers (Grace and Logan, 1996). High values of qP and qL express an intense photochemical process with decreased fluorescent emission. The fluorescent coefficient of photochemical quenching can be used for estimations of opened PS II reaction centers (oxidized state of Q_A) or closed PS II reaction centers (reduces state of Q_A) (Huner *et al.,* 1998).

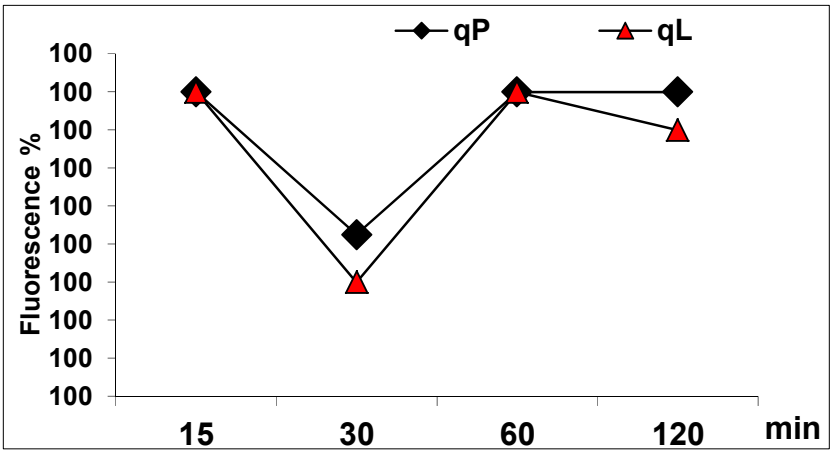

Figure 6. Evolution of photochemical coefficient in *Synechococcus* sp. PCC 7002 under microoxic conditions

Changes in fluorescence yield reflect direct changes in photochemical competing de-excitation paths, in excitation transfer and heat dissipation. When PS II reaction centers are opened and photochemical potential is maximal, fluorescent photochemical quenching is also very high while fluorescence yield is decreased. When reaction centers are closed no photochemical processes are active, photochemical quenching is absent and fluorescence yield is maximal. qP indicates the balance between excitation of PS II centers that are thereby closed, and removing of electrons from PS II by photosynthetic electron transport chain which reopens the centers. This balance in excitation pressure responds to light intensity, temperature and the availability of final acceptors.

The loss of photoinhibition was correlated with the redox state of the primary acceptor Q_A. Relative redox state of Q_A *in vivo* can be estimated by 1-qP parameters (excitation pressure) and Fv/Fm (quantum yield) (Öquist *et al.,* 1993). As in cyanobacteria phycobilisomes provide the greatest capacity to capture light, production of photosynthesis rely on the energy transfer efficiency (Foguel *et al.,* 1992).

In PS I, the Pm signal, as well as Fm, represents the maximal change in P_{700} reaction center, equivalent with differences between oxidized and reduces P_{700}. Total reduction can be achieved only in dark, while total oxidation is obtained after brief illumination, when PS I is limited. Increasing in Pm signal depends on the total chlorophyll content of P_{700} reaction center, and decrease is due to limitation in P_{700} reaction center acceptors. P_{700} values varies between 0 (totally oxidized P_{700} centers) and 1 (totally reduced P_{700} centers, in standard dark state).

By exposure to argon Pm signal was stimulated in the first 30 minutes, followed by a significant decrease towards the end of the stress treatment suggesting a decrease in the reduction state of P_{700} reaction center compared to oxidized state (Fig.7). Maximum oxidation can be reached at illumination with intense light, before the electrons leave PS II to re-reduce P_{700}.

Effective PS I photochemical quantum yield Y(I) dropped significantly in the first 30 minute compared to the control. The decrease in quantum yield Y(I) reveals decreased reduction state due to the lack of limitation by the acceptor, respectively, decrease in photochemical energy conversion in PS I. Y(I) expresses the quantum yield of photochemical energy conversion in PS I and it is complementary to the non-photochemical quantum yield of energy conversion. The non-photochemical quantum yield of PS I, Y(ND) increased compared to the control. Y(ND) defines the quantum yield non-photochemical energy conversion in PS I due to limitation of electron donors, and represents the fraction of overall P_{700} oxidized in a given state ($P_{700}^{+}{}_{A}$). Oxidized P_{700} reaction centers transform the quantitatively absorbed excitation energy in heat. Limitation due to donors is increased by the trans-thylakoid proton gradient (photosynthetic control of the cytochrome complex b_6f as well as the down regulation of PS I) and damages caused in PS II.

PS I contribution to the fluorescence is low: 5% at 720 nm and 1-2% at 685 nm. Closed PS I centers do not contribute to Fv. This can be explained by the relative stability of P_{700} in oxidized state.

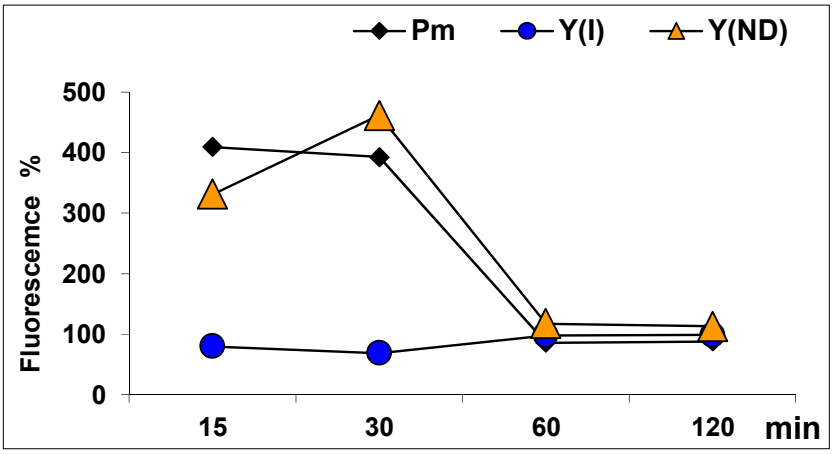

Figure 7. Photochemical activity of photosystem PS I under microoxic conditions in *Synechococcus* sp. PCC 7002

To induce photosynthetic activity pulse amplitude modulation technique (PAM measurements) was used (Schreiber, 2004). Fluorescence transition follows the O-J-I-P sequence, a polyphasic curve of the initial fluorescence F_0 and maximum fluorescence F_m, these can be visualized on a logarithmic scale (Schreiber and Neubauer 1987; Strasser *et al*., 1997; Srivastava *et al.,* 1999). The intermediate J-I level seems to relate to the heterogeneity of plastoquinone volume and refers to the thermal phase of the photosynthetic process. P is reached when all plastoquinone molecules are reduced to PQH_2. Additional DCMU result in curve of O-J. This curve is similar to the kinetics of $O\text{-}I_1 – I_2 – P$ obtained by Neubauer and Schreiber (1987).

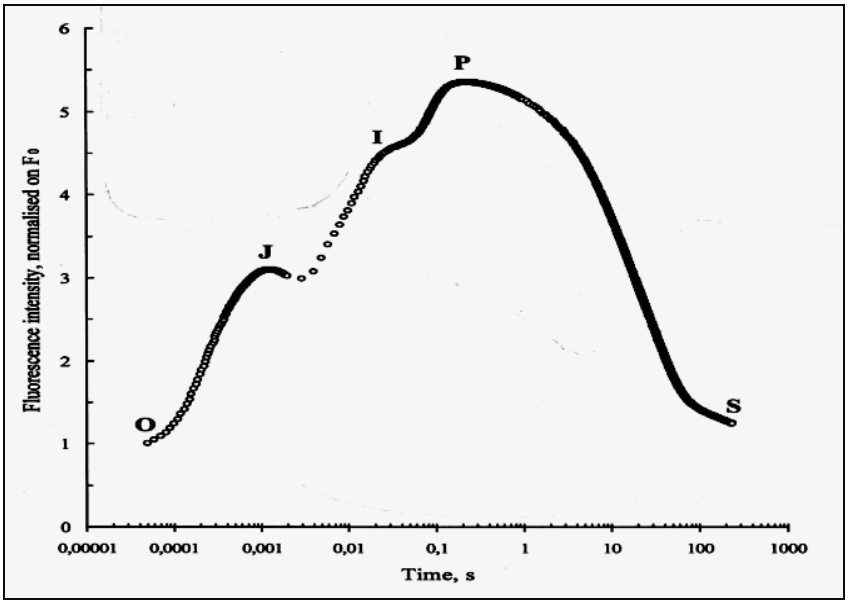

Figure 8. Transition of chlorophyll fluorescence in samples adapted to microoxic conditions and excited with red light of 650 nm (Strasser *et al.,* 1995)

The kinetics of the chlorophyll fluorescence induction by pulse saturation in control and at the end of stress treatment are presented for PS II and PS I in Fig. 9. Fluorescence yield is related to the photochemical activity of PS II. The kinetics of fluorescence variation from F_0 to maximum Fm displays the accumulation of reduced Q_A in reaction centers. Fluorescence kinetics showed on the logarithmic scale revealed important modifications in I – P spectrum due to reduction of the plastoquinone nuclei (Fig. 9, A, C, E, G, I). Changes in the induction curve are shown in Fig. 9, B, D, F, H, J. The length of fluorescence and its amplitude is proportional to the number of antenna molecules (Krause and Weis, 1991).

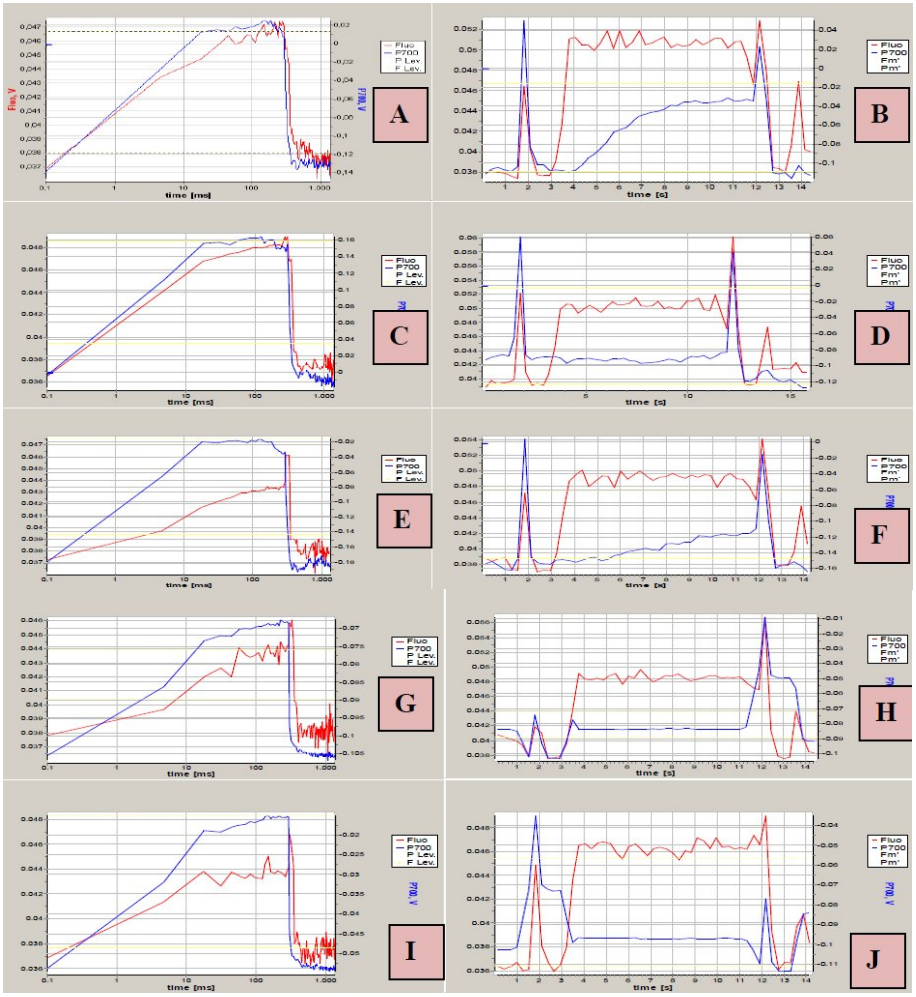

Figure 9. Chlorophyll fluorescence in standard conditions and under microaerobiosis using the saturation-pulse method: A – logarithmic kinetics of the fluorescence in the control; B – fluorescence induction curve in control; C – fluorescence logarithmic kinetics of the sample after 15 minutes of microaerobiosis; D – fluorescence induction curve of the sample after 15 minutes of microaerobiosis; E - fluorescence logarithmic kinetics of the sample after 30 minutes of microaerobiosis; F - fluorescence induction curve of the sample after 30 minutes of microaerobiosis; G - fluorescence logarithmic kinetics of the sample after 60 minutes of microaerobiosis; H - fluorescence induction curve of the sample after 60 minutes of microaerobiosis; I - fluorescence logarithmic kinetics of the sample after 120 minutes of microaerobiosis; J - fluorescence induction curve of the sample after 120 minutes of microaerobiosis. Red – PS II fluorescence; Blue – PS I fluorescence

Conclusions

The cyanobacterium *Synechococcus* sp. PCC 7002 displays a specific composition and concentration of assimilatory pigments, according to the physiological condition of the cells.

For PS II under argon treatment, minimal fluorescence F_0 and maximal fluorescence F_m decreased. Fluorescence yield shows that the primary acceptor Q_A is in oxidized state, and RC II reaction centers are opened, photochemical processes and excitation energy harvesting are maximal, and all redox component of PS II are reduced. Maximum fluorescence shows that primary electron acceptor (Q_A) of PS II becomes totally reduced, photochemical reactions are blocked and reaction centers are closed. Decrease of Fm parameter represents an increase in closed reaction centers, respectively activation of plastoquinone reduction processes and increase of fluorescence emission.

Variable fluorescence, expresses the difference between Fm and F_0, showed positive values compared to the control, except after 60 minutes of argon treatment. All decrease in opening and closing of PS II reaction centers exhibit a functional imbalance.

Maximal quantum yield (Fv/Fm) of PS II photosynthesis weakly stimulated by the argon treatment, except at 60 minutes of argon effect when negative values were observed compared with the control. Fv/Fm allows the determination of maximum quantum yield (efficiency) of PS II photochemistry, or of the photosynthetic electron transport. Final value recorded was 0,167 that represent 20% of the theoretical value, respectively the proportion of photoinhibited reaction centers. Fv/Fm has a theoretical value of 0.82 and indicates the maximum fraction of photons absorbed and used in photochemical reactions. Values below 0.82 indicate the amount of photoinhibited PS II reaction centers. Effective quantum yield (YII) decreased after 15 minutes of argon treatment. Y(II) corresponds to the fraction of photochemical converted energy. Quantum yield of non-regulated energy dissipation Y(NO) dropped, reaching 94% after 15 minutes of stress condition, compared to the control. Theoretically, the quantum yield of non-regulated energy dissipation summarizes the energy dissipation processes that occurs in antennas of the photosystems. Because of the decrease in fluorescence emission due to photoinhibition, non-regulated energy dissipation is slightly lower.

Coefficient of photochemical quenching, qP and qL, were maintained at higher values, except when 30 minute exposure to argon treatment. qP is a measure of the overall „openness", and the high values observed proves the high open state of the RC II reaction centers, respectively the heavily oxidized state of the primary acceptor Q_A. He coefficient of photochemical quenching qL, is a measure of the fraction of open PS II reaction centers, high values measured in our cyanobacterial suspensions indicate the high amount of opened PS II reaction centers. High values of qP and qL express an intense photochemical process with decreased fluorescent emission.

For PS I, by exposure to argon Pm signal was stimulated in the first 30 minutes, followed by a significant decrease towards the end of the stress treatment suggesting a decrease in the reduction state of P_{700} reaction center compared to oxidized state . Maximum oxidation can be reached at illumination with intense light, before the electrons leave PS II to re-reduce $P_{700.}$

Effective PS I photochemical quantum yield, Y(I) dropped significantly in the first 30 minute compared to the control. The decrease in quantum yield Y(I) reveals decreased reduction state due to the lack of limitation by the acceptor, respectively, decrease in photochemical energy conversion in PS I. Y(I) expresses the quantum yield of photochemical energy conversion in PS I and it is complementary to the non-photochemical quantum yield of energy conversion. The non-photochemical quantum yield of PS I, Y(ND) increased compared to the control. Y(ND) defines the quantum yield non-photochemical energy conversion in PS I due to limitation of electron donors, and represents the fraction of overall P_{700} oxidized in a given state ($P_{700}^{+}{}_{A}$). Oxidized P_{700} reaction centers transform the quantitatively absorbed excitation energy in heat. Limitation due to donors is increased by the trans-thylakoid proton gradient (photosynthetic control of the cytochrome complex b_6f as well as the down regulation of PS I) and damages caused in PS II.

Alternation of oxidative/reduced state of the plastoquinone nuclei was revealed in the kinetics of the chlorophyll fluorescence induction by pulse saturation in control. Fluorescence yield is related to the photochemical activity of PS II. The kinetics of fluorescence variation from F_0 to maximum Fm monitors the accumulation of reduced Q_A in reaction centers. Fluorescence kinetics showed on the logarithmic scale revealed important modifications in I – P spectrum due to reduction of the plastoquinone nuclei. The length of fluorescence and its amplitude is proportional to the number of antenna molecules.

Acknowledgements. Funding for this research was provided by the Romanian Ministry of National Education, project PN 09-360201.

REFERENCES

Arnon, D. (1949) Copper enzymes in isolated chloroplasts. Polyphenoloxidase in *Beta vulgaris*, *Plant Physiol*., **24**, 1-15

Arteni, A.A., Ajlani, G., Boekema, E.J. (2009) Structural organisation of phycobilisomes from *Synechocystis* sp. strain PCC6803 and their interaction with the membrane, *Biochim. Biophys. Acta,* **1787**, 272-279

Bissati, K.E., Delphin, E., Murata, N., Etienne, A.L., Kirilovsky, D. (2000) Photosystem II fluorescence quenching in the cyanobacterium *Synechocystis* PCC 6803: involvement of two different mechanisms, *Biochim. Biophys. Acta,* **1457**, 229-242

Bhogavalli, P.K., Murthy, S.D.S, Prabhakar, T. (2012) Combination stress mediated alterations in the photosynthetic electron transport activities of Cyanobacterium *Spirulina platensi, Euro. J. Exp. Bio.,* **2,** 374-377

Boekema, E.J., Hifney, A., Yakushevska, A.E., Piotrowski, M., Keegstra, W., Berry, S., Michel, K.P., Pistorius, E.K., Kruip, J. (2001) A giant chlorophyll-protein complex induced by iron defciency in cyanobacteria, *Nature*, **412**, 745-748

Bryant, D.A. (1995) *The molecular biology of cyanobacteria*, Kluwer Academic Publisher, Dordrecht

Bryant, D.A. (1987) The cyanobacterial photosynthetic apparatus: comparison to those of higher plants and photosynthetic bacteria, In: *Photosynthetic picoplankton*, *Vol. 214*, Platt, T. and Li, W.K.W. (eds), Can. Fish. Aquatic Sci., Ottawa, pp 423-500

Butler, W.L. (1978) Energy distribution in the photochemical apparatus of photosynthesis, *Annu. Rev. Plant Physiol.*, **29**, 345-378

Campbell, D., Hurrz, V., Clarke, A.K., Gustafsson, P., Öquist, G**.** (1998) Chlorophyll fluorescence analysis of cyanobacterial photosynthesis and acclimation, *Microbiol. Mol. Biol. Rev*., **62**, 667-683

Campbell, D., Zhou, G., Gustafsson, P., Öquist, G., Clarke, A.K. (1995) Electron transport regulates exchange of two forms of photosystem II Dl protein in the cyanobacterium *Synechococcu, EMBO J.,* **14**, 5457- 5466

Cruz, J.A., Avenson, T.J., Kanazawa, A., Takizawa, K., Edwards, G.E., Kramer, D.M. (2005) Plasticity in light reactions of photosynthesis for energy production and photoprotection, *J. Exp. Bot.,* **56**, 395-406

Davison, I.R. (1991) Environment effects on algal photosynthesis: temperature, *J. Phycol.*, **27**, 2-8

Diner, B.A. (1979) Energy transfer from the phycobilisome to photosystem II reaction centers in wild type *Cyanidium caldarium*, *Plant Physiol*., **63**, 30-34

Falk, S., Samuelsson, G., Öquist, G. (1990) Temperature-dependent photoinhibition and recovery of photosynthesis in the green alga *Chlamydomonas reinhardtii* acclimated to 12 and 27°C, *Physiol. Plantarum*, **78**, 173-180

Falkowski, P.G, Raven, J.A. (1997) *Aquatic photosynthesis*, Blackwell Scientific, Malden

Foguel, D., Chaloub, R.M., Silva, J.L., Crofts, A.R., Weberll, G. (1992) Pressure and low temperature effects on the fluorescence emission spectra and lifetimes of the photosynthetic components of cyanobacteria, *Biophys. J*., **63**, 1613-1622

Gantt, E. (1986) Phycobilisomes, In: *Photosynthesis III. Encyclopedia of plant physiology. New ser., V,* Staehelin., L.A., Arntzen, C.J. (eds), Springer-Verlag, Berlin, pp. 260-268

Gantt, E. (1981) Phycobilisomes, *Annu. Rev. Plant Physiol.*, **32**, 327-347

Gantt, E. (1975) Phycobilisomes: light harvesting pigment complexes, *Bio-Science,* **25**, 781-787

Genty, B., Briantais, J.M., Baker, N.R. (1989) The relationship between the quantum yield of photosynthetic electron transport and quenching of chlorophyll fluorescence, *Biochim. Biophys. Acta*, **990**, 87-92

Glazer, A.N. (1989) Light guides directional energy transfer in a photosynthetic antenna, *J. Biol. Chem.,* **264**, 1-4

Glazer, A.N. (1985) Light harvesting by phycobilisomes, *Annu. Rev. Biophys. Chem*., **14**, 47-77

Glazer, A.N. (1982) Phycobilisomes: Structure and dynamics, *Annu. Rev. Microbiol.*, **36**, 173-198

Grace, S.C., Logan, B.A. (1996) Acclimation of foliar antioxidant systems to growth irradiance in three broad- leaved evergreen species, *Plant Physiol.*, **112**, 1631-1640

Harnischfeger, G., Codd, G.A**.** (1978) Factors affecting energy transfer from phycobilisomes to thylakoids in *Anacystis nidulans*, *Biochim. Biophys. Acta*, **502**, 507-513

Holzwarth, A.R., Bittersmann, E., Reuter, W., Wehrmeyer, W. (1990) Studies on chromophore coupling in isolated phycobiliproteins. 3. Picosecond excited state kinetics and timeresolved fluorescence spectra of different allophycocyanins from *Mastigocladus laminosus*, *Biophys. J.,* **57**, 133-145

Huner, N.P.A., Gunnar, Ö.G., Sarhan, F. (1998) Energy balance and acclimation to light and cold, *Trends Plant Sci.*, **3**, 224-230

Huner, N.P.A., Maxwell, D.P., Gray, G.R., Savitch, L.V., Krol, M., Ivanov, A.G., Falk, S. (1996) Sensing environmental temperature change through imbalances between energy supply and energy consumption: redox state of photosystem II, *Physiol. Plant.,* **98**, 358-364

Kawamura, M., Mimuro, M., Fujita, Y**.** (1979) Quantitative relationship between 2 reaction centers in the photosynthetic system of blue-green algae, *Plant Cell Physiol.,* **20**, 697-705

Köhler, J., Hilt, S., Adrian, R., Nicklisch, A., Kozerski, H.P., Walz, N. (2005) Long-term response of a shallow, moderately flushed lake to reduced external phosphorus and nitrogen loading, *Freshwater Biol*., **50**, 1639–1650

Krause, G.H. (1993) Photoinhibition induced by low temperatures, In: *Photoinhibition of photosynthesis*, Baker, N. R., Browyer, J. R. (eds), BIOS Scientific, Oxford, pp 331-348

Krause, G.H., Weis, E. (1991) Chlorophyll fluorescence and photosynthesis: the basics, *Annu. Rev. Plant Physiol. Plant Mol. Biol.*, **42**, 313-349

Ley, A.C. (1984) Effective absorption cross sections in *Porphyridium cruentum* – implications for energy transfer between phycobilisomes and photosystem-II reaction centers, *Plant Physiol.,* **74**, 451-454

Lichtenthaler, H.K., Wellburn, A.R. (1983) Determination of total carotenoids and chlorophylls a and b of leaf extracts in different solvents, *Biochem. Soc. Trans.,* **603**, 591-592

Mimuro, M., Fujita, Y. (1978) Excitation energy transfer between pigment system-2 units in blue-green algae, *Biochim. Biophys. Acta*, **504**, 406-412

Miskiewicz, E., Alexander G. Ivanov, A.G., Huner, N.P.A. (2002) Stoichiometry of the photosynthetic apparatus and phycobilisome structure of the cyanobacterium *Plectonema boryanum* UTEX 485 are regulated by both light and temperature, *Plant Physiol.,* **130**, 1414–1425

Miskiewicz, E., Ivanov, A.G., Williams, J.P., Khan, M.U., Falk, S., Huner, N.P.A. (2000) Photosynthetic acclimation of the filamentous cyanobacterium, *Plectonema boryanum* UTEX 485, to temperature and light, *Plant Cell Physiol.,* **41**, 767-775

Mondori, A., Melis, A. (1986) Cyanobacterial acclimation to photosystem I or photosystem II light, *Plant Physiol.,* **82**, 185-189

Mur, L.R., Skulberg, O.M., Utkilen, H. (1999) Cyanobacteria in the environment. Chapt. 2, In: *Toxic Cyanobacteria in Water: A guide to their public health consequences, monitoring and management*, Chorus, I., Bartram, J. (eds.), St Edmundsbury Press, Suffolk

Murakami, A. (1997) Quantitative analysis of 77K fluorescence emission spectra in *Synechocystis* sp. PCC 6714 and *Chlamydomonas reinhardtii* with variable PS I/PS II stoichiometries, *Photosynth. Res.,* **53**, 141–148

Neubauer, C., Schreiber, U. (1987) The polyphasic rise of chlorophyll fluorescence upon onset of strong continuous illumination. I. Saturation characteristics and partial control by the photosystem II acceptor side. *Z, Naturforsch*., **42c**, 1246-1254

Nicklisch, A., Shatwell, T., Köhler, J. (2008) Analysis and modelling of the interactive effects of temperature and light on phytoplankton growth and relevance for the spring bloom. *J. Plankton Res*., **30**, 75–91

Öquist, G., Hurry, V.M., Huner, N.P.A. (1993) The temperature dependence of the redox state of Q_A and susceptibility of photosynthesis to photoinhibition, *Plant Physiol. Biochem.,* **31**, 683-691

Pfündel, E. (1998) Estimating the contribution of photosystem I to total leaf chlorophyll fluorescence, *Photosynth. Res.,* **56**, 185-195

Redlinger, T., Gantt, E. (1982) A Mr 95,000 polypeptide in *Porphyridium cruentum* phycobilisomes and thylakoids - possible function in linkage of phycobilisomes to thylakoids and in energy transfer, *Proc. Natl. Acad. Sci.* USA, **79**, 5542-5546

Riethman, H.C., Sherman, A. (1988) Purification and characterization of an iron stressinduced chlorophyll-protein from the cyanobacterium *Anacystis nidulans* r_2, *Biochim. Biophys, Acta*, **935**, 141-151

Robarts, R.D., Zohary, T. (1987) Temperature effects on photosynthetic capacity, respiration, and growth rates of blocm-forming cyanobacteria, *New Zealand J. Mar. Fres. Res.,* **21**, 391-399

Schreiber, U. (2004) Pulse-amplitude-modulation (PAM) fluorometry and saturation pulse method: an overview, In: *Chlorophyll a Fluorescence: A Signature of Photosynthesis,* Papageorgiou, G. C. (ed.), Springer, Dordrecht, pp 279- 319

Schreiber, U., Endo, T. Mi, H. and Asada, K. (1995) Quenching analysis of chlorophyll fluorescence by the saturation pulse method: particular aspects relating to the study of eukaryotic algae and cyanobacteria, *Plant Cell Physiol*., **36**, 873–882

Schreiber, U., Neubauer, C. (1987) The polyphasic rise of chlorophyll fluorescence upon onset of strong continuous illumination: II. Partial control by the photosystem II donor side and possible ways of interpretation, *Zeitschrift Naturforschung* **42**, 1255–1264

Schreiber, U., Schliwa, U., Bilger, W. (1986) Continuous recording of photochemical and non-photochemical chlorophyll fluorescence quenching with a new type of modulation fluorometer, *Photosynth. Res.,* **10**, 51-62

Srivastava, A.M., Strasser, R.J., Govindjee (1999) Greening of pea leaves: parallel measurement of 77K emission spectra, OJIP chlorophyll a fluorescence transient, period four oscillation of the initial fluorescence level, delayed light emission, and P700, *Photosynthetica*, **37**, 365–392

Strasser, B.J. (1997) Donor capacity of the photosystem II probed by chlorophyll fluorescence transients, *Photosynth. Res.* **52**, 147–155

Straus, N. (1994) Iron deprivation: Physiology and gene regulation, In: *The molecular biology of cyanobacteria,* Bryant, D.A., Kluwer Academic Press, Dordrecht, pp 731-750

Szalontai, B., Domonkos, I., Gombos, Z. (2012) The role of membrane structure in acclimation to low-temperature stress, In: *Photosynthesis: Plastid Biology, Energy Conversion and Carbon Assimilation*, Eaton-Rye, J.J., Tripathy, B.C., Sharkey, T.D. (eds.), Springer Science and Business Media B.V., Van Godewijckstraat, pp 233–250

Tang, E.P.Y., Vincent, W.F. (1999) Strategies of thermal adaptation by high latitude cyanobacteria, *New Phytol*., **142**, 315-323

Van Kooten, O., Snel, J.F.H. **(**1990) The use of chlorophyll fluorescence nomenclature in plant stress physiology, *Photosynth. Res.,* **25**, 147-150

Van Thor, J.J., Mullineaux, C.W., Matthijs, H.C.P., Hellingwerf, K.J. (1998) Light harvesting and state transitions in cyanobacteria, *Bot. Acta*, **111**, 430-443

Wang, R.T., Stevens, C.R.L., Meyers, J. (1977) Action spectra for photoreaction I and II of photosynthesis in the blue-green algae *Anacystis nidulans*, *Photochem. Photobiol*., **25**, 103-108

Wieland, A., Kühl, M. (2000) Irradiance and temperature regulation of oxygenic photosynthesis and O_2 consumption in a hypersaline cyanobacterial mat (Solar lake, Egypt), *Mar. Biol.,* **137**, 71-85

Young, A.J. (1993) Factors that affect the carotenoid composition of higher plants and algae, In: Carotenoids in photosynthesis, Young, A.J., Britton, G. (eds.), Chapman and Hall, London, pp 160-205

Zak, E., Pakrasi, H.B. (2000) The BtpA protein stabilizes the reaction center proteins of photosystem I in the cyanobacterium *Synechocystis* sp. PCC 6803 at low temperature, *Plant Physiol.,* **123**, 215–222

*** (2006) *Dual-PAM-100 measuring system for simultaneous assessment of P_{700} and chlorophyll fluorescence*, Heinz Walz GmbH, Germany

STUDIA UNIVERSITATIS BABEŞ-BOLYAI BIOLOGIA, LIX, 1, 2014 (p. 41-53)

RAPID ASSESSMENT OF CARBON SUBSTRATE UTILIZATION IN THE EPILIMNION OF MEROMICTIC URSU LAKE (SOVATA, ROMANIA) BY THE BIOLOG ECO PLATE™ APPROACH

ADORJÁN CRISTEA[1], ADRIAN-ŞTEFAN ANDREI[2], ANDREEA BARICZ[1,3], VASILE MUNTEAN[1] and HORIA L. BANCIU[1,2,✉]

SUMMARY. Ursu Lake is a large saline, meromictic and heliothermal lake located in the eastern part of the Transylvanian Basin (Sovata, Mureş County, Romania). The investigated lake is characterized by a strong vertical stratification of physical and chemical parameters that indicate a corresponding stratification of biodiversity. Using BIOLOG Ecoplate™ method we were able to describe the community-level physiological profile of the microbial population inhabiting the moderately saline epilimnion (5-6% salinity) of Ursu Lake. The metabolization of 31 different carbon sources was monitored in the water samples collected at 0.5 m depth from two different seasons: October 2013 and March 2014. Physico-chemical parameters (temperature, salinity, pH, oxidation-reduction potential, and dissolved oxygen) were measured along with the estimation of the total chlorophylls, carotenoids, and prokaryotic cell count. The results revealed a higher rate of C substrate consumption in the water sample collected in spring compared to that found in the autumn sample. This finding is paralleled by the differences observed in some of the chemical parameters (salinity, dissolved oxygen) between the seasons suggesting a time-based modification of the microbial activity. Alpha-cyclodextrin, glycogen, D-cellobiose, D-mannitol, and N-acetyl-D-glucosamine were the fastest metabolized C sources in both seasons. This is the first report of using BIOLOG Ecoplate™ approach in profiling the microbial activity in a Romanian deep, meromictic and heliothermal salt lake and one of the very few attempts reported to use the BIOLOG system for the characterization of microbial communities in hypersaline ecosystems.

Keywords: BIOLOG Ecoplate™, biopolymer degradation, community-level physiological profile, meromictic lake, microbial activity.

[1] *Department of Molecular Biology and Biotechnology, Faculty of Biology and Geology, Babeş-Bolyai University, 5-7 Clinicilor Str., 400006 Cluj-Napoca, Romania.*

[2] *Institute for Interdisciplinary Research in Bio-Nano-Sciences, Babeş-Bolyai University, 400271 Cluj-Napoca, Romania.*

[3] *National Institute of Research and Development for Biological Sciences (NIRDBS), Institute of Biological Research, 48 Republicii Street, 400015 Cluj-Napoca, Romania.*

✉ ***Corresponding author: Horia L. Banciu***, *Department of Molecular Biology and Biotechnology, Faculty of Biology and Geology, Babeş-Bolyai University, 5-7 Clinicilor Str., 400006 Cluj-Napoca, Romania. E-mail: Horia.Banciu@ubbcluj.ro*

Introduction

Saline and hypersaline lakes are natural (karstosaline) or man-made (anthroposaline) environments that provide living place for halotolerant and halophilic organisms. These ecosystems are characterized by salt concentration exceeding that of the sea water (i.e., salinity > 30 $g \cdot L^{-1}$ or 3 %) and sometimes reaching the saturation point (i.e., salinity > 300 $g \cdot L^{-1}$) (Oren, 2002). The majority of organisms flourishing in these conditions are prokaryotes belonging to *Bacteria* (Ventosa *et al*., 1998) and *Archaea* (Andrei *et al*., 2012), and only a few are representatives of fungi, protozoa, and algae (Oren, 2002; 2008).

The Romanian territory comprises a significant number of anthroposaline and karstosaline salt lakes dispersed between two distinct geographic areas: the Transylvanian Basin (Central and north-western) and the Dacic Basin (Southern, SE and eastern Romania) (Alexe, 2010; Bulgăreanu, 1996). More than 40 saline and hypersaline lakes are found in the Transylvanian Basin, with locations following a circular line of the inner Carpathians belt. Among these bodies of water, several lakes (e.g. Ocnei and Rotund Lakes in Turda, Fără Fund and Brâncoveanu Lakes in Ocna Sibiului, Ursu Lake in Sovata etc.) are characterized by a strong and relatively stable stratification of physical and chemical parameters, a property termed meromixis (Boehrer and Schultze, 2008). In a similar manner as other meromictic lakes worldwide, the Transylvanian stratified saline lakes display an upper water layer (epilimnion or the uppermost part of the mixolimnion), down to about 2 m depth, an intermediate stratum showing a steep change of physico-chemical parameters (chemocline or the lowermost part of the mixolimnion) at around 2.5-3.5 m depth, and a deep, stable and hypersaline layer (monimolimnion) that starts right below the chemocline (Alexe, 2010; Baricz *et al*., 2014; Máthé *et al*., 2014). Although some of these atypical lakes have long been known and exploited for their touristic value, there is a scarcity of data concerning their biodiversity, especially with respect to their microbial diversity and activity. Systematic investigation of the microbial communities hosted by a number of Transylvanian meromictic salt lakes is just at its beginning and it dealt with the diversity of phototrophic algae and cyanobacteria (Keresztes *et al*., 2012), heterotrophic bacteria (Borsodi *et al*., 2010; 2013; Crognale *et al*., 2013; Máthé *et al*., 2014) and halophilic archaea (Baricz *et al*., 2014). In an earlier study, Muntean *et al*. (1996) were the first to explore the biological activity in the sediment (mud) samples of therapeutic value collected from the bottom of many Romanian salt lakes, including a few of Transylvanian ones.

A fast and convenient approach for profiling the metabolic requirements, sole carbon source utilization and community level physiological profiles (CLPP) was developed by BIOLOG Inc., an R&D company based in Hayward, CA, USA. BIOLOG Ecoplate™ microplates are tools designed for the analysis of whole microbial community from soil and water. One plate has 96 wells containing 31

different carbon sources and a negative control (no carbon substrate) in triplicate. Each well also contains a redox dye indicator (tetrazolium violet) which indicates the positivity of metabolization with color development toward blue-violet (Garland and Mills, 1994; Weber *et al*., 2008). The benefit of the triplicate nature of the microplates is the capacity to use different samples on the same plates or to have an indicator of experimental variation (Weber *et al*., 2007). The Ecoplates offer the opportunity to calculate several substrate-based diversity indices including substrate richness, substrate diversity, and substrate evenness (Zak *et al*., 1994). Several CLPPs of aquatic ecosystems were performed using BIOLOG Ecoplate™ predominantly for freshwater systems such as lakes (Dickerson and Williams, 2014), ponds (Lear *et al*., 2013) or wetland mesocosms (Weber *et al*., 2008). Only a few data exist on CLPP applied in saline environments (Litchfield and Gillevet, 2002; Phillips *et al*., 2011) for the main reason that this approach seems to work unreliably at high salt concentration (Litchfield *et al*., 2001; Pierce *et al*., 2014). CLPP using BIOLOG Ecoplate approach was performed by Crognale *et al*. (2013) in the top and bottom water samples from shallow saline Mierlei Lake, nearby Ursu Lake in Sovata, but the tests were apparently applied to samples with salinities exceeding 10%. However, to date, no approach for a direct estimation of the microbial activity within the water mass has been employed in the Romanian deep, meromictic salt lakes.

The present work intended to provide a first glimpse at the metabolic diversity of microbial community populating the moderately saline epilimnion of the meromictic and heliothermal Ursu Lake. Our aims were: 1) to assess the capacity of carbon substrate metabolization *via* BIOLOG Ecoplate™ approach in the water samples collected during two different seasons (autumn and spring), and 2) to scrutinize the influence of some physico-chemical parameters on the metabolic requirement for carbon sources of the epilimnetic, heterotrophic microbial community of Ursu Lake.

Materials and methods

Description of sampling site

Ursu Lake is located in Sovata (Mureş County), in the eastern part of the Transylvanian Basin, and is the largest heliothermal lake in Romania with an area of about 41000 sqm and maximum depth of 18 m (Muntean *et al*., 1996; Alexe, 2010; Máthé *et al.*, 2014). Ursu Lake is a karstosaline lake formed following a natural event in the late nineteenth century. Continuous water input is provided by brackish Topliţa River and the freshwater Auriu River (Alexe, 2010).

Measurement of physico-chemical parameters and sampling of water

Measurements of physico-chemical parameters of lake water as well as sampling were performed as described previously in Baricz *et al.* (2014), during October 2013 and March 2014. The choice for these sampling times was justified by: 1) ease of accessibility and sampling, 2) the favorable thermal conditions that might support the microbial activity, and 3) the absence of bathing activity. The temperature, salinity, concentration of dissolved oxygen (DO), oxidation-reduction potential (ORP), and pH of the water were measured *in situ*, at a depth of 0.5 m, using a portable water multiparameter device (HI 9828/20, Hanna Instruments, USA). Water samples (1 L) aimed for testing of total microbial activity by BIOLOG Ecoplate approach were collected from 0.5 m depth in sterile plastic containers using an electrical layer sampler. The samples were kept on ice during transportation to laboratory.

Total cell counts

Ten milliliters of water samples were fixed with glutaraldehyde at 2% final concentration and stored for 24 hours at 4^{o}C, in the dark. Fixed samples were filtered through 0.45 µm-pore-size, black, gridded, MCE membrane filters (Fioroni, France). The cells retained on the membrane filters were directly stained with DAPI (4', 6'-diamidino-2-phenylindole) at 5 µg ml^{-1} final concentration and examined by epifluorescence microscopy (BX60, Olympus Optical, Tokyo, Japan). The images were recorded using the microscope's digital camera (Olympus XC50) and analyzed with the CellC software (Porter and Feig, 1980).

Measurement of single-carbon substrate degradation

To test for the CLPP in the collected environmental samples, all the 96 wells of the plates were filled with 150 µl of untreated water samples in sterile conditions, by using an 8-channel automatic pippetor. After inoculation, the plates were incubated and daily monitored during 5 days (120 hrs) in aerobic condition at 30^{o}C. As we aimed for a quick approach to estimate the bulk metabolic activity in the water samples, the consumption of various carbon sources was followed by direct observation of color change at every 24 hours. A reaction was considered roughly positive when the clear blue-violet hue appeared. An extension of incubation (up to 10 days) was employed to estimate whether there are carbon sources that need a prolonged time for degradation. In this situation, the plates were wrapped in plastic foil to avoid evaporation.

Results

Physico-chemical and biological properties of the sampled water layer

The *in situ* measurement of the physical and chemical parameters at 0.5 m depth indicated the moderately saline nature (estimated salinity 57-68 $g \cdot L^{-1}$) of the upper water layer (epilimnion) of Ursu Lake (Table 1). Two environmental factors, temperature and pH, were similar, while other parameters were slightly (salinity and ORP) or significantly (DO) different. The lower salinity found in the epilimnion during March 2014 compared to that estimated in October could be a consequence of the higher fresh water input during late autumn and winter seasons (i.e. rainfalls and ice/snow melting). Other physical and chemical features of the surface lake water are very susceptible to changes that reflect the fluctuations of the surrounding environment. While the temperature value measured during October (around 23°C), followed warm days recorded in summer, the similar value recorded in the epilimnion during March was probably due to the heliothermal effect of the lake water. The measured pH values were also comparable (8.44 in October and 8.53 in March, respectively) but the explanation lays in the buffering effect of the HCO_3^- ions that are present in millimolar concentration (data not shown).

Dissolved oxygen (DO) measurements showed a higher value in October 2013 (6.71 $mg \cdot L^{-1}$) than in March 2014 (0.17 $mg \cdot L^{-1}$). This finding could be explained by an intense activity of oxygenic phototrophic community in deeper layer during warm season (summer 2013) that allowed accumulation of oxygen in the epilimnion. On the turn, the drop of oxygen level during spring season might be triggered either by high metabolic activity of aerobic heterotrophs and/or by a reduced production of photosynthetic oxygen following winter season. The ORP measurements indicated a slightly higher reduction capacity of the water layer during October (-20.7 mV) than that of March sample (+ 6.6 mV). The difference is however too small to assume a clear external cause, ORP probably fluctuating as a consequence of daily or weekly biological activity.

Some of the biological properties were estimated in the epilimnion (0.5 m) (Table 1). In October 2013 the water sample collected at 0.5 m depth presented higher values of total chlorophyll and carotenoid concentrations as well as of cell density compared to that estimated in the March sample. Based on these results one might expect a significantly denser microbial community and possibly higher biological activity in the epilimnion of Ursu Lake during October than March. As stated above, the imbalance of biological parameters recorded in the epilimnion of Ursu Lake could be a direct consequence of varying external environmental factors such as air temperature and amount of water inflow. Higher chlorophyll and carotenoid concentrations during autumn (14.91 and 668.13 $\mu g \cdot L^{-1}$, respectively) than that found during spring (2.30 and 319.60 $\mu g \cdot L^{-1}$, respectively) might be due to the warm, sunny summer season that favored the blooming of primary producers.

Table 1.

Physical, chemical, and biological properties of sampled water layer (0.5 m depth) from Ursu Lake

Parameter (Measurement Units)	Season	
	October 2013	March 2014
Salinity ($g \cdot L^{-1}$ or approx. psu)	68.3	57.5
Temperature (^oC)	23.7	23.6
Dissolved oxygen ($mg \cdot L^{-1}$)	6.71	0.17
ORP (mV)	-20.7	6.6
pH	8.44	8.53
Total chlorophylls ($\mu g \cdot L^{-1}$)	14.9	2.3
Total carotenoids ($\mu g \cdot L^{-1}$)	668.1	319.6
Total cell count ($*10^6$ cells $\cdot$ mL^{-1})	5.36	2.96

Single-carbon substrate degradation

The two BIOLOG Ecoplates were monitored for color changes every 24 hrs during 5 days of incubation. The triplicate format of the plates warrants a reliable repetition of the experiment and provides exact results of different substrate metabolization. The reaction was accounted as positive when color turns to blue-violet in at least two duplicate wells (Fig. 1.).

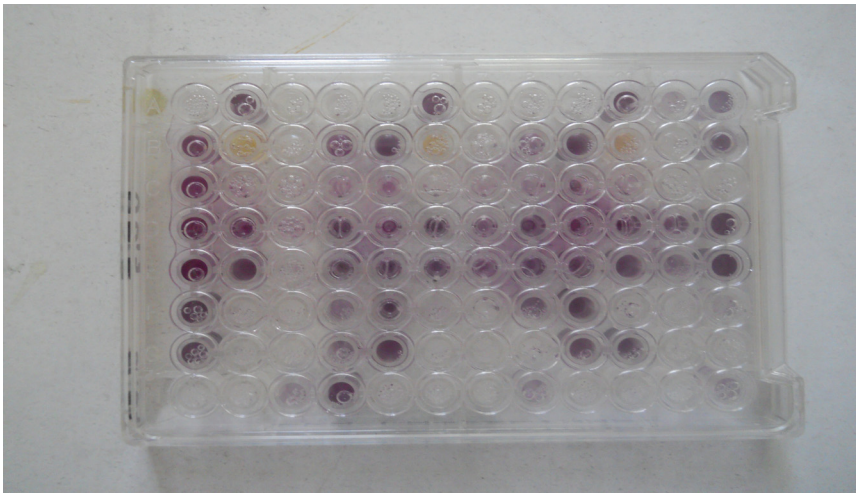

Figure 1. Photographic image of BIOLOG™ EcoPlate inoculated with water sample collected at 0.5 m depth from Ursu Lake, during March 2014, after 48 hrs. of incubation.

The full list of the 31 carbon substrates is presented in Table 2 along with the results (positive or negative) of their degradation.

Table 2.

Microbial utilization of single-carbon sources in the water sample collected at 0.5 m depth from the Ursu Lake during two seasons (October 2013 and March 2014). For the positive samples, the incubation time at which the color change was observed is given

ID	Carbon source	Incubation time (hrs)	
		Oct-13	Mar-14
C1	Pyruvic acid methyl ester	72	24
C2	Tween 40	72	48
C3	Tween 80	72	24
C4	Alpha-cyclodextrin	24	24
C5	Glycogen	24	24
C6	D-cellobiose	24	24
C7	Alpha-D-lactose	-	-
C8	Beta-methyl-D-glucoside	48	24
C9	D-xylose	-	-
C10	i-erythritol	-	-
C11	D-mannitol	24	24
C12	N-acetyl-D-glucosamine	24	24
C13	D-glucosaminic acid	120	120
C14	Glucose-1-phosphate	120	120
C15	D,L-alpha-glycerol phosphate	-	120
C16	D-galactonic acid-gamma-lactone	-	-
C17	D-galacturonic acid	-	-
C18	2-Hydroxy benzoic acid	-	-
C19	4-Hydroxy benzoic acid	-	72
C20	Gamma-hydroxybutyric acid	72	72
C21	Itaconic acid	-	72
C22	Alpha-ketobutyric acid	-	-
C23	D-malic acid	120	120
C24	L-arginine	72	120
C25	L-asparagine	48	48
C26	L-phenylalanine	72	96
C27	L-serine	48	48
C28	L-threonine	48	24
C29	Glycyl-L-glutamic acid	72	72
C30	Phenylethylamine	-	96
C31	Putrescine	72	48

Note: *For a better visualization, we emphasized the name of substrates with colored background: light gray for substrates metabolized in both water samples; blue for substrates metabolized by only one water sample, and white for carbon sources that were not degraded after 10 days of incubation. To highlight the metabolization rates of C sources the backgrounds of positive scores were colored in black (24 hrs), red (48 hrs), orange (72 hrs), dark yellow (96 hrs), and light yellow (120 hrs).*

Out of 31 carbon sources, five substrates were quickly metabolized (i.e., after 24 hours of incubation) by both samples: alpha-cyclodextrin, glycogen, D-cellobiose, D-mannitol, and N-acetyl-D-glucosamine. The first two are polymers, while the latter are a disaccharide, a sugar alcohol, and a monosaccharide derivative, respectively. Other substrates that are degraded in a fairly short time (within 48 hrs.) by both samples are the monosaccharide derivative beta-methyl-D-glucoside and the amino acids L-asparagine, L-serine, and L-threonine. Substrates such as methyl pyruvate, Tween 40, Tween 80, gamma-hydroxybutyric acid, L-arginine, L-phenylalanine, glycyl-L-glutamic acid, and putrescine are equally used in both samples during first 72 hours, apparently slightly quicker in the sample collected during spring season. Three substrates were metabolized in 120 hrs. in both samples: D-glucosaminic acid, glucose-1-phosphate, and D-malic acid. The first two carbon sources are monosaccharide derivatives and the last one is a carboxylic acid.

There are some carbon sources metabolized in only one sample, namely in the March sample: 4-hydroxy benzoic acid and itaconic acid (24 hrs.); phenylethylamine (96 hrs.); D, L-alpha-glycerol phosphate (120 hrs.).

Seven different carbon sources were not metabolized in any of the two samples after 5 days of incubation and up to 10 days of monitoring: alpha-D-lactose, D-xylose, i-erythritol, D-galactonic acid-gamma-lactone, D-galacturonic acid, 2-Hydroxy benzoic acid, and alpha-ketobutyric acid.

In the sample collected and inoculated in October 2013, the BIOLOG Ecoplate™ results indicated that 20 different carbon sources (64.5 % of total carbon sources) were biologically degraded within 120 hours. In the March sample, positive results were observed for 24 different carbon sources (77.4 % of total C sources) within same time interval (Table 3). A number of seven C sources were not metabolized in any of the samples up to 10 days of monitoring: the monosaccharides D-xylose, D-galactonic acid-gamma-lactone, the disaccharide alpha-D-lactose, the sugar alcohol i-erythritol, the phenolic derivative 2-hydroxy benzoic acid (also known as salicylic acid), and the carboxylic acid alpha-ketobutyric acid and D-galacturonic acid.

Table 3.

Summary table of carbon substrate utilization in water samples tested by BIOLOG Ecoplates™ approach

Parameters	**Sampled season**	
	October 2013	**March 2014**
Total metabolized substrates	20 (64.5%)	24 (77.4%)
Number of substrates metabolized within 24 hrs	5	9
Number of substrates metabolized within 72 hrs	17	17
Number of substrates with slow metabolization (after 96 hrs)	3	7
Substrates metabolized in only one sampled season	0	4
Total substrates metabolized in both sampled seasons	20	

Discussion

The data attained from the present study is a first reported indicative for the range of metabolic requirements of heterotrophic microbial community residing the saline epilimnion (0.5 m depth, 5-6 % salinity) of meromictic Ursu Lake (Sovata, Romania). Since the microorganisms are considered the primary decomposers in any environment, revealing the metabolic availability of whole microbial community brings valuable information on their functioning status. As already stressed in the introductory part of the present work, no similar studies were performed for the water collected from meromictic salt lakes located in Romania. Comparable studies were, however, performed in saline environments worldwide: solar salterns from Newark, California and Eilat, Israel (Litchfield *et al*., 2001; Litchfield and Gillvete, 2002), La Sal del Rey salt lake from Texas (Phillips *et al*., 2012), and alkaline Mono Lake, California (Litchfield and Gillevet, 2002).

Our results showed that in October 2013 (autumn), the salinity of water layer (0.5 m) was around 68.3 $g \cdot L^{-1}$ (or 6.8 %) with a total cell number of 5.36 $x10^6$ $cell \cdot mL^{-1}$. This sample accommodated a heterotrophic microbial community capable of using at least 20 different compounds as sole carbon sources. In the sample collected in March 2014 (spring), the salinity was estimated as 57.5 $g \cdot L^{-1}$ (5.75 %) and cell density as 2.96 $x10^6$ $cell \cdot mL^{-1}$. Twenty-four different carbon sources were metabolized by the microbial community existing here at a two-fold lesser cell density than in October. In the case of La Sal del Rey salt lake (Texas, USA), the samples were collected during June 2010 and July 2010 (Phillips *et al*., 2012). The results indicated that in the surface sample with low salinity (4 ppt or 0.4%) and a cell density of around 5.2 x 10^3 cfu mL^{-1}, a total of 29 carbon substrates were metabolized. In a moderately saline water sample (86 ppt, 8.6%), at a higher cell density, the entire range of 31 carbon sources from the plate were metabolized (Phillips *et al*., 2012). In Eilat solar saltern (Israel) and Mono Lake (California, USA), the capacity of the microbial community to use different C sources was tested with BIOLOG GN (Gram-negative) plates. This type of plate contains 95 different carbon sources of which 25 are identical with those in BIOLOG Ecoplates (Table 4). In a previous comparative work it was statistically demonstrated that the two types of plates could reliably be used to discern between the aerobic heterotrophic bacterial communities from various aquatic environments (Choi and Dobbs, 1999). The approach of BIOLOG GN Plates indicated that the Eilat-4 sample (3.9% salinity) from the inlet of the saltern, had the highest carbon metabolization capacity a number of 57 substrates (15 also found in Ecoplates) being used at an estimated cell count of 6 x 10^2 – 3.1 x 10^3 $cfu \cdot mL^{-1}$. The Eilat-3 sample (same 3.9% salinity), also collected from the inlet of solar saltern, had a total capacity of degrading 39 C sources at a higher cell density (2 x 10^4 – 3.5 x 10^5 $cfu \cdot mL^{-1}$). In Mono Lake, the BIOLOG GN plates results revealed that a total of 23 carbon sources were used (5 matches with Ecoplates) at a microbial density of 5.4 x 10^4 $cfu \cdot mL^{-1}$ and a salinity of about 8% (Litchfield and Gillevet, 2002). These findings may suggest that at similar salinity

(3.9 to 8%), the epilimnetic microbial community of Ursu Lake would be more active or at least more receptive to a larger range of C sources than those tested in Eilat solar saltern and the surface shore water of the alkaline Mono Lake (Table 4). The high metabolic potential of Ursu Lake is supported by a recent study of Máthé *et al*. (2014) that dealt with the cultivable and molecular diversity of microbial population along the salinity gradient in the water column. The molecular analysis based on the 16S rRNA gene amplification and analysis showed that all three domains of the life are present at the depth of 0.5 – 1 m. The heterotrophic bacterial isolates likely to degrade some of the C sources present in the Ecoplates under aerobic conditions were assigned to *Pseudoalteromonas* sp., *Idiomarina* sp., *Vibrio* sp., *Marinobacter* sp., *Halomonas* sp., *Thalassospira* sp., *Roseovarius* sp., *Bacillus* sp. and *Staphylococcus* sp. (Máthé *et al*., 2014).

Table 4.

Comparison of carbon utilization pattern assessed by BIOLOG GN plates and BIOLOG Ecoplates in three saline systems. The positive reactions were emphasized with black background

Carbon substrates shared between the two types of BIOLOG plates	Saltern pond (E-4, Eilat, Israel)[a]	Shore water (Mono Lake, USA)[a]	Epilimnion (Ursu Lake, Romania)[b]
Pyruvic acid methyl ester	+	+	+
Tween 40	+	+	+
Tween 80		+	+
Alpha- Cyclodextrin	+	-	+
Glycogen	+	-	+
Cellobiose	+	-	+
Alpha-D-Lactose	+	-	-
Beta-methyl-D-glucoside	-	+	+
i-erythritol	-	-	-
D-mannitol	+	-	+
D,L-alpha-glycerol phosphate	-	-	+
Glucose – 1- phosphate	+	-	+
N-acetyl-D-glucosamine	+	+	+
D- Galacturonic acid lactone	-	+	-
Gamma-hydroxybutyric acid	-	-	+
Itaconic acid	-	-	+
Alpha-ketobutyric acid	+	-	-
L-arginine	+	-	+
L-asparagine	+	-	+
L-phenylalanine	-	-	+
L- serine	+	-	+
L-threonine	+	-	+
Glycyl-L-glutamic acid	+	-	+
Phenylethylamine	-	-	+
Putrescine	-	-	+
Total substrates used	**15**	**6**	**21**

[a] *- data from Litchfield and Gillevet (2002).*
[b] *- Data from March 2013 sample, present study.*

The capacity to use different carbon sources by the microbial community plays a key role in maintaining the equilibrium of the organic substrate composition and implicitly in the carbon cycling within aquatic ecosystems (Christian and Lind, 2006; Weber *et al*., 2008). For example, the hypothetical occurrence of N-acetyl-D-glucosamine in the epilimnion of Ursu Lake and subsequent appetite for its metabolization can be explained through the presence of Gram-positive bacterial population. This monosaccharide is a major component of the bacterial cell wall that could be released in the surroundings by bacterial decomposition and further used as carbon substrate by other microbes. Plant materials originating from the lush temperate vegetation neighboring Ursu Lake could provide other organic compounds like D-cellobiose, D-mannitol, 4-Hydroxy benzoic acid (also present in algae). Some of the amino acids used in the investigated Ecoplates (L-arginine, L-serine, L-asparagine, L-threonine, L-phenylalanine) as well other compounds such as itaconic and malic acids (derived from the Krebs cycle) or phenylethylamine, might be released by microbial decomposition of the organic matter.

The epilimnion is the upper layer of water (Baricz *et al*., 2014), a place with a strong interplay between the freshwater inflow, organic matter input, and fluctuating air conditions that ensures the presence of a large spectrum of microbial diversity with a potent metabolic availability. The ability of the epilimnetic microbial community in Ursu Lake (and elsewhere) to metabolize various carbon sources is crucial in preserving the balance between the formation of organic compounds or toxic substances (e.g. putrescine) and the normal biochemical parameters of water layer. Interestingly, biopolymers such as alpha-cyclodextrin, glycogen and non-ionic detergents Tween 40 and Tween 80 are quickly metabolized in both samples, suggesting that the epilimnion of Ursu Lake may host very active polymer decomposers that could be isolated and used as organisms with potential in food industry and bioremediation.

Conclusions

The results of assessing the carbon utilization pattern by the BIOLOG Ecoplate™ approach indicated a promising metabolic potential of the microbial community from the saline epilimnion of Ursu Lake. By a comparative analysis of water samples collected during two seasons (autumn and spring) it has been observed that the epilimnetic aerobic microbial community is readily degrading a broad spectrum of carbon sources at moderate salinity values (5–6%).

Apparently, our results suggested a higher activity of carbon substrate degradation during spring season, a broader range of C substrates being oxidized by a less denser cell population, at slightly lower salinity and higher ORP. The peculiar nature of meromictic, heliothermal Ursu Lake as well as its importance for the local economy encourages further in-depth investigations on the composition and diversity

of the microbial community, its metabolic activity and role in biochemical cycling of major elements with respect to varying enviornmental conditions and human impact on the lake.

Acknowledgments. This work was supported by a grant of the Romanian National Authority for Scientific Research, CNCS–UEFISCDI, project number PN-II-ID-PCE-2011-3-0546. We are grateful to professor Aharon Oren for the critical reading of the manuscript.

REFERENCES

Alexe, M. (2010) Studiul lacurilor sărate din Depresiunea Transilvaniei. Ed. Presa Universitară Clujeană, Cluj Napoca (In Romanian)

Andrei, A-Ş, Banciu, H.L., Oren A. (2012) Living with salt: metabolic and phylogenetic diversity of archaea inhabiting saline ecosystems. *FEMS Microbiol. Lett.*, **330** (1): 1–9

Baricz, A., Coman, C., Andrei, A.-Ş, Muntean, V., Keresztes, Z. G., Păuşan, M., Alexe, M., Banciu, H.L. (2014) Spatial and temporal distribution of archaeal diversity in meromictic, hypersaline Ocnei Lake (Transylvanian Basin, Romania). *Extremophiles*, **18** (2): 399-413

Boehrer, B., Schultze, M. (2008) Stratification of lakes. *Rev. Geophys*., **46** (2): RG2005. doi:10.1029/2006RG000210

Borsodi, A. K., Kiss, R. I., Cech, G., Vajna, B., Tóth, E.M., Márialigeti, K. (2010) Diversity and activity of cultivable aerobic planktonic bacteria of a saline Lake located in Sovata, Romania. *Folia Microbiol. (Praha)*, **55** (5):461-466

Borsodi, A.K, Felföldi, T., Máthé, I., Bognár, V., Knáb, M., Krett, G., Jurecska, L., Tóth, E.M., Márialigeti, K. (2013) Phylogenetic diversity of bacterial and archaeal communities inhabiting the saline Lake Red located in Sovata, Romania. *Extremophiles*, **17**: 87–98

Bulgăreanu, V.A.C. (1996) Protection and management of anthroposaline lakes in Romania. *Lakes & Reservoirs: Research & Management*, **2**: 211–229

Choi, K.H., Dobbs, F.C. (1999) Comparison of two kinds of Biolog microplates (GN and ECO) in their ability to distinguish among aquatic microbial communities. *J. Microbiol. Methods*, **36** (3): 203-213

Christian, B.W., Lind, O.T. (2006) Key issues concerning biolog use for aerobic and anaerobic freshwater bacterial community-level physiological profiling. *Intl. Rev. Hydrobiol.*, **91** (3): 257–268

Crognale, S., Máthé, I., Cardone, V., Stazi, S.R., Ráduly, B. (2013) Halobacterial community analysis of Mierlei saline lake in Transylvania (Romania). *Geomicrobiology*, **30**: 801–812

Dickerson, T.L., Williams, H.N. (2014) Functional diversity of bacterioplankton in three North Florida freshwater lakes over an annual cycle. *Microb. Ecol.*, **67** (1): 34-44

Garland, J.L., Mills, A.L. (1991) Classification and characterization of heterotrophic microbial communities on the basis of patterns of community-level sole-carbon-source utilization. *Appl. Environ. Microbiol*., **57**: 2351–2359

Lear, G., Bellamy, J., Case, B.S., Lee, J.E., Buckley, H.L. (2014) Fine-scale spatial patterns in bacterial community composition and function within freshwater ponds. *ISME J.*, doi:10.1038/ismej.2014.21

Litchfield, C.D., Gillevet, P.M. (2002) Microbial diversity and complexity in hypersaline environments: a preliminary assessment. *J. Ind. Microbiol. Biotechnol.*, **28** (1): 48-55.

Litchfield, C.D., Irby, A., Kis-Papo, T., Oren, A. (2001) Comparative metabolic diversity in two solar salterns. *Hydrobiologia,* **466**: 73-80

Máthé, I., Borsodi, A.K., Tóth, E.M., Felföldi, T., Jurecska, L., Krett, G., Kelemen, Z., Elekes, E., Barkács, K., Márialigeti, K. (2014) Vertical physico-chemical gradients with distinct microbial communities in the hypersaline and heliothermal Lake Ursu (Sovata, Romania). *Extremophiles*, **18** (3): 501-514

Muntean, V., Crişan, D., Kiss, S., Drăgan-Bularda, M. (1996) Enzymological classification of salt lakes in Romania. *Int. J. Salt Lake Res.*, **5**: 35–44

Oren, A. (2002) *Halophilic microorganisms and their environments.* Kluwer Academic, Dordrecht, The Netherlands

Oren, A. (2008) Microbial life at high salt concentrations: phylogenetic and metabolic diversity. *Saline Systems*, **4** (2): 13

Phillips, K., Zaidan, F., Elizondo, O.R., Lowe, K.L. (2012) Phenotypic characterization and 16S rDNA identification of culturable non-obligate halophilic bacterial communities from a hypersaline lake, La Sal del Rey, in extreme South Texas (USA). *Aquatic Biosyst.,* **8:** 2-11

Pierce, M.L., Ward, J.E., Dobbs, F.C. (2014) False positives in Biolog EcoPlates™ and MT2 MicroPlates™ caused by calcium. *J .Microbiol. Methods*, **97**: 20-24

Porter, K., Feig, Y. (1980) The use of DAPI for identifying and counting aquatic microflora. *Limnol. Oceanogr.*, **25:** 943-948

Ventosa, A., Nieto, J.J., Oren, A. (1998) Biology of moderately halophilic aerobic bacteria. *Microbiol Mol. Biol. Rev.*, **62** (2): 504-544

Weber, P.K., Grove, J.A., Gehder, M., Anderson, W.A., Legge, L.R. (2007) Data transformations in the analysis of community-level substrate utilization data from microplates, *J. Microbiol. Methods,* **69**: 461-469

Weber, P.K., Gehder, M., Legge, L.R. (2008) Assessment of changes in the microbial community of constructed wetland mesocosms in response to acid mine drainage exposure, *Water Res.,* **42:**180-188

Zak. J.C., Willig, M.R., Moorhead, D.L., Wildman, H.G. (1994) Functional diversity of microbial communities: a quantitative approach. *Soil Biol. Biochem*., **26**: 1101–1108

STUDIA UNIVERSITATIS BABEŞ-BOLYAI BIOLOGIA, LIX, 1, 2014 (p. 55-62)

MOLECULAR EVIDENCE FOR THE HYBRID ORIGIN OF *HEPATICA TRANSSILVANICA* (RANUNCULACEAE) BASED ON NUCLEAR GENE SEQUENCES

LÁSZLÓ BARTHA[1,2,✉], KUNIGUNDA MACALIK[2] and LUJZA KERESZTES[2]

SUMMARY. Allopolyploidy (hybridisation followed by genome doubling) has been recognised as a major force driving plant speciation. The genus *Hepatica* includes both diploid and polyploid species where the origin of polyploids has not been fully established, yet. In particular, the origin of Romanian endemic, tetraploid *Hepatica transsilvanica* Fuss. remained challenging because a previous study found its incongruent placement between plastid and nuclear phylogenies (suggestive of its hybrid origin). In this study a more direct method was applied in order to shed lights on the hybrid origin of species. A fragment of nuclear *At103* gene was sequenced in *H. transsilvanica* and in both of its putative diploid progenitors, the European distributed *H. nobilis* Schreb. (var. nobilis) and the Central Asian endemic *Hepatica falconeri* Thomson. Direct *At103* sequence of *H. transsilvanica* clearly showed an additive pattern between the parental sequence types, supporting the allopolyploid origin of species. A few additional additive polymorphic sites (i.e. superimposed peaks) neither supporting, nor contradicting the hybrid origin were also found in the sequence of *H. transsilvanica* but these were not shared by all samples analysed. Origin of this 'inconclusive sequence variation' can be explained by various phenomena, like random sorting of ancestral polymorphism or paralogy. In this study a new platform is provided on which the auto- vs. allopolyploid origin of the rest of tetraploid *Hepatica* taxa can be tested.

Keywords: allopolyploidy, At103 gene, Carpathian endemic.

[1] *Institute for Interdisciplinary Research in Bio-Nano-Sciences, Babeş-Bolyai University, 42 A. Treboniu Laurean Street, 400271 Cluj-Napoca, Romania.*

[2] *Faculty of Biology and Geology, Babeş-Bolyai University, 5-7 Clinicilor Street, 400006 Cluj-Napoca, Romania.*

✉ ***Corresponding author**: **László Bartha**, Institute for Interdisciplinary Research in Bio-Nano-Sciences, Babeş-Bolyai University, 42 A. Treboniu Laurean Street, 400271 Cluj-Napoca, Romania. E-mail: lbartha.ubbcluj@yahoo.com.*

Introduction

Allopolyploidisation (hybridisation followed by genome duplication) has been considered as one of the most important processes driving plant speciation (Grant, 1981; Soltis and Soltis, 2009). Exploring patterns of hybrid speciation via sequencing requires the use of biparentally inherited nuclear markers. Identity of hybrid progenitors can be inferred if direct nuclear sequences of hybrid species show additive pattern between the parental sequence types (Campbell *et al.*, 1993). In cases when such parental sequence types are different in length and hamper direct sequencing, they can still be retrieved from hybrid species by cloning. Concerted evolution may homogenise copies of a nuclear DNA region in a hybrid species towards one of the parental (maternal or paternal) sequence type as commonly occurring in the case of internal transcribed spacer (ITS) region of the nuclear ribosomal (nr) DNA (Álvarez and Wendel, 2003). In such cases the hybrid origin can still be inferred based on conflicting topologies between phylogenies based on plastid and nuclear marker systems.

The genus *Hepatica* (*Ranunculaceae*) is a small-sized genus showing interesting biogeographic distribution characterised by intercontinental and deep inner continental disjunctions (Pfosser *et al.*, 2011). Polyploidisation played an evident role in the evolution of genus (Weiss-Schneeweiss *et al.*, 2007). Taxonomic status of several *Hepatica* species is still under dispute and the genus lacks a well-resolved backbone phylogeny. Taxa of the genus are, however, well characterised as far as their ploidy level and morphological circumscription is considered. Traditionally two morphological groups have been recognised within the genus: the one with entirely lobed leaves and another with crenate leaves. Mabuchi *et al.* (2005) proposed that crenate leaved tetraploid (2n=28) species *Hepatica transsilvanica* Fuss, *Hepatica henryi* Nakai and *Hepatica yamatutai* Steward could be autopolyploids of the diploid and crenate leaved *Hepatica falconeri* Thomson. Interestingly, *H. falconeri* grows in Central Asia, *H. transsilvanica* is confined to the Romanian Carpathians whereas the possibly conspecific *H. henryi* and *H. yamatutai* are distributed in Eastern Asia. As an alternative to the suggested autopolyploid ancestry, they could have also raised via allopolyploidisation involving *H. falconeri* (or an extinct relative to it) as one of the parental species (Weiss-Schneeweiss *et al.*, 2007). Weiss-Schneeweiss *et al.* (2007) found incongruence between plastid and nuclear phylogenies at the level of *H. transsilvanica* although these phylogenies were poorly resolved and some of their relationships were not supported. Their findings, therefore, favored the hybrid origin of *H. transsilvanica* over the autoploid origin but the ultimate inference for an allopolyploid origin of species remained largely unfulfilled.

In an effort to test the hybrid origin of the Romanian (Carpathian) endemic *H. transsilvanica* using a 'strictly direct' method, in this study a nuclear DNA marker system was employed in *H. transsilvanica* and two of its potential progenitors, the

European distributed *H. nobilis* Schreb. (var. *nobilis*) and the Central Asian endemic *H. falconeri*. Because a limited utility of the very popular phylogenetic marker nrDNA has already been found in *Hepatica* by a previous study (Weiss-Schneeweiss *et al.*, 2007), here the use of a so-called 'low-copy nuclear gene' has been endeavoured. Low-copy nuclear genes are less susceptible to concerted evolution when compared with nrDNA (Zimmer *et al.*, 1980). For the purpose of the study the nuclear At103 gene was selected due to its short length, variability and amplifiability across different plant groups with the available universal primers (Li *et al.*, 2008; Bruni *et al.*, 2010; Désamoré *et al.*, 2012).

Materials and Methods

a. Taxon and population sampling

As mentioned previously, taxon sampling included *H. transsilvanica*, *H. falconeri* and *H. nobilis*. One sample per population was analysed in the case of each species studied. Care was taken to include samples from distantly located populations of *H. transsilvanica* from the Northern and Western part, as well as from the middle of the species range (Table 1). The two samples of *H. nobilis* originated from and outside of the Carpathian Basin, respectively. The study resorted to a recently collected single Kyrgyzian accession of *H. falconeri* because additional (herbarium) samples originating from Pakistan (and collected several decades ago) turned out to be not suitable for DNA analysis.

b. Plant material, DNA isolation, PCR amplification and sequencing

Freshly collected leaf material of the studied species was desiccated in silicagel prior to DNA extraction. Total genomic DNA was extracted using the ZR Plant/Seed DNA Kit (Zymo Research). A fragment of the nuclear *At103* gene (for putative Mg-protoporphyrin monomethyl ester cyclase) spanning approximately from the middle of exon III to the end of intron IV was amplified by polymerase chain reaction (PCR) using the forward (5'-CTT CAA GCC MAA GTT CAT CTT CTA-3') and reverse (5'-TTG GCA ATC ATT GAG GTA CAT NGT MAC ATA-3') primers by Li *et al.* (2008). PCR was performed in 25 µl reaction volumes containing 12.5 µl 2× MyTaq Red Mix (Bioline), 8.5 µl dd water, 1 µl of each primers (10 µM) and 2 µl DNA-template solution of unknown concentration. Amplification of *At103* required the following PCR reaction program: initial denaturation step at 94°C for 4 min, followed by 40 cycles of denaturation at 94°C for 30 sec, annealing at 50°C for 45 sec and extension at 72°C for 30 sec. A final extension at 72°C for 5 min was inserted before final hold at 18°C. All amplifications were performed using a Gradient Palm-Cycler (Corbett Research). The success of PCR was tested by agarose gel electrophoresis. Since amplifications did not produce non-specific products (data not shown) PCR products were directly column-purified using the PCR Purification Kit of

Jena Biosciences. PCR products were both forward and reverse-sequenced by Macrogen Inc. (The Netherlands) using the amplification primers. GenBank accession numbers for all *At103* sequences generated for this study are listed in Table 1.

c. Data analysis

At103 sequences from the same accession (obtained with forward and reverse primers) were assembled using BioEdit (Hall, 1999). Sequences were aligned manually in software MEGA5 (Tamura *et al.*, 2011) from which the variable nucleotide positions were exported to a common text file.

Results and discussion

Amplification and sequencing of selected region of *At103* gene was straightforward in all accessions analysed and resulted in clear chromatograms. The length of DNA region flanked by forward and reverse primers has been 326 bp in length and showed no length variation between species. Alignment of sequences contained 10 (3 %) variable nucleotide positions (Table 2). Most (8) of these positions were located within the partial third exon which was inferred to have a length of 226 bp within the sequenced fragment of the gene (see GenBank accessions KJ842642-KJ842647).

Most of sequenced species/accessions contained unambiguous double (i.e. 'superimposed') peaks in their *At103* chromatograms (Fig. 1) (except for the species *H. falconeri* and one accession of *H. nobilis*). Nucleotide states corresponding to double peaks were codified according to *IUPAC* codes in the sequence alignment. Two types of sequence variation can be observed in the dataset regarding their *consistency*. The first type includes single nucleotide differences consistently occurring among *H. falconeri* and the two *H. nobilis* accessions at (column) positions '82' (G/A), '106' (T/C), '211' (C/T), and '289' (C/T) (Table 2). Interestingly, so called additive polymorphic sites (APS) consistently occur at the same positions among the three accessions of *H. transsilvanica* and clearly show an additive pattern between *H. falconeri* and *H. nobilis* (Table 2). This lends support to the recognition of *H. transsilvanica* as a hybrid (allotetraploid) species having *H. falconeri* and *H. nobilis* as its progenitors.

The second type of variation concerns 'randomly' occurring single nucleotide differences (with or without additivity) in the dataset at (column) positions different from those mentioned above (Table 2). Contrary to the previously presented variation, none of these nucleotide differences were shared by all samples of *H. transsilvanica* and *H. nobilis*, respectively.

Since the advent of molecular phylogenetics, this type of information (i.e. ITS profiles with additive pattern between putative parental sequence types) have been successfully used for inference of hybrid origin across different taxonomic groups. One of the earliest examples was reported by Campbell *et al.* (1993) who found additivity

of nucleotide states in *Amelanchier* × *neglecta* (Eggelst.) Eggelst. at sites where the hypothesised parental species, *A. bartramiana* (Tausch) Roemer and *A. laevis* Wieg. differed. Some of the most recent examples include the case of heterophyllous *Ranunculus penicillatus* (Dumort.) Bab. Zalewska-Gałosz *et al.* (2014) recently found that ITS sequences of this tetraploid species exhibited a clearly additive pattern between sequences of *Ranunculus fluitans* Lam. and *Ranunculus peltatus* L. illustrating its hybrid origin.

The hybrid origin of *H. transsilvanica* is neither supported nor contradicted by the second type (i.e. 'randomly occurring') sequence variation as recognised previously. Although the presence of this inconclusive variation cannot be neglected in the dataset, the 'consistent' variation is considered here as the preponderance of evidence in supporting the hybrid origin of the target species. Various phenomena can be responsible for the presence of APS in diploid *H. nobilis* and for appearance of those APS in tetraploid *H. transsilvanica* which are apparently not related to the hybrid status of species. These can result from gene flow between populations, incomplete sorting of ancestral polymorphism or paralogy (due to independent duplication events of the gene in certain populations) (Piñeiro *et al.*, 2009). Discerning the relative contribution of these phenomena to the intra-individual polymorphism of *At103* gene in selected taxa of the genus *Hepatica* was beyond the scopes of this study. This will require in the future denser population sampling, analyses of multiple samples per population, as well as sequencing multiple unlinked nuclear loci. Whatever the reason behind the above findings, the pattern of *At103* variation would be worth exploring in a phylogeographic context. Piñeiro *et al.* (2009), for example, found a clear geographic trend within variation of alleles and certain paralogs of the nuclear gene *GapC* in *Armeria pungens* (Link) Hoffmanns. & Link.

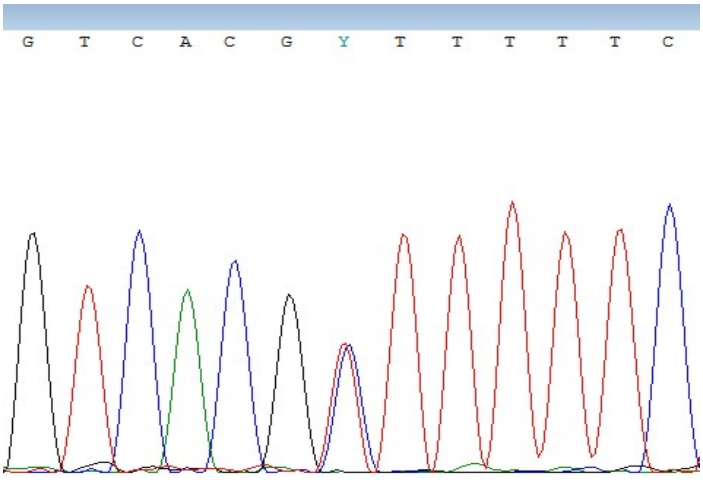

Figure 1. Unambiguous double (i.e. 'superimposed') peak in the chromatogram of *H. transsilvanica At103* sequence at nucleotide position '211' (See Table 2)

Table 1.

Information on the plant samples analysed and list of GenBank accession numbers for *At103* sequences newly generated for the study

Accession	Sampling locality	Name of collectors / suppliers	GenBank acc. numbers
Hepatica falconeri (Thomson) Steward	Kyrgyzstan, Grigorievskaya Gorge	Harry Jans	KJ842642
Hepatica transsilvanica Fuss pop. 1	Romania, Neamț County, Valea Bicăjelului	László Bartha, Bogdan-Iuliu Hurdu	KJ842643
H. transsilvanica pop. 2	Romania, Argeș County, Cheile Dâmbovicioarei Mici	László Bartha, Bogdan-Iuliu Hurdu	KJ842644
H. transsilvanica pop. 3	Romania, Hunedoara County, Hațeg	László Bartha, Kunigunda Macalik	KJ842645
Hepatica nobilis Schreb. pop. 1	Romania, Bihor County, Cetățile Ponorului	László Bartha, Attila Bartók	KJ842646
H. nobilis pop. 2	Romania, Vâlcea County, Cheile Bistriței	László Bartha, Kunigunda Macalik	KJ842647

Table 2.

Variable nucleotide positions in the *At103* sequence alignment. Nucleotide positions exhibiting additive polymorphic sites are in bold and are represented by *IUPAC* codes whereas those supporting the hybrid origin of *H. transsilvanica* are shaded in gray (Accession names as specified in Table 1)

	nucleotide positions									
accessions	73	82	106	133	145	181	184	211	253	289
H. falconeri	A	G	T	A	C	C	T	C	G	C
H. transsilvanica pop. 1	A	**R**	**Y**	**R**	C	C	C	**Y**	**S**	**Y**
H. transsilvanica pop. 2	**R**	**R**	**Y**	G	C	C	C	**Y**	G	**Y**
H. transsilvanica pop. 3	**R**	**R**	**Y**	**R**	C	**Y**	C	**Y**	G	**Y**
Hepatica nobilis pop. 1	A	A	C	A	C	C	C	T	G	T
Hepatica nobilis pop. 2	A	A	C	A	**Y**	C	C	T	G	T

Conclusions

In this study the putative hybrid origin of a polyploid *Hepatica* species has been addressed and confirmed for the first time using comparative analysis of sequences from a low-copy nuclear gene. The authors thus provide a platform on which the auto- vs. allopolyploid origin of the rest of polyploid *Hepatica* species can be tested. Future studies should address the identity of maternal and paternal species of *H. transsilvanica*, as well as its multiple vs. single origin, and – to the extent possible – the age of species.

Acknowledgements. The authors greatly acknowledge Harry Jans for collecting and providing the *Hepatica falconeri* sample analysed in the study. The help of Bogdan-Iuliu Hurdu and Attila Bartók in collecting samples of *Hepatica transsilvanica* and *Hepatica nobilis*, respectively, are also acknowledged. The authors also thank Amir Sultan for providing the Pakistani samples of *H. falconeri* from Herbarium RAW (Islamabad) for the pilot study. This work was supported by a grant of the Ministry of National Education, CNCS – UEFISCDI, project number PN-II-ID-PCE-2012-4-0595.

REFERENCES

Álvarez, I., Wendel, J.F. (2003) Ribosomal ITS sequences and plant phylogenetic inference. *Mol. Phylogen. Evol.*, **29**, 417-434

Bruni, I., De Mattia, F., Galimberti, A., Galasso, G., Banfi, E., Casiraghi, M., Labra, M. (2010) Identification of poisonous plants by DNA barcoding approach. *Int. J. Legal Med.*, **124**, 595-603

Campbell, C.S., Baldwin, B.G., Donoghue, M.J., Wojciechowski, M.F. (1993) Toward a phylogeny of *Amelanchier* (Rosaceae: Maloidae): evidence from sequences of the Internal Transcribed Spacers (ITS) of nuclear ribosomal DNA (nrDNA). *Am. J. Bot.*, **80**, 135-136

Désamoré, A., Laenen, B., González-Mancebo, J.M., Jaén Molina, R., Bystriakova, N., Martinez-Klimova, E., Carine, M.A., Vanderpoorten, A. (2012) Inverted patterns of genetic diversity in continental and island populations of the heather *Erica scoparia* s.l. *J. Biogeogr.*, **39**, 574-584

Grant, V. (1981) *Plant speciation*, Columbia University Press, New York

Hall, T.A. (1999) BioEdit: a user-friendly biological sequence alignment editor and analysis program for Windows 95/98/NT. *Nucleic Acids Symp. Ser.*, **41**, 95-98

Li, M., Wunder, J., Bissoli, G., Scarponi, E., Gazzani, S., Barbaro, E., Saedler, H., Varotto, C. (2008) Development of COS genes as universally amplifiable markers for phylogenetic reconstructions of closely related plant species. *Cladistics*, **24**, 727-745

Mabuchi, T., Kokubun, H., Mii, M., Ando, T. (2005) Nuclear DNA content in the genus *Hepatica* (Ranunculaceae). *J. Plant Res.*, **118**, 37-41

Pfosser, M., Sun, B.-Y., Stuessy, T.F., Jang, C.-G., Guo, Y.-P., Taejin, K., Hwan, K.C., Kato, H., Sugawara, T. (2011) Phylogeny of *Hepatica* (Ranunculaceae) and origin of *Hepatica maxima* Nakai endemic to Ullung Island, Korea. *Stapfia*, **95**, 16-27

Piñeiro, R., Costa, A., Aguilar, J.F., Feliner, G.N. (2009) Overcoming paralogy and incomplete lineage sorting to detect a phylogeographic signal: a GapC study of *Armeria pungens*. *Botany*, **87**, 164-177

Soltis, P.S., Soltis, D.E. (2009) The role of hybridization in plant speciation. *Annu. Rev. Plant Biol.*, **60**, 561-588

Tamura, K., Peterson, D., Peterson, N., Stecher, G., Nei, M., Kumar, S. (2011) MEGA5: Molecular evolutionary genetics analysis using maximum likelihood, evolutionary distance, and maximum parsimony methods. *Mol. Biol. Evol.*, **28**, 2731-2739

Weiss-Schneeweiss, H., Schneeweiss, G.M., Stuessy, T.F., Mabuchi, T., Park, J.-M., Jang, C.-G., Sun, B.-Y. (2007) Chromosomal stasis in diploids contrasts with genome restructuring in auto- and allopolyploid taxa of *Hepatica* (Ranunculaceae). *New Phytol.*, **174**, 669–682

Zalewska-Gałosz, J., Jopek, M., Ilnicki, T. (2014) Hybridization in *Batrachium* group: Controversial delimitation between heterophyllous *Ranunculus penicillatus* and the hybrid *Ranunculus fluitans* × *R. peltatus*. *Aquat. Bot.*, *in press*

Zimmer, E.A., Martin, S.L., Beverley, S.M., Kan, Y.W., Wilson, A.C. (1980) Rapid duplication and loss of genes coding for the alpha chains of hemoglobin. *PNAS*, **77**, 2158-2162

STUDIA UNIVERSITATIS BABEŞ-BOLYAI BIOLOGIA, LIX, 1, 2014 (p. 63-70)

THE ROLE OF *ARABIDOPSIS G*ENES INVOLVED IN ABIOTIC (OSMOTIC, OXIDATIVE AND GRAVITROPIC) STRESS RESPONSE REGULATIONS

GÁBOR RIGÓ[1], GYÖNGYI SZÉKELY[2], DORINA PODAR[3,4], FERHAN AYAYDIN[1], LAURA ZSIGMOND[1], HAJNALKA KOVÁCS[1], ANNAMÁRIA KIRÁLY[1], LÁSZLÓ SZABADOS[1], CSABA KONCZ[1,5] and ÁGNES CSÉPLŐ[1]✉

SUMMARY. The warming of overall climate requires to breed plant cultivars tolerant to extreme osmotic tolerance, e.g. to high salt concentration in order to improve their chance to survive deleterious effects of abiotic stress conditions. Our initial aim is to isolate and characterize abiotic stress response regulatory genes arisen from *Arabidopsis thaliana* which is known as a model species for such investigations in higher plant. For this reason, a Ser/Thr protein kinase, the CRK5 was chosen. The CRK5 protein kinase is partly functionally characterized exhibiting a role in the regulation of gravitropic responses of *Arabidopsis thaliana* roots (Rigó *et al.*, 2013). The CRK5 is a plasma membrane associated kinase that forms U-shaped patterns facing outer lateral walls of root epidermis cells. The CRK5 phosphorylates the hydrophilic loop of the auxin efflux transporter PIN2 *in vitro*. Thus, delayed gravitropic response of *crk5* mutant reflects defective phosphorylation of PIN2 and deceleration of its brefeldin sensitive membrane recycling. Recently, we have been investigating the regulatory role of CRK5 protein kinase under osmotic (salt) and oxidative (hydrogen peroxide) stresses. The aim was to gather additional information regarding its role in the regulation of responses to either high salinity or oxidative stress, and consequently, regarding the impact on the auxin biosynthesis, transport and signaling. CRK protein kinase is hypothesized to be involved in the regulation of the effect of reactive oxygen species (ROS, e.g. hydrogen peroxide).

Keywords: abiotic stress response regulation, *Arabidopsis thaliana*, CRK5 protein kinase, gravitropism, reactive oxygen species

[1] *Institute of Plant Biology, Biological Research Center, H-6726 Szeged, Hungary.*
[2] *Hungarian Department of Biology and Ecology, Faculty of Biology and Geology, Babes-Bolyai University, 400006 Cluj-Napoca, Romania.*
[3] *Department of Molecular Biology and Biotechnology, Faculty of Biology and Geology, Babes-Bolyai University, 400084 Cluj-Napoca, Romania.*
[4] *Institute of Institute for Interdisciplinary Research in Bio-Nano-Sciences Babes-Bolyai University, 400271 Cluj-Napoca, Romania.*
[5] *Max-Planck Institute für Züchtungsforschung, D-50829 Cologne, Germany.*
✉ ***Corresponding author: Dr. Ágnes Cséplő**, Institute of Plant Biology, Biological Research Centre, Hungarian Academy of Sciences, H-6726 Szeged, Temesvári krt. 62, Hungary, Tel: 00-36-62-599703, E-mail: cseplo.agnes@brc.mta.hu.*

Connection of gravitropic response and the plant hormone auxin

Plant roots are involved in many metabolic processes including water and nutrient acquisition, anchorage, propagation, storage functions and secondary metabolite synthesis. All these vital functions are controlled by a number of regulatory genes including transcription factors, protein kinases and transporters controlling local hormone content (Scheres *et al.*, 2002; Petricka *et al.*, 2012). Development of roots is regulated by different plant hormones like auxin, cytokinin, brassinosteroids, abscisic acid and gibberellin. These hormones participate in root development by integrating their signals with auxin biosynthesis, transport, and signaling (Petricka *et al.*, 2012). Among these hormones the auxin is considered to be the master regulator (Benkova *et al.*, 2003; Quint and Gray, 2006; Saini *et al.*, 2013). Auxin is involved in every aspect of plant growth and development such as embryogenesis, organogenesis and tissue patterning. It controls various stages of root development, root elongation, system architecture and tropisms (Sauer *et al.*, 2013).

During evolution, the adaptation to circumstances of Earth gravitation was essential for the developmental processes, for the formation and location of organs and organ systems. Due to the gravitational force, both terrestrial and water plants have growth axis parallel with the gravitation vector. In higher plants the direction of main roots is identical with the gravity vector (positive gravitropism); while the photosynthesizing shoots develop into an opposite direction showing the so called negative gravitropism. The first person who described the root and shoot gravitropism was Charles Darwin (Darwin, 1880). Since his basic discovery, it became clear that the sensors for the gravitational direction in plants are specialized gravity sensing cells called statocytes containing special amyloplasts (starch containing plastids) named statoliths. These specific statocyte cells are found in the root columella and stem endodermis. Mutants impaired in starch synthesis are unable to change their direction of growth according to the direction of gravitation. It was also shown that the movement of statoliths along the gravitational vector alters their interactions with actin filaments which are responsible for statoliths sensing and movement. During the movement of the statoliths, several plasma membrane localized mechanoreceptors are activated which immediately trigger several signaling and secondary messenger molecules. Among these, the release of the Ca^{2+} ions, the Ca^{2+} and calmodulin (CaM) sensing and the consequent phosphorylation cascade are the most important processes. N. Cholodny and F.W. Went described in 1926 that the gravitation sensing signal transduction process results in the asymmetric distribution of plant hormone auxin (Went, 1974). The molecular mechanisms of the amyloplast dependent gravity response and its connection with auxin signaling are largely unknown (Morita, 2010; Hashiguchi *et al*., 2013). During vertical to horizontal rotation, auxin is transported basipetally, from the upper to the lower side of the plant roots, where elevated auxin concentration inhibits cell elongation. The cells at the upper part of the root - due to the

decreasing auxin concentration – will elongate further leading to root bending into the direction of the gravitational vector. Direction of the gravitropic responses are controlled by the asymmetric distribution of auxin, resulting in the downward and upward bending of the horizontally placed roots and shoots, respectively (Blancaflor, 2013). In the last decade, the details of the auxin transport mechanism were mostly clarified by the discovery of the PINFORMED (PIN) proteins which are the main plasma membrane located auxin transporters (Palme and Gailweiler, 1999; Feraru and Friml, 2008; Friml, 2010). However, the question how the secondary Ca^{2+}/CaM signal regulates the asymmetric auxin transport, cell elongation and finally the positive gravitropic root growth response has remained unanswered. Last year Rigó *et al.* (2013) described the functional characterization of *Arabidopsis thaliana* CRK5 protein kinase. This protein kinase is a member of the Ca^{2+}/CaM-dependent protein kinase (CDPK) related CRK family which consists of eight members with unknown functions (Harmon *et al.*, 2000; Harmon, 2003; Harper *et al.*, 2004).

The members of the CDPK superfamily

The Ser/Thr protein kinase CDPK superfamily including the CRK (CDPK-related) and the SnRK (sucrose nonfermenting1-related) protein kinases is found only in the plant kingdom. The most characterized members of this superfamily are the CDPKs and the SnRKs. The *Arabidopsis thaliana* genome analysis revealed 34 CDPKs, 8 CRKs and 38 SnRKs (The Arabidopsis Genome Initiative, 2000; Hrabak *et al.*, 2003). The three plant SnRKs subfamilies (SnRK1, SnRK2 and SnRK3) have different functions involving regulation of energy metabolism (SnRK1, Hardie *et al.*, 1998) or environmental stress reactions (SnRK2 and SnRK3, Gong *et al*., 2002). Many SnRK2 members from several plant species are activated by hyperosmotic and salinity stresses (Umezava *et al.*, 2004) Unlike SnRKs, there is only very few information about the function of plant CRKs *in vivo*. Data concerning mainly their biochemical characterization (e.g. predicting plasma membrane localization of these proteins) has been published (Podell and Gribskov, 2004; Rigó *et al.*, 2008). Information about physiological substrates of individual CRK isoforms is scarce (Harper and Harmon, 2005) and available only for AtCRK3 for which the glutamine synthetase enzyme (AtGLN1;1) participating in leaf senescence was found to act as a substrate (Li *et al*., 2006).

The role of the CRK5 protein kinase in gravitropic regulations

Rigó *et al.* (2013) described the functional analysis of the *Arabidopsis* CRK5 protein kinase. This protein kinase is a member of the CDPK-related CRK family which consists of eight members with unknown functions (Hrabak *et al.*, 2003). They described that the CRK5 protein kinase phosphorylates the PIN2 auxin efflux protein

which is a key transporter of auxin during *Arabidopsis* root gravitropic response. It was also shown that the CRK protein kinase has an important role in the regulation of root and shoots gravitropisms in *Arabidopsis*. At 24 hours after reorientation by 135^0, the wild type (wt) roots completely bended to the direction of gravitational vector, while the roots of the T-DNA mutant allele of CRK5 protein kinase (*crk5-1)* rotated only at 90^0 (Fig. 1). The inflorescence of wild type (wt) *Arabidopsis* has shown normal 90^0 rotation, while inflorescence of the *crk5-1* mutant plants could rotate only at 45^0 as it was demonstrated by Rigó *et al.* (2013). As a conclusion, the inactivation of CRK5 protein kinase inhibits the normal gravitropic responses of roots and shoots in *Arabidopsis,* respectively.

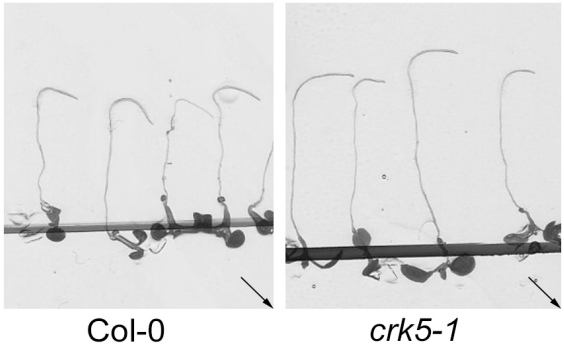

Figure 1. Gravitropic defects caused by the *crk-1* mutation. Root assays: comparison of gravitropic responses of wild type (wt) and the mutant (*crk5-1*) 7 days old seedlings. The direction of gravity is indicated by black arrow.

The reason for the impaired gravitropic responses in *crk5-1* mutant is the alteration of the auxin distribution as compared to those of the wild type. Upon gravistimulation by 135° rotation of the wild type roots, the asymmetric activation of the auxin sensor *DR5::GFP* signal in the columella root cap and epidermis cells was in four hours (Ottenschlager *et al.*, 2003; Rigó *et al.*, 2013). On contrary, in the *crk5-1* mutant, the maximum of the asymmetric localization of *DR5::GFP* expression in the root cap and epidermis was observed only at 9 h after application, thus a five hours delay in the root gravitropic response in *crk5-1*. It was also shown that *in vitro* the CRK5 protein kinase phosphorylates the PIN2 auxin efflux protein which is a key factor of the basipetal auxin transport. The results of immunolocalization of the PIN2 protein - which is the most important basipetal auxin efflux transporter – demonstrated an altered PIN2 pattern in the *crk5-1* mutant when compared to the wild type one (Rigó *et al.*, 2013). The intracellular localization of PIN2 is normally apical in epidermal and basal in cortex cells in *Arabidopsis* wild type roots and this localization is determined by a dynamic phosphorylation/dephosphorylation processes of the PIN2 protein.

Improper phopshorylation of PIN2 in the case of *crk5-1* mutant roots leads to improper auxin transport, and consequently, to a delay of the auxin transport. So, it was found a direct functional correlation between the asymmetric auxin distribution, improper PIN2 phosphorylation and gravitropic response delay in *crk5-1* roots (Rigó *et al.*, 2013).

Additional interesting information is that the intracellular localization of the green fluorescence protein (GFP) tagged CRK5 shows a U-shape facing outer lateral walls of root epidermis cells plasma membrane distribution (Fig. 2 a). Such localization pattern was only observed for boron transporters in *Arabidopsis* (Miwa *et al.*, 2007; Takanoa *et al.*, 2010). This U-shape like pattern may indicate a role for CRK5 protein kinase in the microelement and water transport regulations, too.

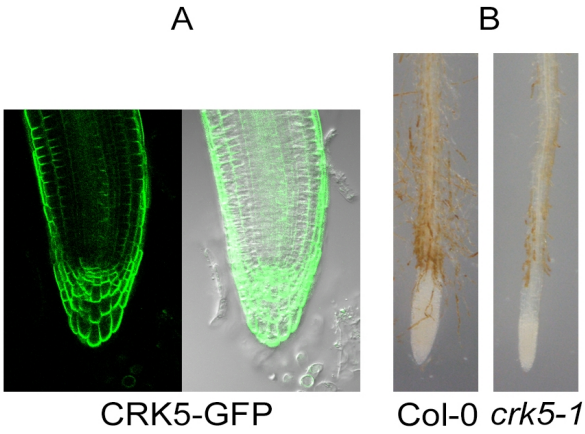

Figure 2. (A) Localization of the *CRK5::GFP* fusion protein in *Arabidopsis* root cap cells. Note U-shape like localization pattern in root tips. **(B)** Demonstration of hydrogen peroxide content in wild type (Col-0) and mutant (*crk5-1*) roots of 6 days old seedlings by 3, 3-diaminobenzidine (DAB) staining. The detection of hydrogen peroxide was performed according to Ren *et al*., 2002

The role of CRK5 protein kinase in abiotic stress responses

The plant ecosystems are significantly influenced by continuous fluctuation of the climate. As a realistic tendency, a serious decrease in plant productivity is forecasted in the near future within considerable parts of Europe. The most critical environmental factors affecting plant productivity are drought, extreme cold and heat and the increase in the salt content of the soil. Therefore, the aim to increase abiotic stress adaptability of plants has become of great interest. For this reason, we continued to further investigate the functional characterization of the CRK5 addressing the study of abiotic (osmotic and oxidative) stress response features of this protein kinase. We

found that one mutant allele of the CRK5 protein kinase develops longer roots than the wild type allele under high saline concentration (Rigó *et al.*, 2011). This means that the CRK5 protein kinase may also influence the osmotic stress regulation. We also found that the hydrogen peroxide level in *crk5* mutant roots was altered compared to wild type roots (Fig. 2 b). It is very intriguing to understand how CRK5 might be a novel player of ROS signal transduction in roots. The hydrogen peroxide is a multifunctional molecule which participates in regulation of several signaling pathways including within the oxidative stress responses of plants (Petrov and Van Breusegem, 2012). We hypothesize that the CRK5 protein kinase may regulate auxin signaling through alteration of redox homeostasis of reactive oxygen species (ROS). Although the functional characterization of the CRK protein kinase is still under examination, the detailed investigations of the loss-of- function mutant of the CRK5 protein kinase revealed that this Ser/Thr type kinase may participate not only in gravitropic response but also in the regulation of the response to abiotic stress.

Acknowledgement. This work was partly supported by the Hungarian-Romanian grant TET_12_RO_1-2013-0010 and Romanian-Hungarian Bilateral Cooperation project 2013-2014/668.

REFERENCES

Benková, E., Michniewicz, M., Sauer, M., Teichmann, T., Seifertová, D., Jürgens, G., Friml, J. (2003) Local, efflux-dependent auxin gradients as a common module for plant organ formation, *Cell,* **115**, 591-602

Blancaflor, E.B. (2013) Regulation of plant gravity sensing and signaling by the actin cytoskeleton, *Am. J. Bot.*, **100**, 143-152

Darwin, C. (1880) *The power of movement in plants*, London, John Murray

Feraru, E., Friml. J. (2008) PIN Polar Targeting, *Plant Physiology*, **147**, 1553-1559

Friml, J. (2010) Subcellular trafficking of PIN auxin efflux carriers in auxin transport, *Eur. J. Cell Biol.*, **89**, 231-235

Gong, D.M., Guo, Y., Jagendorf, A.T., Zhu, J.K. (2002) Biochemical characterization of the *Arabidopsis* protein kinase SOS2 that functions in salt tolerance, *Plant Physiology*, **130**, 256-264

Hardie, D.G., Carling, D., Carlson, M. (1998) The AMP-activated/SNF1 protein kinase subfamily: metabolic sensors of the eukaryotic cells?, *Annual Review Biochemistry*, **67**, 821-855

Harmon, A.C., Gribskov, M., Harper, J.F. (2000) CDPKs - a kinase for every Ca^{2+} signal?, *Trends Plant Sci.*, **5**, 154-159

Harmon, A.C. (2003) Calcium-regulated protein kinases of plants, *Gravity Space Biol. Bull.*, **16**, 83-90

Harper, J.F., Breton, G., Harmon, A. (2004) Decoding Ca (2+) signals through plant protein kinases, *Annu. Rev. Plant Biol.*, **55**, 263-288

Harper, J.F., Harmon, A.C. (2005) Plants, symbiosis and parasites: a calcium signaling connection, *Nature Reviews Molecular Cell Biology*, **6**, 555-566

Hashiguchi, Y., Tasaka, M., Morita, M.T. (2013) Mechanism of higher plant gravity sensing, *Am. J. Bot.*, **100**, 91-100

Hrabak, E.M., Chan, C.W., Gribskov, M., Harper, J.F., Choi, J.H., Halford, N., Kudla, J., Luan, S., Nimmo, H.G., Sussman, M.R., Thomas, M., Walker-Simmons, K., Zhu, J.K., Harmon, A.C. (2003) The *Arabidopsis* CDPK-SnRK superfamily of protein kinases, *Plant Physiology*, **132**, 666-680

Li, R.J., Hua, W., Lu, Y.T. (2006) *Arabidopsis* cytosolic glutamine synthetase AtGLN1; 1 is a potential substrate of AtCRK3 involved in leaf senescence, *Biochemical and Biophysical Research Communication*, **342**, 119-126

Miwa, K., Takano, J., Omori, H., Seki, M., Shinozaki, K., Fujiwara, T. (2007) Plants tolerant of high boron levels, *Science*, **318**, 1417

Morita, M.T. (2010) Directional gravity sensing in gravitropism, *Annu. Rev. Plant Biol.*, **61**, 705-20

Ottenschläger, I., Wolff, P., Wolverton, C., Bhalerao, R.P., Sandberg, G., Ishikawa, H., Evans, M., Palme, K. (2003) Gravity-regulated differential auxin transport from columella to lateral root cap cells, *Proc. Nat. Acad. Sci. U.S.A*, **100**, 2987-2991

Palme, K., Gälweiler, L. (1999) PIN-pointing the molecular basis of auxin transport, *Curr. Opin. Plant Biol*, **2**, 375-381

Petricka, J.J., Winter, C.M., Benfey, P.N. (2012) Control of *Arabidopsis* root development, *Ann. Rev. Plant Biol.*, **63**, 563-90

Petrov, V.D., van Breusegem, F. (2012) Hydrogene peroxide a central hub for information flow in plant cells, *AoB PLANTS*, pls014

Podell, S., Gribskov, M. (2004) Predicting N-terminal myristoylation sites in plant proteins, *BMC Genomics*, **5**, 37-52

Quint, M., Gray, W.M. (2006) Auxin signaling, *Curr Opin Plant Biol*, **9**, 448-453

Ren, D., Yang, H., Zhang, S. (2002) Cell death mediated by MAPK is associated with hydrogen peroxide production in Arabidopsis, *J. Biol. Chem.*, **277**, 559-565

Rigó, G., Ayaydin F., Szabados L., Koncz C., Cséplő A. (2008) Suspension protoplasts as useful experimental tool to study localization of GFP-tagged proteins in *Arabidopsis thaliana*, *Acta Biol. Szeged*., 52, 59-61

Rigó, G., Ayaydin, F., Kovács, H., Szabados, L., Cseplo, A. (2011) AtCRK5, a CDPK-related serine/threonine protein kinase may participate in regulation of salt tolerance in *Arabidopsis thaliana*, In: *Proceedings of the Conference "Protection of the Environment and the Climate": TÁMOP-Humboldt College for Environment and Climate Protection*, Palocz-Andresen, M., Nemeth, R., Szalay, D. (ed), Sopron, University of West Hungary, 70-74

Rigó, G., Ayaydin, F., Tietz, O., Zsigmond, L., Kovacs, H., Pay, A., Salchert, K., Darula, Z., Medzihradszky, K. F., Szabados, L., Palme, K., Koncz, C., Cseplo, A. (2013) Inactivation of plasma membrane-localized CDPK-RELATED KINASE5 decelerates PIN2 exocytosis and root gravitropic response in *Arabidopsis*, *Plant Cell*, **25**,1592-1608

Saini, S., Sharma, I., Kaur, N., Pati, P.K. (2013) Auxin: a master regulator in plant root development, *Plant Cell Rep.*, **32**, 741-757

Sauer, M., Robert, S., Kleine-Vehn, J. (2013) Auxin: simply complicated, *J. Exp. Bot.*, **64**, 2565-2577

Scheres, B., Benfey, P., Dolan, L. (2002) Root development, *Arabidopsis Book*, **1**, e0101

Takanoa, J., Tanakab, M., Toyodab, A., Miwab, K., Kasaib, K., Fujib, K., Onouchia, H., Naitoa, S., Fujiwarab, T. (2010) Polar localization and degradation of *Arabidopsis* boron transporters through distinct trafficking pathways, *Proc. Natl. Acad. Sci.*, **107**, 5220-5225

The *Arabidopsis* Genome Initiative (2000) Analysis of the genome sequence of the flowering plant *Arabidopsis thaliana*, *Nature*, **408**, 796-815

Umezawa, T, Yoshida, R., Maruyama, K., Yamaguchi-Shinozaki, K., Shinozaki, K. (2004) SNRK2C, a SNF1-related protein kinase 2, improve drought tolerance by controlling stress-responsive gene expression in *Arabidopsis thaliana*, *Proc. Natl. Acad. Sci., USA,* **101**,17306-17311

Went, F. W. (1974) Reflections and speculations, *Annu. Rev. Plant Physiol.*, **25**, 1-26

STUDIA UNIVERSITATIS BABEŞ-BOLYAI BIOLOGIA, LIX, 1, 2014 (p. 71-78)

IN VITRO CYTOGENETIC STUDY OF THE MITOTIC DIVISION IN BASIL (*OCIMUM BASILICUM* L.) PLANTS

DIANA-ELENA MAFTEI[1,✉]

SUMMARY. The cytogenetic studies on the in vitro - derived plants of Ocimum basilicum L. (var. Greek basil) aimed to evince if and to what extent this type of conventional culture altered the mitotic cell division. There were some differences regarding the mitotic index, the distribution of cells during each phase of mitosis, and also regarding the percentage of abnormal ana-telophases. The shoots obtained on a culture medium supplemented with indole butyric acid (IB2 medium variant) displayed the highest mitotic index (33.09), compared to the control (16.14) and to the other studied variants. The lowest mitotic index (7.39) was registered on the A2 variant, enriched with indole acetic acid. Regarding the cell distribution on mitotic phases, the highest percentage was registered by prophases, followed by telophases, metaphases, and anaphases (in all the analyzed variants, including the control).

Keywords: basil, cytogenetic analysis, mitotic index.

Introduction

Basil (*Ocimum basilicum* L.) is a herbaceous, annual plant belonging to the Lamiaceae family. It requires great amounts of light and high temperatures, being resistant to drought (Muntean, 1990; Păun *et al*., 1988; Pârvu, 2000; Tiță, 2003). Its essential oil comprises estragol, eugenol, linalool, citral, camphor, cineol etc (Stănescu *et al*., 2002; Tiță, 2003). The main actions of basil volatile oil are: digestive, antispastic, antinauseous, carminative, choleretic, antifungic, stomachic, galactagogue, diuretic (Stănescu, 2002). Taking into account that basil is a very important plant from a pharmaceutical and economical point of view, morphogenetic reactions in *in vitro* culture have been tested, as well as some explants' growth and development on several hormonali formulae, in order to evince possible valuable genotypes and to develop an efficient technology for their micropropagation. The present paper reveals several data on the cytogenetic studies in basil, that were aimed to depict the influence of the *in vitro* culture system and of the growth regulators

[1]✉ ***Corresponding author: Diana - Elena Maftei***, *University "Vasile Alecsandri" of Bacău, Faculty of Sciences, Dpt. of Biology, Ecology and Environmental Protection, +400234542411, 157 Calea Mărăşeşti, Bacău, Romania, E-mail diana.maftei@ub.ro*

within the culture medium on the mitotic index, on the frequency of the abnormal ana-telophases in the mitosis of root meristems, and the range of chromosomal abnormalities, as well. The chromosomal aberrations, their type and frequency are the subject of another research paper on *Ocimum basilicum* L. It was acknowledged that the *in vitro* culture itself triggers a great genetic (somaclonal) variability, that may be further used in amelioration.

Materials and methods

Ever since the 19th century – the moment chromosomes were discovered (Hertwig, 1875), several methods of analysis were perfected, for their study during both the mitotic and the meiotic cell division. One should consider the following essential aspects:

1. To determine the chromosome number, their shape and size during mitosis, and to prepare the karyotype for the respective species;
2. To study the intra- and interspecific chromosome and gene transfer;
3. To depict ploidy level for the intraspecific, interspecific, and intergeneric hybrids, and of the plants treated with chemical substances that induce polyploidy;
4. The study of aneuploids and gene arrangement on chromosomes;
5. To detect the homology degree of the chromosomes by means of studying metaphase I of meiosis and their splitting during other phases of cell division for the interspecific and intergeneric hybrids;
6. To study the chromosomal alterations (numeric or structural) caused by physical or chemical mutagens (Raicu, 1987).

Cytogenetic studies have been conducted on basil roots of 1.5 to 3 cm in length, harvested from vitroplants grown on different nutritive medium variants of MS (Murashige – Skoog, 1962). The original plant belongs to the variety Greek basil, brought from Greece, and cultivated at the 'Stejarul' Research Centre in Piatra Neamt. The control variant was represented by small roots obtained from vitroplants grown on hormone-free MS. The results were compared to the control sample, represented by roots grown *in vitro* on the basic Murashige-Skoog culture medium (hormone-free). The medium variants were: A_2 (comprising 2 ml/l^{-1} indole acetic acid), N_2 (enriched with 2 ml/l^{-1} naphthylacetic acid), BA_1 (comprising 1 ml/l^{-1} benzylaminopurine and 0.5 ml/l^{-1} indole acetic acid), B_2 (2 ml/l^{-1} benzylaminopurine), B_{02} (0.2 ml/l^{-1} benzylaminopurine), IB_2 (2 ml/l^{-1} indole butyric acid).

The plant material was fixed in Farmer solution and hydrolysed with HCl 18.5 % for 8 -10 minutes.

Colouring was achieved in a basic carbol-fuchsin solution, in concentration of 10%.

The slides were prepared using the *squash* technique.

Fresh materials have been examined under an optical microscope (NOVEX), exposed to intense light using a blue filter to highlight the contrast between chromosomes and cytoplasm. The mitotic index was calculated after the analysis of each 10 microscopic fields/medium variant/preparate. All cells were counted, both in mitosis and in interphase. The 10 microscopic fields were chosen at random on the microscope slide, and the cell density was rather high. The same slides used to calculate the mitotic index were studied to detect the abnormal ana-telophases/ preparate/nutritive medium variant. The latter type of microscopic analysis was possible only using the immersion objective of the microscope (due to the cell size and the large number of chromosomes). The chromosomal aberrations were recorded, as well. The best microscopic preparates were rendered permanent (by means of butanol, xylen, and Canada balm). The photos of different phases of the mitotic division have been taken using the 40x and 100x objectives, with an OLYMPUS digital camera.

Results and discussion

The cytogenetic analysis on *Ocimum basilicum* L. (*Greek basil* variety) was aimed to provide data on the mitotic division, the variation of the mitotic index, the frequency of the abnormal ana-telophases, the types of chromosomal abnormalities (simple or complex) that occur during mitotic division in the root tip meristems of the vitroplants cultured on several medium variants enriched with growth regulators, compared to the control sample (vitroplants regenerated on the hormone-free Murashige – Skoog medium).

The *Ocimum* genus comprises about 160 species and many varieties (Păun *et al*., 1988). The chromosome number is 2n = 48 (x = 12).

The cytogenetic studies during mitotic division revealed that there are still variations of the chromosome number. E.g., for *Ocimum basilicum var. citriodorum* (lemon basil) 2n = 72, and for the *crispum* variety 2n = 52; the basic chromosome number is x = 12. The polyploidy and aneuploidy phenomena lead to variations of the chromosome number in *Ocimum basilicum*, (Mukherjee *et al*, 2005).

Our research was done on *Ocimum basilicum* species, the *Greek basil* variety (the explant-donor plants to start the *in vitro* cultures originated from Greece). It was a difficult task to make the microscope slides using root meristems from the basil vitroplants. Because the roots harvested from the *in vitro* basil regenerants were extremely thin and frail there is a risk that the meristematic tip might remain within the hard culture medium.

There was no record of the mitotic processes within the root meristems of the basil vitroplants in the scientific papers published by other authors. This is the reason for searching and implementing the best techniques regarding the hydrolisis

and the best staining method of the biological material (many lab experiments were performed). In an autochtone study on this species, performed on root meristems from germinated basil seeds, not on roots from vitroplants, a series of modifications issued at the material genetic level of meristematic cells of root tips are presented, as a consequence of the treatment with 4-chlorohydrate-bromo-6-methyl-3-dimethylamino-3-chromanone. The 1/10000 dilution induces the increase of frequency of mitotic dividing cells. The cells with chromosome aberrations are in greater number in treated variants, comparatively with control. The aberration spectrum is enough large. (Axente *et al*., 2006).

The attempts to make the microscope slides using the staining with Schiff reagent and acetic orcein were not successful. The genetic nuclear and extranuclear content can be coloured with Carr solution. The chromosomes were evinced on microscope slides within a fortnight since the roots were immersed in the staining solution (a long period of time, compared to the other tested plant species). It normally takes 24-48 hours of colouring, with certain variations due to the analyzed species and the duration of hydrolysis.

To better highlight the genetic material, the roots were treated with a second staining solution (besides Carr solution): they were coloured with acetic orcein, used instead of acetic water for 10-15 minutes, previous to cell layout on the microscope slide by means of the 'squash' method.

The experimental results for basil include the variation of the mitotic index within the meristems of the vitroplants provided on many variants of the basal Murashige – Skoog medium supplemented with growth regulators; the results were compared to the control variant (shoots provided on the basal MS medium).

In case of the vitroplants that were analyzed cytogenetically, one should take into account that the morphogenetic processes and the cell division are caused by a series of internal and external factors, that influence the explant after inoculation. These factors are: the genotype, the hormonal balance, the physiological stage of the cultivated tissue, eventual pre-treatments applied to the explants or to the donor plants, the plant growth conditions. All these factors act simultaneously and stimulate (more or less) the explant development and the processes within the genome. Nevertheless, it is hard to establish which of these factors has the greatest impact in inducing various types of chromosomal aberrations.

In *Ocimum basilicum*, the meristematic cells of the control plants and of those regenerated on various culture medium variants are small, oblong, rather hard to examine and analyze using the 40X objective of the optic microscope. It was ascertained that the mitotic activity was normal, cells in all phases of division have been registered (Fig. 1-6).

In case of the meristematic cells belonging to the vitroplants grown on B_{02} medium (in which the dividing cells were smaller compared to the other analyzed variants) it was rather frequently noticed the presence of several nucleoli inside the

interphasic nuclei (2-4 nucleoli/nucleus), a phenomenon observed in the BA_1 and IB_2 variants. The cytogenetic tests pointed out that the regenerants from the control variant registered a mitotic index (M.I.) of 16.14. The medium variants enriched with indole butyric acid (IB_2) and with cytokinin+auxin (BA_1) displayed a M.I. far superior, of 33.09 and of 29.41, respectively (Fig. 7).

The vitroplants provided on the A_2 variant (supplemented with indole acetic acid) registered a M.I. lower than the witness: 7.39; similar cases were found for three other variants: N_2 (M.I. = 8.88), B_{02} (M.I. = 9.25) and B_2 (M.I. = 9.26) (Fig. 7).

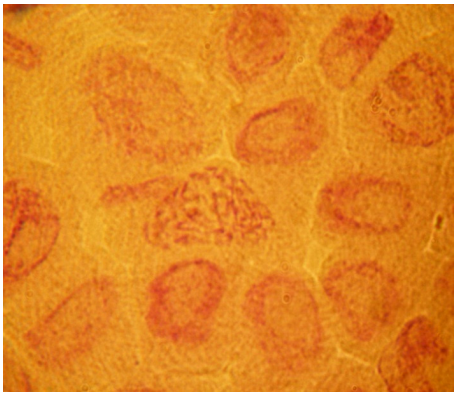

Figure 1. Prophase surrounded by cells in interphase (BA_1 variant)

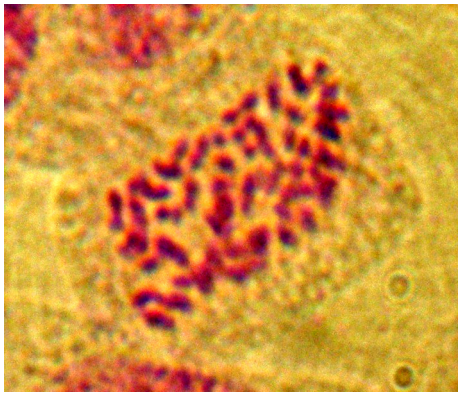

Figure 2. Late prophase (BA_1 variant)

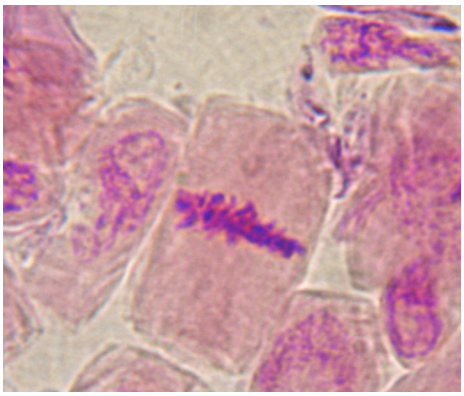

Figure 3. Metaphase (control variant MS)

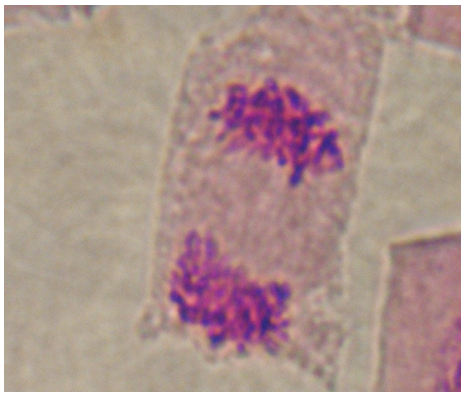

Figure 4. Ana-telophase (BA_1 variant)

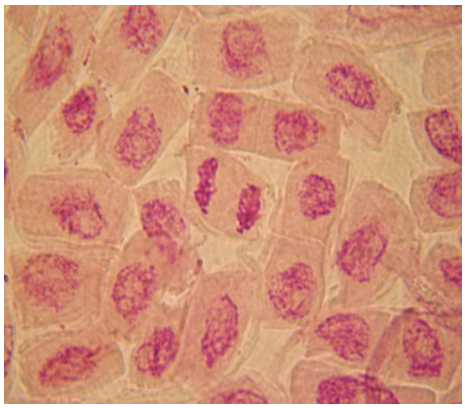

Figure 5. Telophase (BA_1 variant)

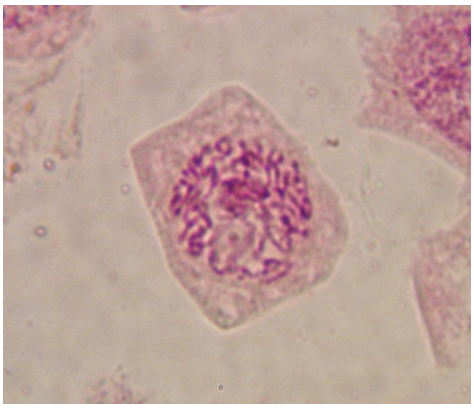

Figure 6. Prophase (BA_1 variant)

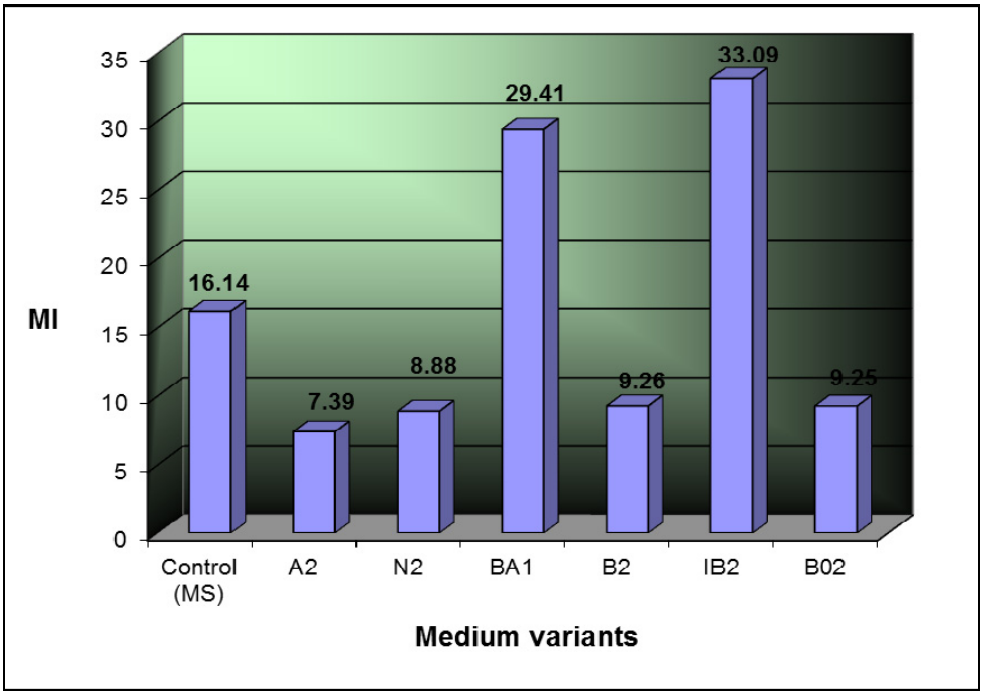

Figure 7. Mitotic index (M.I.) for the vitroplants of *Ocimum basilicum* L.

Table 1.

Mitotic index and number of cells in mitosis in the vitroplants of *Ocimum basilicum* L.

Culture medium	No. of analyzed cells	No. of cells in mitosis	Mitotic index (M.I.)	Cell distribution on mitotic phases							
				PROPHASE		METAPHASE		ANAPHASE		TELOPHASE	
				No. cells	%	No. cells	%	No. cells	%	No. cells	%
MS	5469	883	16.14	513	58.09	160	18.12	45	5.09	165	18.68
A_2	3462	256	7.39	116	45.31	66	25.78	2	0.78	72	28.12
N_2	3940	350	8.88	180	51.42	100	28.57	10	1.00	60	17.14
BA_1	4633	1363	29.41	1180	86.57	74	5.42	16	1.17	93	6.82
B_2	4017	372	9.26	249	66.93	48	12.90	9	2.41	66	17.74
IB_2	2828	936	33.09	828	88.46	36	3.84	4	0.42	68	7.26
B_{02}	3200	296	9.25	212	71.62	40	13.51	4	1.35	40	13.51

Regarding the cell distribution on mitotic phases, the highest percentage was registered by prophases, followed by telophases, metaphases, and anaphases (in all the analyzed variants, including the control). There was one exception: the vitroplants from N_2 medium, in which the percentage of metaphases (28.57%) was higher than the one of the telophases (17.14%).

The number of cells in anaphase decreased in the vitroplants regenerated on several medium variants, compared to the control, excepting the variants A_2 and N_2, where a low percentage of cells in prophase was registered for the control variant (57.93%), compared to 66.93% (B_2 variant), 71.62% (B_{02}), 86.57% (BA_1) and 88.46% (IB_2).

The cytogenetic study on vitroplants of *Ocimum basilicum* L. evinced a normal mitotic activity. Cells in all phases of mitotic division been registered, with a rather low M.I. in the control (16.14), more diminished in the variants A_2 (7.39), N_2 (8.88), B_{02} (9.25) and B_2 (9.26) and higher in the vitroplants regenerated on BA_1 (29.41) and IB_2 (33.09) medium variants (Table 1).

We intend to further expand our cytogenetic studies on this species in order to come with solid conclusions about the influence of the growth regulators on the mitotic division and about the range, frequency and cause of the chromosomal aberrations.

Conclusions

The cytogenetic observations made on root tip meristems of the regenerants obtained by means of *in vitro* cultivation of *Ocimum basilicum* L. have indicated that the growth regulators disturbed the functioning of the mitotic apparatus, i.e.the

mitotic index (M.I.) of the vitroplants was diminished on certain hormonic variants (A_2, N_2, B_{02}, B_2) or augmented on other medium variants (BA_1, IB_2), compared to control plants.

Cells in all phases of mitotic division have been registered.

Further studies should be carried out in order to gain more knowledge about the effect of the growth regulators on the molecular metabolism of the cell division and of the cell cycle.

Acknowledgements. The author would like to thank Prof.dr. Gogu Ghiorghiță (Academy of the Romanian Scientists, Piatra-Neamț Branch, Romania) for his help and suggestions in this scientific study.

REFERENCES

Ahuja, A., Verma, M., Grewal, S. (1982) *Clonal propagation of Ocimum species by tissue culture*. Ind. J. Exp. Biol., **20**, 455-458

Axente, M.F., Căpraru, G., Cîmpeanu, M., Băra, I. (2006) *Cytogenetic effects induced by 4-chlorohydrate-bromo-6-metyl-3-dimethylamino-3-chromanone in Ocimum basilicum* L. species. An. Şt. Univ. „Al.I.Cuza" Iaşi, **VII**, 221-226

Ciulei, I., Grigorescu, E., Stănescu, U. (1993) *Plante medicinale, fitochimie si fitoterapie*, Ed. Medicală, București, **2**, 87 – 90

Ghiorghiţă, G. (1999) *Bazele geneticii,* Ed. Alma Mater, Bacău, pp 377

Maftei, D.E., Ghiorghiţă, G., Nicuţă, D. (2006) *Unele consideraţii privind comportarea in vitro a busuiocului (Ocimum basilicum* L.*)*, An. Şt. Univ."Al.I.Cuza" Iaşi, Ser. Gen. şi Biol. Molec., 151-158

Mukherjee, M., Datta, A.K., Maiti, G.G. (2005) *Chromosome number variation in Ocimum basilicum* L. Cytologia, **70**(4), 455-458

Muntean, L.S. (1990) *Plante medicinale şi aromatice cultivate în România*, Ed. Dacia, Cluj, pp 306

Nuti Ronchi, V. (1990) *Cytogenetics of plant cell cultures*. Progress in Plant Cellular and Molecular Biology, Kluwer Academic Publ., 276-300

Păun, E., Mihalea, A., Dumitrescu, A., Verzea, M., Cojocariu, O. (1988) *Tratat de plante medicinale si aromatice cultivate.* Ed. Acad. RSR, Bucureşti, **2**, 119 – 129

Pârvu, C. (2000) *Universul plantelor. Mică enciclopedie*. Ed. Encicl., Bucureşti, 93-94

Raicu, P. (1987) *Genele şi ingineria genetică*. Ed. Şt. şi Encicl., Bucureşti, 75-97

Sharp, W.R., Evans, D.A. (1981) *Plant Tissue Culture: the Foundation for Genetic Engineering in Higher Plants*. Proc. of the Intern. Symp. on Genet. Engineering, 23-28

Stănescu, U., Miron, A., Hăncianu, M., Aprotosoaie, C. (2002) *Bazele farmaceutice, farmacologice şi clinice ale fitoterapiei*, Ed. „Gr. T. Popa", Iaşi, II, 52, pp 281

Stănescu, U., Miron, A., Hăncianu, M., Aprotosoaie C. (2002) *Plante medicinale de la A la Z; monografii ale produselor de interes farmaceutic*, Ed. „Gr. T. Popa", Iaşi, vol. I, pp 327

Tiţă, I. (2003) *Botanică farmaceutică*, Ed. Did. şi Ped., pp 902

STUDIA UNIVERSITATIS BABEŞ-BOLYAI BIOLOGIA, LIX, 1, 2014 (p. 79-89)

WATER QUALITY ASSESSMENT FROM THE ARIEŞ RIVER CATCHMENT AREA BASED ON BENTHIC INVERTEBRATES

ANA-MARIA PANAITESCU[1,✉], MIRELA CÎMPEAN[1] and KARINA PAULA BATTES[1]

SUMMARY. The present study represents the assessment of the Arieş River water quality in its headwaters, an area heavily affected by intensive tourism activities from the Arieşeni resort. The water quality was assessed using three biotic indices based on benthic invertebrate communities: the Extended Biotic Index (E.B.I.), the Biological Monitoring Working Party adapted for Poland (B.M.W.P.-PL) and the Average Score Per Taxon (A.S.P.T.). Seven sampling sites were considered, located both on the main river course and on its main tributaries from the Arieş River headwaters. The structure of the benthic invertebrate communities, together with their indicative values for water quality showed polluted waters at the source of the Arieş River, an area characterized by intense tourism. However, on going downstream, the river exhibited good and high water quality, due to its self-cleaning capacity.

Keywords: A.S.P.T., B.M.W.P.-PL, E.B.I.

Introduction

Assessing river water quality based on benthic invertebrate communities represents one of the methods recommended by the Water Framework Directive 2000/60/EC of the European Parliament.

Benthic invertebrates play a key role in aquatic ecosystems, representing the link between autotrophs, allochthonous input and top predators (Wetzel, 2001). Benthic invertebrates are a heterogeneous group in terms of their feeding behaviour, habitat preferences or development, including both tolerant and intolerant taxa to pollution, habitat alteration or other human impacts (Wetzel, 2001; Verberk *et al.,* 2002). Benthic communities have long been used as bioindicators for monitoring water quality of streams, considering not only pollution but also other anthropogenic influences (Hering *et al.,* 2006).

[1] *Department of Taxonomy and Ecology, Faculty of Biology and Geology, Babeş-Bolyai University, 5-7 Clinicilor Street, 400006, Cluj-Napoca, Romania.*

✉ ***Corresponding author: Ana-Maria Panaitescu**, Babeş-Bolyai University, Faculty of Biology and Geology, M. Kogălniceanu 1, 400084 Cluj-Napoca, Romania.*
E-mail: anamariapanaitescu@yahoo.com

The Arieş River catchment area represented the subject for many hydrobiological studies, focused on algae, benthic invertebrates or fish communities (Momeu and Peterfi, 2007; Momeu *et al.,* 2007; 2009; Cupşa, 2009), but also on interstitial fauna (Moldovan *et al.,* 2011). These studies showed the major negative impact caused by mining in Roşia Montană and Roşia Poieni areas. The present paper focuses on the headwaters of the Arieş River, upstream of these mining regions, where a prosperous touristic resort developed in the past 20 years. Thus, the objectives of the present paper are: (1) to analyze the structure of the benthic invertebrate communities from the Arieş River headwaters and its tributaries in the area; (2) to present their dynamics and distribution; and (3) to assess the water quality from the study area.

Materials and methods

The Arieş River flows through the Apuseni Mountains (Transylvania, Romania), having its source on the North-Eastern part of the Cucurbăta Massif (1761 m altitude) and a length of 164 km (Ujvari, 1972).

The study area is located in the upper Arieş River catchment area, in the Arieşeni Commune, Alba county, which consists of 18 smaller villages, with a total surface of 6310 ha. The Arieşeni commune is traversed by the springs of the Arieşul Mare River, flowing eastwards on a distance of 14.2 km (Ghinea, 2002). In fact, the Arieşul Mare River is formed in the Arieşeni Commune, and its main tributaries from this area are: the Cobleş River (with a length of 8.5 km), the Ştei River (2 km in length) and the Galbena River (6 km in length).

Benthic invertebrates were sampled from seven sites: three located on the main river course and four located on its main tributaries from the area (The Galbena, the Ştei and the Cobleş Rivers) (Tables 1, 2).

Table 1.

The seven sampling sites with their codes used for the present paper

Sampling site name	Sampling site code
The Arieş River – source	S1
The Arieş River – upstream Arieşeni	S2
The Arieş River – downstream Arieşeni	S3
The Galbena River – source	S4
The Galbena River – upstream the junction with the Arieş River	S5
The Ştei River – upstream the junction with the Arieş River	S6
The Cobleş River – upstream the junction with the Arieş River	S7

The invertebrate communites were sampled seasonally in 2012: in spring on May the 13th, in summer on August the 5th and in autumn on September the 23rd. The samples were collected in plastic vessels, using a 250 μm mesh net, and then preserved in 4% formaldehyde. Subsequently, the samples were sorted in the laboratory, under a dissecting microscope. Taxonomical identifications were made to the genus level for Plecoptera (stoneflies), Ephemeroptera (mayflies), Turbellaria and Hirudinea; and to the family level for Oligochaeta, Copepoda, Amphipoda, Trichoptera (caddisflies), Diptera, Coleoptera, Odonata and Heteroptera. Based on these analyses, the following

biotic indices were calculated: the Extended Biotic Index (E.B.I.) (Ghetti, 1997), the Biological Monitoring Working Party, adapted for Poland (B.M.W.P.-PL) and the Average Score Per Taxon (A.S.P.T.) (Walley and Hawkes, 1996; 1997).

Table 2.

Location of the seven sampling sites from the upper Arieş catchment area, with their major characteristics (sp – spring 2012; su – summer 2012; au – autumn 2012)

Sampling site	Altitude (m a.s.l.)	GPS coordinates	Riverbed width (m)			Maximum depth (m)		
			sp	su	au	sp	su	Au
S1	1172	N 46º30'54.43" E 22º40'51.67"	1.5	1	0.7	0.25	0.25	0.20
S2	1099	N 46º30'29.60" E 22º41'36.93"	3	3	2	0.30	0.30	0.30
S3	799	N 46º27'25.52" E 22º47'40.40"	9	9	6	0.30	0.30	0.40
S4	1419	N 46º28'18.19" E 22º41'07.07"	2	2	2	0.15	0.15	0.15
S5	921	N 46º28'36.53" E 22º44'52.55"	3	2.5	3	0.40	0.40	0.20
S6	908	N 46º28'28.62" E 22º44'25.05."	5	4	3	0.50	0.40	0.60
S7	878	N 46º28'35.50" E 22º45'39.34"	8	8	8	0.40	0.40	0.30

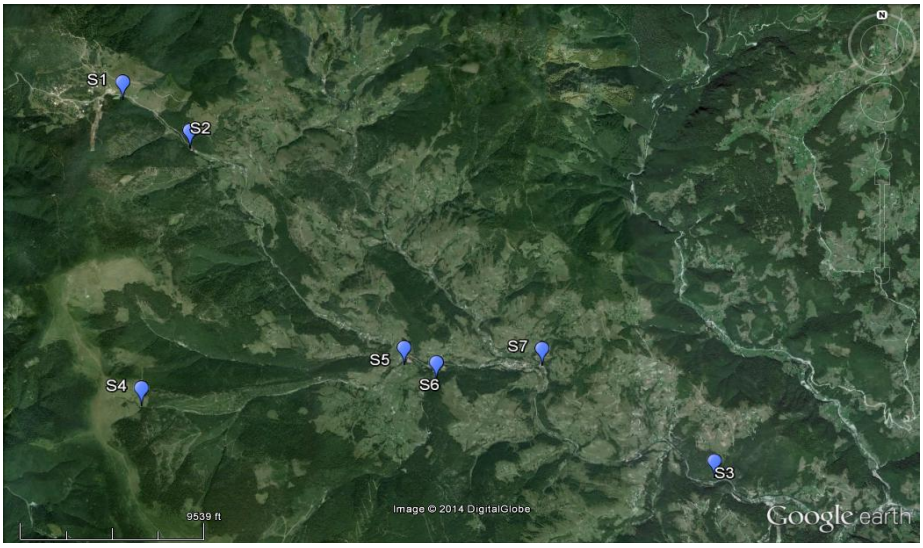

Figure 1. Location of the seven sampling sites from the Arieş catchment area (S1 -The Arieş River – source; S2 -The Arieş River – upstream Arieşeni; S3 -The Arieş River – downstream Arieşeni; S4 -The Galbena River – source; S5 -The Galbena River – upstream the junction with the Arieş River; S6 -The Ştei River – upstream the junction with the Arieş River; S7 -The Cobleş River – upstream the junction with the Arieş River) (source: GoogleEarth)

Results and discussion

The relative percentage abundance was calculated in order to illustrate the structure and dynamics of aquatic invertebrate communities from all the sites sampled in spring, summer and autumn 2012 (Fig. 2 – 4).

Chironomid larvae represended the group with the dominant percentage abundance in all sampling sites, in all three seasons.

At the sampling site S1 - The Arieș River – source, chironomids and oligochaetes recorded the highest values of percentage abundance, because of their ability to survive in very low dissolved oxygen conditions (Abel, 2002). These high percentages indicated organic pollution caused by domestic wastes coming from the touristic guest houses near the Arieşeni ski track. These results differ from the data published by Cupșa (2009), who found low numbers of oligochaetes at the Arieș River source in 2005. These higher oligochaete percentages in the river headwaters could be caused by the increasing number of guest houses, appeared in the past few years, directly related to waste waters and thus organic pollution.

Invertebrates characteristic to clean mountainous rivers: stoneflies, mayflies and caddisflies appeared together with oligochaetes and chironomids at the other sampling sites located on the main river course (S2-The Arieș River – upstream Arieşeni, S3-The Arieș River – downstream Arieşeni), but also at the sites situated on the three tributaries (S4-The Galbena River – source, S5-The Galbena River – upstream the junction with the Arieș River, S6-The Ștei River – upstream the junction with the Arieș River, S7-The Cobleș River – upstream the junction with the Arieș River) (Fig. 2 - 4).

In spring, chironomid larvae dominated the invertebrate communities from the sampling sites S2 and S3, but stoneflies and mayflies became abundand in summer and autumn. Thus, after the organic pollution indicated by tolerant taxa like chironomids, the river was able to recover and intolerant groups returned probably from the tributaries.

Invertebrate communities found in the main tributaries: the Galbena, the Cobleș and the Stre Rivers included the following groups: Plecoptera, Ephemeroptera, Trichoptera and Amphipoda (Fig. 3 and 4), all represended by a small number in S1, the Arieș River source. Thus, the tributaries acted as an important sink of biodiversity, used to repopulate the regions affected by pollution.

For the assessment of water quality, the benthic invertebrates were identified to the taxonomical level required by each of the three indices: the E.B.I. (Ghetti, 1997), the B.M.W.P.-PL and the A.S.P.T. (Walley and Hawkes, 1996; 1997).

A total number of 64 taxa were identified at the seven sampling sites (Table 3). The lowest number of taxa (28) was found at sampling site S1. The taxa richness increased on going downstream, with 31 at S2 and 33 at S3, respectively. Higher numbers of taxa were found on the tributaries: 37 on the Galbena River (sites S4 and S5), 38 on the Ștei River and 39 on the Cobleș River.

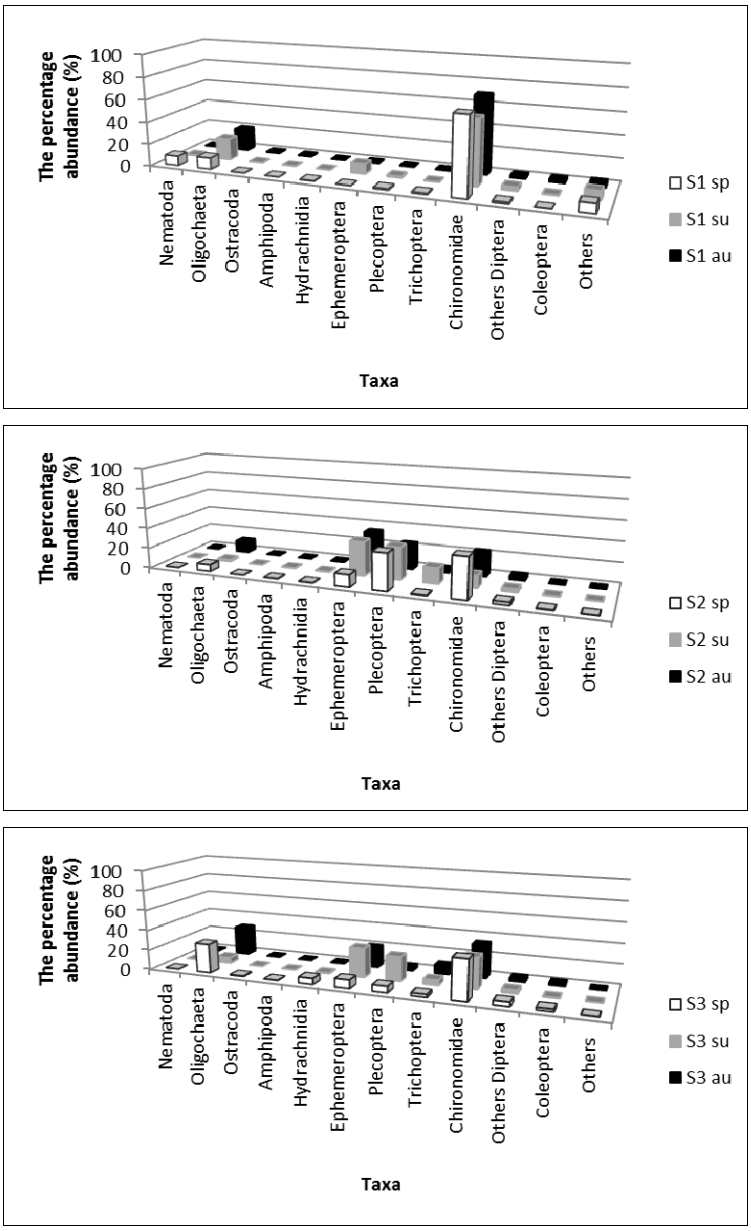

Figure 2. The percentage abundance (%) of benthic invertebrate groups from three sampling sites: S1-The Arieş River – source, S2-The Arieş River – upstream Arieşeni, S3-The Arieş River – downstream Arieşeni, in three different seasons (sp- spring, su- summer, au- autumn)

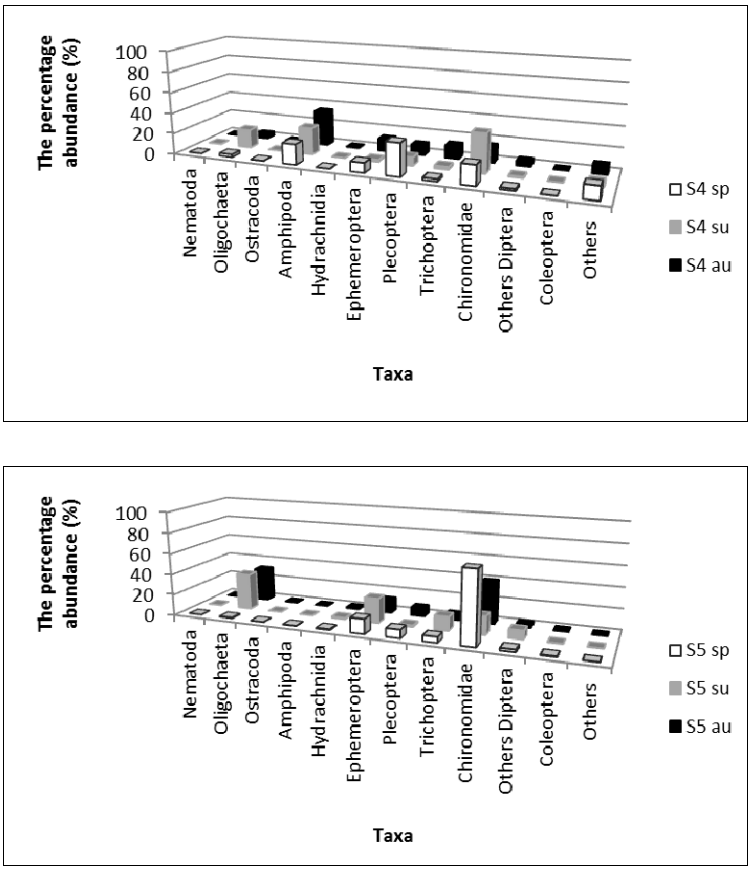

Figure 3. The percentage abundance (%) of benthic invertebrate groups from two sampling sites: S4-The Galbena River – source, S5-The Galbena River – upstream the junction with the Arieş River, in three different seasons (sp- spring, su- summer, au- autumn)

The lowest number of Ephemeroptera, Plecoptera, Trichoptera and Diptera was recorded at sampling site S1, while the sites located on the tributaries (S4 – S7) were characterized by a higher biodiversity, acting as a source for river repopulation after pollution.

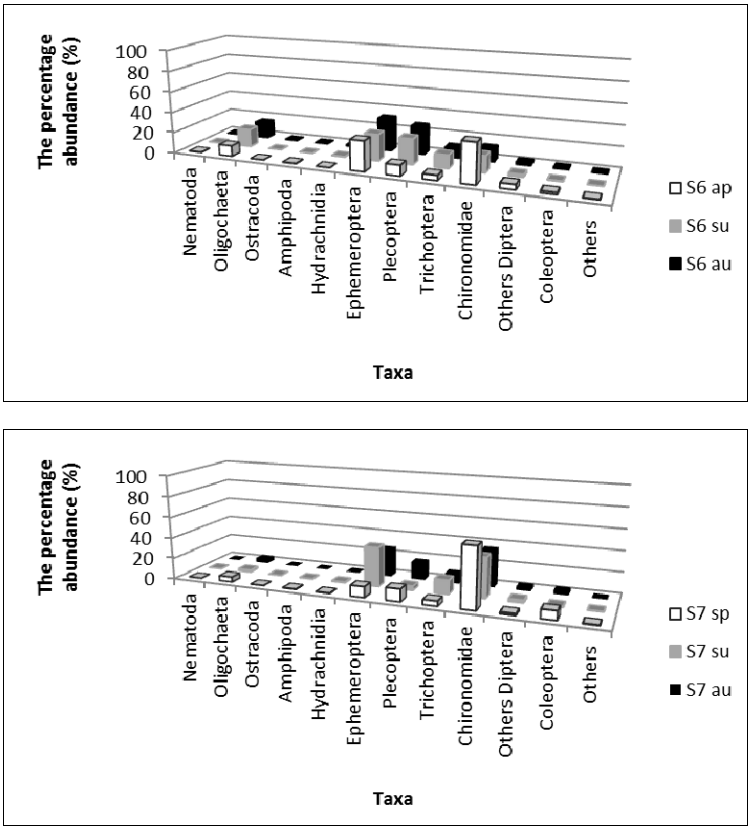

Figure 4. The percentage abundance (%) of benthic invertebrate groups from two sampling sites: S6-The Ştei River – upstream the junction with the Arieş River, S7-The Cobleş River – upstream the junction with the Arieş River, in three different seasons (sp- spring, su- summer, au- autumn)

The three water quality indices (E.B.I., B.M.W.P.-PL and A.S.P.T.) were calculated based on the structure of benthic invertebrate communities from the seven sampling sites. The water quality classes were calculated for each season separatelly (Table 4).

Table 3.

List of benthic invertebrate taxa identified in the seven sampling sites located on the main river course and the main tributaries of the Arieș River (S1-The Arieș River – source, S2-The Arieș River – upstream Arieșeni, S3-The Arieș River – downstream Arieșeni, S4-The Galbena River – source, S5-The Galbena River – upstream the junction with the Arieș River, S6-The Ștei River – upstream the junction with the Arieș River, S7-The Cobleș River – upstream the junction with the Arieș River)

Taxa		**Sites**						
		S1	**S2**	**S3**	**S4**	**S5**	**S6**	**S7**
Nematoda		x	x	x	x	x	x	x
Oligochaeta	Enchytraeidae	x	x	x	x	x	x	x
	Gordiidae				x			
	Haplotaxidae	x	x	x	x	x	x	x
	Lumbricidae	x	x	x	x	x	x	x
	Lumbriculidae	x		x	x	x	x	x
	Naididae	x	x	x	x	x	x	x
	Tubificidae	x	x	x	x	x		x
Copepoda		x						x
Ostracoda		x		x	x			
Amphipoda			x	x	x	x	x	x
Hydrachnidia		x	x	x	x	x		x
Ephemeroptera	*Acentrella*				x	x	x	
	Baetis	x	x	x	x	x	x	x
	Caenis			x			x	x
	Centroptilum							x
	Cloeon	x						
	Echdyonurus		x	x	x	x	x	x
	Epeorus			x			x	x
	Ephemera			x				x
	Habroleptoides		x	x		x	x	x
	Habrophlebia					x		x
	Seratella		x	x		x	x	x
	Rhithrogena		x	x	x	x	x	x
	Torleya		x	x		x		x
Plecoptera	*Arcynopteryx*			x	x	x	x	
	Besdolus				x			
	Brachyptera						x	
	Isoperla		x		x		x	
	Leuctra	x	x	x	x	x	x	x
	Nemoura	x	x		x	x	x	x
	Perla		x	x		x	x	x
	Perlodes		x	x		x	x	x
	Protonemura		x		x	x	x	
	Taeniopteryx						x	

Table 3. continued

Trichoptera	Brachycentridae	x						
	Goeridae					x	x	
	Hydropsychidae		x	x		x	x	x
	Hydroptilidae					x		
	Lepidostomatidae						x	
	Limnephilidae	x	x	x	x	x	x	x
	Polycentropodidae		x		x		x	x
	Rhyacophilidae		x	x	x	x	x	x
Diptera	Athericidae			x	x	x	x	x
	Blephariceridae					x	x	
	Ceratopogonidae	x	x	x	x		x	x
	Chironomidae	x	x	x	x	x	x	x
	Dixidae				x			
	Empididae	x	x	x	x	x	x	x
	Limoniidae	x	x	x	x	x	x	x
	Psychodidae				x			
	Simuliidae	x	x		x	x	x	x
	Syrphidae				x			
	Tabanidae	x						
	Tipulidae	x						
Coleoptera	Dytiscidae	x				x		
	Elminthidae		x	x	x	x	x	x
	Hydrophilidae							x
Altele	Aeshnidae	x						
	Ancylus				x			x
	Dugesia	x		x	x	x		x
	Helobdella				x			
	Lymnaeidae	x						
	Sphaeriidae	x	x					

According to E.B.I., the water quality classes were higher for all seven sampling sites, while B.M.W.P.-PL and A.S.P.T. assigned lower quality classes to all sites. An ”accepted quality class” was considered, averaging the quality classes showed by all the three indices. Only sampling site S1 was rated with moderate water quality (class III); the rest of the sites were considered of good and high water quality (class I-II) (Table 4).

Table 4.

The quality classes calculated according to the three biotic indices, and the accepted quality classes, for the sampling sites considered in the Arieş catchment area (E.B.I. – Extended Biotic Index, B.M.W.P. – Biological Monitoring Working Party, A.S.P.T. – Average Score Per Taxon, S1-The Arieş River – source, S2-The Arieş River – upstream Arieşeni, S3-The Arieş River – downstream Arieşeni, S4-The Galbena River – source, S5-The Galbena River – upstream the junction with the Arieş River, S6-The Ştei River – upstream the junction with the Arieş River, S7-The Cobleş River – upstream the junction with the Arieş River)

Sites	E.B.I. quality classes	B.M.W.P. quality classes	A.S.P.T. quality classes	Accepted quality classes
S1	II-III	III-IV	III	III
S2	I	II	II	I-II
S3	I	II	II	I-II
S4	I	II	II	I-II
S5	I	I-II	II	I-II
S6	I	I-II	I-II	I-II
S7	I	I-II	II	I-II

Conclusions

A total of 64 taxa were identified in the study area, with a minimum richness of 28 at the Arieş River source, a region heavily affected by tourism. The highest number of taxa was found on the three river tributaries from the area, so they might represent an important biodiversity source in repopulating affected river stretches.

In 2012, the water quality from the upper Arieş river catchment area, based on benthic invertebrate communities, was good and high (class I-II), except for the touristic region near the ski track from Arieşeni (where sampling site S1 was located). The severe pollution from this area could be caused by intensive tourism, massive deforestation, overgrazing, but also by the prolonged drought that led to low river discharges, decreasing the self-cleaning capacity of the river.

REFERENCES

Abel, P.D. (2002) *Water Pollution Biology, 2nd Edition*, Technology & Engineering, pp 296

Cupşa, D. (2009) Preliminary data upon the aquatic oligochaeta communities in the upper sector of Arieş River (Transylvania, Romania), *Transylv. Rev. Syst. Ecol. Res*., **7**, 69-76

Ghetti, P.F. (1997) *Manuale di aplicazione - Indice Biotico Esteso (I.B.E.) I macroinvertebrati nel controllo della qualita degli ambienti di acque currenti*, Ed. Provincia Autonoma di Trento, Agenzia provinciale per la protezione dell'ambiente, Trento, pp 222

Ghinea, D. (2002) *Enciclopedia geografică a României, Ediția 3,* Editura Enciclipedică, București

Hering, D., Johnson, R.K., Kramm, S., Schmutz, S., Szoszkiewicz, K., Verdonschot P.F.M. (2006) Assessment of European streams with diatoms, macrophytes, macroinvertebrates and fish: a comparative metric-based analysis of organism response to stress, *Freshwater Biol*., **51**, 1757–1785

Momeu L., Peterfi, L.S. (2007) Water quality evaluation of the drainage basin of the Arieș river, using epilithic diatoms as bioindicators, *Contrib. Bot*., **XLII**, 57 - 65

Momeu, L., Battes K.W., Pricope, F., Avram, A., Battes, K.P., Cîmpean, M., Ureche, D., Stoica, I. (2007) Preliminary data on algal, macroinvertebrate and fish communities from the Arieș catchment area, Transylvania, Romania, *Studia UBB Biologia*, **LII(1),** 25-36

Momeu, L., Battes, K.W., Battes, K.P., Stoica, I., Avram, A., Cîmpean, M., Pricope, F., Ureche, D. (2009) Algae, macroinvertebrate and fish communities from the Arieș River catchment area (Transylvania, Romania), *Transylv. Rev. Syst. Ecol. Res*., **7**, 149-181

Moldovan, O.T., Levei, E., Banciu, M., Banciu, H.L., Marin, C., Pavelescu, C., Brad, T., Cîmpean, M., Meleg, I., Iepure, S., Povară, I. (2011) Spatial distribution patterns of the hyporheic invertebrate communities in a polluted river in Romania, *Hydrobiologia*, **669**, 63–82

Ujvari, I. (1972) *Geografia apelor României*, Ed. Ştiinţifică, Bucureşti, pp 464

Verberk, W.C.E.P., Brock, A.M.T., van Duinen, G.A., van Es, M., Kuper, J.T., Peeters, T.M.J., Smits, M.J.A., Timan, L., Esselink, H. (2002) Seasonal and spatial patterns in macroinvertebrate assemblages in a heterogeneous landscape, *Proceedings of Experimental and Applied Entomology*, **13**, 35-43

Walley, W.J., Hawkes, H.A. (1996) A computer-based reappraisal of Biological Monitoring Working Party scores using data from the 1990 River Quality Survey of England and Wales, *Water Res.*, **30(9)**, 2086-2094

Walley, W.J., Hawkes, H.A. (1997) A computer-based development of the Biological Monitoring Working Party score system incorporating abundance rating, biotope type and indicator value, *Water Res*., **31(2)**, 201-210

Wetzel R. G. (2001) *Limnology, Lake and river ecosystems*, Acad. Press, San Diego, pp 1006

*** (2000) Directive 2000/60/EC of the European Parliament and of the Council of 23 October 2000 establishing a framework for Community action in the field of water policy, Official Journal of the European Communities, L327/72

STUDIA UNIVERSITATIS BABEŞ-BOLYAI BIOLOGIA, LIX, 1, 2014 (p. 91-96)

EFFICIENT METHODS IN TRAPPING WATER RAILS (*RALLUS AQUATICUS*) AND LITTLE CRAKE (*PORZANA PARVA*) FOR BIOLOGICAL STUDIES

ALEXANDRU-NICOLAE STERMIN[1], LIVIU RĂZVAN PRIPON[2], ALIN DAVID[1]✉, ELIANA SEVIANU[3] and IOAN COROIU[1]

SUMMARY. Water rail (*Rallus aquaticus*) and little crake (*Porzana parva*) inhabit wetlands habitats which are hard to penetrate, therefore capturing rails is quite difficult. But this method is in some cases necessary for studies on their biology We shall describe and evaluate two types of traps used in capturing little rails: Potter's traps and automatic fall traps. Potter's traps were mounted on both sides of a net wall or in a funnel formed by the nets' walls, while the automatic fall traps were located on flat polyester plates. Calculating the catching rate for water rail we found that the highest number of birds was trapped in April, when the birds return from the wintering grounds and establish their territory. The Potter traps have advantages for long term studies, in areas with constant water level and also pose a lower risk on birds, while the automatic fall traps have advantages in high fluctuating water level areas and require little effort for their installation.

Keywords: automatic fall traps, catching rate, Potter's traps, small rail.

Introduction

Water rail (*Rallus aquaticus*) and little crake (*Porzana parva*) are elusive rails species, due to their secret life, hidden in the dense marsh vegetation (Ripley, 1977; Taylor, 1998). Wetland habitats dominated by reed (*Phragmites australis*) or cattail (*Typha latifolia* or *T. angustifolia*) are really hard to penetrate, thus making rail trapping a challenging task (Kearns *et al.,* 1998).

Resolving this task allowed access to the specific biological samples (DNA, feathers and measurements) necessary in studies regarding breeding biology, philogeography and some behavioral aspects. In this paper we are describing and evaluating two types of traps used in capturing water rails and little crakes: Potter's traps (Davis, 1981) and automatic fall traps (Bub, 1991).

[1] *"Babeş-Bolyai" University, Department of Taxonomy and Ecology, Cluj-Napoca, Romania.*
[2] *Merops Association for Science, Education and Environment, Braşov, Romania.*
[3] *"Babeş-Bolyai" University, Department of Environmental Science, Cluj-Napoca, Romania.*
✉ ***Corresponding author: Alin David**, "Babeş-Bolyai" University, Department of Taxonomy and Ecology, Cluj-Napoca, Romania, E-mail: adavid.ubb@gmail.com.*

Materials and methods

We used two different field designs for arranging the Potter's traps. Traps were mounted on both sides of a net wall (Fig 1A), or in a funnel formed by the nets' walls (Fig. 1B).

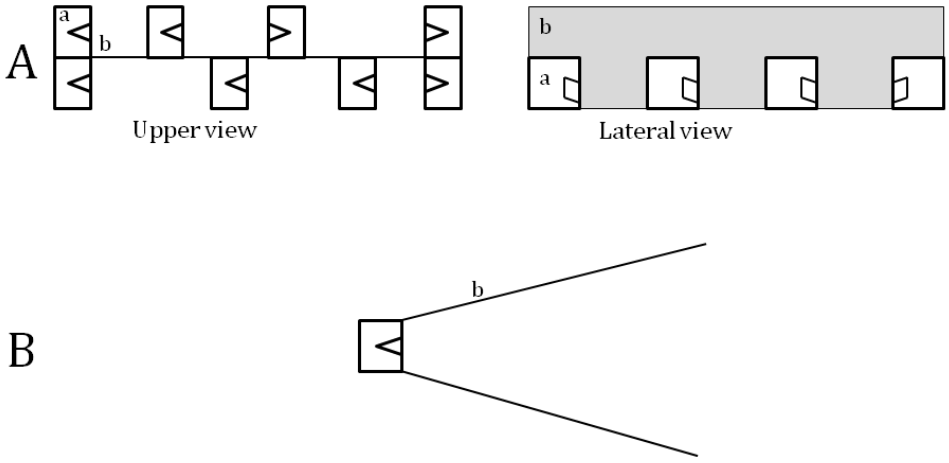

Figure 1. The mounting design of Potter's traps (a- Potter's trap, b- nets wall, A- along a nets wall and B- in a funnel nets).

The design and dimension of the traps are described in Figure 2. The Potter's traps were located on the sides of a net wall, and once the location had been selected, the vegetation was flattened with a 1.5 m long piece of wood. The transect width ranged from 1.7 -2 m, and the length varied depending on the length of the net segment. The net wall was supported and fixed on bamboo sticks. If the water level did not exceed 10 – 20 cm, the traps were fixed at the basis of the net wall. In deeper water, the traps were set at the water level.

In this study we used this type of Potter's traps distribution in three transects, located inside two reed beds where the water level generally ranged from 10 to 20 cm. Transects had a length of 20 m and contained 10 or 11 traps. In 2011 we placed inside the traps small boxes containing fly larvae as bait.

We also used three Potter's traps located on a funnel net wall. In our study three traps of this types were placed, one located in a habitat dominated by reeds, with a water level raging usually from 10 – 20 cm, and two in the habitats dominated by cattail, where the water level exceeded 1 or 1.5 m. This type of traps where checked three to four times a day, first check immediately after sunrise and last check after the night fall.

The automatic fall trap (Bub, 1991) consists of a rectangular metallic wire mesh which is attached to a parallelepiped net (Fig. 3). Located on a flat surface, it is propped with stick made of two complementary pieces, tied with a rope to the distal side of the rectangle. The bait, consisting of live fly and *Tenebrio* sp. larvae, was placed on the string (Fig. 3). Each larva was attached to the rope with a thin wire that was wrapped around it, thus keeping it alive and wiggling to attract the birds. *Tenebrio* sp. larvae, having a larger size than fly larvae, should be more conspicuous and therefore are more easily spotted by the birds.

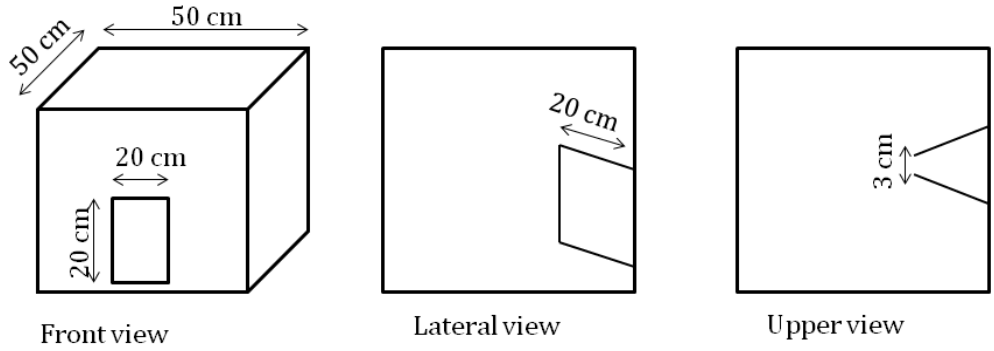

Figure 2. The design of Potter's traps.

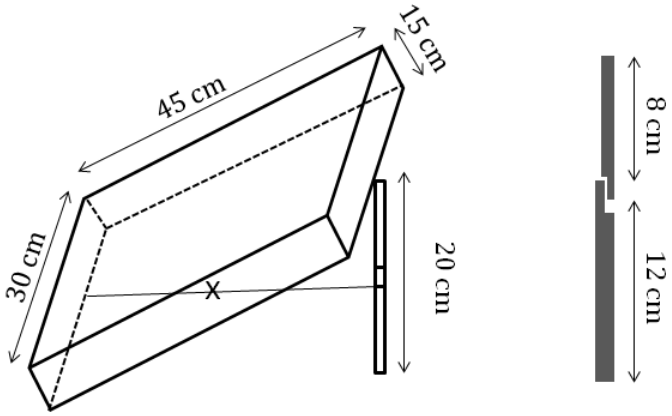

Figure 3. The designee of automatic fall traps.

We used 6 traps in habitats dominated by cattail, where the water level ranged from 1 to 1.5 m and 21 in a habitat dominated by reeds, with a water level raging usually from 10 – 20 cm. We wanted the traps to float on water even when water level fluctuated and therefore we placed each trap on polyester plates covered by reed. Traps were checked at least every two hours, or even once an hour, if the birds' density was higher or if the trap was located inside a bird territory. Frequent checks were necessary to prevent dehydration, as the captured birds had no access to water.

Traps were active from April until the end of July, in different days, from 2010 to 2012. Taking into account the number of water rails captured each month and relating it to the number of traps /days we calculated the catching rate for this species.

All the birds captured in this study were released.

Results

Throughout the entire study period we captured a total of 42 water rails (20 in 2010, 18 in 2011 and 4 in 2012, all of them with Potter's traps) and 10 little crakes (5 in 2011 - with Potter's traps, 5 in 2012 - three with a Potter's and two with the automatic fall traps). Most of the water rails were captured during the morning hours. The little crakes captured in automatic fall traps were caught during the entire day. The highest water rails catching rate (number of birds captured /day) was recorded in April and the lowest in June/July for each of the three years (Table 1).

Table 1.

The water rail catching rate ("-" represents the period when the traps were not active)

	April	**May**	**June**	**July**
2010	0.55	0.30	0.20	-
2011	0.50	0.30	-	0.06
2012	0.15	0.05	-	-

We found that traps covered with reed were more efficient than those left uncovered. Covered traps provide shelter for captured birds, decreasing the stress level and also protecting them against sun light and predators.

In addition to target species, we captured a number of other species. With the Potter's traps were also captured a spotted crake (*Porzana porzana*), four bitterns (*Botaurus stellaris*), two moorhens (*Gallinula chloropus*), six mallards (*Anas platyrhynchos*), a little bittern (*Ixobrychus minutus*), warblers (*Acrocephalus schoenobaenus, A. scirpaceus, A. atrundinaceus* and *Locustella luscinioides*), muskrats (*Ondatra zibethica*), water rats (*Arvicola amphibius*), water turtles (*Emys orbicularis*),

grass snakes (*Natrix natrix*), marsh frogs (*Pelophylax ridibunda*), common spade foot (*Pelobates fuscus*), common rudd (*Scardinius erythrophthalmus*), tench (*Tinca tinca*), european weatherfish (*Misgurnis fossilis*) and crucian carps (*Carassius carassius*).

Discussions

Potter's traps installation requires a considerable effort, but they have a high efficiency over several years, as the vegetation grows around them, still not covering them, this fact being an advantage in long term studies (Table 2). The Potter's traps disadvantage is the fact that they are fixed on bamboo sticks at a certain height, and if the water level changes with more then 10 – 20 cm, they get flooded. Potter's traps should be used only in areas where the water level is relatively constant (Table 2).

Table 2.

Advantages and disadvantages in using Potter's traps or automatic fall traps

	Potter's traps		**Automatic fall traps**	
	Advantage	Disadvantage	Advantage	Disadvantage
Long term studies	x			x
High ranging water level		x	x	
Constant water level	x		x	
Installation effort		x	x	
Low Birds life risk	x			x

Covering the traps with cut vegetation, increased the trapping efficiency and also limited the stress on captured birds. Due to the limited set of data we cannot confirm the favorable effect on trapping efficiency of fly or *Tenebrio* larvae in this type of trap.

In areas with highly variable water level, we found that the automatic fall traps placed on polyester plates were more useful. Another advantage is that these traps are easy to install in the field and require less effort. The disadvantage of this traps is that the birds have no access to water, being exposed to dehydration and sun light, and therefore traps should be checked at least once every one or two hours, but frequent checks might interfere with bird activity in the area.

The highest caching rate was recorded in April, when the birds returned from the wintering grounds and established territory (Cramp and Simmons, 1980; Stermin *et al.,* 2012). During this period, especially males are very active and therefore more trappable. Once their territories and boundaries are defined, the birds activity decrease and so does the capturing rate.

REFERENCES

Bub, H. (1991) *Bird trapping and bird banding – A handbook of methods all over the world.* Corneli University Press, Ithaca, New York

Cramp, S., Simmons, K.E.L. (ed.) (1980) *The birds of Western Palearctic*. Vol. 2. Oxford University Press, Oxford

Dais, G.P. (1981) *Trapping methods for bird ringers*, British trust for Ornithology, Tring

Kearns, G.D., Kwartin, N.B., Brinker, D.F., Haramis, G.M. (1998) Digital playback and improved trep design enhance capture of migrant soras and virginia rails. *J. Field Ornithol*., **69** (3): 466-473

Ripley, S.D. (1977) *Rails of the World, A momograph of the Family Rallidae*. M.F. Feheley Publishers Limited. Toronto

Stermin, A.N., Pripon, L.R., David, A. (2012) The importance of homogenous vs. heterogenous wetlands in rallid (Rallidae) phenological seasons. *Brukenthal Acta Musei*, VII. 3

Taylor, B. (1998) *Rails- A guide to the Rails, Crakes, Gallinules and Coots of the World*. Yale University Press, New Haven and London

STUDIA UNIVERSITATIS BABEŞ-BOLYAI BIOLOGIA, LIX, 1, 2014 (p. 97-100)

=== SHORT COMMUNICATION ===

COMMENT ON MACALIK *ET AL*. (2013) AND AN UPDATE ON THE STATUS OF *SYRINGA JOSIKAEA* (OLEACEAE) IN THE APUSENI MOUNTAINS, ROMANIA

BERTALAN LENDVAY[1,2] and MÁRIA HÖHN[1]✉

SUMMARY. *Syringa josikaea* is a rare and endangered shrub of the Carpathian Mountains. Its distribution was not studied for a century and data on its populations needed re-assessment. Macalik *et al*. (2013) presented data on the distribution of *S. josikaea* in the Apuseni Mountains, which is, however, incomplete. Here we complement the distribution data presented by Macalik *et al*. (2013) from the literature and field survey we performed recently. Populations not mentioned by Macalik *et al*. (2013) exist in the Someşul Cald Valley, the Galbenei Valley and probably also in the Drăgan Valley. We did not find populations reported by earlier literature in the Aleu and Obîrşia Valleys and in the main valley and side valleys of Crişul Repede near Ciucea, Negreni and Lorâu. The population in the Someşul Cald Valley, the largest of all, needs special attention for conserving *S. josikaea* in the Apuseni Mountains.

Keywords: Apuseni Mountains - Romania, distribution, *Syringa josikaea*.

Syringa josikaea Jacq. fil. ex Rchb. is a species of the Carpathians that has attracted the attention of botanists for over a century as it has been considered a Tertiary relict. However, until recently the last comprehensive summary of its distribution was published by Fekete and Blattny (1913), and there was a clear need for the evaluation of its accurate distribution. We have performed a detailed literature and field survey starting in 2009 (Lendvay *et al*., 2012).

In the previous issue of this journal Macalik *et al*. (2013) reported the results of their survey on the actual distribution of *S. josikaea* in the Apuseni Mountains, Romania combined with an environmental niche modeling. Macalik *et al*. (2013) gave detailed data on the size and location of the populations they had found,

[1] *Faculty of Horticulture, Corvinus University of Budapest, Hungary.*
[2] *MTA-MTM-ELTE Research Group for Paleontology, Budapest, Hungary.*
✉ ***Corresponding author: Mária Höhn**, Department of Botany and Soroksár Botanical Garden, Faculty of Horticulture, Corvinus University of Budapest, Villányi út 29-43. 1118 Budapest, Hungary, Phone: +3614826222. Email: maria.hohn@uni-corvinus.hu.*

however the data they presented is not complete with respect to the actual distribution of *S. josikaea* in the Apuseni Mountains. As the accurate knowledge of the distribution of a species as rare as *S. josikaea* is essential for the establishment of its effective conservation strategy, we would like to complement the data presented by Macalik *et al*. (2013) with information on additional populations from our recent survey on the distribution of *S. josikaea* (Lendvay *et al*. 2012).

Macalik *et al*. (2013) claim that *S. josikaea* has gone extinct in the Someşul Cald Valley. However, we found that *S. josikaea* does still exist in the Someşul Cald Valley, moreover this population proved to be the largest of the species in the Apuseni Mountains (Lendvay *et al*., 2012). The exact population size is difficult to estimate due to the dense and extensive clonal growth, but we assess the population to consist of 100 to 200 individual specimens. The location of the population is the extremely remote and hardly accessible bottom of the Someşul Cald Valley between the dam of the Beliş reservoir and the village of Ruseşti. The population in the Someşul Cald Valley is one of the earliest known *S. josikaea* populations (Landoz, 1844), however the most recent herbarium specimens were collected by Aladár Richter in 1908 (deposited in BP herbarium, Budapest) and the last authentic description before our report originated from László Katona, 1912 (Fekete and Blattny, 1913). At Katona's time this population was much larger; he observed it to extend to the present location of the reservoirs constructed along the Someşul Cald Valley in the 1960s and 1970s.

There is another *S. josikaea* population not mentioned by Macalik *et al*. (2013), that in the Galbenei Valley, even though the existence of this population has been known since Michalus discovered it (1887). The population was small and declining already at that time. The one and only herbarium specimen from this population was collected by Emil Pop in 1948 (deposited in CL herbarium, Cluj Napoca), and the most recent personal confirmation of *S. josikaea* at this site before our 2009 visit there originated from 1968 (Stefan, 1971). We found an extremely small population consisting of two individuals in the lower part of the valley (Lendvay *et al*., 2012).

Macalik *et al*. (2013) did not find *S. josikaea* in the Drăgan Valley. Literature reports regarding this population are imprecise (Fekete and Blattny, 1913; Dihoru and Negrean, 2009). Careful analysis of the literature (Lendvay *et al*., 2012) reveals that a report on a population probably referring to the Sebeşului Valley was misunderstood by later botanists as pertaining to the Drăgan Valley. However, when visiting the area, we did find some planted individuals in the village of Tranişu that, according to local people, originate from forests of the Drăgan Valley. Surveying the valley, we have not found any individuals in the wild. As *S. josikaea* exists both in the valleys north (Iad Valley) and south (Sebeşului Valley) of the Drăgan Valley, it would not be surprising to discover *S. josikaea* specimens here as well.

There are some additional sites with *S. josikaea* populations listed in the older literature that Macalik *et al*. (2013) do not mention. We have visited all such sites and have not found live populations. These include a population in the Aleu Valley (on the periphery of Pietroasa village), which was last confirmed by Stefan (1971) and an other one in the Obîrşia Valley (Obîrşia village), which was last seen by Blattny (1913), who claimed it to be extremely small and endangered by logging. Given the fact that currently no *S. josikaea* specimens live at these locations we consider these populations extinct.

The remaining earlier reports on populations are either indirect or obviously originate from misunderstanding or mistranslation of geographical names (reviewed in Lendvay *et al*., 2012). At such locations, namely, Ciucea, Negreni and Lorâu we have not found *S. josikaea* along the river Crişul Repede and its side valleys.

Syringa josikaea is a threatened species of the Apuseni Mountains mostly growing as extremely small populations at distant sites. Special attention is needed to preserve the species in its native environments with increasing human impact. The most well known *S. josikaea* population in the Iad Valley is protected by a designated nature protection area and currently seems not to be endangered. However, attention is required for the maintenance of the large *S. josikaea* population in the Someşul Cald Valley. Forest management or road construction could cause severe damage to this population. It would be desirable to establish a protected area between the dam of the Beliş reservoir and the village of Ruseşti. All other populations may currently be considered as too small to be viable on their own. In these populations care should be taken for the *S. josikaea* specimens individually. For the survival of these populations, it would be desirable to introduce specimens to these sites from nurseries to strengthen these small populations.

REFERENCES

Blattny, T. (1913) Újabb adatok a *Syringa josikaea* Jacq. fil. elterjedéséhez. Botanikai közlemények **12**, 12-14

Dihoru, G., Negrean, G. (2009) *Syringa josikaea*. In: Dihoru, G. and Negrean, G. (eds.) *Cartea rosie a plantelor vasculare din Romania*. (Red book of vascular plants of Romania). Academia Romana Institutul de Biologie Bucureşti, Bucureşti pp 531-532

Fekete, L., Blattny, T. (1913) Az erdészeti jelentőségű fák és cserjék elterjedése a magyar állam területén. Vol 1, Joerges Ágost özv. és fia, Selmecbánya

Landoz, J. (1844) Névsora a' Kolozsvár környékén termő növényeknek, mellyeket több évi vizsgálódásai után összegyüjtött 's a' magyar orvosok és természetvizsgálók 1844-dik év szeptember 2-kán Kolozsvártt tartott nagy gyülésének bémutatott. Ifj. Tilsch János, Kolozsvár

Lendvay, B., Kohut, E., Höhn, M. (2012) Historical and recent distribution of *Syringa josikaea* Jacq. fil. ex Rchb., ecological and conservational evaluation of the remnant populations. *Kanitzia* **19**, 27-58

Macalik, K., Tamás, R., Kolcsár, L.-P., Keresztes, L. (2013) Present status of the *Syringa josikaea* Jacq. ex Rchb., an endemic species which contributes to the diversity of the flora of the Carpathians. *Stud. Univ. Babeş-Bolyai Biol.* **58(2)**:31-40

Michalus, S. (1887) A *Syringa josikaea* előjöveteléről. *Erdészeti lapok* **26**, 982-983

Stefan, E. (1971) *Syringa josikaea* Jacq. in vestul tarii. *Comunicari de Bot.* **12**, 279-284

STUDIA UNIVERSITATIS BABEŞ-BOLYAI BIOLOGIA, LIX, 1, 2014 (p. 101-113)

=== REVIEW ===

BONE DIAGENESIS AND FTIR INDICES: A CORRELATION

ANDRA-SORINA TĂTAR[1,2,✉], OANA PONTA[1] and BEATRICE KELEMEN[1,2]

SUMMARY For the genetic analysis of ancient human remains to be done, the most appropriate bone has to be selected for the extraction procedure. The osseous tissue is already poor in DNA content, and the genetic material begins degradation from the moment of death. The burial conditions influence the diagenesis progress, affecting the composition and microstructure of the mineral component of the bone, the hydroxylapatite, and also the integrity of the organic fraction, which suffers chemical degradation and microbial attack. A complex interaction between the organic and the mineral part, and the impact of different burial site environments render remains with a variety of properties that affect the DNA availability. Using FTIR Spectroscopy (Fourier Transform InfraRed Spectroscopy), many of these variations in bone features can be interpreted, correlated, and used in various further methodological approaches. The crystallinity of the bone mineral and also its organic content can be characterized through FTIR. A higher level of crystal order corresponds to a more degraded bone, but a moderate adsorption of the DNA to the mineral crystallites can protect it from chemical decay, making the interpretation of FTIR spectra a complex and thoughtful procedure.

Keywords*:* ancient remains, crystallinity, diagenesis, FTIR.

Introduction

With the advent of state-of-the-art biological techniques, molecular bioarchaeology has made tremendous progress in the last decades (e.g. Margulies *et al.*, 2005) allowing the scientific world to decipher more and more secrets of the past. Of particular interest is learning the information encoded in the DNA of ancient skeletons. After specific nucleotide sequences are determined, further interpretation can be done, and understanding of the past takes a step forward. However, the

[1] *Interdisciplinary Research Institute on Bio-Nano-Sciences, Cluj-Napoca, Romania/*
[2] *Faculty of Biology and Geology, Babes-Bolyai University, Romania/*
✉ ***Corresponding author: Andra-Sorina Tătar**, Interdisciplinary Research Institute on Bio-Nano-Sciences, Cluj-Napoca, Romania. E-mail: tatar.andra@yahoo.com/*

genetic material is highly degraded and long enough, relevant fragments are difficult to obtain depending on the degree of diagenesis the bone has undergone (Weiner, 2010).

Bone organic and mineral degradation

DNA degradation commences right after death, through autolysis, as the endogenous enzymes from the lysosomes are released within the cells. All types of biomolecules are attacked by specific proteases, lipases, carbohydrases and nucleases, respectively. Some chemicals generated by this enzymatic digestion, such as peroxides and acids may further deteriorate other molecules, increasing damage (Brown and Brown, 2011). After the acute breakdown on the account of putrefaction is over (Collins *et al.*, 2002), remnant fragments of the macromolecules are then slowly suffering a chemical defacement. On one hand, *hydrolysis* manifests through the cleavage of β-N glycosidic bonds, leaving the DNA with an abasic site that will further lead to a nick in the strand. Cytosine and thymine are 20 times less liable than adenine and guanine to this peril (Brown and Brown, 2011, Lindahl, 1993). Furthermore, the packaging of the DNA *in vivo* has an effect on the size of initial fragmentation, affecting mitochondrial DNA differently than the nuclear DNA, as circular molecules are less accessible to nuclease activity (Collins *et al.*, 2002, Allentoft *et al.*, 2012). Hydrolysis also leads to miscoding lesions, where the bases are deaminated: cytosine turning into uracil that will complementary bind adenine instead of guanine, or adenine turning into hypoxanthine that will bind cytosine instead of thymine (Lindahl, 1993, Salamon *et al.*, 2005; Brown and Brown, 2011). Guanine, by deamination turns into xanthine that pairs with cytosine, so no mutation is induced, but xanthine will dislodge from the ribose, leading to the formation of an apurinic site (Lindahl, 1993). On the other hand, *oxidation* produces blocking lesions, scars obstructing the sliding of the DNA-polymerase on the polynucleotide chain, oxygen or its free radicals breaking chemical bonds within the bases or the ribose sugar (Brown and Brown, 2011). Water and oxygen are indeed detrimental to DNA conservation, as ancient spores, protected from excess water and kept anoxic by their shield seem to have a better preserved genetic material (Lindahl, 1993). Also, the Maillard reaction that links sugars and amino-acids, binding peptides to the polynucleotides, leads to blocking lesions. Other major participants at the degradation of the organic material are the ubiquitous microorganisms, whose secreted enzymes break molecules into smaller, absorbable ones (Brown and Brown, 2011). At first, bacteria are mostly of endogenous origin, from the intestinal tract, and after putrefaction is completed the soil microorganisms might continue the process if the environmental conditions are favorable (Jans *et al.*, 2004). Bell *et al.*(1996) considers the time between death and burial as a critical point in the diagenesis of a bone, greatly influencing its fate. Nevertheless, it is important to consider the fact that the DNA macromolecules are located in a complex medium, interacting with the surrounding molecules. Adsorbed to the Ca^{2+} ions in the mineral

hydroxylapatite via the negative phosphate groups, DNA is two times less affected by depurinization (Lindahl, 1993). A DNA molecule moderately adsorbed to the mineral is much more stable over time and less affected by degradation, but a bond too strong, owing to a higher surface area of the mineral crystallites, will heavily impair the DNA isolation rate (Götherström *et al.*, 2002).

The exact chemical reactions affecting the DNA after biological repair processes halt are mainly known, but the genetic material-to-whole bone ratio is infinitesimal, so a study of the other bone components is applied in order to assess the DNA availability.

The mature bone tissue is comprised of ~70% carbonate hydroxylapatite (CHA), 20% organic matter and 10% water. The organic proportion is made up of 90% type I collagen, the most abundant protein in the human body, with most of the rest 10% being osteocalcin (Buckley *et al*., 2008), the second most abundant protein in the bone, other non-collagenous proteins and proteoglycans, lipids, and of course, scarce amounts of DNA (Weiner, 2010). After death, the bone tissue becomes unstable, while part of the water evaporates, a proportion of the organic material is degraded and lost and the mineral fraction suffers extensive reorganization with an increase in crystallinity and changes in porosity (Weiner and Bar-Yosef, 1990; Collins *et al.,* 1995; Nielsen-Marsh and Hedges, 2000; Collins *et al.,* 2002; Hedges, 2002; Trueman *et al.*, 2004; Rogers *et al.,* 2010; Weiner, 2010; Brown and Brown, 2011; King *et al.,* 2011; Muller *et al*, 2011).

Bone diagenesis is a complex process that has numerous variables modeling it, so it is a rather difficult task to completely decipher all participations: microorganisms, temperature, local hydrology, oxygen content, soil organic content, geochemical properties and pH, and so on. A forensic study revealed that microbial attack in bone tissue occurs at around 3 months after death (Bell *et al*., 1996). Microbes digest bone collagen for nutritional purposes – along with the rest of the organic fraction – but neither their secreted enzymes nor they are able to penetrate the mineral lattice (Collins *et al.,* 1995). So a previous dissolution of the surrounding mineral layer is needed. Actually, the two operations are concurrent and limiting each other, in the first 50-100 days after death collagen cannot be attacked owing to an external layer of mineral not yet dissolved. The complete degradation of collagen, known as gelatinization, occurs at 70 °C if it is not mineralized, while in bone tissue this only happens at 150 °C, highlighting an interaction and an increase in stability (Collin *et al.*, 1995; Brown and Brown, 2011). The organic fraction existing in the composite lowers the mineral solubility, passivating its surface, because proteins with high acidic amino-acid content will bind Ca^{2+} atoms with their COO^- residues. Osteocalcin, also named the 'Gla protein' has a conserved central region of γ-carboxyglutamic acid residues representing the calcium binding region. This protein is linked to the mineral fraction tighter than collagen, and the only way to extract it is by dissolving the mineral itself (Buckley *et al.,* 2008; Weiner, 2010). Osteocalcin can be found in fossils, indicating its importance in stabilizing the bone (Berna *et al.*, 2004). The mineral and organic parts are intimately intertwined, a dissolved mineral phase exposing the collagen to degradation, while the

presence of proteins reduces the rate of mineral dissolution (Nielsen-Marsh and Hedges, 2000; Collins *et al.*, 2002). When all conditions for both processes are met the bone can eventually be totally dissolved (Nielsen-Marsh *et al.*, 2000).

Bacteria, fungi or cyanobacteria, in marine environments, greatly accelerate bone degradation by enzymatically degrading the collagen matrix, thus increasing porosity and crystallinity (Hedges, 2002). With higher porosity, water enters more easily into the bone structure, aiding recrystallinisation (Hedges, 2002). Electron microscopy imaging revealed 'microscopical focal destruction' tunnels of 5-10 μm in diameter as a result of fungi attack and hyper-mineralized bacterial remains in areas with small pores and thin channels (0,1- 2,0 μm) where bacteria have resided (Hackett, 1981). Wess *et al.* (2001) also observed hyper-mineralised zones with disoriented crystals in close vicinity to cells with very little organic substances, sustaining the idea that where bacteria have entered and consumed the organic component, the mineral phase also reacted, increasing crystallinity (Müller *et al.*, 2011).

Collagen can, too, be disintegrated by chemical degradation, under the action of water and oxygen from the environment. Chemical, uncatalyzed oxidation and hydrolysis are, however, much slower reactions compared to the enzymatic microbial digestion, but they affect the bone at a macroscopic scale, not only at small destruction foci (Hackett, 1981). A medium with extreme pH and temperature favors a chemical degradation, whilst a more neutral pH is needed for microbial growth (Collins *et al.*, 2002). Triple-helical collagen molecules bind together into structures of tropocollagen via hydrogen bonds and cross-links between lysine residues. Peptide bonds are hydrolysed, leaving nicks in the macromolecule. (Collins *et al.*, 1995). When the broken fragments are short enough that the hydrogen bonds holding them together are weaker than the thermal energy, the molecule breaks down (Brown and Brown, 2011). If the region where this is happening is open enough to the exterior, bacteria can absorb and digest the polypeptide fragments, but if the disintegration occurs in a niche surrounded by mineral, only small scale swelling and unraveling of the collagen occurs (Brown and Brown, 2011). This is because molecules bigger than the water molecule are not able to pass the mineral-protein composite, not even ethanol can, so any eventual bacterial enzymes are secluded (Collins *et al.*, 1995; Collins *et al.*, 1995; Nielsen-Marsh *et al.*, 2000; Brown and Brown, 2011). Cross-linking of collagen with large sized humics infiltrated into the bone from the surrounding soil or condensation with carbohydrates, leading to formation of Maillard products are reactions that help collagen preservation, as they hinder enzymatic digestion (Klinken and Hedges, 1995; Nicholson, 1998; Jans *et al.*, 2004).

The major bone fraction, the carbonate hydroxylapatite [$Ca_{10}(PO_4,CO_3)_6(OH)_2$] is a disordered version of the naturally occurring mineral hydroxylapatite, with some of the phosphates replaced by carbonate moieties. As the PO_4 group has a tetrahedral frame, and the CO_3 is a planar structure, once the natural composition is modified, the 'perfection' of the crystal lattice decreases (Weiner, 2010). Also, using electron microscopy, the size and shape of the crystallites in adult human bone have been determined: 50 x 25 x 2-4 nm and plate-shaped flakes, respectively (Weiner and Price,

1986). Such scanty dimensions determine a very high surface area: volume ratio, the specks having only 12-14 layers of atoms, meaning that a large proportion of them are actually at the surface, not bound to other atoms in a crystalline manner, so a high level of 'unsaturation' is observed. Thereupon, the bone mineral component is actually a pretty disordered structure that would naturally tend toward a thermodynamic equilibrium (Weiner and Price, 1986; Berna *et al.*, 2003; Salamon *et al.*, 2005; Weiner, 2010). After death, when the collagen matrix surrounding the HA crystallites gets degraded, the mineral is no longer caged and the course to equilibrium begins, increasing crystallinity (Collins *et al.*, 2002; Rogers *et al.*, 2010). This explains the hyper-mineralised zones aforementioned (Hackett, 1981, Wess *et al.*, 2001).

As the crystallites grow in dimension and get tighter and more orderly packed, their stability increases, namely their solubility decreases. Berna *et al.*, (2004) studied this property of the bone mineral in relation to phosphate concentration and pH. For fresh bone, on one side, and for a reference HA on the other, two parallel diagonal isotherms were plotted, and the area between them was referred to as a "recrystallization window". As the PO_4 concentration and pH get lower, dissolution occurs, i.e. the left hand side of the HA isotherm, while higher values of the variables induce solidification. A fresh bone subjected to an outset of diagenesis, at a certain – let's assume – *low* PO_4 concentration will have the mineral component dissolved when the surrounding pH drops below the corresponding value on the isotherm. At this point, the water closely enveloping the bone will have a local higher PO_4 concentration, shifting the terms in the "solid" area, thus leading to recrystallization. However, the dissolved mineral will now adhere to an already existing crystal, increasing its size and lattice order. Through this process the crystallinity of the bone mineral increases. Deep in the bone matrix, this water is entrapped in the natural pores, and will not be easily washed away. Still, when the water with diluted minerals from outside the remains is flushed and replaced with fresh water, recrystallization will no longer occur, but the dissolution might continue if the pH allows it. Berna *et al.* estimated that if the surrounding water is replaced every 120 days (seasonally), it would take approximately 25-50 years for 1 gram of bone to be totally disintegrated. In this respect, clay-type soils are extremely good at isolating the micro-environment. If simultaneous collagen digestion takes place, the bone is decomposed.

Each component of the bone composite goes through typical diagenesis paths, but the extent of each of these, and the precise succession leading to the state in which an ancient bone is recovered are governed by sundry factors, discussed below.

Environmental contribution

Different bones exhibit different levels of diagenesis, depending on the local burial site conditions rather than the age of the remains (Weiner and Bar-Yosef, 1990). This implies that the very many variables specific to each site influence the bone

degradation in different ways. (i) Temperature variations are adverse to bone conservation, as the remains found in caves with a constant temperature are well preserved (Weiner and Bar-Yosef, 1990; Collins *et al.*, 2002; Hedges, 2002; Jans *et al.*, 2004). The specific karstic high carbonate concentration in groundwater also enhances mineral deposition, along with a slightly alkaline pH (Wright and Schwarcz, 1996; Collins *et al.*, 2002). Very low temperatures, too, aid the survival of DNA, by slowing down any chemical degradation and halting the microbial growth. DNA fragments of unexpected lengths were successfully found in permafrost remains. On the other hand, high temperatures increase the yield of all chemical reactions and the growth of microorganisms, leading to degradation. (ii) Water is known to degrade the organic components of bone, and an arid environment seems to favor conservation, mostly by inhibition of bacterial development (Collins *et al.*, 2002; Götherström *et al*., 2002; Hedges, 2002; Trueman *et al.*, 2004). However, independently of the medium aridity, the collagen molecules are always hydrated (Collins *et al.*, 1995; Weiner, 2010) and the mineral micropores within the HA matrix are ever filled with a solution of water and mineral ions in equilibrium with the crystallite phase (Hedges, 2002; Berna *et al.*, 2004; Lebon *et al.*, 2010). Similarly, the DNA fragments necessarily have a layer of hydration that allows them a natural conformation, as a chemically dehydrated DNA would have a destroyed double helix structure and a much greater chance of damage (Lindahl, 1993). Excess water, in the case of waterlogged remains, leads to anoxia, blocking some bacterial degradation (Hedges, 2002). Ultimately, water fluctuations and an active soil hydrology are the hostile factors, rinsing the saturated mineral solution from the close vicinity of the bone composite, leading to bone dissolution (Wright and Schwarcz, 1996). (iii) The soil type of the archaeological site strongly marks the diagenesis of the remains, most references stating a clay-type soil as the best retainer. It is not permeable to water, so enclosed cavities around the bones would maintain the carbonate solution, not allowing rain water or other sources of fresh water to dissolve the microenvironment (Weiner and Bar-Yosef, 1990; Nielsen-Marsh and Hedges, 2000; Berna *et al.*, 2004). An organically rich soil, such as peat, guano inside a cave, or a midden becomes anoxic, the glut of organic material consuming all the available oxygen. However, the oxidation lowers the pH, favoring the mineral dissolution (Berna *et al.*, 2004; Jans *et al.*, 2004; Weiner, 2010). Certain chemical elements present in the soil might also influence the bacterial development, soils polluted with mercury, lead or copper maintaining a low microbial population (Jans *et al.*, 2004; Müller *et al.*, 2011). Ions such as sodium, magnesium, barium, iron, manganese, strontium can enter the HA lattice in the position of the calcium ion, lowering crystal neatness. Fluoride is an element that immensely influences the crystallinity of the mineral, by replacing the hydroxyl group, majorly increasing tightness of the lattice and implicitly, decreasing solubility. (Berna *et al.*, 2004; Lebon *et al.*, 2010). A high carbonate content in the soil will lower the crystallinity of the HA, as it disturbs the mineral lattice, but it will also be deposited on the bone surface and in the pores and cracks as calcite (Nielsen-Marsh and Hedges, 2000). (Fig. 1) shows an example of such diagenesis. Trueman *et al.* (2004) assessed the organic content of

bones deposited on the soil surface for as long as 30 years and the collagen lessened by 50% in the surface parts of the remains, and a 25% loss was measured in deeper cortical tissues, suggesting the importance of the condition in which a bone is deposited.

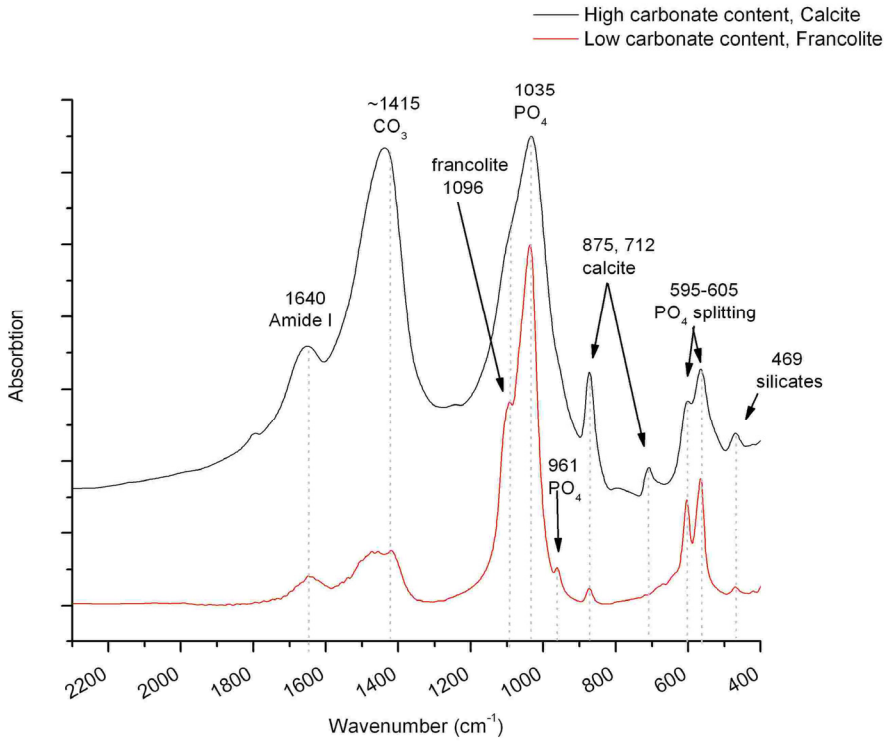

Figure 1. Examples of FTIR absorbtion spectra of bones showing different diagenesis patterns, according to the variables of the environment

The mineral and organic content, as well as the crystallite size, perfection and composition of the crystal lattice are features that are easily assessed with infrared spectroscopy. FTIR (Fourier Transform Infrared Spectroscopy) is a technique widely used in archaeology, together with methods like Raman spectroscopy, electron microscopy, X-Ray Diffraction. The main advantages of FTIR are the accessibility, low cost, relatively short preparation time and the small sample size. Also, FTIR can investigate amorphous samples, too, not only crystals, as XRD and Raman (Termine and Posner, 1966; Weiner, 2010; King *et al., 2011*). Therefore, an entire range of sub-domains can be studied using FTIR, not necessarily focused on ancient bio-molecules, or human remains, but also on non-biological directions, like pottery and cooking, clothing, a whole range of pigments (Damjanovi *et al*., 2011; Karapanagiotis *et al.*, 2011; Rogerio-Candelera *et al.,* 2013).

FTIR indices used to assess bone diagenesis

FTIR is a spectroscopy technique that measures the absorption of infra-red light by the sample. The energy of the IR radiation can excite the chemical bonds, inducing stretchings, bendings, or vibrations between each pair of atoms or groups of atoms-functional groups (Coates, 2000). Every such absorption takes place at a given wavelength of the IR radiation, usually expressed as a wavenumber, the reciprocal of the wavelength, thus measured in cm^{-1}. Tables containing assignments of bond types and their proprietary frequencies can be found in the literature, with focus available on every desired domain, ranging from inorganic molecules to polymers, to any type of organic molecules (Bellamy, 1975; Socrates, 1994; Bryan *et al.*, 2007; Mello and Vidal, 2012). Therefore, when a sample is studied, the characteristics of the IR absorption spectra can lead to understanding the molecular shape of its chemical components.

The first FTIR index used to asses crystallinity in HA was the 'splitting function', an area-to-area ratio characteristic to the degenerating splitting of the 600 cm^{-1} phosphate ion antisymmetric bending frequency as the order of the atoms increased (Termine and Posner, 1966). Sometimes named 'crystallinity index'- CI, and sometimes 'infrared splitting factor'- IRSF, the division between the sum of absorbance values for the two peaks of the splitting and the value corresponding to the valley amid them (i.e. $(A_{595}+A_{605})/A_{588}$) encodes information regarding the degree of diagenesis a bone has undergone. As the organic phase of the bone is chemically or microbially degraded, the mineral lattice around it suffers dissolutions, mostly of the smaller, less stable crystallites, and recrystallizations on the already existing bigger crystals, according to the physicochemical surroundings as previously discussed. Nielsen-Marsh and Hedges (2000) state that the two processes, dissolution and recrystallization can together account for the gain in the IRSF value. This way, the crystallinity increases, and even if at the macroscopic level no differences can be seen, microscopic reorganization is traceable with the use of this parameter (Rogers *et al.*, 2010). A direct correlation between the IRSF and a mean crystal size was revealed by Truman *et al.* (2004), with a slight change in the shape of the crystallites as they matured, from plate-shaped to more needle-shaped: 163 x 28 x 5 nm (Berna *et al.*, 2004).

Several authors calculated the IRSF for modern bone in comparison to the archaeological bones they were studying at the moment, showing a definite increase with degradation: 2.7 *versus* over 3 (Müller *et al.*, 2011); less than 2.8 *versus* 2.7 - 3.4 (Trueman *et al.*, 2004); 3.4 *versus* 3,5 – 3,8 for one burial site and 3.1 – 4.6 for another one (Lebon *et al.*, 2010); 2.6 *versus* 3 (Nielsen-Marsh and Hedges, 2000). Berna *et al.* (2004) pointed out an even wider range of values: 2.6 - 3 for *in vivo* bones, up to 3.4 for bones slightly altered on the soil surface, up to 4.1 for fossil bones, and an IRSF of 7 was determined for highly altered fossils. For comparison, the IRSF for synthetic HA was 5.4. An explanation for why crystallinity in a bone can be higher than a standard HA will be given right away.

When the original chemical structure of the apatite is altered, the whole complex can get loosened, more soluble and less crystalline. This happens when the CO_3 partially replaces the PO_4 or the OH, or when the Ca is substituted by other atoms, such as Na or Mg**.** Figure 1 shows spectra of distinct types of diagenesis, the black plot corresponding to a bone deposited in a carbonated environment (massive carbonate peak at 1415 cm^{-1}): note the poor peak splitting at 595 – 605 cm^{-1}, meeting the explanation above. The reverse situation for HA is when the OH is replaced by a fluoride atom. The fluoroapatite $[Ca_{10}(PO_4)_6(F)_2]$ is actually packed tighter without the hydroxyl moiety, contracting the *a*-axis dimension, making the mineral much more insoluble, crystalline and pH resistant, with an IRSF of almost 7. In bone, the carbonate hydroxylapatite binds fluorine, turning into francolite $[Ca_{10}(PO_4,CO_3)_6(F)_2]$, a mineral with a specific infrared peak at 1096 cm^{-1}, easily recognized on the spectra by the specific 'francolite shoulder', near the main phosphate peak. The red plot in Fig. 1 is an example of a spectrum of a bone that absorbed fluorine, showing a distinctive francolite shoulder and a higher IRSF, as the split 600 cm^{-1} peak shows. King *et al.* (2011) found that burials from a slightly more hydrated linear area in an archaeological site had signs of francolite, as Greenwood and Earnshaw (1998) explained the high affinity of fluorine for water. Very old fossils, such as dinosaur fossils have IRSF values of almost 7 and high fluorine content. Otherwise, they could not have survived all this time (Berna *et al.*, 2004). Still, neither a high IRSF nor a short time of deposition correlate with a good organic conservation, as all the other factors described above outweigh the impact of chronological age (Weiner and Bar-Yosef, 1990). As an example, a mass Civil War grave failed to yield DNA for genetic analyses, while an older Saxon cemetery had interpretable DNA results (Hagelberg *et al.*, 1991). Salamon *et al*., (2005) also failed to find any correlation between DNA amplification yield and the age of the sample, but Allentoft *et al.* (2012) argued that preservation is indeed a function of time, if all the other possible variables would be constant, as expected from pure physical chemistry data.

The 'carbonate content' measures the CO_3/PO_4 peak absorption ratio at 1415 and 1035 cm^{-1}, respectively. Wright and Schwartz (1996) established a good correlation between the C/P ratio and the weight% of CO_3^{2-} measured by CO_2 elimination by acid dissolution. C/P is a disputed parameter, mainly in the interest of performing isotopic labeling, any exogenous carbonate in the examined bone tissue yielding false results regarding age, migrations, dietary habits, climatology (King *et al*., 2011). As for diagenesis, the C/P value simply shows the quantitative ratio between the anions. It might increase over time, if the surrounding carbonate content is high and thus turns the scale of the thermodynamic equilibrium against the HA natural tendency to eliminate CO_3. Such a case will also present with a specific calcite peak at 712 cm^{-1} (Fig. 1), if the calcite represents at least 3% of the bone mineral (Nielsen-Marsh and Hedges, 2000; Müller *et al.*, 2011). A lower C/P value indicates the loss of CO_3 through dissolution and the gain of PO_4 in the crystalline structure. Thereby, an average, modern C/P value in an ancient bone would indicate to both processes, a

deposition of calcite ($CaCO_3$) in and on the bone, with adsorption on the surface of the apatite crystals, but also to an increase in local crystallite perfection by reinstatement of PO_4 in the HA (Nielsen-Marsh and Hedges, 2000,***). Lebon *et al.* (2010) argued a fluctuating value of the C/P index in archaeological samples, on account of the many processes determining it, ranging from 0.15 to 0.35, while modern samples had a lower standard deviation, with an average value of the C/P of 0.28. However, the C/P index does raise some issues because of the organic C - H vibrations that absorb IR energy in the same wavelength as the CO_3 functionality, leading to an overestimation of carbonate along with the organic matrix content (Truman *et al.*, 2004). In Fig. 1 the more carbonated spectrum also has a high Amide I peak (Amide I is the C=O bond in the polypeptide chain), supporting the preceding observation.

The 'collagen content' CC is the index measuring the proteic preservation of the bone matrix, calculated from the peak absorption values of Amide I and PO_4, A_{1640}/A_{1035}. Values of 0.2 correspond to 15 wt% and of 0.8 to 30 wt% of organic material in bone (Truman *et al.*, 2004). The higher the protein signature is, the more organic fraction survived the passing of time in a specific bone. Nielsen-Marsh and Hedges (2000) state a correlation between the CC and the IRSF, as the loss of organic material leads to changes in the mineral microstructure by recrystallization, correlation not attained by Lebon *et al* (2010), probably because the lot investigated by them had some other factors influencing the indices, like fluoride.

Lebon *et al.* (2010) used an additional absorption value ratio to verify the increase in crystallinity, A_{1030}/A_{1020}. The 1030 cm^{-1} indicates phosphates in stoichiometric apatites (i.e. all six positions in $[Ca_{10}(PO_4)_6(OH)_2]$ are occupied by PO_4) and 1020 cm^{-1} is indicative of non-stoichiometric apatites containing CO_3^{2-} and/or HPO_4^{2-}. A direct correlation between this index and the IRSF was observed in a wide range of diagenetically altered bones, demonstrating the possibility to measure the crystallinity of fossil bones using either of the indices, especially when using micro-FTIR, where the IRSF 600 cm^{-1} is outside the detection range. A high non-stoichiometry correlated with high CC, as the non-perfect crystallites were protected from dissolution by the organic matrix (Lebon *et al.*, 2010).

A novel index proposed by Lebon *et al.* (2010) is the position shift of the ν_1PO_4 band at 960 cm^{-1} toward 963 cm^{-1}, linearly correlated with carbonate loss and with an increase of the crystal lattice perfection, as foreign ions are excluded. This index seems to be more sensitive to carbonate loss and lattice strain changes than the IRSF, which mainly refers to crystal size. Some samples might have this peak shifted above 963 cm^{-1}, but only with an accompanying high fluoride content that renders a more ordered atomic arrangement in the fluoroapatite compared to HA. Apatites doped with ions such as Ba^{2+}, Mn^{2+}, Sr^{2+} have the ν_1PO_4 peak shifted below 960 cm^{-1}, so this index could be used to detect ionic substitutions in the mineral lattice during diagenesis (Thomas *et al.*, 2007).

Conclusions

Bone diagenesis affects both fractions of the bone composite, the mineral part going through successive dissolutions and recrystallizations while the organic fraction suffers chemical degradation and microbial digestion. The two are deeply intertwined, influencing the extent to which the external factors can modify them. DNA can not be effectively observed in ancient bones, so its estimation must be done based on the other, much accessible components. The FTIR spectra of the bones examined give values for indices such as infrared splitting factor [(565+605)/588], carbonate-to-phosphate ratio (1415/1035), collagen content (1640/1035), stoichiometry of crystallites (1030/1020) and the perfection of lattice (the shifting of the ν_1PO_4 peak), and can also 'see' other important elements, such as the presence of fluoroapatite, or carbonate. Interpretation of all the accessible information from FTIR spectra of the bones at hand helps the molecular geneticist choose the most appropriate bone for extraction of DNA, in order to have the best DNA yield possible.

AcknowledgementsThis study was supported by funding from the project Genetic Evolution: New Evidences for the Study of Interconnected Structures (GENESIS). A Biomolecular Journey around the Carpathians from Ancient to Medieval Times (CNCSIS-UEFISCDI_ PNII_PCCA_1153/2011).

REFERENCES

Allentoft, M.E., Collins, M., Harker, D., Haile, J., Oskam, C.L., Hale, M.L., Campos, P.F., Samaniego, J.A., Gilbert, M.T.P., Willerslev, E., Zhang, G., Scofield, R.P., Holdaway, R.N., Bunce, M. (2012) The half-life of DNA in bone: measuring decay kinetics in 158 dated fossils, *Proc. R. Soc. B.*, 279: 4724–4733

Bell, L.S., Skinner, M.F., Jones, S.J. (1996) The speed of *post mortem* change to the human skeleton and its taphonomic significance, *Forensic Sci. Internat.*, **82**, 129–40

Bellamy, L.J. (1975) Infrared Spectra Of Complex Molecules, Chapmann & Hall, New York, Vol. 1

Berna, F., Matthews, A., Weiner, S. (2003) Solubilities of bone mineral from archaeological sites: the recrystallization window, *J. Archaeol. Sci*, **31**, 867–882;

Brown, T., Brown, K. (2011) Biomolecular Archaeology - an introduction, John Wiley & Sons

Bryant, M.A., Brauner, J.W., Anderle, G., Flach, C.R., Brodsky, B., Mendelsohn, R. (2007) FTIR studies of Collagen Model Peptides: Complementary Experimental and Simulation Approaches to Conformation and Unfolding, *J. Am. Chem. Soc.*,**129:**7877-7884

Buckley, M., Anderung, C., Penkman, K., Raney, B.J., Gotherstrom, A., Thomas-Oates, J., Collins, M.J. (2008) Comparing the survival of osteocalcin and mtDNA in archaeological bone from four European sites, *J. Archaeol. Sci.*, **35**:1756-1764;

Coates, J. (2000) Interpretation of Infrared Spectra, A Practical Approach, Encyclopedia of Analytical Chemistry, 10815-10837

Collins, M.J., Riley, M., Child, A.M. and Turner, W.G. (1995) A basic mathematical simulation of the chemical degradation of ancient collagen, *J. Archaeol. Sci*, **22**, 175–183

Collins, M.J., Nielsen-Marsh, C.M., Hiller, J., Smith, C.I., Roberts, J.P., Prigodich, R.V., Wess, T.J., Csapo, J., Millard, A.R., Turner-Walker, G. (2002) The survival of organic matter in bone: a review, *Archaeometry*, **44**, 383-394

Damjanovi, L., Holclajtner-Antunovic, I., Mioc, U. B., Bikic, V., Milovanovic, D., Evans, I.R. (2011) Archaeometric study of medieval pottery excavated at Stari (Old) Ras, Serbia, *J. Archaeol. Sci.,* **38**:818-828

Greenwood, N.N., Earnshaw, A., (1998) Chemistry of the Elements, Pergamon, New York;

Götherström, A., Collins, M.J., Angerbjörn, A., Lidén, K. (2002) Bone preservation and DNA amplification, *Archaeometry*, **44**, 395–404

Hackett, C.J. (1981) Microscopical focal destruction (tunnels) in exhumed human bones, *Med. Sci. Law.*, **21**: 243-265

Hagelberg, E., Bell, L.S., Allen, T., Boyde, A., Jones, S.J., Clegg, J.B. (1991) Analysis of ancient bone DNA – techniques and applications, *Philos. T. Roy. Soc. B.*, **333**, 399–407

Hedges, R.E.M. (2002) Bone diagenesis: an overview of processes, *Archaeometry,* **44**, 319–328

Jans, M.M.E., Nielsen-Marsh, C.M., Smith, C.I., Collins, M.J., Kars, H. (2004) Characterisation of microbial attack on archaeological bone, *J. Archaeol. Sci*., **31**: 87-95

Karapanagiotis, I., Mantzouris, D., Kamaterou, P., Lampakis, D., Panayiotou C. (2011),Identification of materials in post-Byzantine textiles from Mount Athos, *J. Archaeol. Sci.,* **38**:3217-3223

King, C.L., Tayles, N., Gordon, K.C., (2011) Re-examining the chemical evaluation of diagenesis in human bone apatite, *J. Archaeol. Sci.*, **38**:2222-2230

Klinken, G.J., Hedges, R.E.M. (1995) Experiments on collagen-humic interactions: speed of humic uptake and effects of diverse chemical treatments, *J. Archeol. Sci.*, **22**:263- 270

Lebon, M., Reiche, I., Bahain, J.-J., Chadefaux, C., Moigne, A.-M., Fröhlich, F., Sémah F., Schwarcz, H.P., Falguères, C., (2010) New parameters for the characterization of diagenetic alterations and heat-induced changes of fossil bone mineral using Fourier transform infrared spectrometry, *J. Archaeol. Sci*., **37**:2265-2276

Lindahl, T. (1993) Instability and decay of the primary structure of DNA, *Nature*, **362**, 709–15

Margulies, M., Egholm, M., Altman, W.E. *et al*. (2005) Genome sequencing in microfabricated high-density picolitre reactors, *Nature*, **437**, 376–80

Mello, M.L.S., Vidal, B.C. (2012) Changes in the Infrared Microspectroscopic Characteristics of DNA Caused by Cationic Elements, Different Base Richness and Single-Stranded Form, *PLOS One,* **7**: 43169

Müller, K., Chadefaux, C., Thomas, N., Reiche, I. (2011) Microbial attack of archaeological bones versus high concentrations of heavy metals in the burial environment. A case study of animal bones from a mediaeval copper workshop in Paris, *Palaeogeogr. Palaeoclimatol. Palaeoecol.*, **310**:39-51

Nicholson, R.A. (1998) Bone degradation in a compost heap, *J. Archaeol. Sci.,* **25**:393–403

Nielsen-Marsh, C.M., Hedges, R.E.M. (2000) Patterns of Diagenesis in Bone I: The Effects of Site Environments, *J. Archaeol. Sci.*, **27**: 1139-1150

Nielsen-Marsh, C., Hedges, R.E.M., Collins, M.J.C. (2000) A preliminary investigation of the application of differential scanning calorimetry to the study of collagen degradation in archaeological bone, *Thermochim. Acta*, **365**, 129–39

Rogerio-Candelera, M.A., Herrera, L.K., Miller, A.Z., Sanjuán, L.G., Molina, C.M., Wheatley, D.W., Justo, A., Saiz-Jimenez, C. (2013) Allochthonous red pigments used in burial practices at the Copper Age site of Valencina de la Concepción (Sevilla, Spain): characterisation and social dimension, *J. Archaeol. Sci.,* **40**: 279-290

Rogers, K., Beckett, S., Samira, K., Chamberlain, A., Clement, J. (2010) Contrasting the crystallinity indicators of heated and diagenetically altered bone mineral, *Palaeogeogr. Palaeoclimatol. Palaeoecol*., **296:** 125-129

Salamon, M., Tuross, N., Arensburg, B., Weiner, S. (2005) Relatively well preserved DNA is present in the crystal aggregates of fossil bones, *PNAS,* **102**, 13783–88

Socrates, G. (1994) Infrared Characteristic Group Frequencies, John Wiley & Sons, New York

Termine, J.D., Posner, A.S. (1966) Infra-red determination of the percentage of crystallinity in apatitic calcium phosphates, *Nature* **211:**268-270

Thomas, D.B., Fordyce, R.E., Frew, R.D., Gordon, K.C. (2007) A rapid, non-destructive method of detecting diagenetic alteration in fossil bone using Raman spectroscopy, *J. Raman Spectrosc.*, **38**:1533-1537

Trueman, C.N.G., Behrensmeyer, A.K., Tuross, N., Weiner, S. (2004) Mineralogical and compositional changes in bones exposed on soil surfaces in Amboseli National Park, Kenya: diagenetic mechanisms and the role of sediment pore fluids, *J. Archaeol. Sci,* **31**: 721-739

Weiner, S., Price, P.A. (1986) Disaggregation of bone into crystals, *Calcified Tissue Int.*, **39,** 365–375

Weiner, S., Bar-Yosef, O. (1990) States of preservation of bones from the prehistoric sites in the Near East: a survey. *J. Archaeol. Sci.,* **17,** 187–196

Weiner, S. (2010) Microarchaeology: Beyond the Visible Archaeological Record, Cambridge University Press

Wess, T.J., Drakopoulos, M., Snigirev, A., Wouters, J., Paris, O., Fratzl, P., Collins, M., Hiller, J., Nielsen, K. (2001) The Use of Small-Angle X-Ray Diffraction Studies for the Analysis of Structural Features in Archaeological Samples, *Archaeometry*, **43**, 117-129

Wright, L.E., Schwarcz, H.P. (1996) Infrared and isotopic evidence for diagenesis of bone apatite at Dos Pilas, Guatemala: palaeodietary implications. *J. Archaeol. Sci.,* **23**, 933–944

STUDIA UNIVERSITATIS BABEŞ-BOLYAI BIOLOGIA, LIX, 1, 2014 (p. 115-126)

=== REVIEW ===

TECHNIQUES USED FOR THE DIAGNOSTIC OF ANCIENT TUBERCULOSIS IN HUMAN REMAINS

CECILIA CHIRIAC[1,2,✉], ANDRA-SORINA TĂTAR[1,2], CLAUDIA RADU[1], IULIA LUPAN[1,2] and BEATRICE KELEMEN[1,2]

SUMMARY. Tuberculosis is today one of the most spread infectious human diseases, being caused by a group of closely related species included in the *Mycobacterium tuberculosis* complex (MTBC). Molecular studies targeting tuberculosis affected human remains are important in order to understand the evolution of specific genomic sites related to virulence. The aim of this review is to describe several techniques that are useful for the confirmation of pathogen persistence in the human archaeological remains. It also presents the genomic loci investigated in the field of molecular bioarchaeology for discrimination of MTBC species.

Keywords: ancient-DNA, FT-IR, HPLC, MALDI-TOF-MS, tuberculosis.

Introduction

World Health Organization (WHO) ranks tuberculosis as the second most dominant infectious disease, exceeded just by HIV/AIDS. Given the incidence of the disease today and the appearance of multi-drug-resistant strains, it is important to obtain information about the conserved and variable genomic loci and about the mutation rate of the pathogen. For this reason, ancient cases of tuberculosis have to be investigated and the co-evolution of the pathogens and modern humans should be tracked.

Tuberculosis is caused by a group of closely related species with exclusively human hosts (*Mycobacterium tuberculosis, M. africanum, M. canetti*) or with a broader host spectrum: *M. bovis* (Brosch *et al*., 2002). These species are included in the *M. tuberculosis* complex (MTBC).

[1] *Molecular Biology Center, Interdisciplinary Research Institute on Bio-Nano-Sciences, "Babeş-Bolyai" University, Cluj-Napoca, Romania.*
[2] *Faculty of Biology and Geology, Babes-Bolyai University, Cluj-Napoca, Romania.*
✉ ***Corresponding author: Cecilia Chiriac**, Molecular Biology Center, Interdisciplinary Research Institute on Bio-Nano-Sciences, "Babeş-Bolyai" University, Cluj-Napoca, Romania.*
E-mail: cecilia.chiriac@yahoo.com

Comas *et al.* (2013) were able to infer the coalescence time of pathogenic species by analyzing the whole genomes of 259 MTBC strains. Thus, it was determined that MTBC accompanied humans in the Out-of-Africa migration and developed as a crowd disease during the Neolithic Demographic Transition (NDT). Evidence of spinal tuberculosis was found throughout the world, in Italy, Denmark and in the Middle East, dating from the Neolithic period (Smith, 2003). Osteological signs (resorption, growth) could not be interpreted as pathognomotic evidence for the disease. Ancient cases of tuberculosis should be confirmed by molecular methods. A number of techniques can be used for this purpose, targeting the ancient DNA (aDNA) of MTBC or the presence of mycolic acids in the human remains.

The aim of this review is to describe how a series of molecular techniques can be used for the diagnosis of ancient tuberculosis cases.

Detection of mycolic acids

The cell envelope of *Mycobacterium* species is composed of arabinogalactan-mycolate linked via a phosphodiester bond to the cell wall peptidoglycan. Mycolic acids are the dominant constituents of the cell envelope. They have structural and functional roles, defending the pathogen from noxious chemicals, oxidative stress or the host's immune system. They are β-hydroxy fatty acids with a long α-alkyl side chain. Mycolic acids are classified in three structural classes: α-; methoxy- and keto-mycolic acids. They contain a carboxylic acid headgroup with two unequal hydrophobic tails. The mero-mycolate chain is composed of 50-70 carbon atoms, with cyclopropane rings, ketones, methoxy groups and/or double bonds. The shorter chain is the α-branch, an alkane chain, consisting of ~25 carbon atoms. Methoxy- and keto-mycolic acids have both *cis*- and *trans*- structural series, depending on the disposition of the cyclopropane rings. The α-mycolic acid has two cyclopropane rings, and a *cis-, cis* configuration. (Takayama *et al.*, 2005; Langford *et al.*, 2011). The chemical structure of mycolates can be seen in Figure 1.

We will present three highly sensitive techniques used for the molecular identification of mycolates in the MTBC infected paleopathological human remains.

FT-IR (Fourier Transform InfRared spectroscopy)

FT-IR is a sensitive and rapid analytical technique. It can provide information about the composition of the sample and about the amount of the compounds. The device contains an interferometer which has the ability to produce a signal that encompasses all infrared frequencies with wavenumbers between 4000 cm^{-1} and 400 cm^{-1}. Specific sets of chemical bonds within the sample will absorb electromagnetic radiation at different frequencies. This will result in chemical bonds vibration which will be recorded as peaks in the infrared spectrum. Because each

substance is a unique combination of atoms, there are no two compounds that will produce the exact same spectrum. Thus, FT-IR is a useful method for the qualitative analysis of the sample. Moreover, the height of the absorption peak is indicative of the amount of material present, rendering this technique also as a quantitative approach (Coates, 2000; Mark *et al*., 2010).

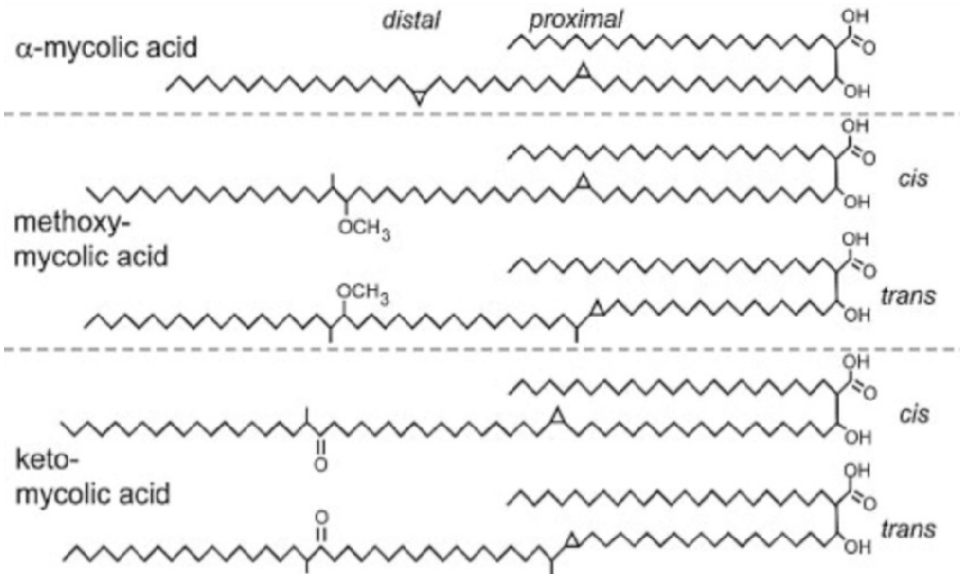

Figure 1. The chemical structure of mycolic acids. There are five forms of mycolic acids: α- type from the H37Ra strain, and methoxy- and keto-mycolates, each having cis- and trans- configurations, from the DT, PN, and C strains (from Takayama *et al.*, 2005).

In the case of the MTBC infected human remains, a set of unique peaks appear in the spectrum. As it can be seen in Fig. 1, mycolic acids are mainly made up of methylene groups and several methyl groups. Coates (2000) emphasized that if there are absorptions at 2935 cm^{-1} and 2860 cm^{-1}, where methylene and methyl groups absorb radiation, and if there are also peaks at 1470 cm-1 and 720 cm-1, as a result of long chain deformations, then the sample probably contains a long linear aliphatic chain. The comparison between a normal bone and one infected with tuberculosis can be seen in Figure 2. It is important to mention that FT-IR spectroscopy has only guiding relevance. Being a low cost method, FT-IR analysis could be used before other more precise, time consuming and expensive techniques, in order to assess if the effort would be worth.

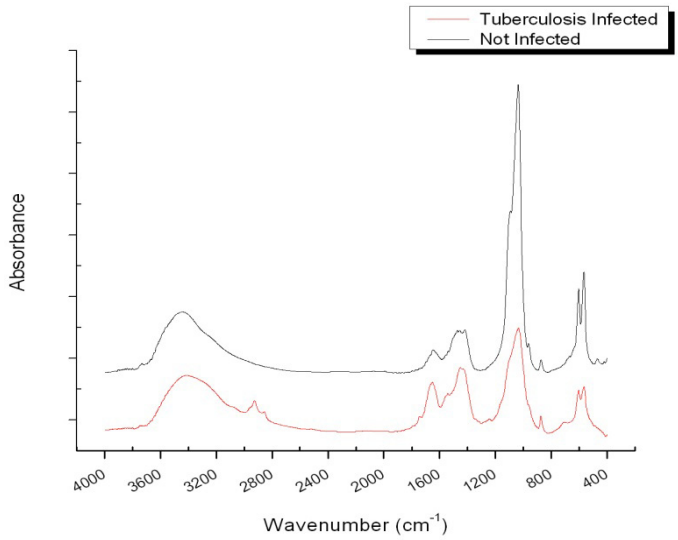

Figure 2. Differences between FT-IR spectra of tuberculosis infected and not infected skeletal remains.

MALDI TOF-MS (Matrix-assisted laser desorption/ionization time-of flight mass spectrometry)

This type of spectroscopy is used for molecule identification and determining their chemical structure by analyzing the m/z ratio. The general principle consists in the photo-volatilization of the sample that is included in an UV-absorbing matrix, followed by time-of-flight mass spectrum analysis. Since the matrix serves as an absorber of UV radiation, it is important for it to be in excess, the optimal matrix:sample ratio being between 100:1 and 10.000:1. The matrix substance is broken down immediately after iradiation and passes into the gaseous phase. Because the sample does not absorb the laser radiation directly, the technique is considered a „soft ionization technique" and allows the analysis of biomolecules up to several hundred kDa (Marvin *et al.*, 2003).

The mixture between the sample and the matrix is applied on a target slide, placed inside the device and irradiated. A beam of UV light is used (N_2 laser), with a wavelength of 337 nm. The matrix vaporizes, together with the sample, which in the process acquire an electric charge. An electric field is applied, which guides the ions into the flight tube and then separates them according to their mass. The result will be displayed as a series of lines in the spectrum that corresponds to the fragments of the initial substance which was broken down. By analyzing the peak patterns in the spectrum, it is possible to identify the structure of the investigated molecule (Marvin *et al.*, 2003; Mark *et al.*, 2010).

Mycolic acids, as they are found in the cell envelope, cover a diverse group of fatty acids, with m/z values between 1000 and 2000. After external calibration, Mark *et al*. (2010) analyzed 11 tuberculosis infected archaeological bone samples. A great majority of the recorded peaks was detected between m/z 1000-1600, the interval which corresponded to the mass spectrum distribution of a standard mixture of mycolic acids used as a positive control. A specific oxygenated methoxy-mycolic acid methyl ester pattern dispalys peaks at 1290, 1318 and 1346 m/z. Also, oxygenated keto-mycolic acids were found to have C82 and C84 respectively, with peaks at m/z 1246 and 1274. A healthy bone was tested as a negative control and a total absence of peaks was obtained in the critical mass range (Mark *et al.*, 2010). These results can be seen in Figure 3.

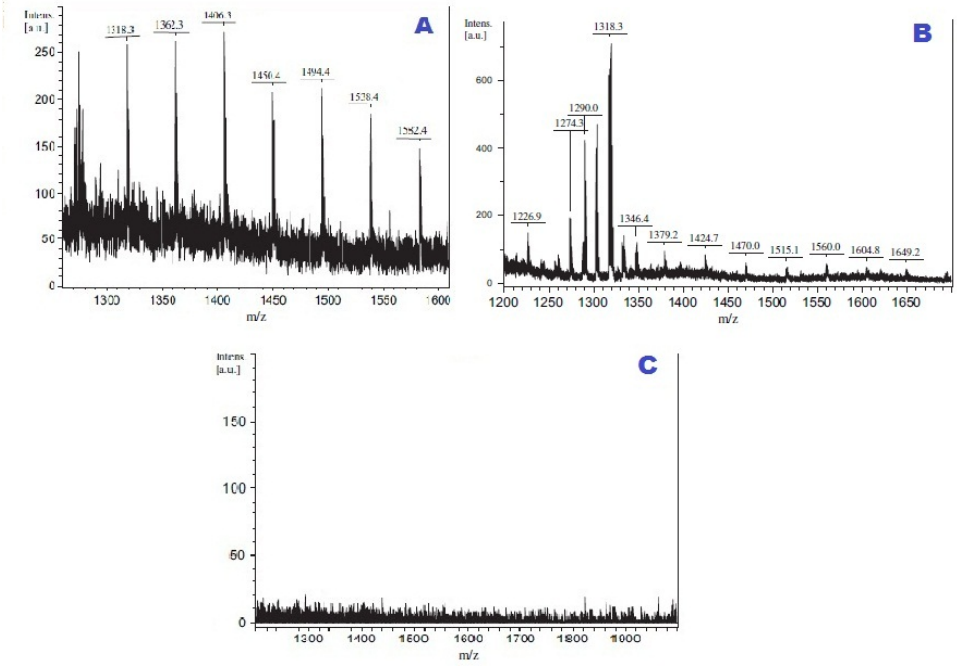

Figure 3. MALDI-TOF spectra of a) the mycolic acids standard mixture; b) a archaeological specimen infected with MTBC; c) a healthy bone as a negative control (after Mark *et al.*, 2010).

HPLC (High-performance liquid chromatography)

HPLC is a powerful chromatography technique able to separate similar substances from a mixture in a short period of time. The method requires a mobile phase (liquid) and a stationary phase (liquid/solid). The stationary is phase usualy

indicated by the column used, while the eluent is the mobile phase. Both phases are selected in order to best suit the sample and the purpose of the separation. The resolution and the order of the elution depends on the stationary and mobile phase selected. Substances that have a higher affinity for the mobile phase will emerge first, while others, with an affinity for the stationary phase will remain in the column longer (Meyer, 2010).

In order to force the mobile phase into the column filled with very small particles, a high constant pressure is necessary to be applied. The basic principle is that under the same conditions, the time between the injection of the component and its elution remains constant. The output is a chart presenting the time-depending changes in the signal intensities as a consequence of substance separation. The technique can be used in qualitative and quantitative approaches, as the height and the area of each peak is proportional to the concentration of the corresponding substance (Meyer, 2010).

Mycolic acids can be recognized based on their chain length (C70 - C90), the presence of double bonds, their long side chain, their additional oxygen or methyl functions. The three main classes of mycolates from mycobacteria can be separated using „normal phase" HPLC, but characteristic peaks for MTBC can not be identified. However, „reserse phase" HPLC (rpHPLC), can separate mycolic acids according to their chain length and their polarity, sensing the difference between pathogenic species and environmental ones (Gernaey *et al*., 2001; Minnikin *et al*., 2011).

Gernaey *et al.* (2001), using rpHPLC, were able to identify the components corresponding to mycolic acids in two ribs belonging to a skeleton affected by tuberculosis dating to Medieval times. The total fraction of mycolates isolated from the two ribs was compared with a standard mixture of MTBC mycolic acids.. The similarity of the profiles suggests that the basic features of the mycolic acids were preserved in the medieval bones. The chromatograms can be seen in Figure 4A. In the chosen negative control, the concentration of mycolates was too low for confirmation of the disease. The soil was also tested for the presence of the mycolic acids, and the sample was shown to be free from MTBC mycolates. Environmental mycobacteria, that produce the same classes of mycolates, are not problematic for the assay, because their mycolic acids are smaller in size and have shorter retention times in rpHPLC. Moreover, individual α-, methoxy- and keto-mycolates were also identified in the two investigated ribs (Figure 4B).

After a discussion of these techniques, we recognize their potential use for the diagnosis of ancient MTBC infection cases. The stability of mycolic acids as biomarkers in tracing the paleoepidemiology of tuberculosis back into antiquity. However, lipid markers could not inform us about important aspects of the pathogen evolution. For this reason it is essential to isolate high quality, informative aDNA.

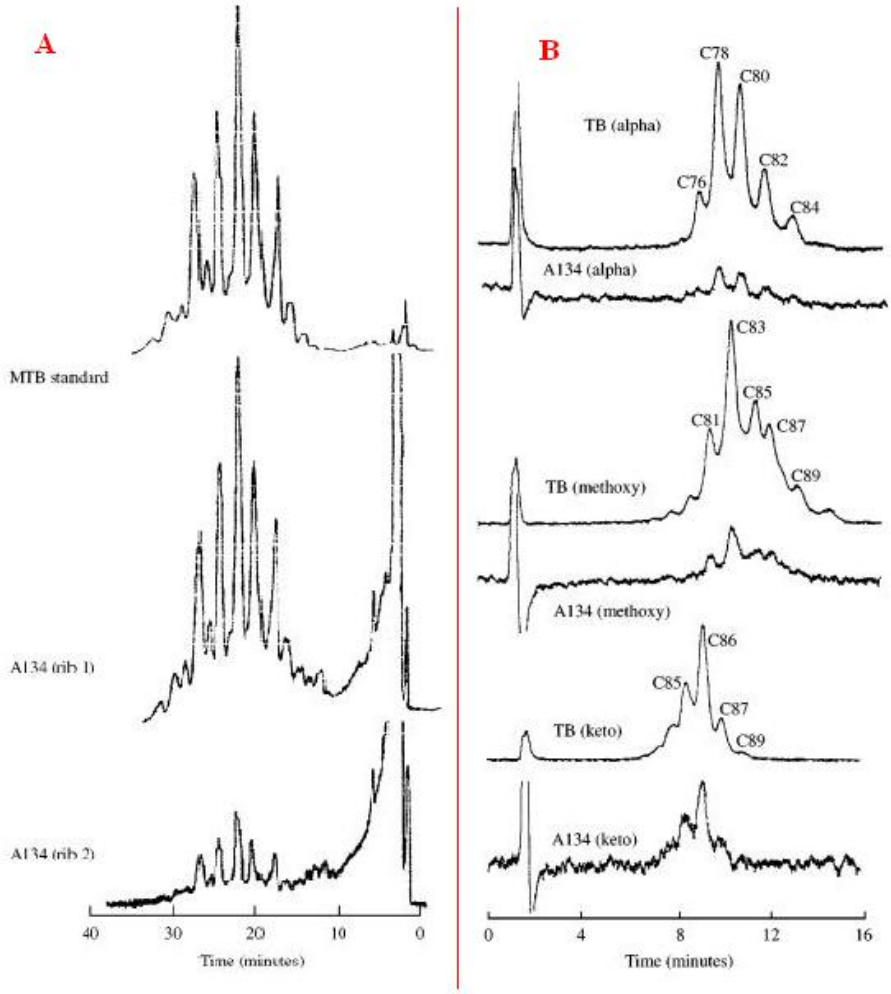

Figure 4. A. Comparable rpHPLC profiles of M. tuberculosis standard and the two investigated ribs; B. The three classes of mycolates found in the MTBC infected samples compared with the standard (from Gernaey *et al*., 2001).

The presence of MTBC inferred from aDNA

Post-mortem degradation of DNA

"aDNA" does not refer to the macromolecule's age, but to its state of conservation (Shapiro and Hofreiter, 2014). Valuable information can be inferred from aDNA sequencing and, for this reason, great efforts are made for proper aDNA

investigation. Immediately after the organisms` death, the DNA degradation occurs in two main stages: microbial digestion and chemical degradation (Smith et al., 2003; Allentoft et al., 2012). In recent years, many authors tried to find a correlation between the sample's age and the amount of high quality endogenous aDNA. This is difficult to achieve as environmental parameters greatly vary (Marota et al., 2002).

The principal chemical degradation paths are: oxidation, hydrolytic depurination and β-elimination. They are influenced by pH, humidity, and mainly temperature (Lindahl, 1993; Smith *et al*., 2003). Also, OH-2' removal in the DNA sugar moiety renders the N-glycosidic links vulnerable leading to the apparition of apurinic and apyrimidinic sites. Apyrimidinic sites occur 20 times less frequently than the apurinic ones. After depurination, the DNA is cleaved in a β-elimination process (Lindahl, 1993). Hydrolitic deamination will result in DNA mutations. Cytosine deamination will result in an uracil in the DNA strand and 5-methyl-cytosine deamination in a thymine (Lindahl, 1993).

DNA depurination, deamination and oxidation will lead to breaks in the DNA chain. After long periods of time, chemical degradation will be too advanced to allow the recovery of informative aDNA.

Detection of MTBC aDNA

The extraction protocol of aDNA follows a similar pattern in almost all cases. The bone sample is first demineralized and then treated with Proteinase K for protein (mainly collagen) digestion. The sample is then usually disaggregated with phenol-chloroform or guanidine thiocyanate, and finally precipitated with ethanol or isopropanol. In the recent years, a switch to silica membranes took place, these being used in the final steps of extraction. Generally, aDNA is poorly preserved, the length of the fragments rarely exceeding 100-200 bp. In this situation, DNA amplification via PCR (Polymerase Chain Reaction) makes possible the recovery of specific informative loci. The yield of a standard PCR can be increased by further amplification through a nested or semi-nested reaction (Minnikin *et al*., 2011).

In many cases, PCR is directed at two insertion sequences (IS). These are mobile genetic elements, that can move within the bacterial genome, and also from one bacterium to another. It is possible that these elements co-mobilize other genes, probably even those for antibiotic resistance. Among the first sequences ever amplified were IS6110 and IS1081. Both of them have more then 20 copies in a single bacterial genome, but IS6110 has the disadvantage of being absent in some M. tuberculosis strains. Thus, a negative PCR result is compatible with both the presence or the absence of the MTBC in the sample. On the other hand, successful IS1081 amplification shows that a member of the complex is present. More specific markers are available now, and they enable the discrimination between MTBC species (Brown and Brown, 2011).

An important distinction to be made is between M. tuberculosis and M. bovis, ruling out the probability that the skeleton may have contacted the bovine form of the disease (Brown and Brown, 2011).

Another distinction is between "ancient" and "modern" M. tuberculosis strains, the classification made on the basis of the tuberculosis TbD1 deletion event (Taylor *et al*., 2005). By doing whole-genome analyses of MTBC, Gordon *et al*. (1999) found ten deletion events. Because their distribution among the samples varied, it is possible that the corresponding genes are related to virulence and host range. The D1 sequence of 5014 bp was determined from X318 BCG strain of M. bovis. In M. tuberculosis the same genomic site was found to be extended with an additional 2.8 kb. Pathogens were found fully virulent in animal models even if the deletion event occurred, suggesting that D1 is not related to virulence (Brosch *et al*., 2002).

A differentiation among MTBC species became possible when a SNP (Single-nucleotide polymorphism) was discovered in the oxyR pseudogene. Initially, this gene encoded an oxidative response regulator, but then it has been disrupted and is now found in the form of a pseudogene. Sreevatsan *et al*. (1996) reported a SNP located at position 285 in the pseudogene. For all M. bovis strains, the nucleotide is an adenine, while in all the other species of MTBC the nucleotide is a guanine.

As time went on, other SNPs were identified. In the pncA gene, at position 169, a nucleotide was shown to distinguish M. tuberculosis from M. bovis. Sequencing clearly established that in M. tuberculosis the nucleotide is cysteine (Taylor *et al*., 2005; Scorpio and Zhang, 1996). This site polymorphism is associated with the natural resistance of M. bovis and the susceptibility of the majority of M. tuberculosis strains to treatment with pyrazinamide (PZA). PZA is a pro-drug of pyrazinoic acids. It displays a broad range of anti-mycobacterial activities, together with its analog 5-chloro-PZA. Zimhony *et al*. (2000) were able to demonstrate that the drug targets the fatty acid synthetase I (FAS I) through the inhibition of the biosynthesis of long-fatty acids from the acetyl-CoA precursor. Furthermore, Shi *et al*. (2011) showed that PZA also inhibits trans-translationation via direct binding to RpsA. This protein is essential for translationation because it binds to the ribosome, and its C-terminus is involved in trans-translationation through the specific recognition of transfer-messenger RNA (tmRNA). In this process, a ribosome that has stalled in the process of decoding mRNA is rescued and the translation of a short tag encoded by tmRNA occurs. This tag encodes a signal for the stalled protein degradation. The process is known to be involved in stress survival, recovery from starvation or virulence. These two methods highlight why mutations in pncA gene are associated with the susceptibility or resistance of the tuberculosis strains.

Another distinction in MTCB could be made based on the combination of polymorphic sites at katG codon 463 and at gyrA codon 95. katG encodes the catalase-peroxidase enzyme, while the gyrA is translated into subunit A of DNA-

gyrase (Taylor *et al*., 1999). Sreevatsan *et al*. (1997) analyzed 842 MTBC isolates recovered from diverse geographical sites and established that they can be divided into three groups, as seen in Table 1.

Table 1.

MTBC genotypic groups based on katG and gyrA polymorphism

Group	*kat*G (codon 463)		*gyr*A (codon 95)	
	sequence	amino acid	sequence	amino acid
I	CTG	Leu	ACC	Thr
II	CGG	Arg	ACC	Thr
III	CGG	Arg	AGC	Ser

Summing all the aforementioned information deduced from the insertion sequences and specific SNPs, researchers can confirm a tuberculosis diagnosis and identify the precise tuberculosis species causing the disease.

Even if Hofreiter *et al*. (2001) formulated several authentication criteria for aDNA, they may not be applicable to the analysis of MTBC cases. Results may not be reproducible because the pathogens are localized in the bone tissue and a repeated experiment may not give a positive result (Minnikin *et al*., 2011).

Conclusions

Tuberculosis accompanied humans in their Out-of-Africa migration and since then it was always a presence in human history. In our days it is one of the most wide-spread infectious disease, developing multi-drug resistance and extremely-drug resistant strains. This article reviewed a set of modern techniques used for the diagnosis of ancient tuberculosis. Studying such cases helps us inferring the mutation rate of the pathogens. Also, variability of specific genomic sites associated with virulence can be investigated.

Acknowledgments The authors would like to acknowledge the project "Genetic Evolution: New Evidences for the Study of Interconnected Structures (GENESIS). A Biomolecular Journey around the Carpathians from Ancient to Medieval Times." (CNCSIS-UEFISCDI_ PNII_PCCA_1153/2011, contract 229/2013).

REFERENCES

Allentoft, M.E., Collins, M., Harker, D., Haile, J., Oskam, C.L., Hale M.L., Campos, P.F., Samaniego, J.A., Gilbert, M.T.P., Willerslev, E., Zhang, G., Scofield, R.P., Holdaway, R.N., Bunce, M. (2012) The half-life of DNA in bone: measuring decay kinetics in 158 dated fossils, *Proc. R. So.c B.* **279**: 4724–4733

Brosch, R., Gordon, S.V., Marmiesse, M., Brodin, P., Buchrieser, C., Eiglmeier, K., Garnier, T., Gutierrez, C., Hewinson, G., Kremer, K., Parsons, L.M., Pym, A.S., Samper, S., van Soolingen, D., Cole S.T. (2002) A new evolutionary scenario for the Mycobacterium tuberculosis complex, Proc Natl Acad Sci USA **99**(6): 3684–3689

Brown. T., Brown, K. (2011) Biomolecular Archaeology - an introduction, John Wiley & Sons

Coates, J. (2000) Interpretation of Infrared Spectra, A Practical Approach, Encyclopedia of Analytical Chemistry 10815–10837

Comas, I., Coscolla, M., Luo, T., Borrell S., *et al*. (2013) Out-of-Africa migration and Neolithic coexpansion of *Mycobacterium tuberculosis* with modern humans, Nature **45**: 1176–1182

Gernaey, A.M., Minnikin, D.E., Copley, M.S., Dixon, R.A., Middleton, J.C., Roberts, C.A. (2001) Mycolic acids and ancient DNA confirm an osteological diagnosis of tuberculosis, Tuberculosis **81**(4): 259-265

Gordon, S.V., Brosch, R., Billault, A., Garnier, T., Eiglmeier, K., Cole, S.T. (1999) Identification of variable regions in the genomes of tubercle bacilli using bacterial artificial chromosome arrays, *Mol. Microbiol.* **32**(3): 643–655

Hofreiter, M., Serre, D., Poinar, H.N., Kuch, M., Pääbo, S. (2001) Ancient DNA, Nat Rev **2**(353): 353-359

Langford, K.W., Penkov, B., Derrington, I.M., Gundlach, J.H. (2011) Unsupported planar lipid membranes formed from mycolic acids of *Mycobacterium tuberculosis, J. Lipid Res*. **52**(2): 272-277

Lindahl, T. (1993) Instability and decay of the primary structure of DNA, Nature **362**:709-715

Mark, L., Patonai, Z., Vaczy, A., Lorand, T., Marcsik, A. (2010) High-throughput mass spectrometric analysis of 1400-year-old mycolic acids as biomarkers for ancient tuberculosis infection, *J. Archaeol. Sci*. **37**: 302–305

Marota, I., Basile, C., Ubaldi, M., Rollo, F. (2002) DNA decay rate in papyri and human remains from egyptian archaeological sites, *Am. J. Phys. Anthropol.* **117**:310–318

Marvin, L.F., Roberts, M.A., Fay, L.B. (2003) Matrix-assisted laser desorption/ionization time-of-flight mass spectrometry in clinical chemistry, *Clin. Chim. Acta* **337**: 11 –21

Meyer, V. (2010) Practical High-Performance Liquid Chromatography, Fifth Edition, John Wiley & Sons

Minnikin, D.E., Lee, O.Y.C., Wu, H.H.T., Besra, G.S., Donoghue, H.D. (2011) Molecular Biomarkers for Ancient Tuberculosis, in Understanding tuberculosis - Deciphering the secret life of the bacilli, InTech

Scorpio, A., Zhang, Y. (1996) Mutations in pncA, a gene encoding pyrazinamidase/ nicotinamidase, cause resistance to the antituberculous drug pyrazinamide in tubercle bacillus, Nat. Med. **2**(6): 662-667

Shapiro, B., Hofreiter, M. (2014) A paleogenomic perspective on evolution and gene function: new insights from ancient DNA, Science 343, 6169

Shi, W., Zhang, X., Jiang, X., Ruan, H. *et al*. (2011) Pyrazinamide inhibits trans-translation in Mycobacterium tuberculosis: a potential mechanism for shortening the duration of tuberculosis chemotherapy, *Science* **333**(6049): 1630–1632

Smith, C.I., Chamberlain, A.T., Riley, M.S., Stringer, C., Collins, M.J. (2003) The thermal history of human fossils and the likelihood of successful DNA amplification, *J. Hum. Evol.* **45**: 203–217

Smith, I. (2003) *Mycobacterium tuberculosis* pathogenesis and molecular determinants of virulence, *Clin. Microbiol. Rev*. **16**(3): 463–496

Sreevatsan, S., Pan, X., Stockbauer, K.E., Connell, N.D., Kreiswirth, B.N., Whittam, T.S., Musser, J.M. (1997) Restricted structural gene polymorphism in the *Mycobacterium tuberculosis* complex indicates evolutionarily recent global dissemination, *Proc. Natl. Acad. Sci. USA* **94**: 9869–9874

Takayama, K., Wang, C., Besra, G.S. (2005) Pathway to synthesis and processing of mycolic acids in *Mycobacterium tuberculosis*, *Clin. Microbiol. Rev.* **18**(1): 81–101

Taylor, G.M., Goyal, M., Legge, A.J., Shaw, R.J., Young, D. (1999) Genotypic analysis of *Mycobacterium tuberculosis* from medieval human remains, *Microbiology* **145**: 899-904

Taylor, G.M., Young, D.B., Mays, S.A. (2005) Genotypic analysis of the earliest known prehistoric case of tuberculosis in Britain, *J. Clin. Microbiol*. **43**(5): 2236–2240

Zimhony, O., Cox, J.S., Welch, J.T., Vilcheze, C., Jacobs, W.R., Jr. (2000) Pyrazinamide inhibits the eukaryotic-like fatty acid synthetase I (FASI) of Mycobacterium tuberculosis, *Nat.Med*. **6**: 1043–1047

STUDIA UNIVERSITATIS BABEŞ-BOLYAI BIOLOGIA, LIX, 1, 2014 (p. 127-134)

=== REVIEW ===

THE EVOLUTION OF GENDER DETECTION PROTOCOLS IN BIOARCHAEOLOGICAL STUDIES

CRISTINA MIRCEA[1,2,✉] and BEATRICE KELEMEN[1,2]

SUMMARY. Accurate gender attribution has always been a priority in forensic casework and has always concerned the archeologists. Characteristics of forensic DNA samples analysis are similar to that of ancient DNA, small quantities of workable molecules being the main resemblance. The most frequently used markers for molecular sex attribution are the single copy gene for amelogenin located on X (AMELX) and Y (AMELY) chromosomes. Worldwide used sex determination kits were designed based on amelogenin genes amplification, especially useful in forensic casework. Sometimes these sex tests fail due to allelic dropout. New molecular markers for sex identification are constantly developed to overcome this problem. Another issue characteristic for ancient DNA studies is the contamination of samples with modern molecules of DNA. The accuracy of sex tests for ancient DNA studies depends on the possibility to discriminate between authentic ancient DNA and modern contaminant DNA.

Keywords: AMELX, AMELY, ancient DNA, molecular sex attribution, physical anthropology, sex attribution.

Introduction

Planktonic organisms, living suspended in the water, form one of the most important pelagic communities, next to the nekton

Correct sex identification has always preoccupied archeologists or anthropologists and has major importance in forensic casework for nowadays population. In past populations, the status of man and woman significantly varied and the dynamics of relations between sexes changed during time. Physical anthropology may work out identifying with a higher degree of certainty the gender of skeletal remains by analyzing a few markers that indicate the sex.

[1] *Molecular Biology Center, Interdisciplinary Research Institute on Bio-Nano-Sciences, "Babeş-Bolyai" University, Cluj-Napoca, Romania.*
[2] *Faculty of Biology and Geology, Babes-Bolyai University, Cluj-Napoca, Romania.*
✉ ***Corresponding author: Beatrice Kelemen**, Molecular Biology Center, Interdisciplinary Research Institute on Bio-Nano-Sciences, "Babeş-Bolyai" University, Cluj-Napoca, Romania.*
E-mail: bea.kelemen@gmail.com

The most common physical markers are the skull and the pelvis. Skull features tend to be more robust in the man than the female and the sub pubic region presents important differences due to the fact that females are capable of giving birth (Buikstra, 1994). The pelvic region markers are more reliable in sex attribution compared to those on the skull. These protocols, however, show no results when infant remains are analyzed. Alternative methods regarding tooth crown diameter in deciduous (Black, 1978) or permanent teeth (Cardoso, 2008) were developed for sex identification of immature individuals.

All anthropological data tend to be influenced by observer subjectivity and cannot be obtained when fragmentary remains are analyzed. Considering these limitations, a molecular sex test can provide additional information. Of course molecular methods have their own limitations regarding DNA's status of preservation or its contamination with modern molecules, but, in connection with traditional anthropological methods can offer a bigger picture, more complete picture.

Sex tests based on the amelogenin gene

The interest in ancient human DNA extraction and molecular analysis begins at the end of the 1980's, when ancient Egyptian mummy DNA was cloned (Pääbo, 1985). Since then, new extraction techniques were developed in order to overcome the degradation process that DNA suffers over time and the contaminants present in each sample. In order to obtain molecular information about an individual's sex, X and Y chromosome investigation is required.

Forensic casework needed methods to determine the sex of individuals from forensic samples. Before the PCR technique was developed other methods for correct sex identification were applied, beginning with the visualization of sex chromatin (Zech, 1969). Alternative methods for detection of the Y chromosome based on the analysis of Southern hybridization patterns were developed (Vergnaud *et al*., 1984). Another technique to discriminate between males and females based on digestion with restriction enzyme (*Hae*III) revealed a specific pattern of bands for the Y chromosome (Ludes *et al*., 1990). The development of the PCR technique (Mullins and Faloona, 1987) offered new avenues of investigation and determination of sex chromosomes in humans.

The most frequently on both X and Y chromosomes is the gene encoding amelogenin. The amelogenin is a fetal tooth matrix protein (Termine *et al*, 1980). Being single copy genes, they are suitable for rapid sex identification. AMELX is located on the X chromosome Xp22.1-22.3, while AMELY on Yp11.2. AMELX gene is expressed at ten times higher levels than AMELY (Haas-Rochholz and Weiler, 1997). Analyzing their sequences, 19 regions of absolute homology can be identified, consisting of 20-80bp, 5 deletions of 1-6bp on the X chromosome and 5 deletions of 1-183bp on the Y chromosome (Haas-Rochholz and Weiler, 1997).

Generally, homologous regions are used for the design of amplification primers. The length of the obtained fragments is different due to the presence of different deletions on both X and Y chromosome.

First amplification of certain X and Y chromosomal regions was carried out using a modern DNA sample, for forensic application (Akane *et al*, 1991). The designed primers amplified fragments of 788bp on Y chromosome, respectively 977bp on X chromosome.

These primers cannot be used when working with ancient DNA due to its degradation. Fragments that long are rarely amplifiable on such samples (Pääbo, 1989). New sets of primers were designed, many of them being suitable to amplify smaller fragments not only important when working with ancient DNA but in forensics too, because analyzed samples may have degraded DNA as well.

Two sets of primers were designed to amplify the same segment on X and Y chromosome obtaining a fragment of 106bp on the X chromosome and a fragment of 112bp on Y, respectively a 212bp fragment on the X chromosome and a 218bp fragment on the Y chromosome (Sullivan *et al*, 1993). The difference in length is due to a deletion of 6bp in the intron 1 of the X chromosome, difference that makes the segments separable by electrophoresis. This method is fast and fragments on both X and Y chromosomes are amplified in one reaction, X chromosome being used as a positive control.

Primers designed by Sullivan were included in commercial kits like AmpFlSTR® SGM Plus® (Holt *et al*, 2000) and used in forensic casework all over the world. Usually when they are contained in commercial kits, the sexual markers are associated with other markers for example Y-STR (Short Tandem Repeats) markers. At least 13 STR loci are used in forensic investigation (Holt *et al*., 2000). This kind of multiplex amplifications may conduct to overlapping fragments. Primers amplifying 80bp on the X chromosome and 83bp on the Y chromosome were designed to better suit multiplex reactions (Haas-Rochholz and Weiler, 1997).

Alternative primers for sex identification were designed targeting other regions of amelogenine genes on both X and Y chromosomes in order to amplify sort segments suitable for ancient DNA studies. Targeting a deletion in the first intron in the Y chromosome, a system of three primers was used to amplify both fragments on X and Y chromosomes in one reaction obtaining a 330bp segment on the X chromosome respectively a 218bp on the Y chromosome (Faerman *et al*, 1995). Forward primers were the same on both chromosomes while the reverse primer on the X chromosome matches an X specific sequence, absent on the Y chromosome. The primer specific for the Y chromosome matches the joint of the deletion break point (Faerman *et al*, 1995). In order to obtain improved results while working with ancient highly degraded DNA, Faerman proposed a new primer for X specific amplification in order to obtain a smaller fragment consisting of 270bp, suitable when working with ancient DNA (Faerman and Bar-Gal, 1998).

On the same principle of using three primers to obtain both segments for X and Y chromosome in one reaction, new primers were designed in order to obtain a 196bp amplification product on the X chromosome and a 136bp amplification product on the Y chromosome (Götherström *et al*., 1997). The downstream primer specific for the Y chromosome matches to a related region on the X chromosome, a 304-312 additional amplification product being expected. This additional product was found just when modern DNA samples were analyzed. While working with ancient DNA, due to its degradation, this undesired additional product couldn't be amplified.

Another method involving amelogenin gene implies using a set of primers amplifying the same segment of 112bp on exon 6 of both the X and Y chromosome (Stone, 1996). Using a dot blot procedure amplification products were assigned to X and Y chromosomes due to the fact that the Y chromosome presented 8 SNPs in the amplified region when compared to the X chromosome.

In order to obtain smaller fragments suitable when working with ancient DNA or forensic samples, new primers were designed that lead to the amplification of even shorter segments. Targeting a deletion of 3bp on the Y chromosome, a 48bp segment was amplified on the X chromosome and a 45bp one on the Y chromosome (Tschentscher *et al*., 2008).

Alternatives to amelogenin gene sex tests

Sometimes sex identification using amelogenin may go wrong. If the fragment specific to the Y chromosome is missing, an individual can be catalogued as female. Using commercial kits based on primers designed by Sullivan, 4.5% of Nepalese males were identified as females because no Y specific amplification took place (Jha *et al*, 2010). The amplification of the Y specific fragment failed because AMELY was missing. Man lacking AMELY - called 'deleted-amelogenin males' (Thangaraj, 2002) - were also identified in India and Malaysia (Chang *et al*., 2003), Israel (Michael and Brauner, 2004), Spain (Bosch *et al*., 2002), Austria (Steinlechner *et al*., 2002). The absence of AMELY is explained by the complete deletion of the Y's chromosome short arm (Michael and Brauner, 2004, Lattanzi *et al*., 2005). In some cases the X chromosome's amplification fails. A rare (C→G) mutation was identified in the binding region of the X specific primer which lead to the failure of the amplification (Maciejewska and Pawłowski, 2009).

For accurate sex identification, especially important in forensic casework, alternative regions to amelogenin are necessary to be investigate since amelogenin tests are not totally reliable. The halphoid satellite family consists of repetitive DNA and is found on the pericentromeric region of each human chromosome (Willard, 1985). Repetitive sequences offer greater amount of template for PCR than single copy gene sequences (Pascal *et al.*, 1991). Specific primers for the Y chromosome,

flank a 170bp fragment (Wolfe *et al*,. 1985), while on the X chromosome a 130bp fragment is expected after amplification (Willard, 1985). Using these primers separately, PCR was performed. Other primers amplifying an X specific segment of 157bp and a Y specific segment of 200bp were designed to be used in the same reaction (Neeser and Liechti-Gallati, 1995).

ZFY is a gene located on the Y chromosome and encodes a zinc finger protein known as testis determining factor (TDF) (Page *et al*., 1987). ZFX is located on the X chromosome. Two primers were designed for amplifying a 209bp fragment on both chromosomes. The X fragment contained a restriction enzyme site for *Hae*III determining two smaller fragments consisting of 172bp and 37bp while the fragment corresponding to the Y chromosome contained a supplementary restriction site for the same enzyme which can split the 172bp segment in two fragments: one of 88bp and the other of 84bp (Stacks and Witte, 1996).

Sex-determination region Y (SRY) is located on the Y chromosome (Santos, 1998) and can be used in addition to the amelogenin test in order to verify the presence of the Y chromosome. Two primers flanking a fragment of 96bp were designed in order to suit the amplification conditions of commercially STR and amelogenin kits (Drobnič, 2006).

Authenticating ancient DNA results

One of the major issues when working with ancient DNA is represented by contamination with modern DNA (Richards *et al*., 1995). Firstly, the remains found come in contact with the archaeologists and they are the major source of contamination (Sampietro *et al*., 2006) compared with the input of modern DNA molecules coming from anthropologists and genetic researchers. Both teeth and bones are equally exposed to contamination especially prior to DNA extraction (Malmström *et al*., 2007, Sampietro *et al*., 2006). To avoid contamination, standard protocols for organizing a laboratory where ancient DNA is analyzed were elaborated (Shapiro, 2012). In order to eliminate the laboratory specific contamination the same probe can be analyzed in other ancient laboratory physically separated from the first one (Richards *et al*., 1995). An efficient method to decrease the quantity of modern DNA present in bone samples is the incubation of the bone powder in bleach (Malmström *et al*., 2007).

To authenticate DNA samples analyzed by PCR techniques a few features of ancient DNA might be taken into account. Molecular size of ancient DNA fragments is low (Pääbo, 1989), more purines are present before strand breaks (Briggs *et al*., 2007), a high number of post mortem C→T substitutions at the ends of fragments are present (Briggs *et al*., 2007) as well as miscoding lesions (Pääbo, 1989). Dealing with contamination requires a large number of cloned amplification products (Kolman and Tuross, 2000).

For sex determination, in order to overcome difficulties characteristic to ancient DNA like the presence of small fragments, small quantities of DNA and high number of cloned amplification products for authenticating the probes, new sequencing techniques can be applied. Using shotgun sequencing reliable sex determination was possible on ancient remains from 100 to 70.000 years ago (Skoglund *et al*., 2013). Discriminating ancient DNA molecules from modern ones was based on the presence of C→T substitutions present at the ends of the fragments. High throughput sequencing starts to be applied to analyze ancient DNA molecules (Bianchi *et al*., 2012).

Conclusions

Molecular sex attribution complements physical anthropological studies applied on ancient human remains and is essential in forensic casework. Amelogenin single-copy genes are widely used for sex determination. Diverse fragments of these genes are targets for PCR reactions. The length of targeted segments gets smaller and smaller to suit ancient DNA work. Failures in amplifying amelogenin genes, especially in man, have been reported. Complementing methods for the X and Y chromosomes are developed. Other molecular methods are applied in order to facilitate the authenticating process of ancient molecules in the context of exogenous DNA contamination.

Acknowledgements This study was supported by funding from the project Genetic Evolution: New Evidences for the Study of Interconnected Structures (GENESIS). A Biomolecular Journey around the Carpathians from Ancient to Medieval Times (CNCSIS-UEFISCDI _PNII_PCCA_1153/2011).

REFERENCES

Akane, A., Shiono, H., Matsubara, K., Nakahori Y., Seki, S., Nagafuchi, S., Yamada, M., Nakagome, Y. (1991) Sex identification of forensic specimens by polymerase chain reaction (PCR): two alternative methods, *Forensic Science International*, **49**, 81-88

Black, T. (1978) Sexual dimorphism in the tooth-crown diameters of the deciduous teeth, *American Journal of Physical Anthropology*, **48**, 77-82

Briggs, A.W., Stenzel, U., Johnson, P.L.F., Green, R.E., Kelso, J., Prüfer, K., Meyer, M., Krause, J., Ronan, M.T., Lachmann, M., Pääbo, S. (2007) Patterns of damage in genomic DNA sequences from a Neandertal, *Proceedings of the National Academy of Sciences,* **104**, 14616-14621

Bianchi, D.W., Platt, L.D., Goldberg, J.D., Abuhamad, A.Z., Sehnert, A.J., Rava, R.P. (2012) Genome-wide fetal aneuploidy detection by maternal plasma DNA sequencing, *Obstretics & Gynecology*, **119**, 890-891

Bosch, E., Lee, A.C., Calafell, F., Arroyo, E., Henneman, P., de Knijff, P., Jobling, M.A. (2002) High resolution Y chromosome typing: 19 STRs amplified in three multiplex reactions, *Forensic Sci. Int.,* **125**, 42–51

Buikstra, J.E., Ubelaker, D.H. (1994) Arkansas archeological survey research series, **44**.

Cardoso, H.F. (2008) Sample-specific (universal) metric approaches for determining the sex of immature human skeletal remains using permanent tooth dimensions, *J. Archaeol. Sci.,* **35**, 158-168

Chang, Y.M., Burgoyne, L.A., Both, K. (2003) Higher failures of amelogenin sex test in an Indian population group, *J. Forensic Sci.*, **48**, 1309–1313

Drobnič, K. (2006) A new primer set in a SRY gene for sex identification, *International Congress Series*, **1288**, 268 – 270

Faerman, M., Filon, D., Kahila, G., Greenblatt, C.L., Smith, P., Oppenheim, A. (1995) Sex identification of archaeological human remains based on amplification of the X and Y amelogenin alleles, *Gene,* **167**, 327-332

Faerman, M., Bar-Gal, G.K. (1998) Determining the sex of infanticide victims from the late Roman era through ancient DNA analysis, *Journal of Archaeological Science*, **25**, 861-865

Götherström, A., Liden, K., Ahlstrom, T., Kallersjo, M., Brown, T.A. (1997) Osteology, DNA and sex identification: morphological and molecular sex identifications of five neolithic individuals from Ajvide, Gotland, *International Journal of Osteoarchaeology,* **7**, 71-81

Holt, C.L., Stauffer, C., Wallin J.M., Lazaruk, K.D., Nguyen, T., Budowle, B., Walsh, P.B. (2000) Practical applications of genotypic surveys for forensic STR testing, *Forensic Science International,* **112**, 91–109

Haas-Rochholz, H., Weiler, G. (1997) Additional primer sets for an amelogenin gene PCR-based DNA-sex test, *Int. J. Legal Med.*, **110**, 312-315

Jha, D.K., Rijal, J.P., Chhetri, N.T. (2010) Nepalese null AMELY males and their Y-haplotypes, *Scientific world,* **8**, 97-101

Kolman, C.J., Tuross, N. (2000) Ancient DNA analysis of human populations, *American Journal of Physical Anthropology*, **111**, 5-23

Lattanzi, W., Di Giacomo, M., Lenato, G.M., Chimienti, G., Voglino, G. (2005) A large interstitial deletion encompassing the amelogenin gene on the short arm of the Y chromosome, *HumGenet,* **116**, 395–401

Ludes, B., Mangin, P., Hanauer, A. (1990) A rapid sex determination using restriction enzymes digestion, *Advances in Forensic Haematogenetics*, **3**, 119-121

Maciejewska, A., Pawłowski, R. (2009) A rare mutation in the primer binding region of the amelogenin X homologue gene, *Forensic Science International: Genetics*, **3**, 265–267

Malmström, H., Svensson, E.M., Gilbert, M.T., Willerslev, E., Götherström, A., Holmlund, G. (2007) More on contamination: the use of asymmetric molecular behavior to identify authentic ancient human DNA. *Molecular Biology and Evolution*, **24**, 998-1004

Michael, A., Brauner, P. (2004) Erroneous gender identification by the amelogenin sex test, *J Forensic Sci*, **49**, 258–259

Mullins, K.B., Faloona, F.A. (1987) Specific synthesis of DNA *in vitro* via a polymerase-catalyzed chain reaction, *Methods Enzymol.,* **155**, 335-350

Neeser, D., Liechti-Gallati, S. (1995) Sex determination of forensic samples by simultaneous PCR amplification of a-satellite DNA from both the X and Y chromosomes. *J. Forensic Sc.,* **40**, 239-241

Pääbo, S. (1985) Molecular cloning of Ancient Egyptian mummy DNA, *Nature***, 314,** 644-645

Pääbo, S. (1989) Ancient DNA: Extraction, characterization, molecular cloning, and enzymatic amplification, *Proc. Natl. Acad. Sci. USA,* 86, 1939-1943

Page, D.C., Mosher, R., Simpson, M.E., Fisher, C.M., Mardon, G., Pollack, J., McGillivary, B., Brown, G.L. (1987) The sex determining region of the human Y chromosome encodes a finger protein, *Cell*, **51**, 1091-1104

Pascal, O., Aubert, D., Gilbert, E., Moisan, J.P. (1991) Sexing of forensic samples using PCR, *Int J Leg Med,* **104**, 205-207

Richards, M., Sykes, B., Hedges, R. (1995) Authenticating DNA extracted from ancient skeletal remains, *J. Archaeol. Sci.*, **22**, 291–299

Sampietro, M.L., Gilbert, T.M.P., Lao, O., Caramelli, D., Lari, M., Bertranpetit, J., Lalueza-Fox, C. (2006) Tracking down human contamination in ancient human teeth, *Oxford Journals,***23**, 1801-1807

Santos, F.R., Pandya, A., Tyler-Smith, C. (1998) Reliability of DNA-based sex tests. *Nature Genetics*. **18**, 103

Skoglund, P., Stora, J., Götherström, A., Jakobsson, M. (2013) Accurate sex identification of ancient human remains using DNA shotgun sequencing, *Journal of Archaeological Science,* **40**, 4477-4482

Stacks, B., Witte, M.M. (1996) Sex determination of dried blood stains using the polymerase chain reaction (PCR) with homologous X-Y primers of the zinc finger protein gene. *J. Forensic Sci.* **41**, 287-290

Steinlechner, M., Berger, B., Niederstatter, H., Parson, W. (2002) Rare failures in the amelogenin sex test. *Int. J. Legal Med.,* **116**, 117–120

Stone, A.C., Milner, G.R., Pääbo, S., Stoneking, M. (1996) Sex determination of ancient human skeletones using DNA, *American Journal of Physical Anthropology,* **99**, 231-238

Sullivan, K.M., Mannucci, A., Kimpton, C.P., Gill, P. (1993) A rapid and quantitative DNA sex test: fluorescence-based PCR analysis of X-Y homologous gene amelogenin. *BioTechniques,* **15**, 637-641

Termine, J.D., Belcourt, A.B., Christner, P.J., Conn, K.M., Nylen, M.U. (1980) Properties of dissociatively extracted fetal tooth matrix proteins, *J. Biol. Chem.,* **255**, 9760-9768

Thangaraj, K., Reddy, A.G., Singh, L. (2002) Is the amelogenin gene reliable for gender identification in forensic casework and parental diagnosis?, *International Journal of Legal Medicine,***116**, 121-123

Tschentscher, F., Frey U.H., Bajanowski, T. (2008) Amelogenin sex determination by pyrosequencing of short PCR products, *International Journal of Legal Medicine,* **122**, 333-335

Vergnaud, G., Kaplan, L., Weisennbach, J., Dumez, Y., Berger, R., Tiollais, P., Guellaen, G. (1984) Rapid and early determination of sex using trophoblast biopsy specimens and Y chromosome specific DNA probes, *Br Med J,* **289**, 73-76.

Willard, H.F. (1985) Chromosome specific organization of human alpha satellite DNA, *Am J. Hun. Genet.*, **37**, 524-532

Wolfe, J., Darling, S.M., Erickson, R.P., Craig, I.W., Buckle, V.J., Rigby, P.W.J., Willard, H.F.K., Goodfellow, P.N. (1985) Isolation and characterization of an alphoid centromeric repeat family from the human Y chromosome, *J. Mol. Biol.*, **182**, 477-485

Zech, L. (1969) Investigation of metaphase chromosomes with DNA-binding fluorochromes, *Exp. Cell Res.,* **58**, 463

STUDIA UNIVERSITATIS BABEŞ-BOLYAI BIOLOGIA, LIX, 1, 2014 (p. 135-144)

=== REVIEW ===

MOLECULAR DIAGNOSIS OF PATHOLOGIES IN ANCIENT HUMAN REMAINS. A CASE STUDY: THE BIOARCHAEOLOGICAL STUDY OF A NEOLITHIC SKELETON DISPLAYING SYMPTOMS OF DIABETES

IOANA MIHALACHE[1,2,✉],CLAUDIA RADU[1] and BEATRICE KELEMEN[1,2]

SUMMARY. Diagnosing diabetes in archaeological human remains is a difficult task. Molecular methods can provide additional information that can help the paleopathologists come closer to a correct diagnostic. A set of skeletal remains from the Suplacu de Barcău (Romania) archaeological site, dated to the Neolithic period, displays pathological changes that indicate diabetes.This would become the oldest documented case of diabetes. This paper describes the strategy we designed for further ancient DNA analysis.

Keywords: ancient DNA, diabetes, Neolithic, paleopathology.

Introduction

One of the goals of bioarchaeology is to understand how the health status of past populations is affected by cultural, socioeconomic and demographic changes.

Determining how disease affected past populations is a laborious task and the methods used for this type of study have rapidly evolved over the past decades. The first step in the analysis of archaeological remains is the visual examination and recording of specific measurements used for assessing the age and sex of an individual, and to discover any signs of pathology. Since the soft tissues are usually absent, for a disease to be diagnosed in ancient remains it should produce changes

[1] *Bioarchaeology Laboratory, Molecular Biology Center, Interdisciplinary Research Institute onBio & Nano Sciences, Babeş-Bolyai University, Cluj-Napoca, Romania.*
[2] *Faculty of Biology and Geology, Babeş-Bolyai University, Cluj Napoca, Romania.*
✉ ***Corresponding author: Ioana Mihalache**, Bioarchaeology Laboratory, Molecular Biology Center, Interdisciplinary Research Institute onBio & Nano Sciences, Babeş-Bolyai University, Cluj-Napoca, Romania. E-mail: ioana.mihalache@yahoo.com.*

that affect the bones and teeth. Diseases that impact the bones perturb the normal turnover balance, and they can be either proliferative or erosive (Waldron, 2009). Diseased bone is relatively easy to recognise. Determining what caused the abnormality is the more challenging task. There may be a number of conditions that cause pathological changes in bones; there are cases where distinguishing between them is difficult and misdiagnosis is quite frequent. Further scientific analysis can be used to increase the certainty of the diagnostic in these cases.

Diagnosis in paleopathology differs greatly from the one in clinical practice. The formal approach for clinical diagnosis is based on knowing the medical history and examining the signs and symptoms of the disease; with this information the clinician will arrange for a series of investigations (e.g. blood tests, biopsies, biochemistry, ultrasound etc.) by which the initial diagnostic can be confirmed. The purpose of a diagnostic is to indicate the proper treatment. In contrast, when it comes to examining ancient remains, the paleopathologist can obtain the information about his 'patient' based on the visual examination of the bones, radiography, histology and ancient DNA analyses.

Examination of individuals affected by various conditions can provide answers to a number of questions. Diseases affecting the bone are more often chronic than acute, which means that the individual lived with the disease enough time to allow the changes in the bone to develop. Therefore, examination of these cases can indicate how the quality of lifeof the individual was affected by the symptoms during his lifetime and how the disease reflected the social status of the individual (is there a difference in the burial rituals between these individuals and the rest of the population?). Also, it can hint at the level of medical care and compassion in populations that leave no written evidence.

Infectious diseases in ancient populations have been a major preoccupation for those studying the history of medicine. Molecular methods to detect human pathogens (*Mycobacterium*, *Treponema*, *Yersinia,* etc.) have been developed and are continuously expanding. Some notable examples are presented below.

Tuberculosis is a disease that has been well known throughout human history. Pott's disease or spinal tuberculosis is a complication of tuberculosis that is easily identified in skeletons. Tuberculosis is caused by a bacterium in the genus *Mycobacterium*. There are two species that can infect humans: *M. bovis* and *M. tuberculosis*. The appearance of the infected bones is identical; the only way to distinguish between the two is by detection of specific molecular markers: a series of genes with specific mutations for each of the species (Bachmann *et al*., 2008). Detection of mycolic acids using mass spectrometry is another way to confirm the presence of *Mycobacterium* in archaeological human remains.

Tertiary syphilis is another infectious disease that affects bones. Syphilis is caused by bacteria of the species *Treponema pallidum.* Diagnosing syphilis can sometimes present problems and ancient DNA techniques have been used to confirm the initial diagnostic. Isolating and amplifying genes specific to treponemal DNA can confirm the presence of the pathogen (von Hunnius *et al*., 2007).

Besides infectious diseases, there are many other conditions that affect the bone formation and its remodelling such as vitamin deficiencies (lack of vitamin C causes scurvy, lack of vitamin D causes rickets), osteoporosis, starvation etc. When studying such pathological modifications of metabolism, age, sex, ancestry, and lifestyle are factors that must be taken into consideration, before reaching a conclusion about the health status of the individual.

Ancient DNA studies can be targeted at diseases with a genetic component. The study of these genetic factors in past individuals can help the understanding of how such conditions evolved.

The need for an interdisciplinary approach arises in such cases. The archaeological context of the grave gives information about the lifestyle and the cultural practices of a population and the socioeconomic status of an individual in a population.

Paleobotanical and zooarchaeological data offers an image of the environment where the individual lived.

Stable isotope analysis of carbon and nitrogen in bone collagen is used to reconstruct diet/nutrition. It is possible to determine whether the source of protein in the diet was from animal, plant or a combination of the two. The amount of ^{13}C relative to ^{12}C is a measure of the dietary dependence on C3 or C4 plants. The proportion of ^{15}N to ^{14}N isotopes indicates the trophic level of an organism. (Leatherdale, 2013)

Approaching all these aspects together paints a clearer image and helps to better understand the health of individuals or populations.

When developing a strategy for the study of an ancient pathological case it is crucial to relate to modern studies of clinical characteristics of that particular disease. The investigations rely on modern medical data and medical studies are focused mostly on cohorts from the developed countries of the world. There are differences in lifestyle, diet and habitat between the subjects of modern studies and past populations and this must be taken into account.

Case study: Suplacu de Barcău

The subject of this study are the skeletal remains of an adult male from the Suplacu de Barcău archaeological site dated to the Neolithic period.

Suplacu de Barcău (Bihor, Romania) is an archaeological site that contains a Neolithic settlement specialized in producing polished stone tools for use in the community and for exchange with other settlements (Ignat, 1998).

Radiocarbon dating was used to confirm the age of the remains. They were dated to 3970-3910 B.C.

The physical anthropology analysis was performed using the protocols described in *Standards for data collection from human skeletal remains* (Buikstra and Ubelaker, 1994).

Sex (male) was determined based on morphological features of the skull (the supraorbital margin, glabella and mental eminence) and pelvis (subpubic concavity, ventral arc, greater sciatic notch, preauricular sulcus).

Age at death (33-45 years) was determined based on the morphological changes of the pelvis (pubic symphisis, auricular surface) and the sternal end of the ribs.

A number of dental pathologies have been noted: 4 dental caries, 5 abscesses and 11 teeth lost ante mortem (Fig. 1).

Joint degeneration processes are observed in the right humeral head and right hand phalanges.

Four of the left-side ribs present remodeled fractures.

Cribra orbitalia (Fig. 2) presents itself as macroscopic porosity on the orbital roofs and is a sign of anemia caused by lack of iron or malnutrition. The presence of *cribra obitalia* generally suggests great metabolic stress.

Figure 1. Dental caries, ante mortem tooth loss

Figure 2. *Cribra orbitalia*

L4 and L5 vertebrae are fused with S1 by large exostoses specific for DISH (Diffuse Idiopathic Skeletal Hyperostosis) (Fig. 3). These are formed by the ossification and calcification of the longitudinal ligaments of the spine. DISH is more common in men than in women and rarely occurs below the age of 40. In modern populations, DISH is found in association with obesity and type II diabetes; an association with abnormal vitamin A metabolism has also been noted (Rogers and Waldron, 2001).

On the right calcaneus a major lesion (38.70x19.80 x116.56 mm) can be observed. There is remodeling around the lesion consistent with a bacterial infection affecting both the compact and trabecular bone. On the left calcaneus there are four smaller lesions affecting the compact bone and reaching the trabecular bone (Fig. 4).

DISH, the infection on the calcanei (as part of a diabetic foot complex) and *cribra orbitalia* (as a sign of nutritional stress) considered together are strong indicators of chronic diabetes. Carries and ante mortem tooth loss have also been associated with diabetes. As such, this would become the oldest documented case of diabetes, surpassing an ancient Egyptian case dated to 2055-19110 B.C. *(*Dupras *et al.*, 2010).

Figure 3. DISH (Diffuse Idiopathic Skeletal Hyperostosis)

Figure 4. Lesions on both calcanei

Diabetes is known since ancient times. The Ebers papyrus is one of the oldest preserved medical documents. It was written in Egypt around 1550 B.C. and it is a compendium of incantations and remedies for various mental and physical disorders. It also contains the first known medical reference to diabetes, more precisely to a typical symptom, polyuria: '…to eliminate urine which is too plentiful' (Loriaux, 2006). Indian physicians around the same time identified the same symptom, polyuria, but added the notion of *madhumeha* or "honey urine", noting the urine would attract ants. However, there are few cases of skeletal remains that have been diagnosed with diabetes with any degree of certainty (Dupras *et al*., 2010, Rogers and Waldron, 2001, Bruintjes, 1987).

A notable example is the case of the skeleton from the archaeological site of Dayr al-Barsha, Egypt dated between 2055- 1911 B.C. This skeleton displayed similar pathological changes to the one at Suplacu: DISH, ante mortem tooth loss, abscesses, and degenerative processes in the shoulder joint. However, this individual suffered amputation of the forefoot bilaterally. This could have been a treatment for a case of diabetic foot, treatment that requires certain surgical skills.

In order to obtain more information and increase the certainty of the diagnostic, we proceeded with developing a strategy for further investigations. This is a very challenging task, because diabetes is a complex disease, which is caused by genetic factors as well as lifestyle and environmental factors.

An important factor to consider was the individual's age at the time of death, since different forms of diabetes arise either during childhood or adulthood. Because the individual was a 33-45 years old adult, type 1diabetes is unlikely. At the same time, this is a case of chronic diabetes, so the individual lived with his condition for years before death. This places the debut of the disease somewhere between the ages of 20 and 40.

Other important aspects to consider are the environmental factors: diet, lifestyle, habitat etc.

Archaeological research in the Suplacu de Barcău area provides valuable information about the environment and the lifestyle of the Neolithic population in the area. During the middle Neolithic, Suplacu de Barcău was a permanent settlement of an agricultural community as suggested by the presence of storing pots, grinding stones and traces of wheat. An important part of the economy was stockbreeding. Big cattle (cow and buffalo), small cattle (sheep and goat) and birds (chicken, pheasant, and partridge) were raised. Hunting and fishing were largely practiced in the area. Bones from stags, hares and wild boars were uncovered (Ignat, 1998). The vegetal sources of food in typical European Neolithic populations were cereals (wheat, barley, rye, etc.), lentils and peas (Rottli and Castigliano, 2009).

We believe the presence of diabetes in this population is related to the lifestyle and diet changes during the Neolithic period (i.e. the transformation from hunter-gatherer based to agriculture based). A hunter-gatherer style of nutrition is based on wild game, fruits and roots. With the introduction of agriculture the proportion of carbohydrates in the diet increased. New sources of carbohydrates were the starch in cereals and the lactose in cattle milk.

C/N stable isotope analysis is used to confirm a typical diet for Neolithic agricultural populations: a mixture of food sources based on plants and meat (Richards *et al*. 2003).

Diabetes has also a genetic component. Ancient DNA analysis can be used for detection of certain mutations associated with diabetes by modern studies. There are numerous studies on various groups across Europe. To narrow down the number of mutations to test for, age was the primary factor to take into consideration.

We decided on detecting SNPs in genes involved in glucose metabolism and insulin production associated with Maturity Onset Diabetes of the Young (MODY), insulin resistance and Maternally Inherited Diabetes and Deafness (MIDD).

The term MODY is used to describe a group of clinically heterogeneous, non-insulin-dependent forms of diabetes. All show dominant inheritance and are defects that affect pancreas development/differentiation or normal b-cell physiology. The variations include the age at onset, severity of the hyperglycaemia (and hence risk of complications) and associated clinical features (Ellard and Hattersley, 2008).

Heterozygous loss-of-function mutations in the glucokinase (GCK) and hepatocyte nuclear factor-1 alpha (HNF1A) genes are the most common cause of

monogenic diabetes in the majority of populations studied and account for approximately 80% of UK patients with a genetic diagnosis of monogenic diabetes (Ellard *et al*., 2007).

Glucokinase (GCK) phosphorylates glucose, preparing it for glycolysis and further energy production. Glucokinase is often referred to as the beta cell glucose sensor because its activity level directly reflects the glucose concentration in the cell (Molven and Njølstad, 2011). This glycolytic enzyme plays a key role in maintaining blood glucose homeostasis. In the pancreatic beta cells, GCK controls insulin secretion and biosynthesis. Mutations in this gene raise the glycaemia threshold for insulin release, meaning the glucose levels necessary for stimulation of insulin production are higher. In the liver, GCK regulates glycogen synthesis and gluconeogenesis (Am *et al*., 2009).

Genes that encode the transcription factors HNF1A and HNF4A were also strongly associated with MODY. The hepatocyte nuclear factors (HNFs) constitute a family of transcription factors that are important for the correct development and function of the liver (Molven and Njølstad, 2011).

HNF4A encodes an orphan hormone nuclear receptor that, together with HNF1A, HNF1B, and HNF3B, constitutes part of a network of transcription factors required for gene expression in pancreatic beta cells, liver, and other tissues. In beta cells, these transcription factors regulate expression of the insulin gene as well as genes encoding proteins involved in glucose transport and metabolism, and in mitochondrial metabolism, all of which are linked to insulin secretion. The fact that heterozygous nonsense and missense mutations in HNF4A lead to an insulinopaenic form of MODY strongly suggests that beta cell function is sensitive to the amount of HNF4A and that haploinsufficiency is the likely mode of molecular pathogenesis in that condition (Barroso *et al*., 2003).

Another gene studied in correlation with type 2 diabetes was ABCC8 (ATP-binding cassette transporter sub-family C member 8). This gene encodes an ATP-sensitive potassium channel present in the membrane of beta cells (Florez, 2008). This channel controls the secretion of insulin out of beta cells and into the bloodstream.

There is a type of diabetes caused by mutations in the mitochondrial genome. Proper mitochondrial function is central to maintaining glucose homeostasis. Characteristic for this type of diabetes is strictly maternal inheritance. The patients also tend to suffer from impaired hearing. Mitochondrial diabetes is therefore often denoted Maternally Inherited Diabetes and Deafness (MIDD) syndrome (Molven and Njølstad, 2011). A SNP in MT-TL1 (Mitochondrially encoded tRNALeucine 1) was linked to premature aging of beta cells and a decrease of glucose induced insulin production (Janssen *et al*., 2007).

Polymorphisms in the CAPN10 gene have also been associated with diabetes and insulin resistance by studies made on populations from Germany, Finland,

Denmark, The United Kingdom, Poland, Czech Republic and France (Tsuchiya *et al*., 2006). CAPN10 encodes a protease expressed in the pancreas, liver and muscle. It is considered to have a role in insulin secretion, insulin action and production of glucose by the liver.

Table 1 summarizes the gene polymorphisms that best fit the age of onset and the symptoms in the Suplacu de Barcău case.

Table 1.

Genes of interest and SNPs associated with diabetes

Gene	SNP	Encoded element	Function	Associated with
GCK	rs1799884 C→A C→G	Glucokinase	Phosphorilates glucose to glucose-6-phosphate	MODY
MT-TL1	3243 A→G	Mitochondrially encoded tRNALeucine 1	tRNA for protein sythesis	Maternally Inherited Diabetes and Deafness
HNF4A	rs2144908 A→G	Hepatic nuclear factor 4α	Transcription factor	MODY
HNF1A	rs1169288 G→T	Hepatic nuclear factor1α	Transcription factor	MODY
CAPN10	*rs3792267* A→G	Calpain 10	Protease active in pancreas	Insulin resistance

Considering the age of the skeleton and the probable degradation of DNA sequencing the genes in their entirety would not be feasible. It is safe to expect tofind intact regions of 100-150 base pairs around the mutations of interest. For this a pair of primers was designed for each polymorphism allowing amplification of the neighboring regionby PCR. PCR products are then cloned and sequenced, in order to detect the presence of the SNPs.

Conclusions

Diagnosis of metabolic paleopathologies is a challenging process. There are a number of molecular methods that can be used to increase the certainty of the diagnostic. There is no standard method; it is rather a question of finding the right approach for the given situation.

Acknowledgments The authors would like to acknowledge the project "Genetic Evolution: New Evidences for the Study of Interconnected Structures (GENESIS). A Biomolecular Journey around the Carpathians from Ancient to Medieval Times." (CNCSIS-UEFISCDI_ PNII_PCCA_1153/2011, contract 229/2013)

REFERENCES

Bachmann, L., Däubl, B., Lindqvist, C., Kruckenhauser, L., Teschler-Nicola, M., Haring, E. (2008) PCR diagnostics of Mycobacterium tuberculosis in historic human long bone remains from 18th century burials in Kaiserebersdorf, Austria. *BMC Research Notes*, **1**, 83. doi:10.1186/1756-0500-1-83

Barroso, I., Luan, J., Middelberg, R. P. S., Harding, A., Franks, P. W., Jakes, R. W. (2003) Candidate Gene Association Study in Type 2 Diabetes Indicates a Role for Genes Involved in b -Cell Function as Well as Insulin Action. *PloS Biology*, **1**(1), 41–56. doi:10.1371/journal.pbio.0000020

Brickley, M., Ives, R. (2008) The Bioarchaeology of Metabolic Bone Disease, Academic Press

Bruintjes, T. J. D. (1987) Diffuse idiopathic skeletal hyperostosis(DISH). A 10th century AD case fromthe St Servaas church at Maastricht. *Bone,***1**, 23-28

Buikstra, J., Ubelaker, D. (1994) Standards for data collection from human skeletal remains. Retrieved from http://core.tdar.org/document/323332

Dupras, T., Williams, L., Willems, H., Peeters, C. (2010). Pathological skeletal remains from ancient Egypt: the earliest case of diabetes mellitus? *Practical Diabetes International*, **27**(8), 358–363a. doi:10.1002/pdi.1523

Ellard, S., Hattersley, A. T. (2008). Best practice guidelines for the molecular genetic diagnosis of maturity-onset diabetes of the young. *Diabetologia*, **51**, 546–553. doi:10.1007/s00125-008-0942-y

Ellard, S., Thomas, K., Edghill, E. L., Owens, M. (2007) Partial and whole gene deletion mutations of the GCK and HNF1A genes in maturity-onset diabetes of the young. *Diabetologia*, **50**, 2313–2317. doi:10.1007/s00125-007-0798-6

Florez, J. C. (2008). The Genetics of Type 2 Diabetes : A Realistic Appraisal in 2008. *J Clin Endocrinol Metab*, **93**, 4633–4642. doi:10.1210/jc.2008-1345#

Ignat, D. F. (1998) Grupul Cultural Neolitic: Suplacu De Barcău. Editura Mirton.Timisoara.

Janssen, G. M. C., Hensbergen, P. J., van Bussel, F. J., Balog, C. I. a, Maassen, J. A., Deelder, A. M., Raap, A. K. (2007) The A3243G tRNALeu(UUR) mutation induces mitochondrial dysfunction and variable disease expression without dominant negative acting translational defects in complex IV subunits at UUR codons. *Human Molecular Genetics*, **16**(20), 2472–81. doi:10.1093/hmg/ddm203

Leatherdale, A. (2013) Interpreting Stable Carbon and Nitrogen Isotope Ratios in Archaeological Remains: An Overview of the Processes Influencing the δ13C and δ15N Values of Type I. *Totem: The University of Western Ontario Journal of Anthropology*, **21**(1)

Loriaux, D L. (2006) Diabetes and The Ebers Papyrus: 1552 B.C. *Endocrinologist*, 16 (2) 55-56. doi: 10.1097/01.ten.0000202534.83446.69

Molven, A., Njølstad, P. R. (2011) Role of molecular genetics in transforming diagnosis of diabetes mellitus. *Expert Review of Molecular Diagnostics*, **11**, pp 313–321.

Richards, M. P., Pearson, J. A., Molleson, T. I., Russell, N., Martin, L. (2003) Stable Isotope Evidence of Diet at Neolithic Çatalhöyük, Turkey. *Journal of Archaeological Science*, **30**(1), 67–76. doi:10.1006/jasc.2001.0825

Rogers, J., Waldron, T. (2001) DISH and the Monastic Way of Life, **365**, 357–365

Rottoli, M., Castigliani, E., (2009), Prehistory of plant growing and collecting in northern Italy, based on seed remains from the early Neolithic to the Chalcolithic (c. 5600–2100 cal b.c.), *Vegetation History and Archaeobotany,* **1**(18), pp 91-103. doi:10.1007/s00334-007-0139-1

Tam, C. H. T., Ma, R. C. W., So, W. Y., Wang, Y., Lam, V. K. L., Germer, S., Martin, M., Chan, J., Ng, M. C. Y. (2009) Interaction Effect of Genetic Polymorphisms in Glucokinase (GCK) and Glucokinase Regulatory Protein (GCKR) on Metabolic Traits in Healthy Chinese Adults and Adolescents. *Diabetes*, **58**. doi:10.2337/db08-1277

Tsuchiya, T., Schwarz, P. E. H., Bosque-plata, L., Geo, M. V, Dina, C., Froguel, P., Bell, G. I. (2006) Association of the calpain-10 gene with type 2 diabetes in Europeans : Results of pooled and meta-analyses. *Molecular Genetics and Metabolism*, **68**. doi:10.1016/j.ymgme.2006.05.013

Von Hunnius, T. E., Yang, D., Eng, B., Waye, J. S., Saunders, S. R. (2007) Digging deeper into the limits of ancient DNA research on syphilis. *Journal of Archaeological Science*, **34**(12), 2091–2100. doi:10.1016/j.jas.2007.02.007

Waldron, T., (2009) Paleopathology. Cambridge University Press, Cambridge

STUDIA UNIVERSITATIS BABEŞ-BOLYAI BIOLOGIA, LIX, 1, 2014 (p. 145-156)

=== REVIEW ===

A BRIEF OVERVIEW OF THE MITOCHONDRIAL DNA AS MOLECULAR MARKER IN BIOARCHAEOLOGY

IOANA RUSU[1]✉ and BEATRICE KELEMEN[1]

SUMMARY. The current paper summarizes the key studies that revolutionized the field of ancient DNA research, with special focus on the mitochondrial genome. Differences between molecular markers used in bioarchaeology are presented with emphasis on their advantages and disadvantages. As previously stated the focus of this review is on the mitochondrial DNA as a molecular marker, commonly used to answer bioarchaeological questions. The essential studies on mitochondrial DNA from ancient specimens that reveal key information about the history of Europeans are illustrated.

Keywords: ancient DNA, bioarchaeology, mitochondrial genome.

Introduction

For centuries, people have been trying to solve the mystery of their origin and to answer questions regarding the evolutionary history of the modern *Homo sapiens* species. First insights that shed light on the past of the human race were provided by archaeological records. Their major limitation is their small resolution when prehistoric records are studied. These are in many cases degraded over time carrying little or no information. Once the structure, properties and function of the DNA molecule were deciphered a new perspective on the approach to tracing the ancestry of humans deep into the past was soon embraced. Since the genetic material is inherited from previous generations, the history of our species is written in our DNA. Unlike archaeological records, this kind of record does not fade away over time and enables molecular biologists to unravel messages from the past, far beyond the reach of stone paintings or different types of material inventory, for example.

[1] *Babeş-Bolyai University, Faculty of Biology and Geology, Interdisciplinary Research Institute on Bio & Nano Sciences, Molecular Biology Center, Cluj-Napoca, România.*

✉ ***Corresponding author: IoanaRusu**, Babeş-Bolyai University, Faculty of Biology and Geology, Interdisciplinary Research Institute on Bio & Nano Sciences, Molecular Biology Center, Treboniu Laurian Street 42, 400271, Cluj-Napoca, Cluj, România.*
Mobile: +40755456580, E-mail: rusu.n.ioana@gmail.com

This idea was emphasized by a scientific paper published in 1987, "Mitochondrial DNA and Human Evolution" (Cann *et al*., 1987). For many generations of scientists controversies based on the interpretation of fossil remains regarding the origins of modern humans were intensely debated,. Using a bio-molecular approach, this publication "(Cann *et al.,* 1987) estimated that the most common mitochondrial ancestor of all modern humans lived about 150 000 years ago in Africa. Supporting the "Out of Africa" theory in favor of the multi-regional scheme, these findings had a great impact in the scientific community (Sykes, 2001).

Brief history

In 1984, Higuchi and his co-workers (1984) managed to retrieve DNA sequences from a museum specimen of quagga (140 years old), an extant member of the genus *Equus* (Higuchi *et al*., 1984). By illustrating the potential of long term survival of DNA molecule in ancient remains, this publication had a great impact in various fields of the scientific community. One year later, Alu elements from a 2400 year old Egyptian mummy of a child were molecularly cloned (Pääbo, 1985). It was clear that ancient DNA can be preserved for many hundred of years in archaeological samples, but considering the postmortem degradation of nucleic acids, for how long and in which conditions? The discovery of a human skeleton in the Tyrolean Alps, now widely known as the Ice Man, has provided additional information regarding the preservation of nucleic acids in 5 000 years old remains from an extreme, cold environment. Moreover, mitochondrial DNA sequences were successfully retrieved from this specimen and compared to those obtained from present-day people. Interestingly, the Ice Man was genetically linked to contemporary Europeans suggesting that all people carry information about their ancestors in DNA molecules.

A remarkable breakthrough in the field of ancient DNA research is the determination of the almost complete mitochondrial genome sequence of a hominin from northern Spain, dated to over 300000 years ago (Meyer *et al*., 2014). The analysis of the oldest DNA ever sequenced revealed surprising facts. The results indicate that it is more likely that the hominin discovered in Spain shares a common ancestor with the Denisovans rather than the Neanderthals, despite the fact that the morphological traits of the skeletal remains suggest the contrary.

Recently, due to technological advances in ancient DNA techniques, a series of archaeological and anthropological controversies can be solved, and at the same time new question arise and need answers. The first technology that revolutionized the field of molecular genetics was the development of Polymerase Chain Reaction (PCR). Since Kary Mullis had this original idea in 1983, this amplification technique was improved and has now become widely used. It enables the production of thousands to millions of copies of a specific DNA segment even from a single template molecule (Bartlett and Stirling, 2003). It is essential for the field of ancient DNA, because usually only a small amount of degraded DNA can be recovered from archaic specimens. More recently, high-throughput DNA sequencing methods were

developed and had a considerable impact in ancient DNA research because significant amounts of sequence data can be generated in a short period of time (Knapp and Hofreiter, 2010). Even though costs for Next Generation Sequencing (NGS) have been significantly reduced in the last few years, it is still not affordable for all laboratories as it also involves powerful bioinformatic means to analyze such large amount of sequence data.

Despite the fact that significant technological progress was achieved in the field of ancient DNA research, the investigation of genomes from archaeological samples is still challenging due to contamination with exogenous DNA. For this reason, strict guidelines have to be followed (Poinar, 2003).

Molecular markers

The study of genetic variations represents a powerful tool that helps us form a relatively complete image of human evolution , as major demographic events leave traces in the human genome mainly by inducing changes in allele frequencies. These imprints are recorded by the modern human genomes because they have been inherited from previous generations. Initial molecular markers used to assess the genetic variation among populations were the blood group systems (Jorde *et al*., 1998). Although, in this manner a perspective of the evolutionary history of our species was provided, it was soon remarked that a single system could only open a small window into the past. It was also observed that using only one genetic system, such as the ABO blood groups, can sometimes lead to same gene frequency in two populations, just by chance, rather than common ancestry (Sykes, 2001). To eliminate such misleading results several genetic systems are now analyzed, often in a multidisciplinary approach.

There are several distinct categories of genetic markers used for unraveling the past history of humans. One group includes nuclear markers such as Single Nucleotide Polymorphisms (SNPs) and Short Tandem Repeats (STR) which have different mutation rates. The evolution of STR, also known as microsatellites, is considerably higher than that of SNPs which make them more suitable for assessing recent history and less informative for ancient evolutionary events (Jorde *et al*., 1998). STRs can be found on the Y chromosome and are frequently used for the investigation of paternal ancestry. Mitochondrial DNA is used in a similar way to trace back maternal lineages (Bouwman *et al*, 2008; Cafer, 2010).

Proprieties of mitochondrial DNA

Besides being maternally inherited in most multicellular organisms, mitochondrial DNA possesses some unique features which makes it appropriate for a large variety of studies, including human evolution, migration or establishing relationships between past populations.

Human mitochondrial DNA (mtDNA) is a double-stranded, circular molecule of 16569 base pairs (Anderson *et al*., 1981). This small genome is located in the cell's energy organelles, mitochondria, and it is presumed to have originated from bacteria that were taken inside advanced cells as endosymbionts, hundreds of millions of years ago (Sykes, 2001). The mitochondrial genome contains genes necessary for the production of energy and a non-coding fragment named the control region. Other mitochondrial genes were slowly transferred to the nucleus in the course of evolution (Pakendorf and Stoneking, 2005).

Unlike any nuclear genes which are present in the human cells in only two copies, there is a multitude of mitochondria in most cells. Since one of the major difficulties for ancient DNA studies is the post-mortem degradation of nucleic acids (Höss *et al*., 1996; Pääbo *et al*., 2004; Willerslev and Cooper 2005), a high copy number of mtDNA makes it more accessible mean for tracking matrilineal ancestry.

Another difference between the two types of genomes is their mutation rate, which is higher in mtDNA, being especially high in the control region (Brown *et al*., 1979). This elevated substitution rate offers an insight on the developments that lead to the actual human gene pool over time (Cann *et al*., 1987).

Nuclear DNA, which is inherited from both parents is subjected to recombination processes. In contrast, human mtDNA is inherited only from one parent, the mother, while paternal mitochondria are lost during fertilization. There were controversies regarding the lack of genetic exchange that had significant impact for mtDNA based phylogenetic studies (Hagelberg*et al*., 1999). In a particular case where the recombination of mtDNA was proposed to explain the presence of a rare mutation at high frequency in separate mtDNA lineages from a small island, the explanation turned out to be just a sequence alignment error (Hagelberg *et al*., 2000). Currently, it is suggested that the main cause for homoplasyis is the presence of mutational hotspots which occur preferentially at hypervariable sites (Stoneking, 2000; Galtier *et al*., 2006).

All these characteristics make mtDNA a suitable molecular marker used for the screening of the genetic history of humans. Assuming that neutral mutations accumulate in time with a constant rate, it has been used as a molecular clock, timing evolutionary events. In this context, Sykes reconstructed the evolutionary history of Europeans and suggested that all modern members originated from seven distinct maternal lineages (Sykes, 2001). The mutation rate estimated for the human mitochondrial DNA is quite different from that reported in pedigree and phylogenetic studies. This is caused by several factors, such as: the presence of mutational hot spots, genetic drift, selection, and the lack of detection of high levels of homoplasy in phylogenetic studies (Howell *et al*., 2003). The assumption that a uniform mutation rate exists is considered an oversimplification which doesn't perfectly reflect the true evolutionary and demographic history of our species (Pakendorf and Stoneking, 2005; Pulquério and Nichols, 2007; Galtier *et al*., 2009).

What is analyzed?

Various parts of the human mitochondrial DNA are analyzed, depending mostly on the focus of the study. Until a few years ago, the majority of research included the investigation of the mitochondrial control region. This non-coding region of the mitochondrial genome comprises two highly polymorphic segments, HyperVariable Regions I and II (HVR-I, HVR-II), and thus provides a good image on the diversity of the mitochondrial genome. In order to obtain data on the variability of the human mitochondrial genome, two types of markers are frequently used: restriction fragment length polymorphisms (RFLPs) and sequence analysis of PCR products. It was observed that DNA molecules recovered from ancient human remains are highly degraded and fragmented due to biological and chemical processes that occur postmortem (Gilbert *et al*., 2003). Therefore, the amplification of ancient DNA sequences is restricted to short fragments of approximately 100-200 base pairs (Pääbo *et al*., 2004). The strategy to overcome this limitation is to amplify short overlapping segments that span the hypervariable regions (Gabriel *et al*., 2001). For this reason, it is considered that for the classification of mtDNA variation into haplogroups, in case of large population studies from archaeological remains, RFLP analysis is more suitable (Izaguirre and De La Rua, 2002).

Data from only the HVRI sequence allows a haplogroup prediction, which becomes more accurate when HVRII is also considered. For a more sensitive haplogroup discrimination, which is especially important in forensic cases, single point mutations from the coding region are also screened (Köhnemann *et al*., 2009). These informative SNPs can be determined by RFLP analysis (Torroni *et al*., 1996) or by SNaPshot assay, a multiplex method (Brandstätter *et al*., 2003). Also, to distinguish more precisely between sequences assigned to haplogroup H and non-H haplogroup, a short segment comprising the defining nucleotide for haplogroup H (position 7028) can be additionally sequenced besides HVRI (Dissing *et al*., 2007).

The study of the mitochondrial genome has a great importance for the medical field as it has been revealed that multiple SNPs can be associated with a variety of degenerative diseases (MITOMAP: http://www.mitomap.org, 2013). For example, a homoplasmic mutation that occurs at position 4336 in the nucleotide sequence might be a contributing factor in Alzheimer and Parkinson diseases (Egensperger *et al*., 1997). Homoplasmy appears when all copies of the mitochondrial genome are identical, while be heteroplasmic mutations are present only in some of the copies of the mitochondrial genome (Wallace, 1994). Variations in some mitochondrial genes are associated with Leber Hereditary Optic Neuropathy and contribute, together with nuclear genetic factors, to the expression of the disease (Taylor and Turnbull, 2005). In this light, the analysis of variations in the sequence of mitochondrial genes is essential, as it might be used for the diagnosis of some genetic disorders.

HVRI sequences from ancient human remains are frequently studied to determine the maternal relationships between individuals (Dissing *et al*., 2007). In order to avoid inconclusive results due to ambiguous haplotype assignment, additional diagnostic point mutations from the coding region are sometimes screened (Rudbeck *et al*., 2005; Deguilloux *et al*., 2014). Being maternally inherited, data from mitochondrial genomes can't provide a complete picture of the biological relationships among individuals. As a consequence, autosomal markers, usually STRs, and the non-recombining region of the Y chromosome are analyzed to complete the information about closely related individuals recovered from archaeological sites (Keyser-Tracqui *et al*., 2003).

Recent advances in molecular genetic technologies have enabled direct access to information from the whole mitochondrial genome. Complete mitochondrial genome sequences were reconstructed from ancient specimens, including a 38000 year old hominid, identified as Neanderthal (Green *et al*., 2008). Whole mitochondrial genome sequences were analyzed to gain a more comprehensive idea about human population history. They were used to construct phylogenetic trees which seemed to be based on a more accurate estimate of the mutation rate than the previously reported ones, which considered only the differences in the control region (Ingman *et al.*, 2000). However, it is still uncertain whether whole mitochondrial genome sequencing is always the best approach considering the costs involved. An alternative to gain insights on the past of human populations is to supplement control region sequences with those mutations from the coding region that contain informative nucleotide polymorphisms (Pakendorf and Stoneking, 2005).

How is the mtDNA sequence analyzed?

The mitochondrial genetic variants of modern people and of past populations can be classified into distinct haplogroups. Similarly, mitochondrial sequences that share the same mutations are grouped into a certain haplogroup suggesting that they all have a common ancestor. To screen for the divergence points among various sequences, these are compared to the first complete sequence of a human mitochondrial genome, the revised Cambridge reference sequence (Andrews *et al*., 1999). Considering mitochondrial sequence variation from three distinct European populations, Torroni and his collaborators revealed that almost 100% can be grouped into 10 different haplogroups (H, I, J, K, M, T, U, V, W, X) (Torroni *et al*., 1996). To define these European haplogroups, mutations in the mitochondrial coding region where determined using restriction fragment length polymorphisms.

The evolutionary relationships between human populations are represented as phylogenetic networks in which the haplogroups are major branching points. Such phylogenetic trees were initially built by using information from the non-coding

region because of its high mutational rate (Richards *et al*., 1996; Macaulay *et al*., 1999). A refined, comprehensive, phylogenetic tree that provides a high resolution on global mitochondrial DNA diversity, from the most recent common matrilineal ancestor of all humans is currently available online (van Oven *et al*., 2009; http://www.phylotree.org).

The mitogenomic data from *Homo neanderthalensis* enabled the reconstruction of the genetic sequence of the "Mitochondrial Eve". It was proposed that the Revised Cambridge Reference Sequence which belongs to the European haplogroup H2a2a should be replaced with the Reconstructed Sapiens Reference Sequence (RSRS) (Behar *et al*., 2012). At this point, this approach is still controversial because the switch to a new reference sequence may cause misinterpretations (Bandelt*et al*., 2014). Still, in a recent study aimed to assess the key factors that lead to the current diversity and distribution of haplogroup H, mitochondrial variation observed in ancient DNA recovered from archaeological samples was genotyped against RSRS (Brotherton *et al*., 2013).

Ancient DNA and European mitochondrial genome diversity

The evolutionary history of modern humans is governed by several factors which include changes in the environment, culture and the geographic distribution of populations. Major demographic events contributed to the current European gene pool by altering the allele frequencies. The analysis of genetic variations in multiple modern populations sheds light on the geographic dispersal of our ancestors, that shaped the actual distribution of populations and their genetic structure. Recent demographic events and population genetic processes obscure some aspects of the human evolutionary history (Lacan *et al*., 2013). Direct access to ancient DNA offers invaluable, additional, information to the one revealed by present-day markers, leading to a better understanding of our complex genetic history (Der Sarkissian *et al*., 2013).

In Europe, several major population movements contributed to the actual patters of genetic diversity (Soares *et al*, 2010; Pinhasi *et al*., 2012). These include the first colonization of the continent, movements due to the last glacial maximum and the transition from a hunter-gatherer way of life to farming, during the Neolithic expansion. The reason for the abundance of studies that focus on ancient mitochondrial DNA from archaeological remains is that they explain how these major events influenced the complex evolutionary history of Europe (Hervella *et al.*, 2012; Brandt *et al*., 2013; Brotherton *et al*., 2013). Ancient DNA studies are also performed to identify more recent migration patterns, establish population affinities, origins and evaluate possible maternal relationships (Bogácsi-Szabó *et al*., 2005; Núńez *et al*., 2011; Ottoni *et al*., 2011; Deguilloux *et al*., 2014).

Genetic investigation of archaeological specimens dated to medieval times have the potential to improve our knowledge about past societies, as substantial changes in population movement occurred during the Middle Ages. Since the southeastern part of Europe, including Romania, was one of the key routes in population dispersal during medieval times, the analysis of mitochondrial genetic variation of past populations from this area, almost unrepresented in current literature, could fill a very large knowledge gap and allow us to identify some of the biological, socioeconomic and cultural factors that, in the end, influenced how the European population looks today from a genetic point of view.

Conclusions

All things considered, mitochondrial DNA is a remarkable molecular marker, widely used in forensics, medical studies and bioarchaeology due to its unique characteristics. A common tendency in the bioarchaeology field is to use multidisciplinary approaches and to integrate in the archaeological context, the information revealed by genetic studies. Even though, some of the questions regarding the past of the human species and its populations cannot find answers, the mitochondrial DNA remains the most straightforward tool used to unravel some of the puzzle pieces of the evolutionary history of humans.

Acknowledgments The authors would like to acknowledge the project "Genetic Evolution: New Evidences for the Study of Interconnected Structures (GENESIS). A Biomolecular Journey around the Carpathians from Ancient to Medieval Times." (CNCSIS-UEFISCDI_ PNII_PCCA_1153/2011, contract 229/2013).

REFERENCES

Anderson, S., Bankier, A.T, Barrell, B.G., de Bruijn, M.H., Coulson, A.R., Drouin, J., Eperon, I.C., Nierlich, D.P., Roe, B.A., Sanger, F., Schreier, P.H., Smith, A.J., Staden, R., Young, I.G. (1981) Sequence and organization of the human mitochondrial genome, *Nature*, **290**, 457-465

Andrews, R.M., Kubacka, I., Chinnery, P.F., Lightowlers, R.N., Turnbull, D.M., Howell, N. (1999) Reanalysis and revision of the Cambridge reference sequence for human mitochondrial DNA, *Nature Genetics*, **23**, 147

Bandelt, H.J., Kloss-Brandstätter, A., Richards, M.B., Yao, Y.G., Logan, I. (2014) The case for the continuing use of the revised Cambridge Reference Sequence (rCRS) and the standardization of notation in human mitochondrial DNA studies, *J. Hum. Genet.,* **59**, 66-77

Bartlett, J.M.S., Stirling, D. (2003) A Short History of the Polymerase Chain Reaction, *PCR Protocols,***226**, 3–6

Behar, D.M., van Oven, M., Rosset, S., Metspalu, M., Loogväli, E.L., Silva, N.M., Kivisild, T., Torroni, A., Villems, R. (2012) A "Copernican" reassessment of the human mitochondrial DNA tree from its root, *Am. J. Hum. Genet.*, **90**, 675-84

Bogácsi-Szabó, E., Kalmár, T., Csányi, B., Tömöry, G., Czibula, A., Priskin, K., Horváth, F., Downes, C.S., Raskó, I. (2005) Mitochondrial DNA of ancient Cumanians: culturally Asian steppe nomadic immigrants with substantially more western Eurasian mitochondrial DNA lineages, *Hum. Biol*., **77**, 639-662

Bouwman, A.S., Brown, K.A., Prag, J.N.W., Brown, T.A. (2008) Kinship between burials from Grave Circle B at Mycenae revealed by ancient DNA typing, *Journal of Archaeological Science*, **35**, 2580–2584

Brandstätter, A., Parsons, T.J., Parson, W. (2003) Rapid screening of mtDNA coding region SNPs for the identification of west European Caucasian haplogroups, *Int. J. Legal Med*., **117**, 291-298

Brandt, G., Haak, W., Adler, C.J., Roth, C., Szécsényi-Nagy, A., Karimnia, S., Möller-Rieker, S., Meller, H., Ganslmeier, R., Friederich, S., Dresely, V., Nicklisch, N., Pickrell, J.K., Sirocko, F., Reich, D., Cooper, A., Alt, K.W., Genographic Consortium (2013) Ancient DNA reveals key stages in the formation of central European mitochondrial genetic diversity, *Science*, **342**, 257-261

Brotherton, P., Haak, W., Templeton, J., Brandt, G., Soubrier, J., Jane Adler, C., Richards, S.M., Sarkissian, C.D., Ganslmeier, R., Friederich, S., Dresely, V., van Oven, M., Kenyon, R., Van der Hoek, M.B., Korlach, J., Luong, K., Ho, S.Y., Quintana-Murci, L., Behar, D.M., Meller, H., Alt, K.W., Cooper, A.; Genographic Consortium, Adhikarla, S., Ganesh Prasad, A.K., Pitchappan, R., VaratharajanSanthakumari, A., Balanovska, E., Balanovsky, O., Bertranpetit, J., Comas, D., Martínez-Cruz, B., Melé, M., Clarke, A.C., Matisoo-Smith, E.A., Dulik, M.C., Gaieski, J.B., Owings, A.C., Schurr, T.G., Vilar, M.G., Hobbs, A., Soodyall, H., Javed, A., Parida, L., Platt, D.E., Royyuru, A.K., Jin, L., Li, S., Kaplan, M.E., Merchant, N.C., John Mitchell, R., Renfrew, C., Lacerda, D.R., Santos, F.R., SoriaHernanz, D.F., Spencer Wells, R., Swamikrishnan, P., Tyler-Smith C., Paulo Vieira, P., Ziegle, J.S. (2013) Neolithic mitochondrial haplogroup H genomes and the genetic origins of Europeans, *Nat. Commun*., **4**, 1764

Brown, W.M., George, M. Jr., Wilson, A.C. (1979) Rapid evolution of animal mitochondrial DNA, *PNAS*, **76**, 1967–1971

Cafer, A.M. (2010) Mitochondrial and Y Chromosomal DNA in the Analysis of Kinship: Methods, Current Practices, and Areas of Further Inquiry, *Nebraska Anthropologist*, Paper 52

Cann, R.L., Stoneking, M., Wilson, A.C. (1987) Mitochondrial DNA and human evolution, *Nature*, **325**, 31-36

Deguilloux, M.F., Pemonge, M.H., Mendisco, F., Thibon, D., Cartron, I., Castex, D. (2014) Ancient DNA and kinship analysis of human remains deposited in Merovingian necropolis sarcophagi (JauDignac et Loirac, France, 7th-8th century AD), *Journal of Archaeological Science*, **41**, 399–405

Der Sarkissian, C., Balanovsky, O., Brandt, G., Khartanovich, V., Buzhilova, A., Koshel, S., Zaporozhchenko, V., Gronenborn, D., Moiseyev, V., Kolpakov, E., Shumkin, V., Alt, K.W., Balanovska, E., Cooper, A., Haak, W.; Genographic Consortium (2013) Ancient DNA reveals prehistoric gene-flow from siberia in the complex human population history of North East Europe, *PLoS Genet*., **9**, e1003296

Dissing, J., Binladen, J., Hansen, A., Sejrsen, B., Willerslev, E., Lynnerup, N. (2007) The last Viking King: a royal maternity case solved by ancient DNA analysis, *Forensic Sci. Int*., **166**, 21-7

Egensperger, R., Kösel, S., Schnopp, N.M., Mehraein, P., Graeber, M.B. (1997) Association of the mitochondrial tRNA(A4336G) mutation with Alzheimer's and Parkinson's diseases, *Neuropathol. Appl. Neurobiol*., **23**, 315-21

Gabriel, M.N., Huffine, E.F., Ryan, J.H., Holland, M.M., Parsons, T.J. (2001) Improved MtDNA sequence analysis of forensic remains using a "mini-primer set" amplification strategy, *Journal of Forensic Science*, **46**, 247–253

Galtier, N., Enard, D., Radondy, Y., Bazin, E., Belkhir, K. (2006) Mutation hotspots in mammalian mitochondrial DNA, *Genome Research*, **16**, 215–222

Galtier, N., Nabholz, B., Glémin, S., Hurst, G.D. (2009) Mitochondrial DNA as a marker of molecular diversity: a reappraisal, *Mol. Ecol*., **18**, 4541-4550

Gilbert, M.T., Willerslev, E., Hansen, A.J., Barnes, I., Rudbeck, L., Lynnerup, N., Cooper, A. (2003) Distribution patterns of postmortem damage in human mitochondrial DNA, *Am. J. Hum. Genet*., **72**, 32-47

Green, R.E., Malaspinas, A.S., Krause, J., Briggs, A.W., Johnson, P.L., Uhler, C., Meyer, M., Good, J.M., Maricic, T., Stenzel, U., Prufer, K., Siebauer M, Burbano, H.A., Ronan, M., Rothberg, J.M., Egholm, M., Rudan, P., Brajkovic, D., Kucan, Z., Gusic, I., Wikstrom, M., Laakkonen, L., Kelso, J., Slatkin, M., Pääbo, S. (2008) A complete Neandertal mitochondrial genome sequence determined by highthroughput sequencing, *Cell*, **134**, 416–426

Hagelberg, E., Goldman, N., Lió, P., Whelan, S., Schiefenhövel, W., Clegg, J.B., Bowden, D.K. (1999) Evidence for mitochondrial DNA recombination in a human population of island Melanesia, *Proc.Biol. Sci*., **266**, 485-492

Hagelberg, E., Goldman, N., Lió, P.,Whelan, S., Schiefenhövel, W., Clegg, J.B., Bowden, D.K. (2000) Evidence formitochondrial DNA recombination in a human population of island Melanesia: correction, *Proc. Biol. Sci.*, **267**, 1595–1596

Handt, O., Richards, M., Trommsdorff, M., Kilger, C., Simanainen, J., Georgiev, O., Bauer, K., Stone, A., Hedges, R., Schaffner, W., *et al*. (1994) Molecular genetic analyses of the Tyrolean Ice Man, *Science*, **264**, 1775-1778

Hervella, M., Izagirre, N., Alonso, S., Fregel, R., Alonso, A, *et al*. (2012) Ancient DNA from Hunter-Gatherer and Farmer Groups from Northern Spain Supports a Random Dispersion Model for the Neolithic Expansion into Europe, *PLoS ONE*, **7**, e34417

Howell, N., Smejkal, C.B., Mackey, D.A., Chinnery, P.F., Turnbull, D.M., Herrnstadt, C. (2003) The pedigree rate of sequencedivergence in the human mitochondrialgenome: There is a difference betweenphylogenetic and pedigree rates, *Am. J. Hum. Genet*., **72**, 659–670

Höss, M., Jaruga, P., Zastawny, T.H., Dizdaroglu, M., Pääbo, S. (1996) DNA damage and DNA sequence retrieval from ancient tissues, *Nucleic Acids Res*., **24**, 1304 – 1307

Higuchi, R.G., Bowman, B., Freiberger, M., Ryder, O.A., Wilson, A.C. (1984) DNA sequences from the quagga, an extinct member of the horse family, *Nature*, **312**, 282-284

Ingman, M., Kaessmann, H., Pääbo, S., Gyllensten, U. (2000) Mitochondrial genome variation and the origin of modern humans, *Nature*, **408**, 708-13

Izaguirre, N., De La Rua, C. (2002) Ancient mtDNAhaplogroups: a new insight into the genetic history of European populations*, International Journal of Anthropology*, **17**, 27-40

Jorde, L.B., Bamshad, M., Rogers, A.R. (1998) Using mitochondrial and nuclear DNA markers to reconstruct human evolution, *Bioessays*, **20**, 126-136

Keyser-Tracqui, C., Crubézy, E., Ludes, B. (2003) Nuclear and Mitochondrial DNA Analysis of a 2,000-Year-Old Necropolis in the EgyinGol Valley of Mongolia, *Am. J. Hum. Genet*., **73**, 247–260

Knapp, M., Hofreiter, M. (2010) Next Generation Sequencing of Ancient DNA: Requirements, Strategies and Perspectives, *Genes*, **1**, 227-243

Köhnemann, S., Hohoff, C., Pfeiffer, H. (2009) An economical mtDNA SNP assay detecting different mitochondrial haplogroups in identical HVR 1 samples of Caucasian ancestry, *Mitochondrion*., **9**, 370-375

Lacan, M., Keyser, C., Crubézy, E., Ludes, B. (2013) Ancestry of modern Europeans: contributions of ancient DNA, *Cell. Mol. Life Sci*., **70**, 2473-87

Macaulay, V., Richards, M., Hickey, E., Vega, E., Cruciani, F., Guida, V., Scozzari, R., Bonné-Tamir, B., Sykes, B., Torroni, A. (1999) The emerging tree of West Eurasian mtDNAs: a synthesis of control-region sequences and RFLPs, *Am. J. Hum. Genet*., **64**, 232-249

Meyer, M., Fu, Q., Aximu-Petri, A., Glocke, I., Nickel, B., Arsuaga, J.L., Martínez, I., Gracia, A., de Castro, J.M., Carbonell, E., Pääbo, S. (2014) A mitochondrial genome sequence of a hominin from Sima de los Huesos, *Nature*, **505**, 403-406

MITOMAP (2013) A Human Mitochondrial Genome Database. http://www.mitomap.org

Núnéz, C., Sosa, C., Baeta, M., Geppert, M., Turnbough, M., Phillips, N., Casalod, Y., Bolea, M., Roby, R., Budowle, B., Martínez-Jarreta, B. (2011) Genetic analysis of 7 medieval skeletons from the Aragonese Pyrenees, *Croatian Medical Journal*, **52**, 336-343

Ottoni, C., Ricaut, F.X., Vanderheyden, N., Brucato, N., Waelkens, M., Decorte, R. (2011) Mitochondrial analysis of a Byzantine population reveals the differential impact of multiple historical events in South Anatolia, *Eur. J. Hum. Genet.,***19**, 571-576

Pakendorf, B., Stoneking, M. (2005) Mitochondrial DNA and human evolution, *Annu. Rev. Genomics Hum. Genet*.,**6**, 165–183

Pääbo, S. (1985) Molecular cloning of Ancient Egyptian mummy DNA, *Nature*, **314**, 644 - 645

Pääbo, S., Poinar, H., Serre, D., Jaenicke-Despres, V., Hebler, J., Rohland, N., Kuch, M., Krause, J., Vigilant, L., Hofreiter, M. (2004) Genetic analyses from ancient DNA, *Annu. Rev. Genet*., **38**, 645–679

Pinhasi, R., Thomas, M.G., Hofreiter, M., Currat, M., Burger, J. (2012) The genetic history of Europeans, *Trends Genet*., **28**, 496-505

Poinar, H.N. (2003) The top 10 list: criteria of authenticity for DNA from ancient and forensic samples, *International Congress Series*, **1239**, 575 – 579

Pulquério, M.J., Nichols, R.A. (2007) Dates from the molecular clock: how wrong can we be?,*Trends Ecol. Evol*., **22**, 180-184

Richards, M., Corte-Real, H., Forster, P., Macaulay, V., Wilkinson-Herbots, H., Demaine, A., Papiha, S., Hedges, R., Bandelt, H.J., Sykes, B. (1996) Paleolithic and Neolithic lineages in the European mitochondrial gene pool, *Am. J. Hum. Genet*.,**59**, 185–203

Rudbeck, L., Gilbert, M.T., Willerslev, E., Hansen, A.J., Lynnerup, N., Christensen, T., Dissing, J. (2005) mtDNA analysis of human remains from an early Danish Christian cemetery, *Am. J. Phys. Anthropol*., **128,** 424-429

Soares, P., Achilli, A., Semino, O., Davies, W., Macaulay, V., Bandelt, H.J., Torroni, A., Richards, M.B. (2010) Thearchaeogenetics of Europe, *Curr. Biol*. **20**, 174-183

Stoneking, M. (2000) Hypervariable sites in the mtDNA control region are mutational hotspots, *Am. J. Hum. Genet*., **67**, 1029-1032

Sykes, B. (2001) *The Seven Daughters of Eve: The Science that Reveals our Genetic Ancestry, 1st Edition*, W.W. Norton & Company New York, pp 8-51

Taylor, R.W., Turnbull, D.M. (2005) Mitochondrial DNA mutations in human disease, *Nat. Rev. Genet*., **6**, 389-402

Torroni, A., Huoponen, K., Francalacci, P., Petrozzi, M., Morelli, L., Scozzari, R., Obinu, D., Savontaus, M.L., Wallace, D.C. (1996) Classification of European Mtdnas from an Analysis of Three European Populations, *Genetics*, **144**, 1835–1850

van Oven, M., Kayser, M. (2009) Updated comprehensive phylogenetic tree of global human mitochondrial DNA variation, *Hum. Mutat*., **30**, 386-394, http://www.phylotree.org

Wallace D.C. (1994) Mitochondrial DNA sequence variation in human evolution and disease, *ProcNatlAcadSci U S A*., **91**, 8739–8746

Willerslev, E., Cooper, A. (2005) Ancient DNA,*Proc. R. Soc. B*., **272**, 3–16

STUDIA UNIVERSITATIS BABEŞ-BOLYAI BIOLOGIA, LIX, 1, 2014 (p. 157-167)

=== REVIEW ===

THE EVOLUTION AND GENETIC BASIS OF HUMAN PIGMENTATION

ENIKŐ KOCSIS[1]✉ and BEATRICE KELEMEN[1]

SUMMARY. Studies in the field of ancient DNA began thirty years ago. Key discoveries proved that ancient DNA is an important tool in the search for difficult answers pertaining to our past. Studies on pigmentation genetics showed that adaptation for different UV radiations was the major factor contributing to the formation of the current pigmentation pattern in Europe, but there is evidence which highlights the additional effect of sexual selection. From the various genes described to play a role in the determination of human skin, hair and eye color, HERC2, SLC24A4 and SLC45A2 seem to be most strongly associated with this phenotypic characteristics.

Keywords: ancient DNA, melanin, pigmentation genetics.

Introduction

The DNA of archaeological human remains is an important tool in the search for difficult answers on our past: the evolution and the origin of the human species, the origin of our diseases, the genetics and evolution of our phenotypic characteristics. The first results in this field were obtained in 1985 by Pääbo *et al*. from a 2430 year old Egyptian mummy (Kefi, 2011). This study used bacterial cloning to amplify small, old DNA sequences. With the development of improved techniques such as PCR and new generation sequencing technologies, it became possible to isolate and routinely amplify ancient DNA, and to surmount problems related to the alteration of ancient DNA (Rizzi *et al.*, 2012).

[1] *Department of Molecular Biotehnology, Faculty of Biology and Geology, University of Babeş-Bolyai, 5-7 Clinicilor str., 400006, Cluj-Napoca, Romania; Interdisciplinary Research Institute on Bio-Nano-Science, 42 Treboniu Laurean str., 400271, Cluj-Napoca, Romania.*

✉ ***Corresponding author: Kocsis Enikő**, Department of Molecular Biotehnology, Faculty of Biology and Geology, University of Babeş-Bolyai, 5-7 Clinicilor str., 400006, Cluj-Napoca, Romania; Interdisciplinary Research Institute on Bio-Nano-Science, Cluj-Napoca, Romania.*
Phone no: (+40) 0740 082578, E-mail: kocsis.eniko@yahoo.com

The preservation of ancient DNA depends not only on the age and type of the sample (Grigorenko *et al.,* 2009), but also on environmental conditions. The alteration of ancient DNA is a consequence of autolysis and microbial degradation, but humidity, high or very variable temperatures and very alkaline or acidic pH also contributes to this effect (Kefi, 2011).

Thus, ancient DNA is difficult to amplify because of the small quantity and size of the DNA fragments, the presence of postmortem chemical DNA modifications and due to the presence of contaminants, in particular modern DNA (Kefi, 2011). The contamination with modern DNA can be prevented by following strict precautionary steps during collection and laboratory work (Hummel, 2003). The main advantage of PCR is the selective amplification of a target region of the DNA. The amplification of other fragments than the target sequences can thus be avoided. Approaches as Multiplex PCR proved to be a powerful tool for the analysis of small quantities and highly degraded source ancient DNA (Kefi, 2011).

The methods and techniques used depend on the age and type of the sample and the questions the researchers want answered. The majority of the studies focus on the origin, relationship and migration of human populations, but other studies which focus on the reconstruction of the diet, the determination of sex or of phenotypic characteristics are of interest (Mulligan, 2006). Even though working with ancient DNA is difficult and circumstantial, it represents a more scientific bridge to our past.

Key discoveries in skin, hair and eye pigmentation in ancient populations from Europe

The field of ancient DNA studies began thirty years ago, when Higuchi *et al.* (1984) examined and extracted DNA from dried muscle of the quagga, a zebra-like species and showed its phylogenetic relationship with modern zebra (Higuchi *et al.*, 1984). A year later, Pääbo (1985) obtained DNA from a 2400-year-old Egyptian mummy (Pääbo, 1985).

A key discovery in this field was the extraction of a pigmentation gene, MC1R from the bones of two Neanderthals by Lalueza-Fox *et al.* (2007), who showed that some of the Neanderthals had pale skin and reddish hair similarly to some of the *Homo sapiens* who today inhabit Europe (Lalueza-Fox *et al.*, 2007). Three years later Green *et al.* (2010) sequenced the Neanderthal genome, which showed that they are likely to have had a role in the genetic ancestry of present day humans outside of Africa. This research team found a number of genomic regions and genes, in particularly those involved in cognitive abilities and cranial morphology, as candidates for positive selection early in modern human history (Green *et al.*, 2010).

In 2009 Bouakaze *et al.* examined 10 SNPs from six genes (MC1R, HERC2, OCA2, SLC45A2, SLC24A5 and DCT) in the case of 25 archeological human remains and found that they had blue or green eye color, light hair color and pale skin. This was the first research which used a multiplexed genotyping assay on aged and degraded DNA and underlined the importance of pigmentation genetics in the case of ancient DNA (Boukaze *et al.,* 2009).

The most useful study was carried out by Walsh *et al*. in 2011. They developed the IrisPlex system, a powerful tool for eye color prediction from DNA. This study finds that the most strongly eye color associated SNP is rs12913832 in the HERC2 gene. This SNP determines whether the eye color will be brown or non-brown. The further determination of non-brown color is provided by rs12896399 from SLC24A4 and rs16891982 from SLC45A2, while the further darkening of brown color is determined by rs1800407 from OCA2, rs1393350 from TYR and rs12203592 from the gene IRF4 (Walsh *et al.*, 2011). Two years later, this research team developed the HIrisPlex System, which uses the 6 SNPs and genes from the IrisPlex system and 18 additional SNPs from 5 other genes to predict hair and eye color from DNA. In this study, they also found that HERC2 seems to be the gene most strongly associated with hair and eye color (Walsh *et al.*, 2013).

The evolution of pigmentation

The human species originates from Africa and our closest evolutionary relatives are the chimpanzees. It is likely that the first members of hominids were similar to other primates, they had light skin color covered with dark hair (Jablonski and Chaplin, 2000). The hairless condition appeared as the first adaptation to living in a hot environment, and was facilitated by the increase in the number of sweat glands (Jablonski and Chaplin, 2010). As the density of the dark body hair decreased and the density of sweat glands increased, the need for protection against the destructive effect of UV radiation also increased. The solution was found by evolution in the beneficial effect of melanization (Jablonski and Chaplin, 2000). Melanin acts as a filter to attenuate and prevent UV radiation from entering into subepidermal tissues. Another protective effect of melanin is accomplished by scavenging free radicals and other oxidants, by which it prevents the destruction of the skin (Parra, 2007).

Thus, the evolution of naked, dark skin occurred early in the evolution of hominids as a protective character against UV radiation, which is highest near the Equator and in the tropics (Jablonski and Chaplin, 2000). The effects of UV radiation are harmful: they damage sweat glands, disrupt thermoregulation, increase risk of infection and of skin cancer (Parra, 2007). Folate, which plays a key role in human health and reproductive success is also sensitive to UV radiation. Folate plays a crucial role in the maturation of bone marrow, development of red blood cells, purine

and pyrimidine biosynthesis, neurulation and spermatogenesis. In incomplete neurulation, which could be a consequence of the lack of this essential nutrient, embryos fail early in their development, which leads to spontaneous abortion. Folate deficiency caused by UV radiation also leads to male infertility. Thus, protection against UV radiation through a darker skin color had a crucial role in the maintenance of reproductive success, and the survival of the species (Jablonski and Chaplin, 2000).

The effects of UV radiation described above are harmful. There is one exception: UVB radiation is essential for the synthesis of vitamin D, which plays an important role in bone metabolism, immunoregulation, cell differentiation and proliferation (Parra, 2007). As hominids migrated far from the Equator a selective pressure acted on pigmentation to permit UVB induced synthesis of vitamin D. The higher melanin content of dark skin became nonadaptive and ineffective under conditions where higher concentrations of melanin did not allow the sufficient synthesis of vitamin D. That is why depigmentation and the appearance of lighter skin color far from the Equator was a necesary development (Jablonski and Chaplin, 2000).

Charles Darwin stated that several human traits, such as pigmentation, could be the result of sexual selection and there are researchers who affirmed that sexual selection has been an important role in determining the distribution of skin, hair and eye color across the globe, pigmentation being an important criterion of mate choice in humans (Parra, 2007). Human hair and eye color are unusually diverse in Europe, but fairly uniform on the other continents. As one moves outward from this area, eye color becomes uniformly brown, while hair color becomes uniformly black (Frost, 2006). There are authors who affirm that this pattern is due primarily to natural selection and there are others who believe that sexual selection had a more prominent role (Parra, 2007).

The first theory, which seems to support sexual selection is rare-color advantage studied in fruit flies, guppies and reported in ladybugs, red flour beetles and some bird species. This theory postulates that mates with unusual characters are most likely to be chosen. This rare color advantage has also been reported in humans by several authors. For example, Thomas Thelen presented three series of slides showing females with blonde and brown hair and asked male participants to indicate the one that they would most prefer to marry. The firs series of slides showed 6 females with brown hair, the second 1 female with brown and 5 female with blonde hair, while the third series showed 1 female with brown and 11 female with blonde hair. The participants selected females with brown hair with significantly increased preference from the one to the third series of slides. The males preferred females which had the rarer hair color in the specific population (Frost, 2006). Bruno Laeng *et al.* (2005) also tested the effect of eye color on mate choice. They showed the same man and female with different eye colors to a group of young individuals, and

asked them to select the one they feel the most attractive. The study presented positive correlation only in the case of men with blue eyes (Laeng *et al.*, 2005). The effect of the rare color advantage on human hair, eye and skin color is not completely clear, but it may have added selective pressure on pigmentation diversification (Frost, 2006).

If sexual selection is the answer for this unusual pattern of pigmentation in Europe, a competitive force must exist to support this theory. As humans migrated from Africa northward, they had to accommodate to the new environment and they had to obtain their food mostly from hunting. The importance of food gathering became negligible as they entered in the Arctic environment, which implied that females were dependent on males, who were the principal hunters. With the increase in distances to hunting grounds, the survival of men decreased. Thus, females had to compete for males and the theory may explain this unusual distribution pattern, but more research needs to be done in order to prove this theory with certainty (Frost, 2006).

Natural selection and sexual selection are not exclusive processes, and it is likely that both were involved in the evolution of humans. Pigmentation patterns and their diversification in Europe, may have resulted from their combined effect (Parra, 2007).

Melanocytes and melanin

Melanocytes are dendritic cells derived from the neural crest that are able to produce melanin. Mammalian melanocytes are categorized in two groups: cutaneous melanocytes, which are involved in hair and skin pigmentation, and extracutaneous melanocytes, which represent the melanogenic cells of the eye, inner ear, adipose tissue, brain, heart and bone (Kawakami and Fisher, 2011). The life cycle of melanocytes is split into several steps: lineage specification from neural crest cells, migration and proliferation, differentiation into melanocytes, maturation of melanocytes, transport of mature melanosomes to keratinocytes in the case of cutaneous melanocytes and cell death (Cichorek *et al.*, 2013).

Melanogenesis happens during the phase of melanocyte maturation in specialized organelles, called melanosomes. Melanosomes are large organelles (~500 nm), which are the cellular sites of the synthesis, storage and transport of melanin (Wasmeier *et al.*, 2008). Two types of melanin pigment are synthesized during melanogenesis: the brown/black colored eumelanin and the yellow/ red colored pheomelanin. The color of the skin, eye and hair depend on the amount of pigment and on the balance between the synthesis of eumelanin and pheomelanin. It is important to note that only eumelanin can efficiently protect against UV radiation (Borovanský and Riley, 2011).

Melanosomes are transferred to keratinocytes only in the case of cutaneous melanocytes and it has important roles in the immune response to various stimuli and in the protection against UV caused DNA damage and oxidative stress. The melanocytes of hair follicles are involved not only in hair pigmentation, but also in the elimination of toxic byproducts of melanin synthesis (Borovanský and Riley, 2011). Melanocytes of the hair are restricted below keratinocytes, to the bulb of the hair, and from here the minimally digested melanosomes are transported to keratinocytes, which ultimately form the outer pigmented shaft of the hair. Instead of this, follicular and epidermal melanocytes both originate from neural crest cells; during development, the follicular melanocytes become larger, more dendritic and produce larger melanosomes. In addition melanogenesis in the hair bulb melanocytes is coupled with the growth cycle of the hair (Slominski *et al.*, 2005).

The melanocytes of the skin are found not only in the basal layer of the epidermis but also in the dermis. In contrast to epidermal melanocytes of the skin, which are surrounded by keratinocytes and are able to transport completely degraded melanosomes to the surrounding cells, the melanocytes of the dermis are surrounded mostly by fibroblasts and are not able to transport melanosomes. Melanosomes of the epidermis have a protective role against the destructive effect of UV radiation by reducing the penetration of UV rays and also by scavenging reactive oxygen species generated in response to UV exposure. The reactive intermediates generated during melanin synthesis have antimicrobial and antifungal properties, and in addition, melanocytes are active components of the skin's immune system, as they respond to the presence of cytokines, growth factors and they can present antigens to immune T cells (Borovanský and Riley, 2011).

The human eye contains two different types of pigment cells: the pigmentary epithelium cells with neural ectodermal origin and the uveal melanocytes with origin in the neural crest. Both types of cells produce and store melanin in their cytoplasm. Pigmentary epithelium cells are more pigmented, contain mostly eumelanin and do not contribute to the color of the eye. The melanin quality and quantity in the uveal melanocytes, in particular the iridial melanocytes differ for each eye color (Wakamatsu *et al.*, 2007). The melanocytes of the iris are located in its anterior layer and the stroma. In the case of brown irises these layers contain abundant melanocytes and melanin, while blue irises contain very little amounts of melanin (Borovanský and Riley, 2011).

Both types of melanin pigment are synthesized during melanogenesis, the so called Raper- Mason pathway, in melanosomes. Melanosomes have four stages. Stage I melanosomes are multivesicular endosomes, which contain matrix and internal vesicles. Stage II melanosomes have a more organized structure, but no melanin is yet synthesized. The deposition of melanin on the fibrillar matrix is found in stage III, while stage IV melanosomes are fully melanized (Park *et al.*, 2009). The Raper Mason pathway has a rate limiting, tyrosinase catalyzed phase, after which the

synthesis of the two types of melanin follows different reactions. The rate limiting first reaction of melanin production is catalyzed by tyrosinase and includes the hydroxylation of L-tyrosine to L-DOPA (L-dihydroxyphenylalanine) and the subsequent oxidation of this to L-dopaquinone (Gillbro and Olsson, 2010).

During eumelanin synthesis, L-dopaquinone spontaneously transforms first into L-cyclodopa, which together with another molecule of L-dopaquinone forms L-dopachrome. L-dopachrome in the eumielin pathway can spontaneously rearrange to DHI (5,6-dihydroxyindole) or enzimatically transform into DHICA (DHI-2 carboxylic acid). IQ (5,6-indolequinone) and IQCA (indole-2-carboxylic acid-5,6-quinone) are formed by oxidation from DHI and DHICA, respectively. The black, insoluble eumelanin (DHI-melanin) and the golden-brown poorly soluble eumelanin (DHICA-melanin) are formed during the last phase of the eumelanin pathway by the spontaneous intermixed polymerization of DHI, IQ, DHICA and IQCA (Borovanský and Riley, 2011).

The pheomelanin pathway depends upon the availability of L-cystein. In the presence of this compound, L-dopaquinone transforms into various isomers of cysteinildopa (5-cysteinildopa, 2-cysteinildopa, 6-cysteinildopa). 5-cysteinildopa is the one from which the monomers of pheomelanin, alanyl-hydroxy-benzothiazines are formed. The production of eumelanin and pheomelanin depends on the regulatory effects of various enzymes, proteins and transcription factors. The mutation of several genes determines the melanin synthetic activity of melanocytes (Borovanský and Riley, 2011).

Human pigmentation genes

The color of the human skin, eye and hair is a polygenic trait and multiple genes work together to determine it, under the influence of several environmental factors. The gene MC1R (melanocortin-1 receptor) is one of the major genes in determining human skin and hair color. A large amount of the photoprotective eumelanin is found among humans with dark skin color and pheomelanin among humans with fair skin. The MC1R gene regulates the production of eumelanin in melanosomes and is located on chromosome 16q24.3. The gene encodes a G-protein coupled receptor found on the cell membrane of melanocytes and keratinocytes. Point mutations in the gene lead to the loss of receptor function and to decreased eumelanin production, which will determine fair skin and carrot red hair (Metzelaar-Blok *et al.*, 2001). The gene shows little variation within Africa, probably in order to maintain the production of the photoprotective eumelanine. Outside Africa, the gene has various polymorphisms. The global pattern of variation of the gene suggests that mutant alleles were favored during the movement of the human populations towards the North as an adaptation to the new environment (Jablonski, 2013).

Mutation in another gene, MATP (Membrane Associated Transporter Protein) is also responsible for hypopigmentation. The gene is located on chromosome 5p13.2 and encodes for a membrane protein, which mediates the melanin synthesis by tyrosinase trafficking and proton transport to melanosomes (Fracasso *et al.*, 2013). Several studies indicate that the MATP gene plays important roles in the normal pigmentation variations and shows a strong signature of selection in the European populations (Parra, 2007)

The rate limiting reactions of melanogenesis depend on the catalytic activity of tyrosinase. The gene which encodes this enzyme is located on chromosome 11q14.3. This enzyme is part of the tyrosinase family together with TYRP1 (tyrosinase related protein1) and TYRP2 (tyrosinase related protein 2). The TYRP1 and TYRP2 proteins also contribute to the catalytic effect of tyrosinase and influence the stability of the enzyme. The TYRP1 gene is located on chromosome 9p23, while the TYRP2 gene on chromosome 13q32. Mutations in these genes lead to a decreased melanin production (Sturm, 2001).

The gene MITF (Microphthalmia Associated Transcription Factor) is a transcription factor, which regulates melanogenesis by binding upstream of the tyrosinase promoter and stimulating tyrosinase transcription (Wang *et al.*, 2014). The gene is located on chromosome 3p and m14.1 (Sturm *et al.*, 2001), and mutations in this gene lead to hypopigmentation.

The OCA2 (Oculocutaneous Albinism Type II) and HERC2 (Hect Domain and RCC1-like Domain 2) are also involved in eye, hair and skin color pigmentation. OCA2 is located on chromosome15q13.1 and encodes for a transmembrane protein, P protein, which plays a role in tyrosinase traffic and pH regulation of the melanosomes. Mutations in this gene in Europeans are associated primarily with blue eye color. The HERC2 gene is located upstream from the regulatory region of OCA2 and has a possible regulatory effect on OCA2. Mutations in HERC2 are associated with green/hazel eyes in Europeans (Donnelly *et al.*, 2012).

Conclusions

Ancient DNA is an important molecular tool used to answer problematic questions about humanity's past. It represents a new field in anthropology. Working with ancient DNA is circumstantial and difficult, due to several factors: lack of material, alterations caused by postmortem modifications and degradation under environmental conditions during time, contamination with exogenous DNA. The information about the evolution of human phenotypic characteristics and the unusual pattern of pigmentation in Europeans is incomplete. There are authors (Jablonski, 2013; Frost, 2006) which state that natural selection contributed to this pattern, but there are others (Laeng, 2005; Frost, 2006) who affirm that sexual selection had the primary effect in this diversification. This lack of clarity is understandable because

the pigmentation of human skin, hair and eye is not a simple trait determined by a single gene; it is a polygenic trait determined by the combined effect of multiple genes. Studies on past populations may contribute to the reconstruction of evolutionary paths followed by human pigmentation patterns during historical periods across Europe, thus shedding more light on the molecular mechanisms involved.

Acknowledgements This work was financially supported by the project Genetic Evolution: New Evidence for the Study Interconnected Structures (GENESIS). A Biomolecular Journey around the Carpathians from Ancient to Medieval Times (CNCSIS-UEFISCDI_PNII_PCCA_ 1153/2011).

REFERENCES

Borovanský, J., Riley, P.A. (2011) *Melanins and melanosomes*,Wiley-VCH Verlag & Co. KGaA, Germany, pp 21-109

Boukaze, C., Keyser, C., Crubézy, E., Montagnon, D., Ludes, B. (2009) Pigment phenotype and biogeographical ancestry from ancient skeletal remains: inferences from multiplexed autosomal SNP analysis, *International Journal of Legal Medicine*, **123**(4), 315-325

Cichorek, M., Wachulska, M., Stasiewitcz, A., Tymińska, A. (2013) Skin melanocytes: biology and development, *Postepy Dermatol Alergol* **30**(1): 30-41

Donnelly, M.P., Paschou, P., Grigorenko, E., Gurwitz, D., Barta, C., Lu, R.B., Zhukova, O.V., Kim, J.J., Siniscalco, M., New, M., Li, H., Kajuna, S.L.B., Manolopoulos, V.G., Spee, W.C., Pakstis, A.J., Kidd, J.R., Kidd, K.K. (2012) A global view od the OCA2-HERC2 region and pigmentation, *Human Genetics*, **131**, 683-696

Fracasso, N.C.A., Andrade, E.S., Andrade, C.C.F., Zanão, L.R., Silva, M.S., Marano, L.A., Wiezel, C.E.V., Donadi, E.A., Simões, A.L., Mendes-Junior, C.T. (2013) Association of SNPs from the SLC45A2 gene with human pigmentation traits in Brazil, *Forensic Science International*, **4**, e342-e343

Frost, P. (2006) European hair and eye color: a case of frequency- dependent sexual selection?, *Evolution and Human Behavior*, **27**, 85-103

Gillbro, J.M., Olsson, M.J. (2010) The melanogenesis and mechanisms of skin-lightening agents- existing and new approaches, *International Journal of Cosmic Science*, **33**, 210-221

Green, E.R., Krause, J., Briggs, A.W., Maricic, T., Stenzel, U., Kircher, M., Patterson, N., Li, H., Zhai, W., Fritz, M.H.Y., Hansen, N.F., Durand, E.Y., Malaspinas, A.S., Jensen, J.D., Marques-Bonet, T., Alkan, C., Prüfer, K., Meyer, M., Burbano, H.A., Good, J.M., Schultz, R., Aximu-Petri, A., Butthof, A., Höber, B., Höffner, B., Siegemund, M., Weihmann, A., Nusbaum, C., Lander, E.S., Russ, C., Novod, N., Affourtit, J., Egholm, M., Verna, C., Rudan, P., Brajkovic, B., Kucan, Ž., Gušic, I., Doronichev, V.B., Golovanova, L.V., Lalueza-Fox, C., Rasilla, M., Fortea, J., Rosas, A., Schmitz, R.W., Johnson, P.L.F, Eichler, E.E., Falush, D., Birney, E., Mullikin, J.C., Slatkin, M., Nielsen,

R., Kelso, J., Lachmann, M., Reich, D., Pääbo, S. (2010) A draft sequence of the Neandertal genome, *Science*, **328**, 710-722

Grigorenko, A.P., Borinskaya, S.A, Yankovsky, N.K., Rogaev, E.I. (2009) Achievments and peculiarities in studies of ancient DNA and DNA from complicated forensic specimens, *Acta Naturae*, **3**, 58-69

Higuchi, R., Bowman, B., Freiberger, M., Ryder, O.A, Wilson, A.C. (1984) DNA sequences from the quagga, an extinct member of the horse family, *Nature*, **312**, 282-284

Hummel, S. (2003) *Ancient DNA typing:methods, strategies, and applications*, Springer-Verlag Berlin Heidelberg, Germany, pp 131-155

Jablonski, N.G. (2013) *Skin: a natural history*, University of California Press, England, pp 1-39

Jablonski, N.G., Chaplin, G. (2000) The evolution of human skin coloration, *Journal of Human Evolution*, **39**, 57-106

Jablonski, N.G., Chaplin, G. (2010) Human skin pigmentation as an adaptation to UV radiation, *Proceeding of the National Academy of Sciencies of the United States of America*, **107**(2), 8962-8968

Kawakami, A., Fisher, D.E. (2011) Key discoveries in melanocyte develompent, *Journal of Investigative Dermatology*, **131**, E2-E4

Kefi, R. (2011) Ancient DNA investigations:a review on their significance in different research fields, *International Journal of Modern Anthropology*, **4**, 61-76

Laeng, B., Mathisen, R., Johnsen, J.A. (2006) Why do blue-eyed men prefer women with the same eye color?, *Behavioral Ecology and Sociobiology*, **61**(3), 371-384

Lalueza-Fox, C., Römpler, H., Caramelli, D., Stäubert, C., Catalano, G., Hughes, D., Rohland, N., Pilli, E., Longo, L., Condemi, S., Rasilla, M., Fortea, J., Rosas, A., Stoneking, M., Schöneberg, T., Bertranpetit, J., Hofreiter, M. (2007) A melanocortin 1 receptor allelesuggest varying pigmentation among Neanderthals, *Science*, **318**, 1453-1455

Metzelaar-Blok, J.A.W., Huurne, J.A.C., Hurks, H.M.H., Keunen, J.E.E., Jager, M.J., Gruis, N.A. (2001) Characterization of melanocortin-1 receptor gene variants in uveal melanoma patient, *Investigative Ophtalmology and Visula Science*, **42**(9), 1951-1954

Mulligan, C.J. (2006) Anthropological applications of ancient DNA: problems and prsopects, *American Antiquity*, **71**(2), 365-380

Pääbo, S. (1985) Molecular cloning of Ancient Egyptian mummy DNA, *Nature*, **314**, 644-645

Park, H.Y., Kosmadaki, M., Yaar, N., Gilchrest, B.A. (2009) Cellular mechanism regulation human melanogenesis, *Cellular and Molecular Life Sciences*, **66**, 1493-1506

Parra, E.J. (2007) Human pigmentation variation: evolution, genetic basis, and implications for public health, *Yearbook of Physical Anthropoly*, **50**, 85-105

Rizzi, E., Lari, M., Gigli, E., Bellis, G., Caramelli, D. (2012) Ancient DNA studies: new perspectives on old samples, *Genetics Selection Evolution*, **44**, 21

Slominski, A., Wortsman, J., Plonka, P.M., Schallreuter, K.U., Paus, R., Tobin, D.J. (2005) Hair follicle pigmentation, *Journal of Investigative Dermatology* **124**(1): 13-21

Sturm, R.A., Teasdale, R.D., Box, N.F. (2001) Human pigmentation genes: identification, structure, and consequences of polymorphic variations, *Gene*, **277**, 49-62

Wakamatsu, K., Hu, D.N., McCormick, S.A., Ito, S. (2007) Characterization of melanin in human iridal and choroidal melanocytes from eyes with various colored irides, *Pigment Cell Melanoma Research* **21**: 97-105

Walsh, S., Liu, F., Ballantyne, K.N., Oven, M., Lao, O., Kayser, M. (2011) IrisPlex: a sensitive DNA tool for accurate prediction of blue and brown eye colour in the absence of ancestry infromation, *Forensic Science International*: *Genetics*, **5**, 170-180

Walsh, S., Liu, F., Wollstein, A., Kovatsi, L., Ralf, A., Kosiniak-Kamysz, A., Branicki, W., Kayser, M. (2013) The HIrisPlex system for simultaneous prediction of hair and eye colour from DNA, *Forensic Science International: Genetics***, 7**, 98-115

Wang, Y., Li, S.M, Huang, J., Chen, S.Y., Liu, Y.P. (2014) Mutation of TYR and MITF genes are associated with plumage colour phenotypes in Geese, Asian-Australasian *Journal of Animal Science*, **27**(6), 778-783

Wasmeier, C., Hume, A.N., Bolasco, G., Seabra, M.C. (2008) Melanosomes at a glance, *Journal of Cell Science*, **121**, 3995-3999